Funktionelle Untersuchungen zur Reaktion der Haut auf exogene Noxen:

Die Rolle des Arylhydrocarbon-Rezeptors

Inaugural-Dissertation

zur Erlangung des Doktorgrades
der Mathematisch-Naturwissenschaftlichen Fakultät

der Heinrich-Heine-Universität Düsseldorf

vorgelegt von

Julia Tigges

aus Duisburg

Düsseldorf, November 2011

aus dem Leibniz Institut für umweltmedizinische Forschung (IUF)

an der Heinrich-Heine Universität Düsseldorf gGmbH

Gedruckt mit der Genehmigung der

Mathematisch-Naturwissenschaftlichen Fakultät der

Heinrich-Heine-Universität Düsseldorf

Referent: Prof. Dr. Ellen Fritsche

Koreferent: Prof. Dr. Peter Proksch

Tag der mündlichen Prüfung: 14.12.2011

„Man kann nichts dagegen tun, dass man altert.

Aber man kann sich dagegen wehren,

dass man veraltet.“

Lord Samuel

Für Ida und Klara

Danksagung

Inhaltsverzeichnis

1   Einleitung

1.1   Aufbau und Funktion der Haut

1.1.1   Allgemeines

Die Haut stellt das Grenzflächenorgan des Körpers gegenüber den äußeren Faktoren der Umwelt dar. Mit einer Gesamtfläche von durchschnittlich 2 m^2 und einem Gewicht von 20 kg, einschließlich des Unterhautfettgewebes, ist sie das größte Organ des Menschen. Als Barriere schützt die Haut vor physikalischen, chemischen und biologischen Einflüssen von Außen, dient aber auch der Regulation des Wasser-, Temperatur- und Elektrolythaushalts. In der Haut eingebettete Merkel- und Nervenzellen nehmen Druck, Temperatur und Schmerz wahr. Mit den Langerhanszellen, Mastzellen und Makrophagen stellt sie den periphersten Außenposten des Immunsystems dar (Fritsch, 2009).
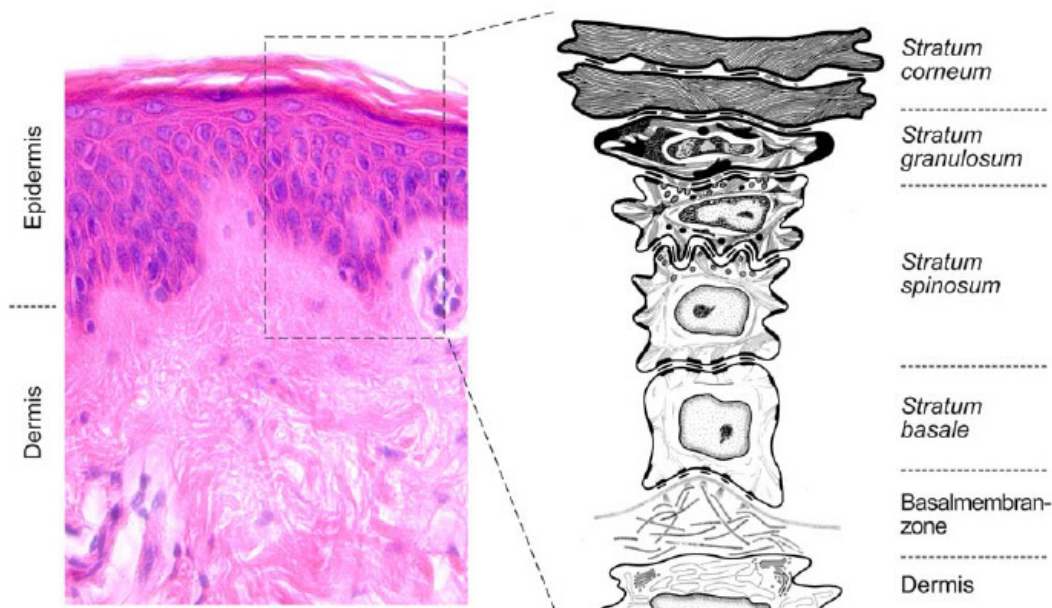
Abb. 1.1: Aufbau der humanen Haut. Die humane Haut unterteilt sich in Epidermis, Basalmembranzone und Dermis. Die Epidermis wird in das *Stratum basale*, *Statum spinosum*, *Stratum granulosum* und *Stratum corneum* unterteilt (entnommen aus Boehnke K, 2009).

Die Haut gliedert sich in drei Schichten: die Epidermis (Oberhaut), die bindegewebige Dermis (Lederhaut) und Subkutis (Unterhautfettgewebe) (Abb. 1.1).

1.1.2 Epidermis

Als Epidermis bezeichnet man das mehrschichtige, verhornende Plattenepithel ektodermalen Ursprungs, das zu über 90 % aus Keratinozyten besteht (Abb. 1.1 und 1.2). Die anderen 10 % sind Langerhans-Zellen (die dendritischen Zellen der Epidermis), pigmentbildende Melanozyten und neuroendokrine Merkelzellen. Die Epidermis besteht aus vier Schichten (Abb. 1.1), die verschiedenen Differenzierungsgraden der Keratinozyten entsprechen und zueinander in einem homöostatischen Gleichgewicht stehen: dem *Stratum corneum* (Hornschicht), dem *Stratum granulosum* (Körnerschicht), dem *Stratum spinosum* (Stachelschicht) und dem *Stratum basale* (Basalschicht) (Fritsch, 2009). Die Grenzzone zwischen Epidermis und Dermis verläuft wellenartig mit epidermalen Retezapfen und dermalen Papillen, was der Verbesserung der Stabilität und der Dehnungsreserve dient. Dieser Grenzschicht sitzt in apikaler Richtung die Epidermis mit einer einzelligen Basallamina auf, welche die epidermalen Stammzellen beherbergt, aus denen die Keratinozyten hervorgehen. Die Keratinozyten des *Stratum basale* sind über Hemidesmosomen mit der Basalmembran verbunden (Fritsch, 2009). Sie durchwandern einzeln und aktiv das *Stratum basale* und *Stratum spinosum*, wobei sie einen streng regulierten Differenzierungsgang durchlaufen. Desmosomen stellen die Verbindung der Zellen untereinander sicher und der Zellkontakt mittels *gap junctions* gewährleistet den interzellulären Stoffaustausch. Dieser Teil der Keratinozytendifferenzierung dauert durchschnittlich 14 Tage (Fritsch, 2009).

Während der nächsten 14 Tage erfolgt im *Stratum corneum* der finale epidermale Differenzierungsprozess der Keratinozyten zu toten Korneozyten (Hornzellen). Dabei werden in den Keratinozyen verschiedene Lipide synthetisiert und in den Extrazellularraum ausgeschleust, wo sie sich in Schichten zusammenlagern. Dieser sogenannte *Cornified Envelope* (CE) ist eine robuste Protein/Lipid-Polymerstruktur, die sich unterhalb der zytoplasmatischen Membran auf der Außenseite der Korneozyten befindet. Die Ceramide A und B sind kovalent mit den Proteinen des CE verbunden und bilden das Grundgerüst für die Anlagerung von freien Ceramiden, Fettsäuren und Cholesterol im *Stratum corneum*. Fillagrin ist mit dem CE quervernetzt und aggregiert Keratinfilamente zu Makrofibrillen. Die Funktion und Aufrechterhaltung der Barrierefunktion wird durch Zytokine, zyklische Adenosinmonophosphate und Calcium beeinflusst (Fritsch, 2009).
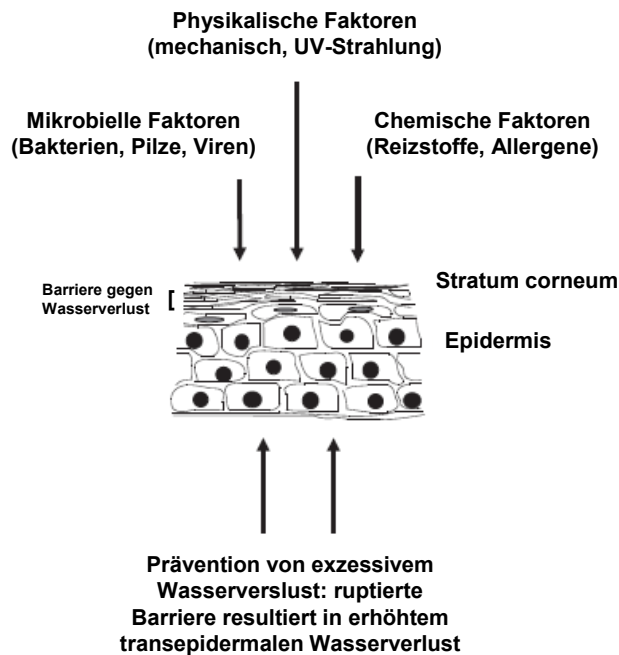
Abb. 1.2: Funktionen der epidermalen Barriere (adaptiert nachProksch *et al.*, 2008)

Veränderungen in der epidermalen Differenzierung und Lipidzusammensetzung führen zu einer Störung der Hautbarriere, und damit zum unerwünschten Eintritt von äußeren Faktoren wie Allergenen und Chemikalien (zusammengefasst in Proksch *et al.*, 2008).

1.1.3 Dermis

Als Dermis bezeichnet man das fibroelastische Bindegewebe unterhalb der Epidermis und oberhalb der Subkutis. Es besteht aus dem *Stratum papillare* mit den die Haut versorgenden Gefäßen und Nerven und dem *Stratum reticulare*, welches sich durch hohe Reißfestigkeit (vermittelt durch Kollagenfaserbündel) und Elastizität (vermittelt durch elastische Fasern) ausweist (Fritsch, 2009). Die Hauptzellpopulation in der Dermis wird von Fibroblasten gestellt. Dabei handelt es sich um mesenchymale spindelförmige Zellen mit langen zytoplasmatischen Fortsätzen, die untereinander und mit ihrer Umgebung durch Integrine (membranständige Rezeptoren) verbunden sind (Heckmann M, 1999). Sie synthetisieren sowohl Komponenten der Extrazellulären Matrix (ECM) wie Proteoglykane und Glukosaminglykane, sowie Strukturproteine wie Laminin,

Fibronektin und Elastin (Fritsch, 2009), als auch spezifische Proteasen, die für die Degradation und Modifikation der ECM verantwortlich sind (Fritsch, 2009; siehe auch Abschnitt 1.2). Ein weiterer in der Dermis vorkommender Zelltyp sind Mastzellen, die unter anderem Histamin und Heparin sekretieren und somit für hypersensitive Reaktionen der Haut verantwortlich sind (Chu DH *et al.*, 2003). Außerdem finden sich in diesem Hautkompartiment Makrophagen, die als immunologisch aktive Zellen sowohl anfallende Abbauprodukte wie Proteine oder Fette, als auch abgestorbene Zellen phagozytieren und durch die Speicherung von Antigenen und Produktion von Interferon an der Immunantwort der Haut beteiligt sind (Jung EG, 1998).

Die Fasern und Zellen der Dermis sind von einer gelartigen Grundsubstanz umgeben. Zusammen mit den Fasern wird diese als extrazelluläre Matrix (ECM) bezeichnet (Fritsch, 2009).

1.1.4 Extrazelluläre Matrix (ECM)

Unter Extrazellulärer Matrix (ECM) versteht man die Füllsubstanz von Dermis und Subkutis. Sie besteht aus einem Gemisch von langkettigen, unverzweigten Glykosaminglykanen und Proteoglykanen, die über glykosidische Bindungen an kleinere Proteine gebunden sein können. Ein wichtiges Glykosaminglykan sind Hyaluronsäuren. Proteoglykane sind in der Lage verschiedene Moleküle wie z.B. Versikan zu binden, dem eine wichtige Funktion bei der Zellhaftung zukommt. Die Synthese von Glykosaminglykanen und Proteoglykanen erfolgt durch Fibroblasten. Da sie von Hyaluronidasen und lysosomalen Enzymen rasch abgebaut werden, haben sie eine Halbwertszeit (HWZ) von nur wenigen Tagen (HWZ Hyaluronsäure: 3 Tage; Fritsch, 2009).

Ein weiterer wichtiger Bestandteil der ECM sind Kollagene. Diese Proteinfamilie stellt die Hauptfraktion der extrazellulären Stütz- und Strukturproteine in allen Organen des Körpers. Bei Kollagenmolekülen handelt es sich um Tripelhelices aus je drei α-Polypeptidketten mit der Aminosäure Glyzin an jeder dritten Position. Wie Glykosaminglykane werden auch Kollagene durch Fibroblasten synthetisiert (Fritsch, 2009). Diese sezernieren das lösliche Prokollagen, von dem extrazellulär terminale

Peptide abgespalten werden. Das so entstandene unlösliche Kollagen wird durch Lysyloxidase (LOX) quervernetzt und aggregiert zu Fibrillen, welche zu Fasern gebündelt vorliegen (Hulmes DJS, 2008). Insgesamt sind beim Menschen 28 Kollagen-Typen bekannt, wovon die Dermis 8 enthält (Kadler *et al.*, 2007). Die wichtigsten Kollagentypen in der Dermis sind Kollagen Typ I mit einem Anteil von 80 - 90 %, Typ III mit 8 – 12 %, Typ V mit 5 % und Typ VI (Fritsch, 2009; Hulmes DJS, 2008; Chu DH *et al.*, 2003).

1.2   Intrinsische und Extrinsische Hautalterung

Die Haut altert sowohl intrinsisch (die rein chronologische Alterung), als auch extrinsisch (beeinflusst durch äußere Faktoren wie z.B. UV-Strahlung). Beide Formen der Hautalterung führen zu Falten und Verlust der Elastizität, allerdings kommt es bei der extrinsischen Form zu einem früheren Einsetzen und zu stärkeren Effekten der pathologischen Unterschiede (Montagna *et al.*, 1989; Agache *et al.*, 1980; Warren *et al.*, 1991; Escoffier *et al.*, 1989). Des Weiteren weisen die Modulierungsprozesse der ECM in der Haut bei beiden Formen der Hautalterung deutliche Unterschiede auf: in intrinsisch gealterter Haut gibt es nicht nur Hinweise auf die Degradation von faserigen ECM-Komponenten wie Elastin (Robert *et al.*, 1988) und den Kollagenen I, III und IV (El-Domyati *et al.*, 2002), sondern auch auf Verluste in der Oligosaccharid-Fraktion, die die Möglichkeit der Haut, Wasser zu speichern, beeinflusst (Ghersetich *et al.*, 1994; Naylor *et al.*, 2011; Abb. 1.3).

Im Gegensatz zu der generellen extrazellulären Atrophie in intrinsisch gealterter Haut, ist extrinsisch gealterte Haut sowohl durch katabolische als auch durch anabolische Umstrukturierungen charakterisiert. Diese betreffen unterschiedliche Matrixkomponenten, lokal begrenzt und abhängig von der Dosis der exogenen Noxe. Insbesondere in erheblich lichtgealterter Haut ist ein Verlust nicht nur von fibrillären Kollagenen (I und III) in der Dermis (El-Domyati *et al.*, 2002; Talwar *et al.*, 1995), sondern auch der Verlust von Kollagen VII-Ankerfibrillen an der *Dermal/Epidermal Junction* (DEJ) zu verzeichnen (Craven *et al.*, 1997). Im Gegensatz dazu ist der dermale

Gehalt an Glykosaminglykanen erhöht und umverteilt (Bernstein *et al.*, 1996a; Bernstein *et al.*, 1996b; Bernstein und Uitto, 1996).
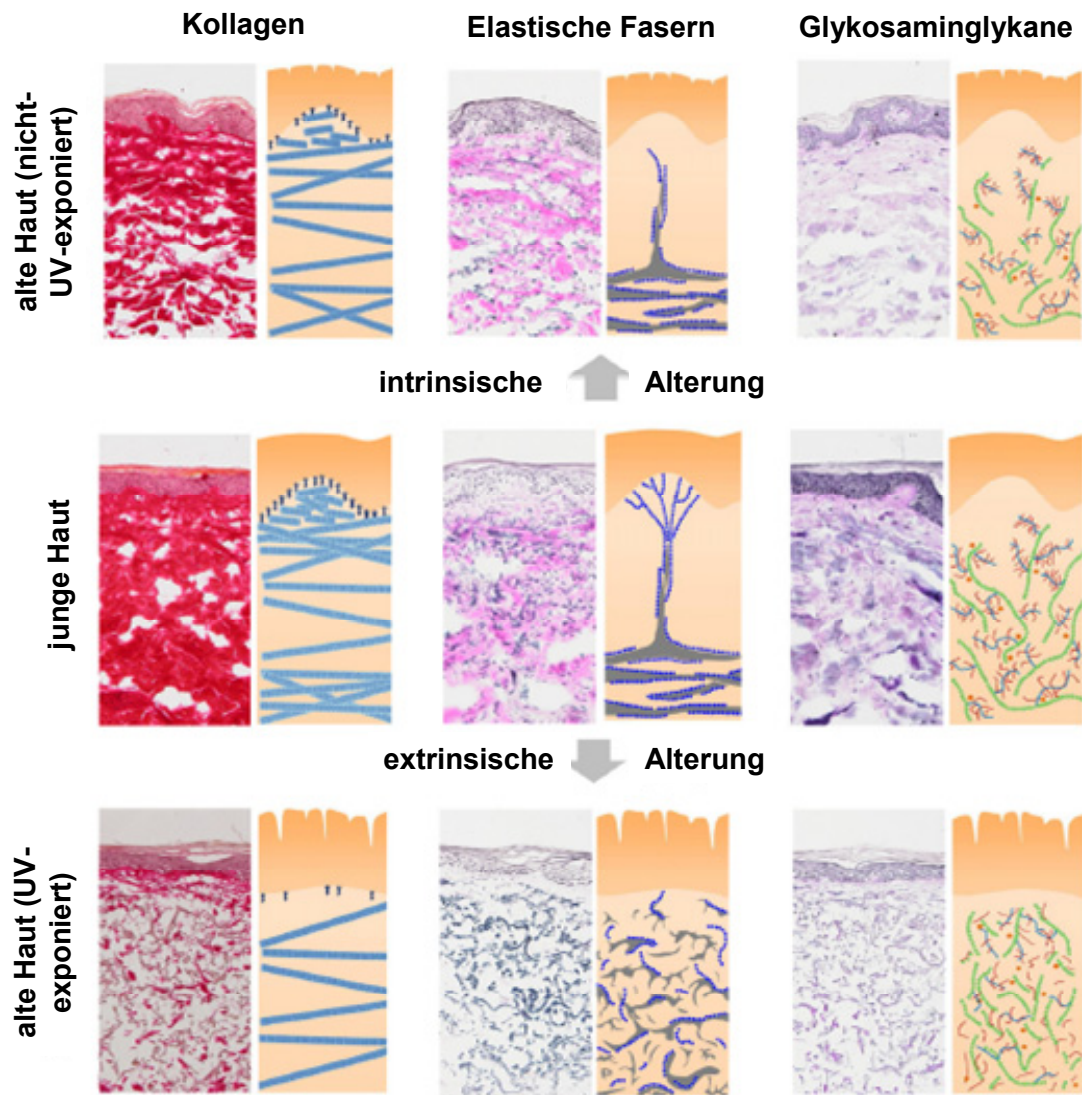
Abb. 1.3: ECM Modulation in intrinsisch und extrinsisch gealterter Haut. Dermales Kollagen, elastische Fasern und Glykosaminglykane (gefärbt mit Picrosirius Rot, Miller's Elastin und Periodsäure) durchlaufen signifikante, aber unterschiedliche Modulationen der ECM in UV-exponierter und nicht UV-exponierter Haut (jung: 23 Jahre, oberer Innenarm; alt nicht UV-exponiert: 75 Jahre, unterer Rücken; alt UV-exponiert: 75 Jahre, Unterarm) (entnommen aus Naylor *et al.*, 2011).

Das Netzwerk der elastischen Fasern ist in milder und akuter lichtgealterter Haut unterschiedlich verändert. Während der frühen Phase der Lichtalterung kommt es an der DEJ zu einem Verlust von Fibrillin-1 (Watson *et al.*, 1999) und -5 (Kadoya *et al.*, 2005). In

schwer lichtgealterter Haut jedoch ist die retikuläre Dermis von großen, desorganisierten Proteinen von elastischen Fasern durchzogen (Kadoya *et al.*, 2005; Mitchell, 1967; Bernstein *et al.*, 1994; Karonen *et al.*, 1997; Hunzelmann *et al.*, 2001). Daraus lässt sich schließen, dass Elemente des elastischen Fasersystems besonders empfänglich für altersbezogene Degradation sind, der zu Grunde liegende Mechanismus ist bis jetzt allerdings noch nicht vollständig charakterisiert (zusammengefasst in Naylor *et al.*, 2011).

1.1.2   Mechanismen der Hautalterung

Intrinsische Faktoren wie z.B. der Hormonspiegel im Blut können zur Hautalterung beitragen. So klagen insbesondere Frauen jenseits der Menopause oftmals über eine rasche Zunahme von Anzeichen der Hautalterung wie Faltenbildung und Verlust von Elastizität, die zumindest teilweise durch eine Hormonersatztherapie oder lokale Applikation von Östrogen aufgehoben werden können (Brincat, 2000a; Brincat, 2000b; Fuchs *et al.*, 2003; Sator *et al.*, 2001; Schmidt *et al.*, 1996; Affinito *et al.*, 1999).

Dem gegenüber stehen Mechanismen der extrinsischen Hautalterung. Ein wesentlicher Faktor sind DNS-Schäden, welche durch Umweltnoxen induziert werden (Lombard *et al.*, 2005). Dass DNS-Schäden eine wichtige Rolle in Alterungsprozessen spielen, wird durch eine starke positive Korrelation zwischen der DNS-Reparatur-Kapazität und der Lebensspanne, die in vielen Spezies zu beobachten ist, verdeutlicht (Hart und Setlow, 1974). In diesem Zusammenhang spielen Telomere eine große Rolle. Telomere sind kurze wiederkehrende DNS-Sequenzen (TTAGGG), die an den Enden der Chromosomen sitzen (Greider, 1996) und nicht der Kodierung von Genen, sondern dem Schutz der Chromosomenenden dienen. Fehlen sie, oder erreichen sie eine kritisch kurze Länge, kommt es zu Fusionschromosomen (Benn, 1976; Blackburn, 2001). Die letzten 100 – 200 Basen auf einem Chromosom werden bei der Zellteilung nicht repliziert, dieses führt nach etwa 60 Mitosen zu kritisch verkürzten Telomeren und die Zelle tritt in die proliferative Seneszenz ein (Harley *et al.*, 1990). Dieser Vorgang existiert nicht nur in instrinsischen Alternsprozessen, sondern kann durch extrinsische Faktoren verstärkt werden, so führt z.B. UV-Strahlung zu einer beschleunigten

Telomerverkürzung (Li *et al.*, 2003). Zudem konnte in humanen Zellen, in denen das für den Wiederaufbau der Telomere nach Mitose verantwortliche Enzym Telomerase ausgeschaltet wurde, eine erhöhte β-Galaktosidase-Aktivität im Vergleich zu Telomerase-profizienten Kontrollen gezeigt werden (Bodnar *et al.*, 1998). Bei diesem Enzym handelt es sich um einen Marker für zelluläre Seneszenz (Itahana *et al.*, 2007).

Mitochondrien wird ebenfalls eine wichtige Rolle in der extrinsischen Alterung zuge-schrieben. Diese Organellen sind der Ort der Atmungskette, die zur Bildung von ATP führt. Während des dafür nötigen Prozesses kommt es zur Freisetzung von Reaktiven Sauerstoffspezies (ROS), die wiederum zu Mutationen in der mitochondrialen (mt) DNS führen können. Während des Alterungsprozesses kommt es zu einer Akkumulation von mtDNS-Mutationen, begleitet von einem damit einhergehenden Funktionsverlust (Wallace, 1992). In lichtgealterter Haut finden sich vermehrt mtDNS Mutationen im Vergleich zu intrinsisch gealterter Haut (Berneburg *et al.*, 1997; Birch-Machin *et al.*, 1998; Yang *et al.*, 1995; Gilchrest BA und Krutmann J, 2006). Die häufigste Art der Veränderungen ist die *Common Deletion*, ein 4977-bp großes mtDNS-Fragment, das in lichtexponierter Haut ein und des selben Individuums etwa 10 Mal häufiger vorkommt als in nicht lichtexponierter Haut und keine Korrelationen zur intrinsischen Alterung der Donoren aufwies, weshalb die *Common Deletion* als Marker für lichtinduzierte Hautalterung gilt (Koch *et al.*, 2001). Induziert man die *Common Deletion* in humanen Fibroblasten, z.B. durch UVA-Strahlung, kommt es zu einer In-duktion der Matrixmetalloproteinase (MMP)-1, während die Expression der gewebe-spezifischen Inhibitoren der MMP (TIMP) unverändert bleibt (Berneburg *et al.*, 2006).

Viele physiologische und pathologische Prozesse wie Embryogenese, Wundheilung, Entzündung, Zellmigration, Tumorigenese, aber eben auch Hautalterung, machen einen Ab- bzw. Umbau des Kollagens erforderlich. Dieser erfolgt durch sogenannte Matrix-Metalloproteinasen (MMP). Diese meist kalziumabhängigen Metalloenzyme bestehen aus einem Propeptid, das bei der Aktivierung abgespalten wird, einer zinkbindenden katalytischen Einheit und einer C-terminalen Hemopexindomäne (Visse und Nagase, 2003). Insgesamt sind bisher 26 MMP bekannt, darunter MMP-1, -8, -13, -18 (Kollagenasen), MMP-2 und -9 (Gelatinasen), MMP-3, -10 und -11 (Stromelysine) und MMP-14 und -17 (membranständige MMP). Kollagenasen und Gelatinasen spalten Kollagene des Typs I – III und ermöglichen dadurch deren weiteren Abbau. Die

Induktion von MMPs erfolgt durch Wachstumsfaktoren, Zytokine (IL-1, TNF-α, PGDF, EGF) und mehreren Onkogene, während TGF-β, INF-γ und Kortikosteroide zur Herab-regulierung führen. Viele Zellen sind in der Lage MMPs zu produzieren, darunter Fibroblasten, Keratinozyten und Neutrophile. Pro-MMPs werden von den Zellen sekretiert und durch Abspaltung eines Propeptids in einem Mehrstufenprozess aktiviert. Die Aktivierung von MMPs wird durch spezifische Gewebeinhibitoren, die *tissue inhibitors of metalloproteinases* (TIMP) gehemmt (Fritsch, 2009). Von diesen Inhibitoren existieren vier Formen (TIMP-1, -2, -3 und -4), die in einem Eins-zu-eins-Gleichgewicht mit den MMPs stehen (Visse und Nagase, 2003). Die Regulation der Expression von MMP und TIMP erfolgt über mitogen-aktivierte-Proteinkinase (MAPK)-Signalwege und die Aktivierung von Transkriptionsfaktoren wie c-Jun, was wiederum zur Bildung und Aktivierung des Transkriptionsfaktor Aktivator-Protein (AP)-1 führt. AP-1 ist in der Lage, an entsprechende Promotorregionen zu binden und initiiert somit die Transkription der Gene (Schieke *et al.*, 2002).

Bereits vor ca. 10 Jahren konnte gezeigt werden, dass MMP-1 größtenteils für die durch UV-Strahlung verursachten Schäden der ECM in menschlicher Haut verantwortlich ist (Fisher und Voorhees, 1998; Brennan *et al.*, 2003), demnach ist die UV-induzierte vorzeitige Faltenbildung durch den von MMP-1 verursachten Kollagenabbau bedingt (Gilchrest BA und Krutmann J, 2006). Ein weiterer Hinweis auf den Einfluss von MMP-1 auf die Hautalterung war der Nachweis der Verknüpfung zwischen Kollagenfragmentation, oxidativem Stress und MMP-1-Induktion in gealterter Haut (Fisher *et al.*, 2009). Zudem korreliert der Faktor Rauchen mit der Induktion von MMP-1 in der Haut (Morita, 2007). Da sich im Zigarettenrauch polyzyklische aromatische Kohlenwasserstoffe (PAK) wie z.B. Benzo(a)pyren (B(a)P) befinden, ist eine Involvierung des Arylhydrocarbon-Rezeptor (AhR)-Signalwegs in diesen Prozess der extrinsischen Hautalterung denkbar. Dazu kommt eine kürzlich veröffentliche epidemiologische Studie, die eine Korrelation von Zeichen der Hautalterung mit der Exposition gegenüber Autoabgasen zeigt (Vierkotter *et al.*, 2010). Da die in Autoabgasen präsenten Nanopartikel mit PAKs wie z.B. B(a)P assoziiert sind, die als Ligand für den AhR fungieren, ist auch hier eine Involvierung des AhR-Signalwegs denkbar.

1.3   Die Rolle des Arylhydrocarbon-Rezeptors in der Haut

Die Haut ist einer Vielzahl an exogenen Noxen wie UV-Strahlung, Pharmazeutika und Umweltschadstoffen direkt ausgesetzt und stellt die Grenzfläche zwischen diesen äußeren Faktoren und dem Organismus dar. Aus diesem Grund ist es essentiell für die Homöostase des Organismus, dass Hautzellen auf diese extrinsischen Faktoren reagieren können (Merk *et al.*, 2006). Der Arylhydrocarbon-Rezeptor (AhR) als intrazellulärer Stresssensor spielt in dieser Hinsicht eine zentrale Rolle, wie in den folgenden Abschnitten verdeutlicht werden soll.

1.3.1   Der Arylhydrocarbon-Rezeptor

Der Aryhlhydrocarbon Rezeptor (AhR) ist ein evolutionsbiologisch hoch konserviertes Protein, welches sowohl in Einzellern, als auch in komplexeren Organismen wie Insekten, Mollusken, Fischen, Amphibien und Säugern exprimiert wird (Hahn, 2002). Der AhR ist einer der am besten charakterisierten und zudem toxikologisch bedeutsamsten nukleären Transkriptionsfaktoren. Er gehört zur Gruppe der basic Helix-Loop-Helix (bHLH)-PAS (Homologe von Per (*Drosophila period*)/ARNT (*Säuger Arylhydrocarbon Receptor Nuclear Translocator*)/Sim (*Drosophila single minded*)) Proteine, welche intrazelluläre Sensoren für Redoxpotential, Sauerstoff, Licht und Fremdstoffe darstellen (Taylor und Zhulin, 1999). Der AhR kodiert für ein Protein, das über einen Rückkopplungsmechanismus eine Transkriptionskontrolle übernimmt, in diesem Fall den AhR-Repressor (AhRR) (Mimura *et al.*, 1999; Haarmann-Stemmann *et al.*, 2007). In der großen Gruppe der bHLH-PAS-Proteinfamilie erfüllt der AhR bisher das Alleinstellungsmerkmal einer Ligandenbindungsstelle (Coumailleau *et al.*, 1995).

Im inaktiven Zustand ist der AhR als Multiproteinkomplex im Zytoplasma der Zelle lokalisiert. Bestandteil des Multiproteinkomplexes sind zwei Hitzeschockproteine (hsp90; Denis *et al.*, 1988), das AhR-interagierende-Protein (AIP; auch als ARA9 oder XYP bekannt; Ma and Whitlock, Jr., 1997), welches sowohl die Stabilisierung des Komplexes (Bell and Poland, 2000), als auch die zytosolische Lokalisation unterstützt (Kazlauskas *et al.*, 2000), und p23 (Kazlauskas *et al.*, 1999), das nach Ligandenbindung bei der Abspaltung von hsp90 vom Rezeptor assistiert. Des Weiteren ist die

Tyrosinkinase c-src mit den Chaperonen assoziiert, welche ebenfalls nach Aktivierung des Rezeptors durch einen Liganden abgespalten wird (Enan und Matsumura, 1996).
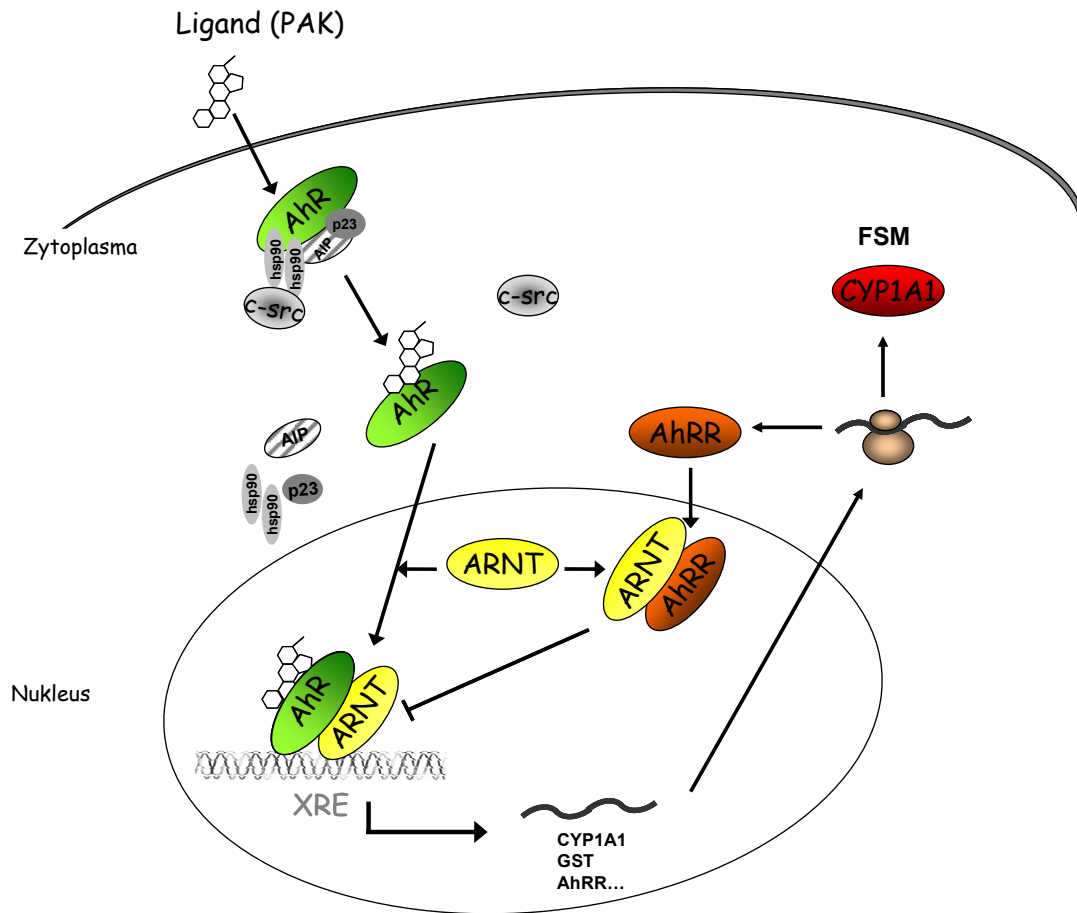
Abb.1.4: Die klassische Regulation der AhR-Signalkaskade: Die Aktivierung des AhR führt zu ARNT- und XRE-abhängiger transkiptioneller Aktivierung von AhR-Zielgenen, u.a. AhRR. Das AhRR Protein konkurriert mit dem AhR um den Dimerisierungspartner ARNT sowie um die Bindung an das XRE. AhRR/ARNT-Komplexe führen zur Inhibierung der Transkription XRE-abhängiger Gene; FSM = Fremdstoffmetabolismus (modifiziert nach Mimura *et al.*, 1999).

Nach Abdissoziation der Kochaperone transloziert der AhR in den Kern, wo er mit seinem Dimerisierungspartner A̲hR̲ *nuclear* t̲ranslocator (ARNT) heterodimerisiert und mit sogenannte X̲enobiotika-R̲esponsiven-E̲lementen (XRE) (5'-TGCGTG-3') in der Promoterregion von AhR-Zielgenen interagiert und zur Initiation der Transkription von mRNS dieser Gene führt (Rowlands und Gustafsson, 1997; Abel und Haarmann-Stemmann, 2010; Abb 1.4).

Auf Grund von transienter Überexpression von AhR, ARNT und AhRR *in vitro* wurde 1999 von Mimura *et al.* mit dem AhR-Repressor (AhRR) ein Protein identifiziert, das über eine Rückkopplungsschleife die Funktion des AhR hemmen kann. Der AhRR gehört selbst zu den AhR regulierten Genen und konkurriert mit dem AhR um den Dimerisierungspartner ARNT (Mimura *et al.*, 1999). Der AhRR/ARNT-Komplex konkurriert mit dem AhR/ARNT-Dimer um das XRE und reguliert somit die Transkription von AhR-Zielgenen (Mimura *et al.*, 1999; Gradin *et al.*, 1993).

Die Art der AhR-vermittelten Zellantwort ist dabei sowohl Liganden- als auch Zelltyp-abhängig (Shimada *et al.*, 2003; Yamamoto *et al.*, 2004; Dohr *et al.*, 1996; Li *et al.*, 1994). Zu den „klassischen" AhR-Liganden gehören polyzyklische aromatische Kohlenwasserstoffe (PAK, z.B. Benzo(a)pyren (B(a)P)) oder halogenierte aromatische Kohlenwasserstoffe (HAK, z.B. 2,3,7,8-Tretrachlorodibenzo-*p*-Dioxin (TCDD)) (Denison und Nagy, 2003), beide entstehen bei unvollständigen Verbrennungsprozessen. Zusätzlich gibt es die Gruppe der „nicht klassischen" Liganden. Zu diesen gehören in Obst und Gemüse enthaltene Polyphenole wie die Flavonoide Naringenin und Quercitin (Kim *et al.*, 2004; Amakura *et al.*, 2003; Ciolino *et al.*, 1999) und auch das in grünem Tee enthaltene Epigallocatechingallat (EGCG) (Williams *et al.*, 2000). In Abhängigkeit vom Zelltyp und der angewandten Konzentration können diese Substanzen den AhR aktivieren oder inhibieren (Zhang *et al.*, 2003). Schließlich gibt es auch physiologische Liganden des AhR. Zu diesen zählen vor allem Tryptophan-Photoprodukte, wie der hochaffine AhR-Ligand 6-formylindolo(3,2-*b*)carbazol (FICZ) und dessen Metabolite (ausführlich zusammengefasst in Rannug und Fritsche, 2006), die nach UV-Bestrahlung intrazellulär in der Haut entstehen können (Fritsche *et al.*, 2007).

Klassische Zielgene des AhR sind Fremdstoff metabolisierende Enzyme der Phase1 und 2 (Okey, 2007; Fujii-Kuriyama and Mimura, 2005; Nebert *et al.*, 2004). Untersuchungen an AhR-KO-Mäusen veranschaulichen die Bedeutung des AhR bei der Vermittlung der toxischen Wirkungen von HAK (z.B. TCDD) und PAK (z.B. B(a)P). Diese Tiere sind resistent gegenüber den akuten und chronischen Wirkungen von TCDD wie Enzyminduktion (Fernandez-Salguero *et al.*, 1997), Thymusatrophie (Fernandez-Salguero *et al.*, 1995), Leberhypertrophie (Fernandez-Salguero *et al.*, 1997)

(Schmidt *et al.*, 1996b), Teratogenität (Abbott *et al.*, 1999), und auch gegen PAK-
induzierte Hauttumoren (Shimizu *et al.*, 2000).

1.3.2   Die Bedeutung des Arylhydrocarbon-Rezeptor-Signalwegs in der Haut

Die Haut ist einer Vielzahl an exogenen Noxen wie UV-Strahlung, Pharmazeutika und
Umweltschadstoffen direkt ausgesetzt und stellt die Grenzfläche zwischen diesen
äußeren Faktoren und dem Organismus dar. Aus diesem Grund ist es essentiell für die
Homöostase des Organismus, dass Hautzellen auf diese extrinsischen Faktoren
reagieren können (Merk *et al.*, 2006).
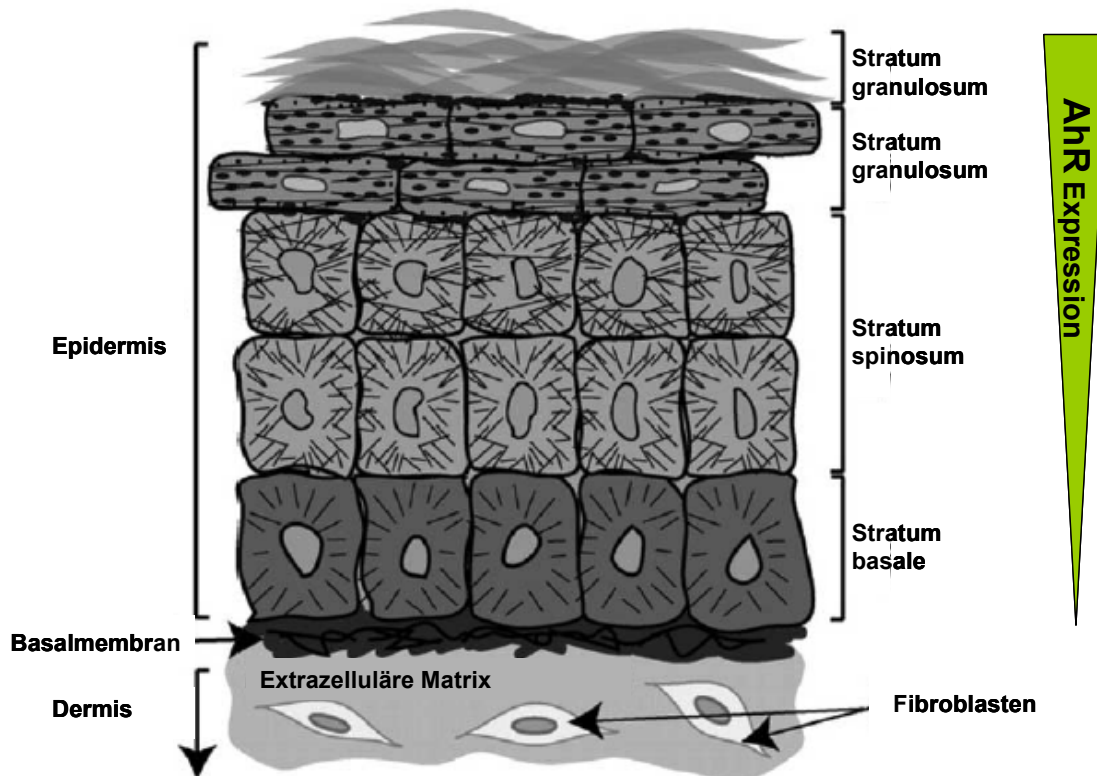
Abb. 1.5: Die zelluläre Architektur der Haut: Die Epidermis ist aus proliferierenden und sich nach
apikal differenzierenden Keratinozyten zusammengesetzt. Die Dermis setzt sich aus
Fibroblasten zusammen, die in einer extrazellulären Matrix eingebunden sind (modifiziert nach
Swanson, 2004).

Die Epidermis stellt dabei die vorderste Barriere dar, demnach ist der Hauptanteil an der
zellulären Abwehr in den Keratinozyten, die mit über 90 % die größte Zellpopulation in

der Epidermis sind (Fritsch, 2009), lokalisiert. Dass der AhR bei dieser Schutzfunktion eine entscheidende Rolle spielt, zeigt sich auch daran, dass seine Expression in der Epidermis von basal nach apikal zunimmt (Swanson, 2004; Abb. 1.5).

Epidermale Keratinozyten exprimieren sowohl Enzyme der Phase 1 (CYP1A1, 1B1, 2A6, 2B6, 2D6, 2E1, 3A4 und 3A5; Du 2006, Swanson 2004), als auch der Phase 2 (NQO1, NAT, GST; Kawakubo and Ohkido, 1998; Afaq and Mukhtar, 2001; Radjendirane V *et al.*, 1997), um die schnelle Metabolisierung von Fremdstoffen zu gewährleisten (Details in Abschnitt 1.3.3 und 1.3.4).

Obwohl der AhR in Keratinozyten eine essentielle Komponente des Fremdstoffmetabolismus darstellt, ist dies in dermalen Fibroblasten nicht der Fall. In diesen Zellen ist der Rezeptor zwar exprimiert, es ist jedoch schon seit den 90er Jahren bekannt, dass weder CYP1A1 noch CYP1B1 in Fibroblasten induziert werden können (Gradin *et al.*, 1993; Gradin *et al.*, 1999). Der zugrunde liegende Mechanismus dieses Phänomens ist bis heute nicht eindeutig aufgeklärt, es wurde jedoch die hohe Expression des AhRR in diesen Zellen als möglicher Grund postuliert (Gradin *et al.*, 1993; Mimura *et al.*, 1999). Da Fibroblasten gegenüber Keratinozyten eine deutlich verringerte Regenerationsfähigkeit haben, sind sie anfälliger für eine Akkumulation von geschädigten Makromolekülen und Organellen (wie z.B. Mitochondrien). Daher könnte die Reprimierung des AhR Signalweges in der Dermis als Schutz gegenüber oxidativem Stress dienen, der bei der Aktivierung von CYP-Monooxygenasen entsteht.

Bereits in den 1980er Jahren wurde im Nager beobachtet, dass eine UV Bestrahlung der Haut zur Induktion der AhR-abhängigen CYP1-Aktivität in verschiedenen Organen führt (Goerz *et al.*, 1983; Mukhtar *et al.*, 1986; Paigen *et al.*, 1981). Die Arbeitsgruppe von Katiyar konnte diese Beobachtung 2000 auch für menschliche Haut *in vivo* bestätigen, die mit UVB (289 – 320 nm) bestrahlt wurde (Katiyar *et al.*, 2000). Weitere *in vitro* Untersuchungen untermauern diese Befunde. So führt die UV-Bestrahlung von HaCaT-Keratinozyten zur Induktion der CYP1A1 mRNS und auch AhR-defiziente Leberzellen zeigten eine AhR-abhängige UV-Antwort (Wei *et al.*, 1999). Aus diesen Beobachtungen ergab sich die Frage, ob der AhR auch an der Antwort der Haut auf UV-Strahlung beteiligt ist. Die Beobachtung, dass die CYP1A1-Induktion durch Zugabe des Chromophors Tryptophan vor der Bestrahlung noch verstärkt wurde (Wei *et*

al., 1999) war ein Hinweis auf die Entstehung von Tryptophanphotoprodukten, die als AhR-Liganden fungieren können. Die Arbeitsgruppe um Rannug zeigte *ex vivo*, dass tatsächlich nach UV-Bestrahlung einer wässrigen Tryptophanlösung Photoprodukte entstehen, die an den AhR binden. Dabei wurden 6-formylindolo(3,2-*b*)carbazol (FICZ; Abb. 1.6) und 6,12-diformylindolo(3,2-*b*)carbazol (dFICZ) als die Produkte mit der höchsten AhR-Affinität identifiziert (Rannug *et al.*, 1987; Rannug *et al.*, 1995).
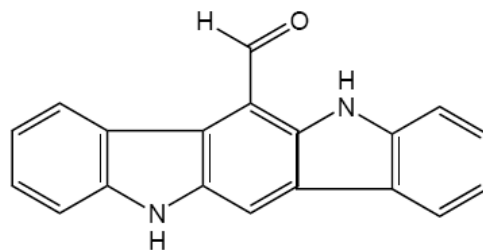
Abb. 1.6 6-formylindolo(3,2-*b*)carbazol: Strukturformel des durch UVB-Bestrahlung entstandenen Tryptophan-Dimers 6-formylindolo(3,2-*b*)carbazol (FICZ).

Erst kürzlich wurde in HaCaT-Keratinozyten die intrazelluläre Formierung des AhR-Liganden FICZ (bestehend aus einem Tryptophan Dimer) nachgewiesen (Fritsche *et al.*, 2007). Die Bindung von FICZ an den AhR führt zur Aktivierung des Rezeptors und somit zur Abspaltung der Kochaperone, darunter c-src. Der aktivierte AhR transloziert in den Nukleus, wo er mit ARNT dimerisiert und zur Transkription von AhR-Zielgenen wie z.B. CYP1A1 führt (zusammengefasst in Abel und Haarmann-Stemmann, 2010). Durch einen bislang noch unbekannten Mechanismus (in Abb. 1.7 durch gestrichelte Linie angedeutet) führt c-src zur Aktivierung und Internalisierung des *Epidermal Growth Factor Receptor* (EGFR) (Enan und Matsumura, 1996; Kohle *et al.*, 1999), was in einer Aktivierung des ERK1/2 Signalwegs mit erhöhter COX-2 Expression und Aktivität resultiert (Fritsche *et al.*, 2007; Agostinis *et al.*, 2007).

Da die Exposition der Haut gegenüber UVB-Strahlung sowohl zur Entstehung von Tumoren beiträgt (Situm *et al.*, 2008; Narayanan *et al.*, 2010), als auch eine Ursache für vorzeitige Hautalterung (Gilchrest BA und Krutmann J, 2006) und Immunsuppression (Schwarz, 2002) ist, kommt dem AhR nun eine wichtige Rolle in der Präventivmedizin zu. Dass der AhR an der Hauttumorigenese beteiligt ist, zeigen *in vivo* Arbeiten an

AhR-defizienten Mäusen, die gegen PAK-induzierte Hauttumoren geschützt sind (Shimizu *et al.*, 2000). Vorzeitige Hautalterung geht ebenfalls mit der Aktivierung der AhR-Signalkaskade einher. So ist z.B. bei Rauchern eine beschleunigte Alterung der Haut zu beobachten (Leung und Harvey, 2002).
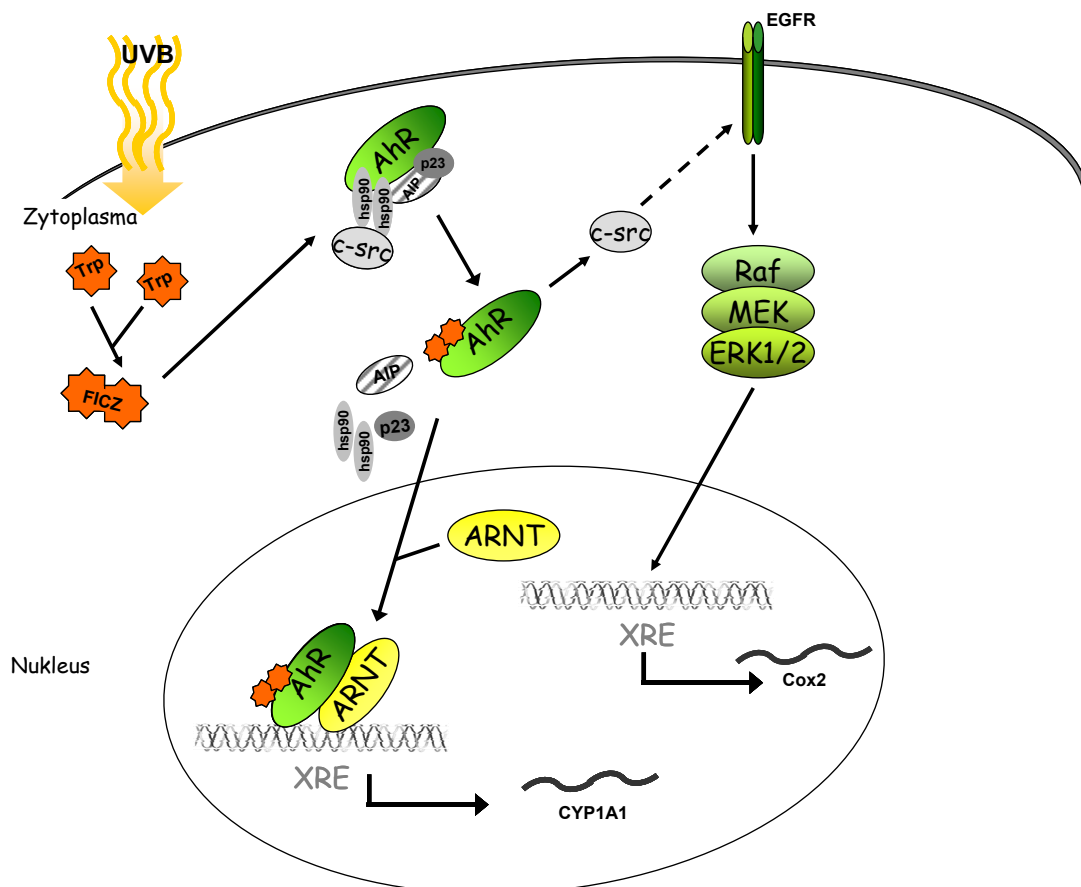
Abb.1.7: AhR Signaltransduktion in humanen Keratinozyten nach UVB-Bestrahlung. In unbehandelten Zellen liegt der AhR als inaktiver Multiproteinkomplex im Zytosol vor. UVB-Absorption durch Tryptophan (Trp) führt zur intrazellulären Bildung des AhR-Liganden FICZ, welches den AhR aktiviert und u. a. c-src abspaltet. Der aktive AhR transloziert in den Nukleus, wo er mit ARNT heterodimerisiert und die Transkription von CYP1A1 einleitet. Über einen bisher unbekannten Mechanismus (gestrichelte Linie) bewirkt c-src die Internalisierung des aktivierten EGFR und aktiviert so die ERK1/2-Signalkaskade mit erhöhter COX-2 Expression und Aktivität. (adaptiert nach Agostinis *et al.*, 2007)

Zudem wurde in nicht sonnenexponierter Haut von Rauchern eine induzierte Expression von MMP-1 nachgewiesen (Lahmann *et al.*, 2001). Für diesen Effekt sind möglicherweise die im Zigarettenrauch enthaltenen PAK (wie z.B. B(a)P) verantwortlich. Arbeiten von Murphy, in denen TCDD-Belastung von Keratinozyten auf mRNS-Ebene

zu einer Induktion von MMP-1 führt, untermauern diese Hypothese (Murphy *et al.*, 2004). Des Weiteren zeigen sowohl AhR- als auch ARNT-defiziente Mäuse einen typischen Hautalterungsphänotyp mit Hyperplasien, Hyperkeratosen und gestörter epidermaler Barrierefunktion (Fernandez-Salguero *et al.*, 1997; Takagi *et al.*, 2003).

1.3.3   Fremdstoffmetabolismus der Phase I in der Haut

Eine wichtige Funktion des AhR liegt in der Regulation des Fremdstoffmetabolismus (FSM). Durch Aktivierung des AhR nach Ligandenbindung werden AhR-abhängige Gene exprimiert, die für Enzyme des Phase 1 FSM kodieren (Bock und Kohle, 2006). Dazu gehören die Cytochrom (CYP) P450-Monooxygenasen CYP1A1, 1B1, 1A2, 2S1 (Ramadoss *et al.*, 2005). Diese Enzyme katalysieren Reaktionen, die funktionelle Gruppen in lipophile Chemikalien (wie z.B. B(a)P) einführen, deren Hydrophilie dann nachfolgend durch Enzyme der Phase 2 (siehe Abschnitt 1.2.4 für Details) erhöht wird, um die biliäre oder renale Elimination zu ermöglichen (Wätjen W und Fritsche F, 2010). Lange Zeit wurde angenommen, dass die Haut von Säugetieren keinen nennenswerten Fremdstoffmetabolismus aufweist. Inzwischen gibt es jedoch viele Arbeiten, die zeigen, dass die meisten Enzyme des Fremdstoffmetabolismus in der Haut exprimiert werden, wenn auch zum Teil mit niedrigen Aktivitäten (für eine ausführliche Zusammenfassung siehe Oesch *et al.*, 2007). In gesunder unbehandelter menschlicher Haut sind die meisten CYPs in der Epidermis und den Schweißdrüsen lokalisiert, was für CYP1A1 und 1B1 Protein (Katiyar *et al.*, 2000) und CYP2A6, 2B6 und 3A4 mRNS (Janmohamed *et al.*, 2001) gezeigt werden konnte. Da es sich bei der Haut um ein aus verschiedenen Zelltypen aufgebautes Organ handelt, ist es nicht überraschend, dass nicht alle Zelltypen die gleiche Verteilung in der CYP-Expression aufweisen. Eine vergleichende Studie in Keratinozyten, Melanozyten, Langerhanszellen und Fibroblasten von sechs verschiedenen Individuen konnte zeigen, dass CYP mRNS für CYP1A1, 1B1 und 2E1 in allen vier Zelltypen auf transkriptioneller Ebene vorhanden ist (Saeki *et al.*, 2002). Keratinozyten exprimierten des Weiteren CYP1A1, 1B1, 2E1 und 3A5 in allen Individuen, CYP2C6 in 5 Individuen und 4B1 in 3 Individuen. In Melanozyten wurde mRNS für CYP1A1, 1B1, 2A6 und 2E1 nachgewiesen, in Langerhanszellen waren es CYP1A1, 1B1, 1E1 und 3A4 in allen untersuchten Zellen, sowie 3A7 in drei der unter-

suchten Individuen. Auch Fibroblasten exprimierten die Gene für CYP1A1, 1B1, 2D6, 2E1 und 3A7 in allen Individuen, CYP3A5 in fünf, 2C in vier und 2A6 in zwei Individuen (Saeki *et al.*, 2002). Eine aktuelle Studie von Du *et al.* wies weiterhin in Keratinozyten eine Änderung im Expressionsmuster von CYP-Genen mit zunehmendem Differenzierungsgrad nach (Du L *et al.*, 2006). So wurden in Keratinozyten, die sich im Differenzierungsstadium des *Stratum spinosum* befanden, CYP1A1, 1A2, 1B1, 2C9, 2C18, 2C19, 2D6, 2E1, 2J2, 2S1, 2U1, 2W1, 3A4 und 4B1 exprimiert. Davon wurden CYP2C9, 3C18, 2C19, 2W1, 3A4 und 4B1 mit zunehmender Differenzierung aufreguliert.

Viele Chemikalien, denen die menschliche Haut ausgesetzt ist, darunter auch Kosmetikprodukte, Allergene, Toxine und Karzinogene, sind Substrate der CYP P450-Monooxygenase Familie (Ahmad *et al.*, 1996). Ähnliches gilt für Therapeutika wie z.B. die endogenen CYP-Substrate Vitamin A (Pavez *et al.*, 2009) und D (Omdahl *et al.*, 2003), die in der Dermatologie eingesetzt werden (Ahmad und Mukhtar, 2004). Durch Enzyme des Fremdstoffmetabolismus in der Haut werden topisch applizierte dermatologische Therapeutika sowie Xenobiotika, denen die Haut ausgesetzt ist, entweder ent- oder gegiftet, wodurch es zu dermatologisch relevanten Pathologien kommen kann (Wätjen W und Fritsche F, 2010). Bereits in den 1970er und 1980er Jahren wurde nachgewiesen, dass humane Haut CYP-abhängige mikrosomale Enzymaktivität gegenüber PAKs besitzt, die durch eben diese induzierbar ist (Alvares *et al.*, 1973; Bickers *et al.*, 1984; Levin *et al.*, 1972). Viele CYPs, die auch in der Leber eine wichtige Rolle im Fremdstoffmetabolismus spielen, konnten auch in der Haut identifiziert werden, allerdings in wesentlich geringeren Mengen. Dazu gehören CYPs, die hauptsächlich Prokarzinogene metabolisieren (CYP1A1, 1A2, 1B1, 2A6, 2B6, 2E1 und 3A4) und CYPs die bei der Metabolisierung vieler Pharmaka eine Rolle (Ahmad und Mukhtar, 2004; Baron *et al.*, 2001; Janmohamed *et al.*, 2001; Vondracek *et al.*, 2001; Yengi *et al.*, 2003; Ahmad *et al.*, 1996). Des Weiteren wurde für CYP kodierende mRNS in *ex vivo* humaner Haut (Yengi *et al.*, 2003; Janmohamed *et al.*, 2001; Vondracek *et al.*, 2001) und in humanen Keratinozytenkulturen (Baron *et al.*, 2001) identifiziert: CYP1A1, 1A2, 1B1, 2A6/7, 2B6/7, 2C9, 2C18, 2C19, 2D6, 2E1, 2S1, 3A4/7 und 3A5. Zusammenfassend werden mindestens 19 Gene der CYP 1-3 Familie in der Haut exprimiert, die hauptsächlich für fremdstoffmetabolisierende CYPs kodieren (CYP1A1,

1A2, 1B1, 2A6, 2A7, 2B6, 2C9, 2C18, 2C19, 2D6, 2E1, 2J2, 2R1, 2S1, 2U1, 2W1, 3A4, 3A5, 3A7) (zusammengefasst in Oesch *et al.*, 2007).

Neben der großen Gruppe der CYP P450-Monooxigenasen werden auch Cyclooxygenasen (COX) in der menschlichen Haut exprimiert, die ebenfalls eine wichtige Rolle im Fremdstoffmetabolismus einnehmen (Oesch F und Arand M, 1999). Die Verteilung der unterschiedlichen COX-Isoformen in der Epidermis ist unterschiedlich. So wird COX-1 in der gesamten Epidermis exprimiert, während COX-2 (beteiligt an der zellulären Antwort auf Entzündungsstimuli; Lee *et al.*, 2003) hauptsächlich in den Keratinozyten der Basallamina zu finden ist (Buckman *et al.*, 1998; Leong *et al.*, 1996).

Weitere Enzyme der Phase 1, die in der menschlichen Haut exprimiert werden, sind die Flavin-abhängige Monooxygenase (FMO), die Alkoholdehydrogenase, die Aldehyddehydrogenase, Esterasen / Amidasen sowie Epoxidhydrolasen (EH) (Oesch *et al.*, 2007). Im Vergleich zur Leber liegen die spezifischen Enzymaktivitäten in der Haut bei unter 10 % (Smith C.K. und Hotchkiss S.A.M., 2001).

1.3.4   Fremdstoffmetabolismus der Phase II in der Haut

Zu den AhR-abhängigen fremdstoffmetabolisierenden Enzymen der Phase 2, die in der Haut exprimiert werden, gehören die Glutathion S-Transferase A (GST-A), die UDP-Glukuronosyltransferase (UGT) und NADPH Chinonoxidoreduktasen (Ramadoss *et al.*, 2005). Die Enzyme der Phase 2 erhöhen die Hydrophilie von lipophilen Chemikalien, in die bereits in Phase 1 funktionelle Gruppen eingeführt wurden, um die biliäre oder renale Elimination zu ermöglichen (Wätjen W und Fritsche F, 2010).

GSTs sind an der Entgiftung von vielen Chemikalien, vor allem elektrophilen Substanzen, beteiligt (Eaton und Bammler, 1999). Die am meisten verbreiteten Formen sind die im Zytosol lokalisierten löslichen GST-A, -M, -T und -P, die sowohl Homo- als auch Heterodimere formen können (Hayes und Strange, 2000). In humaner Haut wurde GST-Aktivität im Zytosol bereits in den 1990er Jahren beschrieben, wobei GST-P als die dominante Isoform in der Epidermis identifiziert wurde (Raza *et al.*, 1991).

Bei der Glucuronidierung werden Glucuronsäurekonjugate an funktionelle Gruppen eines Fremdstoffes angehängt, um dessen Wasserlöslichkeit zu erhöhen (Tukey und Strassburg, 2000). Dieser Metabolismusweg spielt eine wichtige Rolle im Schutz der Zelle (Grancharov *et al.*, 2001). Die Reaktion wird durch das Enzym UGT katalysiert und benötigt UDP-Glucuronsäure als Kofaktor, welcher in Fibroblastenkulturen aus humaner embryonaler Haut gefunden wurde (Sarnstrand *et al.*, 1987). Es gibt nur wenige Daten zu diesem Enzym in der Haut, allerdings belegen die Bildung von Indolylessigsäure Glucoroniden und Triclosan Glucuroniden, dass in der Haut UGT Aktivität vorhanden ist (Ademola *et al.*, 1993; Moss *et al.*, 2000). Des Weiteren ist berichtet worden, dass 3-Methylcolanthren (3-MC) in der Haut und in Hautzellen von verschiedenen Spezies die UGT auf mRNS-Ebene induziert (zusammengefasst in Oesch *et al.*, 2007).

Ein weiteres Phase 2 Enzym, das in humaner Haut hohe Aktivitäten aufweist, ist die zytosolische N-Acetyltransferase (NAT), die vor allem zur direkten Entgiftung von aromatischen Aminen, wie sie z.B. in oxidativen Haarfärbemitteln vorkommen, beiträgt (Kawakubo *et al.*, 2000; Nohynek *et al.*, 2005), wodurch es in der Haut zu einem „First Pass"-Metabolismus kommt (Goebel *et al.*, 2009). Die NAT-1 ist dabei die Isoform des Enzyms, die sich in den Keratinozyten der Haut wiederfinden lässt (Minchin *et al.*, 2007; Kawakubo *et al.*, 2000).

Des Weiteren finden sich Sulfotransferasen (SULT) in humaner Haut, von denen gezeigt werden konnte, dass sie viele Substanzen wie z.B. Triclosan nach topischer Applikation *in vitro* und *in vivo* sulfatieren (Moss *et al.*, 2000). Diese Klasse der Phase 2 fremdstoffmetabolisierenden Enzyme ist essentiell bei der Metabolisierung des endogenen AhR-Liganden FICZ. Dieser wird in erster Instanz durch die Phase 1 Enzyme CYP1A1, 1A2 und 1B1 funktionalisiert und letztendlich durch SULT 1A1, 1A2, 1B1 und 1E1 konjugiert (Bergander *et al.*, 2004; Wincent *et al.*, 2009). Sulfatierte Konjugate von FICZ-Metaboliten wurden in humanem Urin nachgewiesen (Wincent *et al.*, 2009).

Allgemein liegen, ähnlich wie bei den Phase 1 Enzymen des Fremdstoffmetabolismus, die spezifischen Aktivitäten dieser Enzyme in der Haut bei unter 10 %, vergleicht man sie mit den entsprechenden Enzymen in der Leber (Smith C.K. und Hotchkiss S.A.M., 2001).

1.4   Ziel der Dissertation

Die Haut reagiert auf exogene Noxen wie UV-Strahlung oder PAK mit vorzeitiger Organalterung. Zur Entwicklung präventiver Strategien ist das tiefgreifende Verständnis der diesen Prozessen zugrunde liegenden Mechanismen von außerordentlicher Bedeutung.

Innerhalb dieses übergeordneten Ziels wurde im Rahmen der vorliegenden Dissertation Folgendes untersucht:

I.   Die fremdstoffmetabolisierende Kapazität im Bezug auf Enzyme der Phase 1 und 2 von humaner Haut im Vergleich zu zwei- und dreidimensionalen (2D/3D) *in vitro* Zellmodellen.

II. Untersuchung der funktionellen Rolle des AhRR in der fehlenden Induzierbarkeit von primären humanen Fibroblasten durch AhR-Liganden.

III. Die Rolle der AhR-Signalkaskade in der extrinsischen Hautalterung.

IV. Die Rolle von Östrogen in der lichtinduzierten vorzeitigen Hautalterung.

2   Manuskripte

Im Folgenden sind die Publikationen als Erst- und Koautor angefügt. Bei den ersten drei Publikationen (2. 1 – 2. 3) handelt es sich um Untersuchungen zum Fremdstoffmetabolismus der Phase 1 und 2. Insbesondere liegt das Augenmerk auf dem Vergleich zwischen humaner *ex vivo* Haut und verschiedenen Keratinozyten-basierten *in vitro* Alternativmodellen, da es im Bezug auf zukünftige dermatotoxikologische und kosmetische Studien essentiell ist, deren metabolische Kapazität zu charakterisieren. Da viele fremdstoffmetabolisierende Enzyme über den AhR reguliert werden und der AhR in der Homöostase der Haut von Bedeutung ist, beschäftigen sich die folgenden beiden Publikation mit der AhR-Signalkaskade in verschiedenen Hautzellen. In Publikation 2. 4: „AhRR function revisited: Investigations in adult primary human fibroblasts" wird diskutiert, dass der nicht funktionelle AhR-Signalweg in humanen Fibroblasten, entgegen der landläufigen Literaturmeinung, nicht durch eine hohe AhRR-Expression, sondern durch einen bisher unbekannten Faktor verursacht wird. Dahingegen wird in der darauf folgenden Publikation „The Arylhydrocarbon Receptor (AhR) in keratinocytes is a universal sensor for environmental stress that mediates skin aging" (2. 5) eben dieses Molekül in den metabolisch kompetenten Keratinozyten der Epidermis als gemeinsamer Nenner PAK- und UVB-vermittelter extrinsischer Hautalterung diskutiert, indem er die MMP-1-Expression induziert. Die letzte Publikation „Estradiol protects dermal hyaluronan / Versican matrix during photoaging by release of EGF from keratinocytes" (2. 6) greift das Thema der extrinsischen Hautalterung auf. Hierin wird deutlich, dass der protektive Effekt des Östrogens auf die extrazelluläre Matrix durch Keratinozyten vermittelt wird, die durch EGF parakrin die Synthese von Hyaluronsäure und Versikan in den Fibroblasten der Dermis vermitteln.

2.1   Publikation 1

Xenobiotic metabolism capacities of human skin in comparison to 3D-epidermis models and keratinocyte-based cell culture as *in vitro* alternatives for chemical testing: Phase I

Obwohl die Haut ein wichtiges Organ für die Absorption und die Metabolisierung von Chemikalien, Kosmetika und Pharmazeutika darstellt, ist ihre metabolische Kompetenz bis jetzt noch nicht ausreichend charakterisiert. Da die siebte Änderung der EG-Kosmetik-Richtlinie (76/768/EWG) seit 2009 den Gebrauch von *in vivo* Modellen zur Testung von Kosmetika für einige Endpunkte wie z.B. Genotoxizität verbietet, gibt es dringenden Bedarf die fremdstoffmetabolische Kapazität der *in vitro* Alternativmethoden mit der der menschlichen Haut zu vergleichen. In dieser Publikation wurden Phase 1 Enzymaktivitäten von Cytochrom P450 (CYP) und Cyclooxygenase (COX) in *ex vivo* humaner Haut, dem 3D-Epidermis-Model Epi-Derm™ (EPI-200), immortalisierten Keratinozytenzelllinien (HaCaT und NCTC 2455) und primären normalen humanen epidermalen Keratinozyten (NHEK) gemessen und verglichen. Die basalen CYP-Enzymaktivitäten in Keratinozyten, EPI-200 und humaner Haut waren sehr gering. Zudem unterschieden sich die Aktivitäten aller untersuchten *Monolayer* Zellen von denen der 3D-Äquivalente nach Induktion durch 3-Methylcolanthren (3-MC). Die basale COX-Aktivität hingegen war in *ex vivo* Haut und EPI-200 vergleichbar, variierte aber stark in den untersuchten 2D-Zellkulturmodellen, wobei die Aktivität in den immortalisierten Zelllinien HaCaT und NCTC deutlich geringer war, als in den auf Primärzellen basierenden Modellsystemen NHEK und EPI-200. Signifikante Induktion nach 3-MC Behandlung wurde nur in EPI-200 Modellen beobachtet. Zusammengefasst sind die basalen CYP-Aktivitäten im Vergleich zu den beträchtlichen COX-Aktivitäten in rekonstruierter Epidermis (EPI-200) und Mikrosomen humaner Haut sehr gering. Daraus ergibt die Schlussfolgerung, dass 3D-Kulturen wie EPI-200 ein passenderes Model für dermatotoxikologische Studien darstellen könnten als *Monolayer*-Zellkulturen, da sie der *in vivo* Kompetenz der Phase 1 Enzymaktivität in humaner Haut am nächsten kommen. Zusammengefasst helfen diese Daten, den Metabolismus in der Haut besser zu verstehen und das Wissen von *in vitro* Alternativsystemen für die dermatotoxikologische Testung zu verbessern.

XENOBIOTIC METABOLISM CAPACITIES OF HUMAN SKIN IN COMPARISON TO A 3D-EPIDERMIS MODEL AND KERATINOCYTE-BASED CELL CULTURE AS IN VITRO ALTERNATIVES FOR CHEMICAL TESTING: PHASE I

XENOBIOTIC METABOLISM CAPACITIES OF HUMAN SKIN IN COMPARISON TO A 3D-EPIDERMIS

MODEL AND KERATINOCYTE-BASED CELL CULTURE AS IN VITRO ALTERNATIVES FOR CHEMICAL

TESTING: PHASE I

Christine Götz[1], Roland Pfeiffer[1], Julia Tigges[1], Veronika Blatz[2], Christine Jäckh[2], Eva-Maria Freytag[1],

Eric Fabian[2], Robert Landsiedel[2], Hans F Merk[3], Jean Krutmann[1], Robert J Edwards[4], Camilla Pease[5],

Carsten Goebel[6], Nicola Hewitt[7] and Ellen Fritsche[1,3]

[1] Institut für Umweltmedizinische Forschung (IUF), Heinrich-Heine-University Düsseldorf, Germany

[2] BASF SE, Experimental Toxicology and Ecology, Ludwigshafen, Germany

[3] Department of Dermatology and Allergology, University Clinic RWTH Aachen, Germany

[4] Imperial College London, Hammersmith Campus, London UK

[5] Unilever, Safety & Environmental Assurance Centre, Sharnbrook, Bedford, UK

[6] Procter and Gamble, Darmstadt, Germany

[7] Nicky Hewitt Scientific Writing Services, Erzhausen, Germany

Corresponding author: ellen.fritsche@uni-duesseldorf.de

Running title: Phase I xenobiotic metabolism in human skin and in vitro skin models

Words: 3998

Figures: 4

Supplements

Supplemental Figures: 1

Supplemental Tables: 2

2

ABSTRACT:

Skin is important for the absorption and metabolism of exposed chemicals such as cosmetics or pharmaceuticals. The 7th Amendment to the EU Cosmetics Directive prohibits the use of animals for cosmetic testing for certain endpoints, such as genotoxicity; therefore, there is an urgent need to understand the xenobiotic metabolising capacities of human skin and to compare these activities with reconstructed 3D skin models developed to replace animal testing. We have measured phase I enzyme activities of cytochrome P450 (CYP) and cyclooxygenase (COX) in ex vivo human skin, the 3D skin model EpiDerm™ (EPI-200), immortalized keratinocyte-based cell lines and primary normal human epidermal keratinocytes. Our data demonstrate that basal CYP enzyme activities are very low in whole human skin and EPI-200 as well as keratinocytes. In addition, activities in monolayer cells differed from organotypic tissues after induction. COX activity was similar in skin, EPI-200 and NHEK cells, but was significantly lower in immortalized keratinocytes. Hence, the 3D model EPI-200 might represent a more suitable model for dermatotoxicological studies. Altogether, these data help to better understand skin metabolism and expand the knowledge of in vitro alternatives used for dermatotoxicity testing.

Keywords: skin; xenobiotic metabolism; cytochrome P450-monooxygenase; cyclooxygenase

Abbreviations: CYP=cytochrome P450-monooxygenase; COX=cyclooxygenase; PGE$_2$=prostaglandin E2; 3-MC=3-methylcholanthrene; EPI-200=reconstituted epidermis model EpiDerm™ (MatTek); NHEK=normal human keratinocytes; HLM=human liver microsomes

3

INTRODUCTION

Skin is the largest organ and represents the body's protective surface as the first and outermost contact site for topically applied substances. Beside the skin's important tasks in preventing mechanical and physical harm its potential to detoxify chemicals often remains unconsidered. However, skin plays a key role in not only controlling the penetration and distribution but also the metabolism of topically applied chemicals (1) and is thus a first-pass organ for penetrating substances. Numerous examples exist showing that skin metabolism is not only protective but also contributes to skin pathologies such as contact dermatitis or carcinogenesis (2;3). This implies a need for safety assessment for all ingredients of cosmetic products and the need to employ appropriate models to test chemical ingredients for their potential to cause skin irritation, sensitization, as well as genotoxic damage.

Animal testing was the method of choice for dermatotoxicological testing for decades. Decreasing acceptance of animal use in cosmetic testing in the public, arising from ethical concerns, forces the revision of traditional procedures and the establishment of alternative methods. In addition, animal testing for cosmetics was prohibited by the 7th Amendment to the EU Cosmetics Directive including skin irritation and genotoxicity. The need for adequate substituting test models is evident, but even though several alternative skin models are available only little knowledge exists about the resemblance of their xenobiotic metabolizing capacities compared to native human skin.

For years, keratinocyte-derived cell lines have been used for investigations of mechanisms of action of dermatotoxic compounds or the prevention of skin diseases (4-10) as they represent a cost- and time-effective tool to address these questions. They may also be appropriate to explore human metabolic inter-individual differences (11). The most critical issues concerning immortalized keratinocyte-based monolayer models have been the lack of three-dimensional tissue (3D) properties as well as accumulation of spontaneous chromosomal aberrations. Due to these insufficiencies, 3D human epidermal equivalents were developed over the last years (12-14). Such 3D skin models consist of primary human keratinocytes which are grown at the air-liquid interphase and differentiate into a multilayered 3D tissue. They were already examined e.g. by COLIPA for their suitability for genotoxicity testing (15-17). However, until now, a systematic assessment of xenobiotic metabolism capacities of monolayer cultures in comparison to human skin and 3D models has never been performed.

Therefore, the aim of this study was the characterization of the xenobiotic metabolizing activities of native human skin compared to *in vitro* models such as (i) the commercially available 3D epidermal model EpiDerm™ (EPI-200, MatTek Corp.) based on human primary keratinocytes and (ii) several

4

human skin-derived cell monolayers. The latter one including the well-known keratinocyte-based cell lines, HaCaT (18) and NCTC 2544 (19) as well as primary human epidermal keratinocytes (NHEK). For use in dermatotoxicology it is necessary that alternative testing methods reproduce xenometabolic pathways of human skin so that the results of *in vitro* testing are meaningful. Particular concern for the evaluation of the toxicity of compounds is the activation of genotoxic compounds via CYP and also the effect of compounds to induce the activity of these enzymes. In order to characterize the enzyme metabolism of skin models compared with human skin in this study, cells and EPI-200 epidermal models were primarily treated with 3-methylcholanthrene (3-MC) as a prototypical arylhydrocarbon receptor agonist and CYP inducer.

5

MATERIALS AND METHODS

Chemicals and materials

All chemicals, if not otherwise specified, were purchased from Sigma-Aldrich (Germany) in highest purity available. Cell culture media were obtained from PAA (Austria) and PromoCell (Germany), the DC protein quantification kit from BioRad (Germany). Prostaglandin E2 EIA monoclonal and fluorescent COX kit was acquired from Cayman Chemical Company (USA). Liver microsomes were bought from Celsis In Vitro Inc. (USA).

Keratinocyte / tissue culture

HaCaT cells were cultured in DMEM, NCTC 2544 and A431 cells were cultured in MEM each containing 10 % (v/v) fetal calf serum (FCS) and 1 % (v/v) of antibiotic-antimycotic solution (PAA, Cat. No. P11-002). A431 were supplemented with non-essential amino acids (PAA, Austria). Primary NHEK keratinocytes from 30- 40 year old female donors were cultured in KGM-2 containing supplements from Promocell (Germany). For subsequent enzyme assays, media were FCS-free if not otherwise specified.

The human reconstituted epidermis EpiDerm™ (EPI-200) was purchased from MatTek Corporation, Ashland, USA (donor 1188 and for one experiment 254). After delivery, the tissue recovered for 24 h at 37 °C and 5 % CO_2 in serum-free EPI-100-NMM-PRF media (900 μL per model). Induction experiments were carried out in EPI-100-NMM-PRF medium.

Enzyme induction

Cells and EPI-200 epidermal models were treated with 3-methylcholanthrene (3-MC), rifampicin (RIF), dexamethasone (DEX) and 6-(4-chlorophenyl:imidazo[2,1-b]thiazole-5-carbaldehyde O-(3,4-dichlorobenzyl)oxime (CITCO, (20) in DMSO (stock concentration 10, 50, 100 and 10 mM, respectively) and cyclophosphamide (CP, 50 mM in PBS). Incubation times for induction were 24 h (CYP1), 48 h (CYP3A) and 72 h (CYP2) unless otherwise noted (timepoints chosen and adjusted in accordance to hepatocyte data (Hewitt et al., 2007a)). Maximum solvent concentration was 0.1 %.

Cell viability, cytotoxicity and protein content assessment

Assay kits for measurement of cell viability (Cell Titer Blue and CytoTox One, Promega Corp) were applied according to the manufacturer. Protein in monolayer cell culture was determined using CBQCA protein quantification kit (Molecular Probes/Invitrogen, Germany) and bovine serum albumin as reference protein.

6

Human *ex vivo* skin samples

Skin samples were obtained from the hospital Kaiserswerther Diakonie in Düsseldorf, Germany. The samples originated from female patients of different age and unknown pharmacological background. Patients were informed and agreed to donate removed tissue for scientific purpose. The use of *ex vivo* skin from breast reduction has been fully approved by the local Ethics Committee at the Heinrich-Heine-University of Düsseldorf. Skin samples were collected immediately after surgery and kept cold during the transport (< 1 h).

Preparation of subcellular fractions from human ex vivo skin and EPI-200 models

Microsomal and cytosolic fractions from human skin were prepared in accordance to previously described methods (21) using a Ultra Turrax T25 homogenizer. The number of individual microsomal preparations was n=8 for EPI-200 and n=10 for skin biopsies. The functionality of the preparation protocol was confirmed by comparing CYP enzyme activities of commercially available mouse liver microsomes with obtained results of in house preparation of mouse microsomes which were highly comparable (data not shown).

Cytochrome P450 enzyme activity assays

CYP1/2B activities were measured via resorufin-based substrates (supplemental material and methods). Dicoumarol (10 µM) was added to all resorufin-based CYP experiments to prevent metabolism of the reaction product resorufin by NQO1 (22) and Phase II enzymes.

The multi-CYP1/2 substrate 7-methoxy-4-trifluoromethylcoumarin was assayed according to the method described by (23).

CYP3A was assayed by using 7-benzyloxyquinoline as substrate according to (24). The luminescent Luc-BE CYP3A-assay was carried out as recommended by the manufacturer (Promega, USA; supplemental material and methods).

Cyclooxgenase enzyme activity assays

PGE_2 formation as a measure for COX-2 activity (25) was measured using a monoclonal EIA and a COX fluorescent activity assay kit (Cayman Chemical Company, Ann Arbor, USA; supplemental material and methods).

Statistics

All experiments were conducted at least n=3. Using the Student's unpaired t-test; $p < 0.05$ was considered significant. LOD was defined as mean of blank measurements plus 3 times standard deviation of the blank. LOQ was defined as the 2-fold LOD.

RESULTS

XENOBIOTIC PHASE I METABOLISM IN HUMAN SKIN AND EPI-200 MODELS

Performance of all CYP assays was verified with rat, mouse, minipig and human liver microsomes (HLM). All of those displayed substantial hepatic enzyme activities for CYP1A1/1B1 (EROD), CYP1A2 (MROD), CYP2C9 (MFC *O*-dealkylase) and CYP3A (BQ-dealkylation and luminescence generated from Luc-BE), whereas no CYP2B6 activity (PROD) was seen above the limit of detection (LOD; < 0.2 pmol min^{-1} mg^{-1} in resorufin dealkylase assays) in any human sample (Fig. 1a- e). In contrast to liver, human skin and EPI-200 microsomes displayed no EROD, MROD, MFC *O*-dealkylase and – in common with the human liver samples – no PROD activities above the LOD. In our coworkers' study at BASF, similar results in native human skin as well as reconstructed epidermal (MatTek) and full thickness skin (Phenion) models were obtained (supporting table 1; (26)).

In contrast to resorufin dealkylase activities, BQ- and Luc-BE (CYP3A) rates were 76 ($\pm$ 41) and 94 ($\pm$ 13) pmol BQ min^{-1} mg^{-1} and 0.05 ($\pm$ 0.03) and 0.08 ($\pm$ 0.05) pmol Luc-BE min^{-1} mg^{-1} in skin and EPI-200 microsomes, respectively. These values just exceeded the given LOD. In the study conducted by our coworkers (BASF), CYP3A examined via BROD also remained below their respective LOQ. These data indicate very low to undetectable basal enzyme activities in human skin as well as in the EPI-200 model.

CYP-mediated biotransformation is increased upon treatment with specific inducers. Therefore we investigated CYP induction in intact EPI-200 models by systemic application of prototypical inducers. In intact models, basal EROD, MROD, PROD and MFC activities were below the LOD and the BQ turnover was 5.5 ($\pm$ 0.9) pmol min^{-1} mg^{-1} (Fig. 2b) confirming our measurements in microsomes. EROD and MROD activities, however, were inducible by 3-MC after 24 h in a concentration-dependent fashion up to 1.7 ($\pm$ 0.8) pmol min^{-1} mg^{-1} for EROD and 0.7 ($\pm$ 0.3) pmol min^{-1} mg^{-1} for MROD (Fig. 2a). Basal and rifampicin- or CITCO-induced (72 h) PROD and MFC activities remained below the LOD. CYP3A4 activity was not inducible by rifampicin or dexamethasone after 48 h (Fig. 2b).

Basal COX activity in microsomes was present (23.5 ± 8.7 pg min^{-1} mg^{-1} and 33.7 ± 19.8 pg min^{-1} mg^{-1} of PGE$_2$ formation; Fig. 1 f). Basal PGE$_2$ production in intact EPI-200 tissue was about 10-fold lower (3.6 ± 1.9 pg min^{-1} mg^{-1}). After treatment with 3-MC, PGE$_2$ formation in intact tissues increased approximately 2-fold to 7.6 pg min^{-1} mg^{-1} within 24 h in a concentration dependent manner (Fig. 2c).

9

Inter-individual variability and the duration of inducer treatment may impact on enzymatic activities. Therefore, basal microsomal CYP1A/1B and COX activities were measured in EPI-200 models from two different donors (donors 1188 and donor 254) after 24, 48 and 72 h upon tissue arrival. Independently from donor and time point after arrival, EROD activity was below the LOD. Also PGE_2 formation over time was similar under all conditions tested (supporting online material, Figure 5).

XENOBIOTIC PHASE I METABOLISM IN CELL LINES

As shown in figure 3a, basal EROD activity for HaCaT was below detection and for NCTC and NHEK cells just above the LOD at 0.2 - 0.3 pmol min^{-1} mg^{-1}. EROD and MROD activities were increased by 3-MC in all three cell lines (Fig. 3a). At 5 µM 3-MC, the highest EROD and MROD induction was seen in NCTC 2544 with 114 ± 77 pmol min^{-1} mg^{-1} and 70 pmol min^{-1} mg^{-1}, respectively. At that concentration HaCaT cells showed 75 pmol min^{-1} mg^{-1} for EROD and 35 pmol min^{-1} mg^{-1} for MROD. NHEKs displayed maximal EROD activity with 2.5 µM 3- MC (11.1 ± 6.6 pmol min^{-1} mg^{-1}). Similar results were obtained using MFC (data not shown). Thus, immortalized cell lines like NCTC 2544 and HaCaT are more responsive to CYP-induction by 3-MC than primary keratinocytes. Moreover, inducer concentrations for maximum differ between cell types (Figure 3a).

The ability to induce CYP2B in hepatocytes decreases rapidly when cells are transferred to monolayer cultures (27) (28). To find out if this is also the case for keratinocyte cultures, we tested the inducibility of CYP2B (PROD) by rifampicin (RIF, 0-50 µM), CITCO (0-10 µM) and cyclophosphamide (CP, 0-500 µM) which was reported to induce CYP2B6 more than 2-fold in hepatocyte culture (29). None of these chemicals elevated PROD activity in any cell type after 24 to 72 h (example for cyclophosphamide shown in Fig. 3a).

Basal CYP3A activity was detectable in the immortalized HaCaT und NCTC cell lines with 38 ± 13 pmol min^{-1} mg^{-1} and 33 ± 5 pmol min^{-1} mg^{-1}, respectively, as measured by BQ as CYP3A substrate for monolayer cells. These values were comparable with turnover rates obtained for microsomal activities of human skin and EPI-200. In contrast, no BQ turnover was measured in NHEKs (Fig. 3b). As serum conditions affect metabolic activities *in vitro* (30), we also assayed BQ in immortalized cells using inactivated serum. Treatment with either serum, rifampicin or dexamethasone treatment for 48 h failed to increase BQ metabolism above basal levels in HaCaT and NCTC cells. Dexamethasone decreased BQ turnover in NCTC, an effect which was similar to that seen in intact EPI-200 (Fig. 2b).

PGE_2 formation as a measure of COX activities was detected in HaCaT (0.05 ± 0.03 pg min^{-1} mg^{-1}), NCTC (0.02 ± 0.01 pg min^{-1} mg^{-1}) and the epidermal squamous cell carcinoma strain A431 (0.07 ± 0.02 pg min^{-1} mg^{-1}) employed as a tumor cell line control. In contrast, primary NHEKs exhibited more than

10

100-fold higher PGE_2 production (5.1 ± 2.8 pg min^{-1} mg^{-1}; Fig. 4). Incubation of monolayers with 3-MC did not significantly affect COX activities (Fig. 3c). The highest increase in PGE_2 production in the cell culture experiments was measured at inducer concentrations between 1 to 2 µM 3-MC, which caused an up to 1.7-fold, 1.5-fold and 1.4-fold increase, though not significant induction of PGE2 production in HaCaT, NCTC and NHEK.

11

DISCUSSION

For the first time, drug metabolizing enzyme activities of human skin, 3D epidermal models and keratinocytes were compared. Thereby, CYP1A1, 1B1, 1A2, 2B6 and 3A activity were below the limits of quantification in any of the cell models tested. However, basal CYP3A4 and COX activities were present in all human skin models except for CYP3A4 in NHEKs.

Studies from two groups determined that human skin possesses CYP-dependent microsomal enzyme activity metabolizing polycyclic aromatic hydrocarbons or is induced by such compounds (31-33). Moreover, high CYP activities were observed in epidermal hair follicles (34). As skin is a compartmented organ, it was a major finding that the main CYP metabolism of skin takes place in the epidermal layer, i.e. epidermal keratinocytes, rather than in dermal fibroblasts (35;36) and references therein). This is why only epidermal models were chosen in this study.

A variety of researchers have studied CYP mRNA, protein and/or activity in skin and keratinocyte-derived *in vitro* models (11;17;30;37-39). As CYP mRNA expression does not always correlate well with enzyme activity (36;39), CYP mRNA expression in skin will not be discussed here although others have made extensive investigations into this aspect (17;36;38;39). With regard to enzyme activity, previous results are ambiguous. For example, while one group identified CYP1A1 and 1B1 protein and EROD activity in human untreated epidermis (40), others, in agreement with our findings, did not (30). In 3D epidermal models, CYP activity measurements were more in harmony with our findings in that basal CYP1A1/1B1 protein expression and basal EROD activity were consistently below limits of detection (41;42). Basal CYP1 activity measured in some human skin microsomes may arise from lifestyle or nutrition as food constituents and contaminants are well known to induce AhR-dependent CYP expression (43) or might be due to seasonal variation as CYP expression is dependent on seasonal UV irradiation (44). These inconsistencies will not be present in 3D skin models as primary keratinocytes used for generation of such models are cultivated under standard conditions before application.

Wattenberg and Leong (45) illustrated that cutaneous arylhydrocarbon hydroxylase activity is induced by 3-MC in rats. Similar findings were reported in human skin (31;32). EROD and MROD inducibility by 3-MC in 3D skin models in agreement with Harris et al. (41) was confirmed in this study clearly demonstrating the presence of functional CYP protein (Fig. 2a).

Keratinocyte monolayers differ from the more complex 3D epidermal model. NHEKs and NCTC cells showed very low basal CYP1A/1B activity while these activities were below the limit of detection in HaCaT cells. Moreover, CYP1A/1B in all three cell types were inducible by 3-MC with the lowest

induction rate in NHEKs. These basal CYP1A/1B activities as well as their induction responses in HaCaT and NHEK or NCTC measured in this study support the recently reported data using B(a)P or 3-MC as inducers (46;47). It was also observed that CYP1A/1B activities decreased in all monolayer keratinocytes after maximal induction (Fig. 3a). Since no significant cytotoxicity of 3-MC was detected in our setup (LDH, data not shown), the proposed mechanism for this observation is substrate inhibition, as reported for resorufin-based CYP substrates like EROD earlier (48). CYP1A1/1B induction by 3-MC was also observed in 3D models, but, in contrast to monolayers, no substrate inhibition occurred. This is possibly due to a different distribution of the compound within the 3D model where all cells are exposed via the medium. Also, the amount of cells/surface area is much higher in a 3D model. These data suggest that EpiDerm models due to their 3D structure are suitable alternative models for studying CYP1A/1B induction in skin (Fig. 2a).

CYP2B6 activitiy was not detectable at the basal nor at induced levels in skin microsomes (basal), EPI-200 models or cell lines (Fig. 1b,2a,3) and is most probably not transcribed in human skin as indicated by Hu *et al.* (2010). In contrast to our findings, Gelardi *et al.* (2001) reported measurable PROD activity in NCTC cells. Here, PROD activity in HLM did not exceed the detection limit, while rodent liver samples showed significant PROD activity (Fig. 1b) indicating that the suitability of the PROD assay for human samples is questionable and rather suited for experiments based on rodent catalytic activity. Such species-specificities of CYP towards particular substrates have been reported previously (49).

To answer the question if native skin and/or skin cell-derived *in vitro* models possess basal or inducible CYP2B6 activity, we employed the broad spectrum CYP substrate MFC, which is mainly metabolized by CYP2B6 (50). In contrast to HLM, human skin and EPI-200 microsomes did not metabolize MFC (Fig. 1c). Induction experiments in the cell lines of this study with model inducers for a variety of CYP enzymes suggest that induced MFC turnover is due to enhanced CYP1A/1B activity since selective inducers of CYP2B6, 2E1 and 3A did not significantly alter MFC metabolism (Suppl. Table 2). Lack of basal MFC turnover in skin and epidermal models/cell lines also indicates that there is no measureable basal MFC turnover via CYP1A1, 1B1, 1A2, 2B6, 2C19 and 2E1. These data are in agreement with Rolsted et al. (2007) who reported that two keratinocyte cell lines lack basal CYP2B6 activity. However, these authors did find CYP2C9 (a minor pathway in MFC metabolism) and CYP2E1 enzyme activities in human skin microsomes. Lack of MFC turnover in our studies does not necessarily contradict these reported activities for CYP2C9 and 2E1 as the MFC substrate might have lower sensitivity and specificity towards these enzymes.

The CYP3A family is of particular importance for xenobiotic detoxification in skin as many drugs employed in dermatology are metabolized by these enzymes. Members of the CYP3A family have been reported to be present in rodent (51) as well as in human skin, where CYP3A5 appears to be the key enzyme at the basal level without inducer (35;52). Both CYP3A substrates utilized in this study indicate low basal CYP3A activity in skin which is in agreement with Rolsted et al. (30). For the first time, this study shows that CYP3A activity in EPI-200 models and human skin is very similar (Fig. 1d, e). In contrast to Rolsted et al. (30), basal CYP3A activities were detected in HaCaT cells. This might be due to different HaCaT sub-clones because this cell line has been existing for a long time (18). Differences in HaCaT sub-clones were observed recently also for N-acetylation activities (47). NCTC cells also exhibited basal CYP3A activity. In any of these *in vitro* models, CYP3A activity was not inducible above a factor of 1.2 under the conditions tested (Fig. 2b & 3b). CYP3A activity was lacking in NHEKs as was also seen in the Rolsted et al. (30) study. This was not due to lack of FCS in the culture medium of primary cells which, in contrast to immortalized cell lines, are cultured without serum since (i) Rolsted et al. (30) tested this hypothesis and (ii) EPI-200 expressed basal CYP3A activity in serum-free medium (Fig. 1 & 2). These data suggest that keratinocytes like NHEK are not a suitable alternative model for studying CYP3A metabolism-dependent effects in skin cells and that the choice of cell line, sub-clone and culture conditions may be crucial for the experimental outcome.

A very different picture is obtained for COX activities. COX is thought to play a major role in activation of chemicals during the COX catalyzed peroxidase reaction (53). This is especially important for genotoxins and sensitizers. COX enzyme activities were measured at well-detectable levels in all models tested. In EPI-200, duration of incubation (24-72 h; Fig. 5) or donor (Suppl. Fig. 1) did not affect COX activities. The largest difference in COX activities is seen between immortalized and non-immortalized cellular systems: PGE_2 production is lower in immortalized than in primary cells or native skin (Fig. 1f, 4). Thereby, e.g. EPI-200 and HaCaT PGE_2 production was found to be very similar to COX metabolism rates reported by others (54;55). One possibility causing differences in COX activity – as already discussed for CYP3A - was presence/absence of serum. We ruled out this option by cultivating NHEK in serum-containing media (data not shown). We also included a squamous cell carcinoma line (A431) in our studies because COX-2 is known to be a major player in inflammation and tumorigenesis (56;57). However, these cells produced the same low amount of PGE_2 as the other immortalized lines (Fig. 4). Therefore, a further possibility might be loss of cellular PGE_2 production during the cellular immortalization process. This hypothesis is supported by the observation that COX-2 expression is lower in breast cancer cell lines and specimens compared to normal mammary epithelial cells (MEC) and that immortalization of hMEC causes a dramatic decrease in COX-2 expression by an unknown mechanism (58).

Data on COX induction by xenobiotics in skin is rare. We have recently shown that AhR activation causes COX-2 induction in mouse skin and HaCaT cells (4). Here, PGE_2 formation was induced via the AhR ligand 3-MC in HaCaT, NHEK and EPI-200 (Fig. 2c, 3c). However, induction was only statistically significant in EPI-200. These data indicate that *in vitro* models based on primary cells are the method of choice and that EPI-200 models are the most suitable for experiments involving COX induction.

In conclusion, basal CYP activities are very low in comparison to substantial COX activities in reconstructed epidermis and human skin microsomes. In contrast, basal and inducible biotransforming capacities from monolayer cells differed from organotypic tissues and most interestingly also from each other. Hence, reconstructed tissues such as EPI-200 should rather be considered for dermatotoxicological studies as they maintain phase I native-like metabolic competence. For some chemical testing queries, usage of simple monolayer cultures might also be plausible but they have to be chosen with care.

CONFLICT OF INTEREST

The authors state no conflict of interest.

Reference List

1 Kao J, Patterson FK, Hall J. Toxicol Appl Pharmacol 1985; **81**(3, Part 1): 502-516.

2 Shimizu Y, Nakatsuru Y, Ichinose M, Takahashi Y, Kume H, Mimura J *et al.* Proc Natl Acad Sci USA 2000; **97**(2): 779-782.

3 Aeby P, Sieber T, Beck H, Gerberick GF, Goebel C. J Invest Dermatol 2008; **129**(1): 99-109.

4 Fritsche E, Schäfer C, Calles C, Bernsmann T, Bernshausen T, Wurm M *et al.* Proc Natl Acad Sci USA 2007; **104**(21): 8851-8856.

5 Schwarz A, Maeda A, Gan D, Mammone T, Matsui MS, Schwarz T. Photochem Photobiol 2008; **84**(2): 350-355.

6 Afaq F, Zaid MA, Pelle E, Khan N, Syed DN, Matsui MS *et al.* J Invest Dermatol 2009; **129**(10): 2396-2403.

7 Fernau NS, Fugmann D, Leyendecker M, Reimann K, Grether-Beck S, Galban S *et al.* J Biol Chem 2010; **285**(6): 3896-3904.

8 Adhami VM, Khan N, Mukhtar H. Nutrition and Cancer 2009; **61**(6): 811-815.

9 Ott H, Bergstroem MA, Heise R, Skazik C, Zwadlo-Klarwasser G, Merk HF *et al.* Chem Res Toxicol 2009; **22**(2): 399-405.

10 Li Y, Liu Y, Xu Y, Voorhees JJ, Fisher GJ. J Dermatol Sci 2010; **60**(2): 105-113.

11 Gibbs S, van de Sandt JJM, Merk HF, Lockley DJ, Pendlington RU, Pease CK. Curr Drug Metab 2007; **8**: 758-772.

12 Slivka SR, Landeen LK, Zeigler F, Zimber MP, Bartel RL. J Invest Dermatol 1993; **100**(1): 40-46.

13 Roguet R, Ragnier M, Cohen C, Dossou KG, Rougier A. Toxicol in Vitro 1994; **8**(4): 635-639.

14 Cannon CL, Neal PJ, Southee JA, Kubilus J, Klausner M. Toxicol in Vitro 1994; **8**(4): 889-891.

15 Zhao JF, Zhang YJ, Kubilus J, Jin XH, Santella RM, Athar M *et al.* Biochem Biophys Res Com 1999; **254**(1): 49-53.

16 Curren RD, Mun GC, Gibson DP, Aardema MJ. Mutat Res-Gen Tox En 2006; **607**(2): 192-204.

17 Hu T, Khambatta ZS, Hayden PJ, Bolmarcich J, Binder RL, Robinson MK *et al.* Toxicol in Vitro 2010; **24**(5): 1450-1463.

18 Boukamp P, Petrussevska RT, Breitkreutz D, Hornung J, Markham A, Fusenig NE. J Cell Biol 1988; **106**(3): 761-771.

19 Bakken PC, Evans VJ, Earle WR, Stevenson RE. Am J Epidemiol 1961; **73**(1): 96-104.

20 Hewitt NJ, Lecluyse EL, Ferguson SS. Xenobiotica 2007; **37**(10-11): 1196-1224.

21 Nelson AC, Huang W, Moody DE. Drug Metab Dispos 2001; **29**(3): 319-325.

22 Asher G, Lotem J, Kama R, Sachs L, Shaul Y. Proc Natl Acad Sci USA 2002; **99**(5): 3099-3104.

23 Turpeinen M, Korhonen LE, Tolonen A, Uusitalo J, Juvonen R, Raunio H *et al.* Eur J Pharm Sci 2006; **29**(2): 130-138.

24 Hakkola J, Maenpaa J, Mayer RT, Park SS, Gelboin HV, Pelkonen O. Brit J Clin Pharmacol 1992; **34**(5): 415-420.

25 Giuliano F, Warner TD. J Pharmacol Exp Ther 2002; **303**(3): 1001-1006.

26 Jäckh C, Blatz V, Fabian E, Guth K, van Ravenzwaay B, Reisinger K *et al.* Toxicol in Vitro 2011; **In Press, Corrected Proof**.

27 Nemoto N, Sakurai J, Funae Y. Arch Biochem Biophys 1995; **316**(1): 362-369.

28 Hewitt NJ, Gomez-Lechon MJ, Houston JB, Hallifax D, Brown HS, Maurel P *et al.* Drug Metab Rev 2007; **39**(1): 159-234.

29 Lindley C, Hamilton G, McCune JS, Faucette S, Shord SS, Hawke RL *et al.* Drug Metab Dispos 2002; **30**(7): 814-822.

30 Rolsted K, Kissmeyer A-M, Rist GM, Hansen SH. Arch Dermatol Res 2007; **300**: 11-18.

31 Levin W, Conney AH, Alvares AP, Merkatz I, Kappas A. Science 1972; **176**(4033): 419-420.

32 Alvares AP, Kappas A, Levin W, Conney AH. Clin Pharmacol Ther 1973; **14**(1): 30-40.

33 Bickers DR, Mukhtar H, Duttachoudhury T, Marcelo CL, Voorhees JJ. J Invest Dermatol 1984; **83**(1): 51-56.

34 Merk HF, Mukhtar H, Kaufmann I, Das M, Bickers DR. J Invest Dermatol 1987; **88**(1): 71-76.

35 Baron JM, Holler D, Schiffer R, Frankenberg S, Neis M, Merk HF *et al.* J Invest Dermatol 2001; **116**(4): 541-548.

36 Swanson HI. Chem Biol Int 2004; **149**: 69-79.

37 Ahmad N, Mukhtar H. J Invest Dermatol 2004; **123**(3): 417-425.

38 Oesch F, Fabian E, Oesch-Bartlomowicz B, Werner C, Landsiedel R. Drug Metab Rev 2007; **39**(4): 659-698.

39 Svensson CK. Drug Metab Dispos 2009; **37**(2): 247-253.

40 Katiyar SK, Matsui MS, Mukhtar H. J Invest Dermatol 2000; **114**(2): 328-333.

41 Harris IR, Siefken W, Beck-Oldach K, Brandt M, Wittern KP, Pollet D. Skin Pharmacol Physiol 2002; **15**(Suppl. 1): 59-67.

42 Neis MM, Wendel A, Wiederholt T, Marquardt Y, Joussen S, Baron JM *et al.* Skin Pharmacol Physiol 2010; **23**(1): 29-39.

43 Denison MS, Nagy SR. Annual Review of Pharmacology and Toxicology 2003; **43**(1): 309-334.

44 Rannug A, Fritsche E. Biol Chem 2006; **387**(9): 1149-1157.

45 Wattenberg LW, Leong JL. J Histochem Cytochem 1962; **10**(4): 412-&.

46 Gelardi A, Morini F, Dusatti F, Penco S, Ferro M. Toxicol in Vitro 2001; **15**(6): 701-711.

47 Bonifas J, Hennen J, Dierolf D, Kalmes M, Blömeke B. Toxicol in Vitro 2010; **24**(3): 973-980.

48 Lin Y, Lu P, Tang C, Mei Q, Sandig G, Rodrigues AD *et al.* Drug Metab Dispos 2001; **29**(4): 368-374.

49 Martignoni M, Groothuis GM, de Kanter R. Exp Opin Drug Metab Toxicol 2006; **2**(6): 875-894.

50 Stresser DM, Turner SD, Blanchard AP, Miller VP, Crespi CL. Drug Metab Dispos 2002; **30**(7): 845-852.

51 Zhu Z, Hotchkiss SA, Boobis AR, Edwards RJ. Biochem Biophys Res Com 2002; **297**(1): 65-70.

52 Vyas PM, Roychowdhury S, Khan FD, Prisinzano TE, Lamba J, Schuetz EG *et al.* J Pharmacol Exp Ther 2006; **319**(1): 488-496.

53 Vogel C. Curr Drug Metab 2000; **1**(4): 391-404.

54 Natsch A, Wasescha M. Int J Cosmet Sci 2007; **29**: 369-376.

55 Moeller R, Lichter J, Blömeke B. Toxicology 2008; **249**(2-3): 167-175.

56 Dubois RN, Abramson SB, Crofford L, Gupta RA, Simon LS, De Putte AV *et al.* FASEB J 1998; **12**(12): 1063-1073.

57 Paz ML, Ferrari A, Weill FS, Leoni J, Maglio DHG. Cytokine 2008; **44**(1): 70-77.

58 Zhao X, Goswami M, Pokhriyal N, Ma H, Du H, Yao J *et al.* Cancer Res 2008; **68**(2): 467-475.

59 Vane JR. Nature New Biol 1971; **231**: 232-235.

FIGURE LEGENDS

Figure 1: Specific CYP activity (pmol min^{-1} mg^{-1}) was examined in positive control microsomes from liver compared to untreated human skin (n=10) and EPI-200 (n=8) microsomes. Rat liver microsomes (Rat ARO) were from Aroclor 1254-induced animals, all other microsomes were non-induced samples. LOD = limit of detection. Specific PGE2 formation (pg min^{-1} mg^{-1}) was examined in untreated human skin (n=10) and EPI-200 (n=8) microsomes.
a: Activity of CYP1 measured by ethoxyresorufin O-deethylation (EROD) and methoxyresorufin O-demethylation (MROD) assays.
b: Activity of CYP2B measured by pentoxyresorufin O-depentylation (PROD).
c: Activity of CYP1 and CYP2 measured by the broad spectrum substrate MFC.
d: Activity of CYP3A measured by the substrate BQ.
e: Activity of CYP3A measured by the substrate LucBE.
f: Basal levels of PGE$_2$ production in skin and EPI-200 microsomes. The data are shown as pg PGE$_2$ min^{-1} mg^{-1}.

Figure 2: Induction of enzyme activity in intact EPI-200 models by the model compounds 3-MC, RIF and DEX [μM]. The asterisks indicate significant difference (p=0,05) to solvent (DMSO) control.
a: Induction of CYP1 (EROD, MROD) and CYP2B (PROD) in intact EPI-200 models induced by the model compound 3-MC [μM]. PROD induction was additionally examined by specific CYP2B inducer treatment (CITCO and cyclophosphamide) which lead to the same result as depicted here. Activity is shown as pmol min^{-1} mg^{-1}.
b: Induction of CYP3A in intact EPI-200 models induced by rifampicin (RIF) and dexamethasone (DEX). Activity (pmol min^{-1} mg^{-1}) was determined via benzyloyxquinoline (BQ) assay.
c: PGE$_2$ production in intact EPI-200 upon 3-MC [μM] treatment. The data are shown as pg PGE$_2$ min^{-1} mg^{-1}.

Figure 3: Induction of enzyme activity in immortalized cell lines (HaCaT, NCTC) and primary keratinocytes (NHEK) by the compounds 3-MC, CP, RIF and DEX [μM]. The asterisks indicate significant difference (p=0,05) to solvent (DMSO) control.
a: Induction of CYP1 (EROD, MROD) und CYP2B (PROD) activity induced by 3-MC [μM]. PROD induction was carried out using rifampicin, CITCO and cyclophosphamide (72 h). The latter compound is depicted here (CP), but the same result was obtained with the other two CYP2B inducers. Activity is shown in pmol min^{-1} mg^{-1}.
b: Induction of CYP3A activity rifampicin (RIF) and dexamethasone (DEX) for 48 h. The assay was BQ. The data are shown as specific activity (pmol min^{-1} mg^{-1}). The dagger labels rates that are significantly different to DMSO controls and the RIF group.
c: PGE$_2$ production in keratinocytes upon 3-MC treatment. The data are shown as pg PGE$_2$ min^{-1} mg^{-1}.

Figure 4: Basal levels of PGE$_2$ production in immortalized cell lines (HaCaT, NCTC), a squamous cell carcinoma line (A431) and primary keratinocytes (NHEK). The data are shown as pg PGE$_2$ min^{-1} mg^{-1}.

1
2
3
4
5
6
7
8
9
10
11
12
13
14
15
16
17
18
19
20
21
22
23
24
25
26
27
28
29
30
31
32
33
34
35
36
37
38
39
40
41
42
43
44
45
46
47
48
49
50
51
52
53
54
55
56
57
58
59
60

Figure 1

Figure 2

Figure 3

Figure 4

1
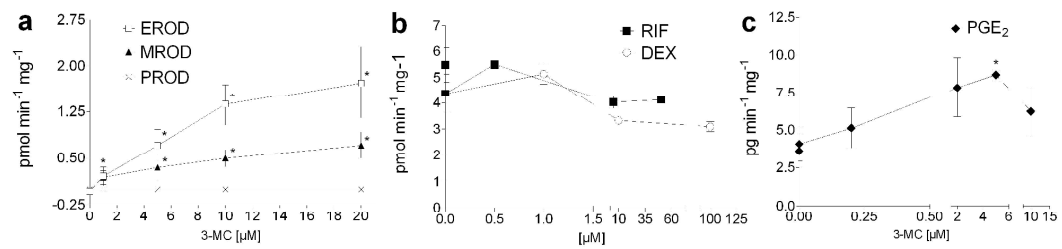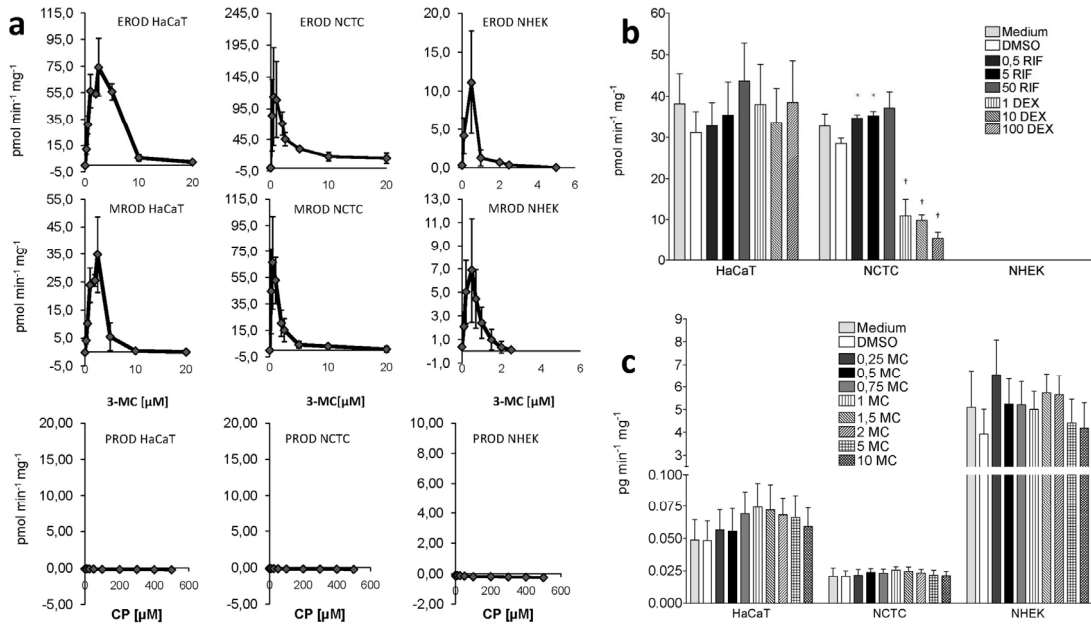
Supporting Online Material

Materials

Positive controls for microsomal enzyme activities

These positive controls included induced Sprague-Dawley rat liver microsomes as well as non-induced liver microsomes from ICR/CD -1 mouse, Goettingen minipig and mixed gender pooled human donors. Rat liver enzymes were induced by Aroclor 1254 except for the CYP3A assays BQ and Luc-BE where dexamethasone-induced rat liver microsomes were used. The human liver microsome (HLM) preparations had moderate CYP activity according to the manufacturer.

Methods

Preparation of subcellular fractions from human ex vivo skin and EPI-200 models

Skin samples without subcutaneous fat were cut into small pieces and homogenized on ice (4 °C) employing a blender (SW18, Ultra-Turrax, Germany) according to Nelson et al. (21). Briefly, ice-cold homogenisation buffer (250 mM Potassiumphosphate, 150 mM KCl, 1 mM EDTA at pH 7,25) was added at approximately 2 times the volume of the tissue sample. Skin tissue was thereafter shred carefully under constant cooling until it yielded a homogeneous suspension that was centrifuged at 9.000 g and 4 °C for 20 min to remove debris. The supernatant was taken to an ultracentrifugation step at 100.000 g and 4 °C for 60 min. The resulting supernatant contained the cytosolic and the pellet the microsomal protein fraction. Microsomes were resuspended in microsome buffer (250 mM potassiumphosphate, 30 % glycerol at pH 7,5) and carefully homogenised. Protein was quantified by the DC assay kit (BioRad, Germany) with bovine serum albumin as standard. Protein samples were stored in aliquots at -80 °C. Protein extraction from EPI-200 was carried out using the same procedure as described above, except that whole epidermis models (at least 20 single models/preparation) were processed in a Potter-Elvehjem-homogeniser containing 2 mL homogenisation buffer.

Cytochrome P450 enzyme activity assays

For measuring CYP1/2B activities in living monolayer cultures and Epi-200 models, resorufin-based substrates (all solved in DMSO) were employed. Resorufin as the reaction product in the respective media or assay solution was used to generate the standard curves. Ethoxyresorufin was used for assaying CYP1A and CYP1B1 (EROD), methoxyresorufin for CYP1A (MROD) and pentoxyresorufin for CYP2B (PROD) according to a protocol described by (30). Shortly, serum-free media containing 2,5 µM resorufin substrate and 10 µM dicumarol were applied to PBS-washed monolayer cells and

2

resorufin formation kinetics were measured 21 min at 37 °C and excitation and emission wavelength of 544 nm and 590 nm on a Thermo Ascent Fluoroskan fluorometric plate reader. To check for glucuronidation or sulfatation of resorufin, cells and cell-free wells were incubated under the same conditions with 1 µM resorufin instead of alkylated substrate.

CYP activity in microsomes was determined in 100 mM Tris-HCl buffer (pH 7,5) containing 10 µM dicumarol, NADPH-regeneration kit with MgCl$_2$ (Promega, USA) according to the manufacturer, 2 µM resorufin substrate and 5 % v/v (ca. 0,1 mg protein in total) of microsome preparations. All measurements were carried out at least in triplicate at a final volume of 100 µL in 96-well plates.

The multi-CYP1/2 substrate 7-methoxy-4-trifluoromethylcoumarin (MFC) was assayed according to the method described by (23). The assay was calibrated with the reaction product 7-hydroxy-4-trifluoromethylcoumarin in the respective media. MFC activity in microsomes was determined in a 200 µL reaction containing 0,1 M Tris-HCl (pH 7,4), 50 µM MFC substrate and 2,5 % microsome preparation (0,1 mg protein in total for positive controls; 0,05 mg for skin and EPI-200 microsomes). The reaction was incubated for 10 min at 37 °C, initiated by the addition of NADPH regenerating kit and terminated after 5 min incubation at 37 °C with 120 µL of ACN/Tris 0,5 M solution (80/20 v/v) and centrifuged at 12.000 g for 10 min to pellet the protein. 100 µL of the supernatant were transferred to a black 96-well plate and measured at 390 nm and 538 nm on a Thermo Ascent Fluoroskan fluorometric plate reader. Media from cell and tissue cultures were treated the same way.

A spectrofluorometric CYP3A assay was carried out by using 7-benzyloxyquinoline (BQ, dissolved in DMSO) as substrate ((50)). The assay procedure was modified according to (24). It was calibrated with the reaction product 7-hydroxyquinoline (TCI GmbH, Germany) in the respective media. The reaction mixture contained 100 mM Tris-HCl buffer (pH 7,5), NADPH-regeneration kit, 120 µM BQ and 5 % microsome preparation (0,02 mg protein for positive controls except for human liver microsomes (0,005 mg); 0,01 mg for skin and EPI-200 microsomes) in a final volume of 100 µL. The reaction mix was incubated 10 min without, subsequently 10 min with BQ substrate at 37°C and stopped by adding 100 µL of TCA (6 % w/v). The sample was centrifuged 10 min at 12.000 g and the supernatant was then removed and added to 400 µL 1,6 M glycine-NaOH-buffer (pH 10,4). All measurements were carried out in triplicates at a final volume of 100 µL in 96well plates at an excitation and emission wavelength of 355 nm and 510 nm on a Thermo Ascent Fluoroskan fluorometric plate reader. In cell culture, 48 h after adding respective inducers, BQ was added to the cells at a final concentration of 120 µM in medium containing 10 µM dicoumarol. Due to the long assay duration, medium contained 10 % FCS (immortalized cells) or EPI-100 NMM PRF (NHEK, EPI-

3

200) was used to maintain the cells viable. Cells incubated with BQ for 24 h at 37°C. The media were then removed and 100 µL aliquots processed as described above.

The luminescent Luc-BE as a second CYP3A-assay was carried out as recommended by the manufacturer (Promega , USA). D-Luciferin was used to calibrate the measurement. Shortly, the substrate (5 mM) was pre-incubated with distilled water and microsomal protein or luciferin standards for 10 min in the dark at room temperature. Positive controls contained 0,1 mg of protein, whereas 0,05 mg of protein were used for assaying activity in skin and EPI-200 microsomes. The reaction was started by the addition of NADPH regenerating solution and kept dark at room temperature for 10 min. Then, detection reagent was added and the mixture was incubated for further 20 min under the same conditions before luminescence was detected using a MicroLumat Plus microplate luminometer (Berthold Technologies GmbH & Co. KG, Germany).

Cyclooxgenase enzyme activity assays

PGE_2 and its metabolites formed by were detected using a monoclonal EIA and a COX fluorescent activity assay kit (Cayman Chemical Company, USA). In monolayer cell culture and intact EPI-200, media from inducer treatment were removed after 24 h incubation using the corresponding media for preparation of the standards. Media samples were incubated overnight on EIA plates and afterwards color (405 nm) was developed with Ellman's reagent according to the manufacturer's protocol. In microsomal preparations, PGE_2 production assay was carried out according to a protocol by Vane (59) using modified Bucher medium, arachidonic acid (final concentration 30 µM) and 5 % microsomal protein in a 100 µL reaction which was incubated for 30 min at 37 °C. The reaction was terminated by heating the sample at 70°C for 60 seconds. After a short centrifugation step at 12.000 g, the sample was transferred to ultrafiltration tubes (Millipore, Germany) and centrifuged at 12.000 g through a 10 kDa cut-off membrane before the solution was analyzed using the above mentioned Cayman EIA kit. The background control contained the reaction mixture with buffer instead of microsomes.

In an additional assay to examine donor- and time-dependent effects on COX activity, the COX fluorescent activity assay kit from Cayman Corp. was used employing the compound 10-acetyl-3,7-dihydroxyphenoxazine (ADHP) forming resorufin upon COX action. The assay was conducted as recommended by the manufacturer and measured at 544 nm and 590 nm on a Thermo Ascent Fluoroskan fluorometric plate reader.

4

SUPPLEMENTAL MATERIAL LEGENDS

Figure 5 (SUPPLEMENT): COX activity (nmol min^{-1} mg^{-1}) was measured by the fluorescent ADHP assay (Cayman Corp.) in microsomes prepared from EPI-200 after different cultivation durations (24-72 h). Ovine COX-1 is shown as positive control. Donor 1188 was the regular donor. Donor 254 is a special donor upon request (MatTek Corp.).

Table 1 (SUPPLEMENT): Specific CYP activity (pmol min^{-1} mg^{-1}) was examined in positive control microsomes from rat liver (Han Wistar) compared to untreated human skin. LOQ EROD: 1.57; LOQ PROD: 5.08; LOQ BROD: 4.42. * Jaeckh et al. 2011 (26)

Table 2 (SUPPLEMENT): MFC turnover (pmol min^{-1} mg^{-1}) 24 h after treatment with respective inducers (n=3). 3-MC= 3-methylcholanthrene; RIF= rifampicin; CP= cyclophosphamide; Et= ethanol p.a. All concentrations are [µM] except for ethanol [‰].

5

1
2
3
4
5
6
7
8
9
10
11
12
13
14
15
16
17
18
19
20
21
22
23
24
25
26
27
28
29
30
31
32
33
34
35
36
37
38
39
40
41
42
43
44
45
46
47
48
49
50
51
52
53
54
55
56
57
58
59
60

SUPPLEMENT: Figure 5

6
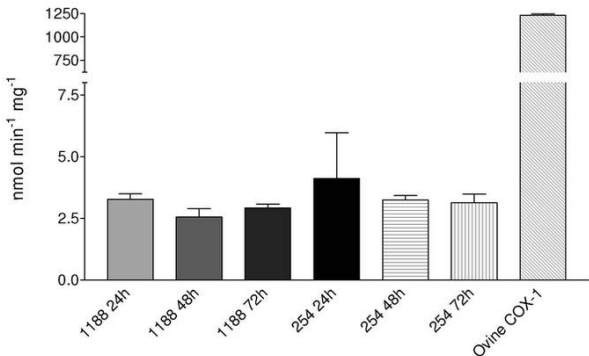
SUPPLEMENT: Table 1

	EROD	PROD	BROD
rat control *	33.93 ± 1.17	16.72 ± 0.2	69.41 ± 0,31
human skin	0.6 ± 0.22	0.82 ± 0.07	0.32 ± 0.09

7

SUPPLEMENT: Table 2

	Medium	DMSO	3-MC				RIF			CP			EtOH		
Conc.	-	-	0.25	2.5	10	20	0.5	5	50	5	50	500	1 ‰	5 ‰	10 ‰
HaCaT	0	0	0	2.1	0	-	0	0	0	0	0	0	0	0	0
NCTC	0	0	1.3	5.3	3.3	-	0	0	0	0	0	0	0	0	0
NHEK	0	0	1.3	7.5	2.7	-	0	0	0	0	0	0	0	0	0
EPI-200	0	0	-	0	0	0	-	-	-	-	-	-	-	-	-

Publikation Nr. 1

Xenobiotic metabolism capacities of human skin in comparison to 3D-epidermis models and keratinocyte-based cell culture as *in vitro* alternatives for chemical testing: Phase I

Christine Götz, Roland Pfeiffer, **Julia Tigges**, Veronika Blatz, Christine Jäckh, Ulrike Hübenthal, Karsten Ruwiedel, Eva-Maria Freytag, Eric Fabian, Robert Landsiedel, Hans F Merk, Jean Krutmann, Robert J Edwards, Josef Abel, Camilla Pease, Carsten Goebel, Nicola Hewitt und Ellen Fritsche

— · — · — · — · — · — · — · — · — · — · — · —

2.2   Publikation 2

Xenobiotic metabolism capacities of human skin in comparison to 3D-epidermis models and keratinocyte-based cell culture as *in vitro* alternatives for chemical testing: Phase II

Die siebte Änderung der EG-Kosmetik-Richtlinie (76/768/EWG) verbietet seit 2009 den Gebrauch von *in vivo* Testmodellen für die kosmetische Testung bestimmter Endpunkte wie z.B. Genotoxizität. Aus diesem Grund ist die Entwicklung und Charakterisierung entsprechender *in vitro* Modelle dringend erforderlich, um neue Substanzen zu testen. Bis zum heutigen Zeitpunkt ist die metabolische Kompetenz weder von humaner Haut, noch von alternativen *in vitro* Modellen zufriedenstellend charakterisiert, obwohl die Haut das First-Pass-Organ für viele Chemikalien, darunter auch Kosmetika und Therapeutika, ist. Daher gibt es einen zunehmenden Bedarf, die fremdstoffmetabolisierende Kapazität von humaner Haut im Vergleich zu den Aktivitäten von *in vitro* Modellen zu verstehen. In dieser Publikation wurden die Aktivitäten der Phase 2 Enzyme GST, UGT und NAT in humaner *ex vivo* Haut, dem 3D-Epidermis-Modell EpiDerm^{TM} 200 (EPI-200), immortalisierten Keratinozytenzelllinien (HaCaT und NCTC 2455) und primären normalen humanen epidermalen Keratinozyten (NHEK) gemessen und verglichen. Alle untersuchten *in vitro* Modelle exprimierten basale GST-Aktivität in der gleichen Größenordnung wie humane Haut. Ähnliches gilt auch für NAT- und UGT-Aktivitäten, daher kommen wir in dieser Publikation zu dem Schluss, dass sowohl *in vitro* 2D-Keratinozyten Modelle, als auch 3D-Modelle die Phase 2 Aktivitäten von humaner *ex vivo* Haut gut widerspiegeln. Aus diesem Grund können auch *Monolayer* Zellkulturen ein schnelles, kostengünstiges und brauchbares Werkzeug zur Abschätzung des Gefährdungspotentials einer Substanz darstellen, z.B. wenn diese in erster Linie durch Phase 2 Enzyme metabolisiert wird. Die in dieser Publikation erhobenen Daten helfen dabei, den Fremdstoffmetabolismus der Haut besser zu verstehen und erweitern das Wissen über *in vitro* Alternativmodelle, die in der dermatotoxikologischen Testung zum Einsatz kommen.

XENOBIOTIC METABOLISM CAPACITIES OF HUMAN SKIN IN COMPARISON TO A 3D-EPIDERMIS MODEL AND KERATINOCYTE-BASED CELL CULTURE AS IN VITRO ALTERNATIVES FOR CHEMICAL TESTING : PHASE II

1

XENOBIOTIC METABOLISM CAPACITIES OF HUMAN SKIN IN COMPARISON TO A 3D-EPIDERMIS
MODEL AND KERATINOCYTE-BASED CELL CULTURE AS *IN VITRO* ALTERNATIVES FOR CHEMICAL
TESTING : PHASE II

Christine Götz[1], Roland Pfeiffer[1], Julia Tigges[1], Karsten Ruwiedel[1], Ulrike Hübenthal[1], Hans F Merk[2],
Jean Krutmann[1], Robert J Edwards[3], Josef Abel[1], Camilla Pease[4], Carsten Goebel[5], Nicola Hewitt[6] and
Ellen Fritsche[1,2]

[1] Institut für Umweltmedizinische Forschung (IUF), Heinrich-Heine-University Düsseldorf, Germany

[2] Department of Dermatology and Allergology, University Clinic RWTH Aachen, Germany

[3] Imperial College London, Hammersmith Campus, London UK

[4] Unilever, Safety & Environmental Assurance Centre, Sharnbrook, Bedford, UK

[5] Procter and Gamble, Darmstadt, Germany

[6] Nicky Hewitt Scientific Writing Services, Erzhausen, Germany

Corresponding author: ellen.fritsche@uni-duesseldorf.de

Running title: Phase II xenobiotic metabolism in human skin and in vitro skin models

Words: 3882

Figures: 4

ABSTRACT

The 7th Amendment to the EU Cosmetics Directive prohibits the use of animals in cosmetic testing for certain endpoints, such as genotoxicity. Therefore, skin *in vitro* models have to replace chemical testing *in vivo*. However, the metabolic competence neither of human skin nor of alternative *in vitro* models have so far been fully characterized, although skin is the first-pass organ for accidentally or purposely (cosmetics and pharmaceuticals) applied chemicals. Thus, there is an urgent need to understand the xenobiotic metabolising capacities of human skin and to compare these activities to models developed to replace animal testing. We have measured the activity of the Phase II enzymes GST, UGT and NAT in *ex vivo* human skin, the 3D epidermal model EpiDerm 200 (EPI-200), immortalized keratinocyte-based cell lines (HaCaT and NCTC 2455) and primary normal human epidermal keratinocytes. We show that all three Phase II enzymes are present and highly active in skin as compared to Phase I. Human skin therefore represents a more detoxifying than activating organ. This and the corresponding work on Phase I metabolism (*Goetz et al.*, submitted) compare for the first time systematically enzyme activities of xenobiotic metabolism in four different *in vitro* models directly to human skin. We conclude from our studies that 3D epidermal models, like the EPI-200 employed here, are superior over monolayer cultures in mimicking human skin xenobiotic metabolism and thus better suited for dermatotoxicity testing.

Keywords: skin; xenobiotic metabolism; Glutathione S-Transferase; *N*-Acetyltransferase; UDP-Glucuronosyltransferase

Abbreviations: GST= Glutathione S-Transferase; UGT= UDP-Glucuronosyltransferase; NAT= *N*-Acetyltransferase; 3-MC= 3-methylcholanthrene; EPI-200= reconstituted epidermis model EpiDerm™ (MatTek); NHEK= normal human keratinocytes; HLM= human liver microsomes

INTRODUCTION

Animal testing has been the method of choice for dermatotoxicological testing for decades. Decreasing acceptance of animal use in cosmetic testing in the public arising from ethical objections forces the revision of traditional procedures and the establishment of alternative methods. In addition, for certain endpoints including skin irritation and genotoxicity animal testing for cosmetics is already prohibited by the 7th Amendment to the EU Cosmetics Directive. The need for adequate substitutes is evident, but even though several alternative skin models are available, only poor knowledge exists about the resemblance of their xenobiotic metabolism capacities compared to human skin. As e.g. genotoxicity and skin sensitization are often caused by metabolites of xenobiotics rather than by the unmetabolized parent compounds, metabolic capacities which resemble the *in vivo* situation of an organ are crucial for correct readouts *in vitro*.

To better understand the resemblance of *in vitro* models for metabolic potential of human skin, we assessed Phase I (Goetz *et al*., submitted) and Phase II enzyme activities in human *ex vivo* skin and keratinocyte-derived skin models: a commercially available 3D epidermal model (EPI-200, MatTek Corp.) which is based on primary keratinocytes, HaCaT keratinocytes (1), NCTC 2544 cells (2) as well as primary normal human epidermal keratinocytes (NHEK). While phase I enzyme activities may determine activation and toxification of compounds as is discussed in part one of this work (Goetz *et al*., submitted), this phase II paper (part two) assesses mainly, though not solely, detoxification capacities of human skin and epidermal *in vitro* models. Enzyme activities determined here are Glutathion-S-transferase (GST), UDP-Glucuronosyltransferase (UGT) and N-acetyltransferase (NAT).

MATERIALS AND METHODS

Chemicals and materials

All chemicals, if not otherwise specified, were purchased from Sigma-Aldrich (Taufkirchen, Germany) and were of highest purity available. Cell culture media were obtained from PAA (Pasching, Austria) and PromoCell (Heidelberg, Germany). The CBQCA protein quantification kit was purchased from Molecular Probes/Invitrogen (Darmstadt, Germany). NADPH regeneration system was purchased from Promega (Madison, USA). Liver microsomes were from Celsis In Vitro Inc. (Neuss, Germany).

Cell/tissue culture

HaCaT cells were cultured in DMEM, NCTC 2544 were cultured in MEM each containing 10 % (v/v) fetal calf serum (FCS) and 1 % (v/v) of antibiotic-antimycotic solution (PAA, Cat. No. P11-002). Immortal cells were kindly provided by Helmut Sies, Heinrich-Heine University Düsseldorf. Primary NHEK keratinocytes (Promocell, Heidelberg, Germany) from 30-40 year old female donors (breast) were cultured in Keratinocyte Growth Medium 2 and supplement mix from Promocell (Heidelberg, Germany). All cells were maintained under standard conditions at 37°C and 5% CO_2. Treatment of cells was performed 24h after seeding in 48-well plates in the respective media. For subsequent enzyme assays, the respective media were used without FCS supplement. The human reconstituted epidermis EpiDerm™ (EPI-200) was purchased from Mat Tek Corporation, Ashland, USA (donor 1188 and for one experiment donor 254). After delivery, the tissue recovered for 24 h at 37 °C and 5 % CO_2 in serum-free EPI-100-NMM-PRF media (900 µL per model), unless otherwise noted. EPI-200 induction experiments were carried out in EPI-100-NMM-PRF medium.

Enzyme induction

For enzyme induction, cells and EPI-200 epidermal models were treated systemically with 3-methylcholanthrene (3-MC) dissolved in DMSO as a model genotoxin and incubated for 24 h. Final maximum DMSO concentration was 0.1 %. All experiments were carried out at least in triplicates with 3 independent lots of cells or skin equivalents and 3 repetitions per single lot.

Human *ex vivo* skin samples

Skin samples from breast reduction surgery were obtained from a hospital in Düsseldorf, Germany. The samples originated from n=10 female patients of different age (22-59 years). Patients agreed to donate removed tissue for scientific purpose. The use of *ex vivo* skin from breast reduction has been fully approved by the local Ethics Committee at the Heinrich-Heine-University of Düsseldorf (Project-

Nr.: TOX_EF_D01/2008). Skin samples were collected immediately after surgery, kept cold during the transport (< 1 h) and stored deep-frozen at -80°C until processed.

Preparation of subcellular fractions from human *ex vivo* skin and EPI-200 models

Subcutaneous fat was removed before the skin sample was homogenized in a blender (SW18, Ultra-Turrax, Germany) that was kept on ice (4 °C) during the whole procedure. The homogenization protocol was according to Nelson and coworkers (3). The microsomal fraction was resuspended in microsome buffer (250 mM potassiumphosphate, 30 % glycerol at pH 7.5). Protein quantification was done by using a DC kit (BioRad, Germany) with bovine serum albumin as standard. Protein extraction from EPI-200 was carried out using at least 20 whole epidermis models, which were processed in a glass homogeniser. The number of individual microsome preparations was n=8 for EPI-200 and n=10 for skin biopsies.

Glutathione S-transferase (GST) assay

GST activity was measured using 1-chloro-2,4-dinitrobenzene (CDNB, 1 mM) and reduced glutathione (1mM) according to the protocol by Habig et al. (4). In cell culture and EPI-200, the reaction mixture was applied to monolayers or single EPI-200 models. In EPI-200 induction experiments, S9 protein from topically treated equivalents was measured. Equine liver GST was used as a positive control.

UDP-Glucuronosyltransferase (UGT) assay

UGT was measured with 4-methylumbelliferone (4-MU, 100 µM) and UDP-glucuronic acid (1.7 mM) as published by Sörgel and coworkers (5). Endpoints were measured at 390 nm and 460 nm on a Thermo Ascent Fluoroskan plate reader. Monolayers and EPI-200 were incubated with serum-free assay medium containing 100 µM 4-MU. Media samples were removed after 1 h (monolayer) or 2 h (EPI-200) and diluted 1:20 in 10 mM NaOH before they were measured.

N-Acetyltransferase assay

NAT activity was determined with *p*-toluidine (200 µM) as described (6;7). Keratinocytes and EPI-200 were incubated 1h at 37 °C with serum-free media containing 200 µM *p*-toluidine. Media were then removed and equally processed.

Statistical Analyses

6

All data, if not otherwise specified, are presented as mean ± standard deviation. Data were analyzed using Student's t test (Excel; Microsoft, Redmond, WA). P-values below 0.05 were considered as significant.

RESULTS

XENOBIOTIC PHASE II METABOLISM IN HUMAN SKIN AND EPI-200 MODELS

GST activities were measured in cytosolic fractions of human skin and EPI-200 models because cellular cytosols contain the larger GST superfamily involved in biotransformation of xenobiotics (8). We employed CDNB as a common universal substrate for GST activity in these measurements (9). GST:CDNB activity in untreated whole human skin cytosol was 20 ± 6.8 nmol min^{-1} mg^{-1} with inter-individual differences from 12.8 to 34.2 nmol min^{-1} mg^{-1}. In EPI-200 protein, CDNB conjugation rates were approximately 3-fold higher than in protein from human skin (Figure 1a). GST from equine liver served as positive control and the measured activity of 3505 ± 490 nmol min^{-1} mg^{-1} is similar to published data (10).

In contrast to rates in EPI-200 cytosolic protein, GST activity was substantially lower (4.2 ± 1.6 nmol min^{-1} mg^{-1}) in intact epidermal models (Figure 1b). One hypothesis was that the insert membrane, to which the model is attached, might restrain substrate flow and thus reduce measurable GST activity. Assaying GST with loosely floating EPI-200 tissue (without insert, 1.5 ± 0.4 nmol min^{-1} mg^{-1}), however, demonstrated that lower GST activity of intact EPI-200 was not due to the presence of the insert membrane but most probably due a lack of bioavailability of substrate to the enzyme. The effect of polycyclic aromatic hydrocarbons (PAH) on GST induction in EPI-200 has been examined in a complementary study (Goetz and Hewitt *et al.*, submitted).

4-MU was chosen for assaying UGT activity since it is a preferential substrate for UGT1A (11) and UGT1 is the predominantly expressed group in skin (12). The reaction mixture contained 1 % DMSO to overcome the lipid membrane constraint for the access of the cofactor UDPGA (13-15). This DMSO concentration had no apparent effects on 4-MU glucuronidation in hepatocytes (16) or generally ≤ 20% inhibition in recombinant UGT isoforms (17). UGT rates were 1.3 ($\pm$ 0.2) nmol min^{-1} mg^{-1} in *ex vivo* skin and 1.8 ($\pm$ 0.2) nmol min^{-1} mg^{-1} in EPI-200 microsomes which was not significantly different from each other (Figure 2a). In comparison, rat liver microsomes (3-MC induced) displayed UGT activity of 2.9 ($\pm$ 0.2) nmol min^{-1} mg^{-1} in our setup which is in the range reported in the literature (15). UGT activity in human liver microsomes was similar to the rat (2.7 $\pm$ 0.1 nmol min^{-1} mg^{-1}, data not shown).

UGT activity in whole intact EPI-200 (Figure 2b) was roughly 20 times lower than those measured in the microsomal fraction (0.09 ($\pm$ 0.03) nmol min^{-1} mg^{-1}). Therefore, a similar cell membrane effect as for GST activity was observed for UGT. Again, the influence of the insert membrane was insignificant.

3-MC treatment elicited no relevant induction on UGT activity in EPI-200. At inducer concentrations ranging from 0.2 to 10 µM 3-MC, no significant increase in UGT activity was observed in the epidermal models compared to solvent control (0.11 ± 0.02 nmol min^{-1} mg^{-1} and 0.09 (± 0.01) nmol min^{-1} mg^{-1} for DMSO and 10 µM 3-MC, respectively; data not shown).

For determining NAT activity, a spectrophotometric method with the substrate *p*-toluidine was chosen. Purified NAT from pigeon liver served as positive control (3.4 ±0.7 nmol min^{-1} mg^{-1}). Figure 3a demonstrates that NAT activities were in average approximately two times higher in skin than in EPI-200 cytosol. However, the inter-individual variability was high. NAT polymorphisms might be responsible for this finding (18-21). From 10 individuals tested, four were relatively slow metabolizers of *p*-toluidine in this experimental setup (0.63 – 0.94 nmol min^{-1} mg^{-1}). In comparison, three other donors showed rapid conjugation of the substrate (1.73 – 3.03 nmol min^{-1} mg^{-1}) while the cytosolic protein fractions of the remaining three donors displayed intermediate substrate turnover (Figure 3d). In comparison to the rates from these ten donors, the cytosolic NAT:*p*-toluidine activity of both EPI-200 donors, 1188 and 254, matches the range of the relatively slow metabolizing skin donors (Figure 3c,d).

NAT activity in intact EPI-200 models (0.56 ±0.07 nmol min^{-1} mg^{-1}) was in the range of the rates observed in their cytosolic fractions (Figure 3b), which thus differs to GST and UGT substrate penetration behavior. The presence of the insert was again of minor importance for NAT activity in intact EPI-200. A pre-experiment in EPI-200 confirmed previous knowledge that NAT activity was not inducible by 3-MC (data not shown).

Incubation time and donor may influence enzymatic activities *in vitro*. Therefore, we measured GST, UGT and NAT activities in cytosolic and microsomal fractions prepared from EPI-200 models from two different donors (donors 1188 and donor 254, MatTek Corp.) 24, 48 and 72 h after tissue delivery. Figures 1c-3c demonstrate that enzyme activities of both donors were highly comparable to each other with regard to all enzymes tested. Moreover, enzyme activities did not decrease significantly over the 72 h tested.

XENOBIOTIC PHASE II METABOLISM IN CELL LINES

Basal GST:CDNB activity of all three keratinocyte monolayer cells – HaCaT, NCTC and NHEK - was approximately 50 nmol min^{-1} mg^{-1} total protein (Figure 4a) and thus in the range of GST activity in skin and EPI-200 cytosolic protein (Figure 1a). Monolayer cells were treated with various

concentrations of 3-MC. The PAH did not cause a statistically significant GST induction in comparison to the solvent control (Figure 4a).

At the basal level, UGT activity in all three keratinocyte cell types tested (Figure 4b) was in the range of activity measured in skin microsomes (Figure 2b). The highest basal activity of UGT:4-MU (1.99 ± 0.97 nmol min^{-1} mg^{-1}) was observed in HaCaT cells. There was no significant induction of UGT by 3-MC (0.25 – 10 μM).

The most distinct differences in basal activity of monolayers were observed for NAT:p-toluidine (Figure 4c). HaCaT showed the highest substrate turnover (0.65 ± 0.37 nmol min^{-1} mg^{-1}), while the rates where approximately half in NCTC (0.35 ± 0.22 nmol min^{-1} mg^{-1}) and only a forth in NHEK cells (0.16 ± 0.08 nmol min^{-1} mg^{-1}). No induction of NAT was observed in the cell lines, while a significant reduction in activity after treatment with 1 μM 3-MC in NCTC cells was detected.

DISCUSSION

There is the urgent need for sophisticated and well-characterized *in vitro* models as alternatives to animal testing to assess hazards for human health with the overall goal of consumer protection. In this regard, our work contributes to this necessity by characterizing xenobiotic metabolism capacities of epidermal *in vitro* models and comparing such to human skin. As enzyme activities for phase I xenobiotic metabolism from cytochrome P450 enzymes and cyclooxygenases (COX) is shown elsewhere (Goetz *et al.,* submitted), this work here focuses on phase II drug metabolism of GST, UGT and NAT.

GSTs comprise a multi-gene family of enzymes involved in the detoxification of a wide variety of chemicals, especially electrophilic compounds (22). The most abundant forms are thereby the soluble, cytosolic GST-A, -M, -T and –P forming homo- and heterodimers (8). Human epidermal keratinocytes are known to express significant levels of GST activity towards the universal substrate CDNB (23) and also in human skin cytosol, GST activity has been described (24). Corresponding to these reports, we found noticeable total GST activity in cytosolic protein from human skin which was in the nanomolar range. This compares to cytosolic protein from EPI-200 models with a 3-fold lower GST activity. This finding matches the results reported for human epidermal and EPI-200 protein by Harris et al. (25). A proposed reason for the higher GST activity in the 3D epidermal models compared to human skin was that protein preparations from human whole skin contains dermal protein, which is lacking in the epidermal model. However, epidermal cells presumably represent the major site of xenobiotic metabolism (26;27) and, in contrast to this study, Harris et al. (2002) used scraped-off epidermis for their protein preparation which excludes dilution of epidermal by dermal protein. From this data we conclude that basal cytosolic GST:CDNB activity seems to be constitutively higher in EPI-200 keratinocytes than in cells derived from human skin, possibly due to donor variation or culture conditions used for the EpiDerm. This is also in accordance to a recent study (12) detecting about 2-3 times higher gene expression of GSTA4 and P1 in EPI-200 from various donors compared to full thickness buttock skin. GST-Pi was earlier described as the predominant epidermal GST isoform (24).

That GST activity in intact EPI-200 models was 15-fold lower than in the cytosolic preparations was probably due to barred accessibility of CDNB to the enzyme. It must also be kept in mind that the membrane passage of the lipophilic compound before conjugation is faster than that of the water-soluble glutathione conjugate which is produced intracellularly. CDNB accesses the cell via the membrane by diffusion, while excretion of the conjugate is conducted in an ATP-dependent manner by an organic anion transporter (28). In contrast, excretion is likely to occur faster in cells grown as a

monolayer than in a complex epidermal model. Indeed, CDNB conjugation rates in all intact keratinocyte monolayers were higher than in intact EPI-200. The difference to intact EPI-200 was significant in NHEK. Cell monolayer GST activities were also up to two-fold higher than activities from human skin cytosols. However, we related activities from cells to total cellular protein, while human skin activity was matched to total cytosolic protein. This probably explains the slightly different mean GST activities between these systems. The basal GST activity of keratinocytes detected in our experiments is thereby in agreement with reported ranges (23;29). With regard to induction of GST, 3-MC did not induce enzyme activity in keratinocytes monolayers or 3D epidermal models. This might be due to an already high GST activity in these cells as in comparison e.g. human liver cytosols possess 3 to more than 600 nmol min^{-1} mg^{-1} CDNB:GST activity (30;31). Lack of significant GST induction was also seen in NCTC 2544 by 3-MC (32).

The GST results indicate that human skin as well as all *in vitro* skin alternatives exhibit GST activities in the low nanomolar range which is high compared to liver, an organ which primary role is metabolism and detoxification. This is also true for intact 3D epidermal models although our measurements show that caution has to be exercised to ensure penetration of compounds when used as an *in vitro* test system. GST with CDNB as substrate exhibited the highest conjugation rates of all skin Phase II enzymes examined in these experiments. Therefore, all *in vitro* models tested represent GST metabolism of human *ex vivo* skin well.

Glucuronidation involves the conjugation of a suitable functional group present on a variety of structurally unrelated substrates with glucuronic acid (in our setup 4-MU) and plays an important cytoprotective role (33). The reaction requires UDP-glucuronic acid (UDPGA) as cofactor and is catalyzed by the enzyme UGT (17). This metabolic pathway leads to the formation of water-soluble metabolites (11) similar to the metabolism product of the GSTs. Reports on UGT enzyme activity mostly refer to liver, while activity data on skin UGT is rare. However, reports on indolylacetic acid glucuronides and generation of triclosan glucuronides demonstrate the presence of UGT activity in skin (34;35). Our results support these findings by measuring 4-MU:UGT activity in microsomal preparations from human *ex vivo* skin. UGT activity of EPI-200 microsomes compares very similarly to skin preparations. Remarkably, the ability of human skin to glucuronidate xenobiotics was found to be approximately 50 % of the UGT rates in human liver microsomes. Similar data have been reported for rat skin UGT, whose activity was 10-50 % of that in rat liver (36). In the intact EPI-200 models there was 20 times lower UGT activity than in respective microsomes. Membrane diffusion and excretion are assumed as factors influencing UGT activity. Basal UGT activities in HaCaT, NCTC and NHEK monolayer cells were in the range of skin and EPI-200 microsomes and thus, these keratinocytes/keratinocyte-derived cells represent UGT activity of *ex vivo* human skin.

Previous publications report inducibility of UGT by 3-MC in skin and skin cells in various species (as reviewed in Oesch et al. 2007 (36)) on the expression level. In our experiments UGT was not induced by 3-MC neither in intact EPI-200 nor in keratinocytes. Besides, enzyme activity and gene expression data might not necessarily correlate well. Nevertheless, UGT activity of epidermal *in vitro* models display human *ex vivo* skin adequately.

Human skin also bears high activity of cytosolic *N*-acetylation for detoxification of e.g. arylamines or hydrazines (37;38) and therefore provides 'first-pass' metabolism in skin (39). Unlike the NAT2 enzyme, which is found predominantly in the liver and GI tract, NAT1 is distributed widely in extrahepatic tissues of the body including skin (20;40). Our determination of NAT activities in human skin and EPI-200 cytosols revealed activities in the nanomolar range. This is in agreement with previous data on human skin (37;40). NAT1 is a polymorphic enzyme. Especially the *10 allele seems to determine fast acetylation, whereby fast and slow acetylaters are distinguished by a factor of 4 in enzyme activity within a Chinese population (41). The 10 skin donors investigated in this study reveal an approximately 5-fold difference between the fastest and the slowest metabolizers which is in the same order of magnitude than the Chinese study (Fig. 3d). Based on these results we attributed NAT activity of EPI-200 models, both donors 1188 and 254, the slow metabolizer phenotypes. NAT rates in such EPI-200 cytosolic preparations were in the same range than in intact EPI-200 models implying that the substrate penetrates cell membranes very well. β-naphthylamine and *o*-toluidine penetrate human skin fast and at high percentages (42). Presumably, *p*-toluidine, the NAT substrate employed in this study, shares related penetration characteristics and thus infuses the tissue of the epidermal model faster and at higher concentrations than substrates for GST and UGT. Moreover, the product of *N*-acetylation, as opposed to the other Phase II reactions, is not rendered hydrophilic, but retains its lipophilic character which facilitates membrane passage. This leads to faster enrichment of the conjugate in the medium.

Basal NAT activity towards *p*-toluidine in monolayer cells varied across cell types. While HaCaT displayed the highest and NHEKs showed the lowest NAT activity, NCTC cells found themselves in the middle. Thereby, NHEKS had an approximately 4-fold lower NAT activity than HaCaT cells, which is in accordance to recently published data on NAT rates towards the substrate pABA (43). Bonifas and coworkers (43) also reported that the difference in NAT activity in HaCaT cells and NHEKs is not due to cell culture conditions. However, one would expect NAT activity of NHEKs to vary amongst different donors and thus must be assessed for each individual. Our data shows that HaCaT have the closest NAT activity to human skin. Despite differences in acetylation capacities, skin and all epidermal *in vitro* models possess comparable NAT activities in the very low nanomolar range and thus reflect NAT activity found in human *ex vivo* skin.

Oesch et al. (36) comprehensively reviewed that drug metabolism is different in skin from various species and also in skin cells and assumed that 3D organotypic models come closest to the situation of whole skin. This and the respective work on phase I metabolism (Goetz et al., submitted) provide an experimental rationale to this assumption comparing for the first time systematically enzyme activities of xenobiotic metabolism in four different *in vitro* models directly to human skin. This work clearly indicates that 3D epidermal models, like the EPI-200 employed here, are superior over monolayer cultures in mimicking human skin xenobiotic metabolism. This superiority ensues not so much from phase II metabolism which is present at high and similar rates in skin and all epidermal *in vitro* models tested, but relates to distinct phase I enzyme activities, especially cyclooxygenases, in monolayer compared to 3D organotypic cultures. Therefore, depending on the proposed metabolism of a compound, e.g. mainly acetylation, monolayer cultures might still represent a quick, inexpensive and useful tool for hazard assessment.

CONFLICT OF INTEREST

The authors state no conflict of interest.

14

Reference List

1 Boukamp P, Petrussevska RT, Breitkreutz D, Hornung J, Markham A, Fusenig NE. J Cell Biol 1988; **106**(3): 761-771.

2 Bakken PC, Evans VJ, Earle WR, Stevenson RE. Am J Epidemiol 1961; **73**(1): 96-104.

3 Nelson AC, Huang W, Moody DE. Drug Metab Dispos 2001; **29**(3): 319-325.

4 Habig WH, Pabst MJ, Jakoby WB. J Biol Chem 1974; **249**(22): 7130-7139.

5 Sörgel E, Beyhl FE, Mutschler E. Experientia 1980; **36**: 861-863.

6 Andres HH, Klem AJ, Szabo SM, Weber WW. Anal Biochem 1985; **145**: 367-375.

7 Dairou J, Atmane N, Rodrigues-Lima F, Dupret JM. J Biol Chem 2004; **279**(9): 7708-7714.

8 Hayes JD, Strange RC. Pharmacology 2000; **61**(3): 154-166.

9 Lyubenova L, Götz C, Golan-Goldhirsh A, Schröder P. Int J Phytorem 2007; **9**: 465-473.

10 Nebbia C, Dacasto M, Carletti M. Life Sci 2004; **74**(13): 1605-1619.

11 Tukey RH, Strassburg CP. Ann Rev Pharmacol Toxicol 2000; **40**(1): 581-616.

12 Hu T, Khambatta ZS, Hayden PJ, Bolmarcich J, Binder RL, Robinson MK *et al.* Toxicol in Vitro 2010; **24**(5): 1450-1463.

13 Soars MG, Ring BJ, Wrighton SA. Drug Metab Dispos 2003; **31**(6): 762-767.

14 Notman R, Noro M, O'Malley B, Anwar J. J Am Chem Soc 2006; **128**(43): 13982-13983.

15 Letelier ME, Lagos F, Faúndez M, Miranda D, Montoya M, Aracena-Parks P *et al.* Chem Biol Int 2007; **167**(1): 1-11.

16 Easterbrook J, Lu C, Sakai Y, Li AP. Drug Metab Dispos 2001; **29**(2): 141-144.

17 Uchaipichat V, Mackenzie PI, Guo XH, Gardner-Stephen D, Galetin A, Houston JB *et al.* Drug Metab Dispos 2004; **32**(4): 413-423.

18 Rodrigues-Lima F, Dupret JM. Curr Pharm Des 2004; **10**: 2519-2524.

19 Dupret JM, Rodrigues-Lima F. Curr Med Chem 2005; **12**: 311-318.

20 Minchin RF, Hanna PE, Dupret JM, Wagner CR, Rodrigues-Lima F, Butcher NJ. Int J Biochem Cell Biol 2007; **39**(11): 1999-2005.

21 Grant DM, Hughes NC, Janezic SA, Goodfellow GH, Chen HJ, Gaedigk A *et al.* Mut Res Mol Mech Mutagen 1997; **376**(1-2): 61-70.

22 Eaton DL, Bammler TK. Toxicol Sci 1999; **49**(2): 156-164.

15

23 Zhang Y, Gonzalez V, Xu MJ. J Dermatol Sci 2002; **30**(3): 205-214.

24 Raza H, Awasthi YC, Zaim MT, Eckert RL, Mukhtar H. J Invest Dermatol 1991; **96**(4): 463-467.

25 Harris IR, Siefken W, Beck-Oldach K, Brandt M, Wittern KP, Pollet D. Skin Pharmacol Physiol 2002; **15**(Suppl. 1): 59-67.

26 Baron JM, Holler D, Schiffer R, Frankenberg S, Neis M, Merk HF *et al.* J Invest Dermatol 2001; **116**(4): 541-548.

27 Swanson HI. Chem Biol Int 2004; **149**: 69-79.

28 Roelofsen H, Schoemaker B, Bakker C, Ottenhoff R, Jansen PL, Elferink RP. Am J Physiol Gastrointest Liver Physiol 1995; **269**(3): G427-G434.

29 Hirel B, Chesne C, Pailheret JP, Guillouzo A. Toxicol in Vitro 1995; **9**(1): 49-56.

30 Pacifici GM, Franchi M, Colizzi C, Giuliani L, Rane A. Arch Toxicol 1988; **61**(4): 265-269.

31 Howie AF, Forrester LM, Glancey MJ, Schlager JJ, Powis G, Beckett GJ *et al.* Carcinogenesis 1990; **11**(3): 451-458.

32 Gelardi A, Morini F, Dusatti F, Penco S, Ferro M. Toxicol in Vitro 2001; **15**(6): 701-711.

33 Grancharov K, Naydenova Z, Lozeva S, Golovinsky E. Pharmacol Ther 2001; **89**: 171-186.

34 Ademola JI, Wester RC, Maibach HI. J Pharm Sci 1993; **82**(2): 150-154.

35 Moss T, Howes D, Williams FM. Food Chem Toxicol 2000; **38**(4): 361-370.

36 Oesch F, Fabian E, Oesch-Bartlomowicz B, Werner C, Landsiedel R. Drug Metab Rev 2007; **39**(4): 659-698.

37 Kawakubo Y, Yamazoe Y, Kato R, Nishikawa T. Skin Pharmacol Physiol 1990; **3**(3): 180-185.

38 Summerscales JE, Josephy PD. Mol Pharmacol 2004; **65**(1): 220-226.

39 Goebel C, Hewitt NJ, Kunze G, Wenker M, Hein DW, Beck H *et al.* Toxicol Appl Pharmacol 2009; **235**(1): 114-123.

40 Kawakubo Y, Merk HF, Masaoudi TA, Sieben S, Blömeke B. J Pharmacol Exp Ther 2000; **292**(1): 150-155.

41 Zhangwei X, Jianming X, Qiao M, Xinhua X. Clin Chim Acta 2006; **371**(1-2): 85-91.

42 Luersen L, Wellner T, Koch HM, Angerer J, Drexler H, Korinth G. Arch Toxicol 2006; **80**(10): 644-646.

43 Bonifas J, Hennen J, Dierolf D, Kalmes M, Blömeke B. Toxicol in Vitro 2010; **24**(3): 973-980.

FIGURE LEGENDS

Figure 1: GST activity towards CDNB (nmol min^{-1} mg^{-1}).

a: Enzyme activity in the cytosolic fraction from skin and EPI-200.

b: Enzyme activity in fully intact EPI-200 models assayed with insert (+ insert) or without (- insert).

c: Enzyme activity in cytosolic fractions prepared from EPI-200 after different cultivation durations (24-72 h) in donors 1188 and 254 (MatTek Corp.).

Error bars are mean +/- SD. The asterisk indicates significant difference (p=0.05).

Figure 2: UGT activity towards 4-MU (nmol min^{-1} mg^{-1}).

a: Enzyme activity in microsomes from skin and EPI-200.

b: Enzyme activity in fully intact EPI-200 models assayed with insert (+ insert) or without (- insert).

c: Enzyme activity in microsomes prepared from EPI-200 after different cultivation durations (24-72 h) in donors 1188 and 254 (MatTek Corp.).

Error bars are mean +/- SD.

Figure 3: NAT activity towards p-toluidine (nmol min^{-1} mg^{-1}).

a: Enzyme activity in the cytosolic fraction from skin and EPI-200.

b: Enzyme activity in fully intact EPI-200 models assayed with insert (+ insert) or without (- insert).

c: Enzyme activity in cytosolic fractions prepared from EPI-200 after different cultivation durations (24-72 h) in donors 1188 and 254 (MatTek Corp.).

d: Individual NAT activities depending on skin donor (D= donor number).

Error bars are mean +/- SD.

Figure 4: Specific phase II enzyme activities measured in living monolayer cell culture (HaCaT, NCTC, NHEK).

a: GST:CDNB, b: UGT:4-MU, c: NAT:p-toluidine, induced by the model compound 3-MC [μM]. For each substrate, cells from n=3 independent passages were used.

Error bars are mean +/- SD. The asterisk indicates significant difference (p=0.05) to solvent control (DMSO).
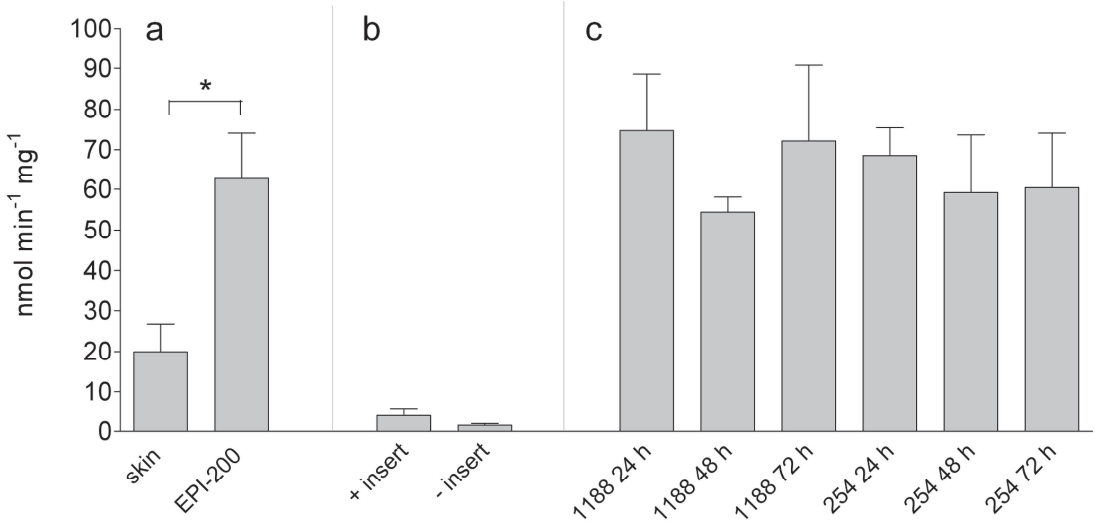
1
2
3
4
5
6
7
8
9
10
11
12
13
14
15
16
17
18
19
20
21
22
23
24
25
26
27
28
29
30
31
32
33
34
35
36
37
38
39
40
41
42
43
44
45
46
47
48
49
50
51
52
53
54
55
56
57
58
59
60

Figure 2
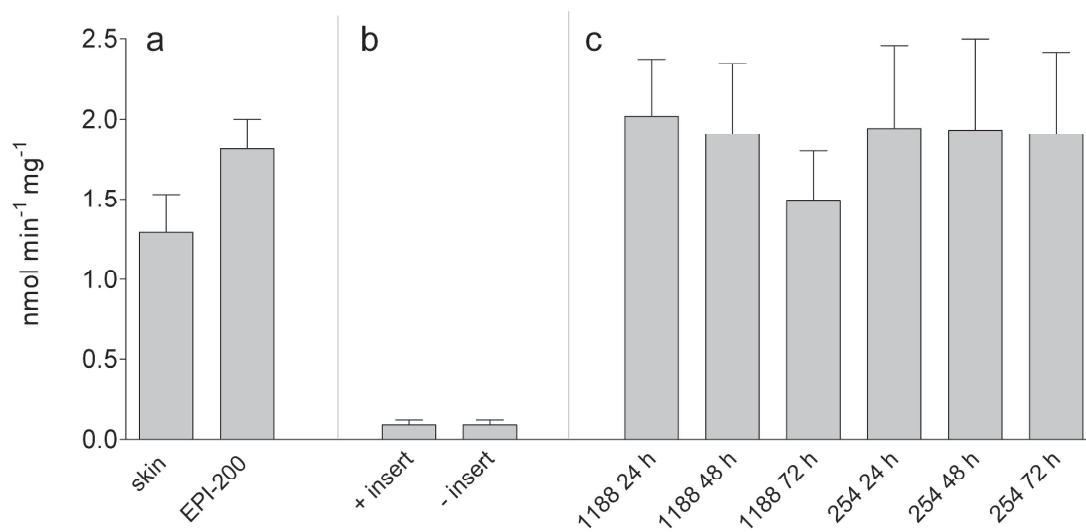
Figure 2

1
2
3
4
5
6
7
8
9
10
11
12
13
14
15
16
17
18
19
20
21
22
23
24
25
26
27
28
29
30
31
32
33
34
35
36
37
38
39
40
41
42
43
44
45
46
47
48
49
50
51
52
53
54
55
56
57
58
59
60

Figure 3
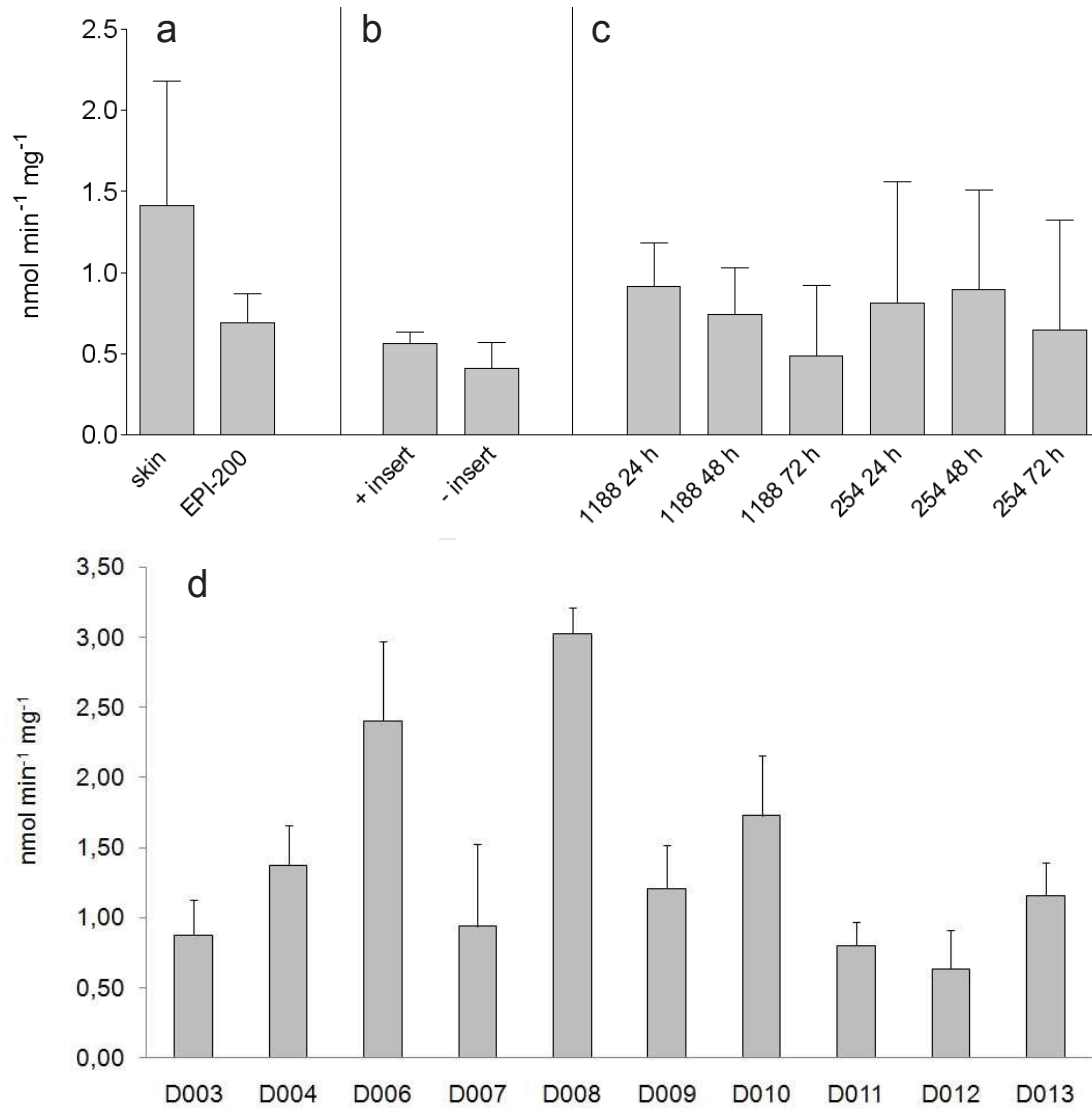
1
2
3
4
5
6
7
8
9
10
11
12
13
14
15
16
17
18
19
20
21
22
23
24
25
26
27
28
29
30
31
32
33
34
35
36
37
38
39
40
41
42
43
44
45
46
47
48
49
50
51
52
53
54
55
56
57
58
59
60

Figure 4
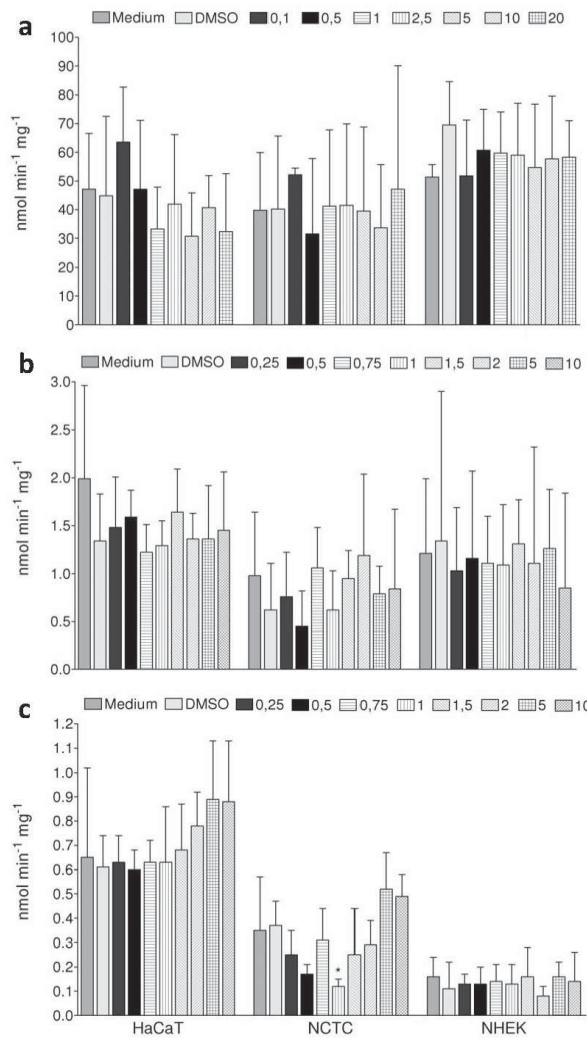
Publikation Nr. 2

Xenobiotic metabolism capacities of human skin in comparison to 3D-epidermis models and keratinocyte-based cell culture as *in vitro* alternatives for chemical testing: Phase II

Christine Götz, Roland Pfeiffer, **Julia Tigges**, Ulrike Hübenthal, Hans F Merk, Jean Krutmann, Robert J Edwards, Josef Abel, Camilla Pease, Carsten Goebel, Nicola Hewitt und Ellen Fritsche

— · — · — · — · — · — · — · — · — · — · — —

2.3   Publikation 3

Effects of the genotoxic compounds, benzo(a)pyrene and cyclophosphamide on phase 1 and 2 activities in EpiDerm[TM] models

Da die siebte Änderung der EG-Kosmetik-Richtlinie (76/768/EWG) seit 2009 den Gebrauch von *in vivo* Modellen zur Testung von Kosmetika auf Genotoxizität untersagt, besteht die Notwendigkeit passende *in vitro* Alternativmethoden zu entwickeln. Der Mikronukleus Assay in dreidimensionalen (3D) EpiDerm[TM] Epidermismodellen (EPI-200) (RSMN) bietet daher einen vielversprechenden neuen Ansatz für die Evaluierung des genotoxischen Potentials dermal applizierter Chemikalien. Die durchgeführten Untersuchungen zeigten, dass sowohl die Aktivität von Phase 1 Enzymen des Fremdstoffmetabolismus (7-Ethoxyresorufin-O-Deetylierung und Testosteron Metabolismus), die bei der metabolischen Aktivierung vieler potentiell genotoxischer Substanzen von Bedeutung ist, als auch entsprechende Phase 2 Aktivität (GST und UGT) in dem untersuchten *in vitro* Modell EPI-200 basal vorhanden ist. Mit Ausnahme von GST, dessen Aktivität zwischen 24 und 48 Stunden abfiel, waren die untersuchten Enzymaktivitäten über einen Zeitraum von 72 Stunden konstant. Für weiterführende Untersuchungen wurden die genotoxischen Chemikalien Cyclophosphamid (CPA) und Benzo(a)pyren (B(a)P) appliziert. Die EROD Aktivität wurde durch B(a)P signifikant induziert, nicht aber durch CPA. CPA, B(a)P und die Kontrollsubstanz β-Naphtoflavon führten alle zu einer geringen Induktion der GST-Aktivität, wobei das Ausmaß der Induktion, literaturkonform, deutlich hinter dem für EROD ermittelten zurückblieb. Zusammenfassend ist eine Anzahl an metabolischen Enzymaktivitäten in EPI-200-Hautmodellen vorhanden und zumindest die CYP1 Familie ist auch signifikant induzierbar. Aus diesem Grund benötigt der RSMN Assay möglicherweise kein exogenes metabolisches Aktivierungssystem für Substanzen, die über diese Wege aktiviert oder detoxifiziert werden.
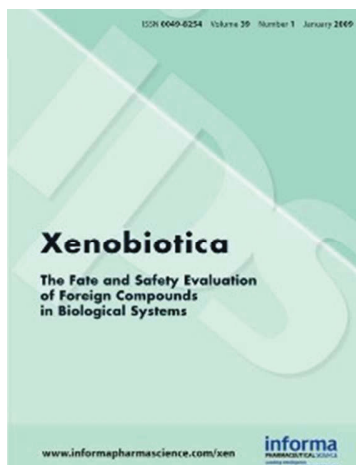
Effects of the genotoxic compounds, benzo[a]pyrene and cyclophosphamide on phase 1 and 2 activities in EpiDerm™ models

Journal:	*Xenobiotica*
Manuscript ID:	TXEN-2011-0183
Manuscript Type:	Original Article
Keywords:	skin metabolism, 7 ethoxyresorufin O-deethylation, induction, UDP-glucuronosyltransferases, glutathione S-transferases, Induction

SCHOLARONE™
Manuscripts

Abstract

1. The micronucleus assay in the 3D human reconstructed EpiDerm^{TM} skin model (RSMN) is a promising new assay for evaluating genotoxicity of dermally applied chemicals.

2. To complement the testing of metabolically activated chemicals, such as cyclophosphamide (CPA) and benzo[a]pyrene (B[a]P), we measured phase 1 (ethoxyresorufin O-deethylation (EROD) and testosterone metabolism) and 2 activities (UGTs and GSTs) in non-treated and genotoxin treated EpiDerm^{TM} models in a study design which mimics the RSMN assay. The assay involved a 3 dose dosing regimen over 72 h to take into account effects e.g. enzyme induction, which require longer than the standard 2 dose 48 h assay.

3. These studies demonstrated the presence of basal phase 1 and 2 activities of EpiDerm™ models.

4. With the exception of GST all of the activities measured did not reproducibly change over time.

5. It was possible to measure enzyme induction using this assay design. EROD activity was significantly induced by B[a]P but not by CPA. CPA and B[a]P had little or no reproducible effects on GST and UGT activities.

6. In conclusion, a number of metabolic enzyme activities were present in the EpiDerm^{TM} skin model and at least the CYP1 family was inducible.

Introduction

As a result of the 7th Amendment of the Cosmetics Directive [EU, 2003], cosmetic ingredients can no longer be tested for genotoxicity in *in vivo* assays. Therefore, much effort has been made on the development of a micronucleus assay in the 3D human reconstructed EpiDerm[TM] skin model (RSMN) [Curren et al., 2006, Dahl et al., 2011, Hu et al., 2009a, Munn et al., 2009]. This is a promising new assay for evaluating genotoxicity of dermally applied chemicals and results to date demonstrate international inter-laboratory and inter-experimental reproducibility of the assay for chemicals that do not undergo metabolism [Aardema et al., 2010]. Ongoing studies in the Colipa-funded (European Cosmetics Association) project include the testing of chemicals which are metabolically activated to the genotoxic metabolite. Initial findings suggest that the EpiDerm[TM] model can also correctly identify a number of genotoxicants which have been shown to be metabolically activated in hepatic models and human lymphocytes (data not shown), e.g. cyclophosphamide [Cao et al., 1993; Elhajouji et al., 1994] and benzo[a]pyrene (B[a]P [Elhajouji et al., 1994; Wu et al., 2003].

EpiDerm[TM] [Hu et al., 2010] and other reconstructed skin models [Luu-The et al., 2009] are prepared from primary human keratinocytes and have been shown to exhibit a metabolic potential which is similar to normal human skin, at least with respect to the mRNA expression of these enzymes [Hu et al., 2010]. However, the presence of mRNA expression does not always infer that the respective enzyme protein is present and, moreover, functional [Pushparajah, 2008a]. There are reports of functional enzyme activity measurements in skin models and, indeed, EpiDerm[TM] models have been reported to have measureable N-acetyltransferase activities [Hu et al., 2009b]. We have extended investigations of the metabolic capacity of EpiDerm[TM] models to include a study design which mimics the pre-validated RSMN [Dahl et al., 2010] with the measurement of a limited number of basal phase 1 and 2 activities. Few have reported whether the chemicals under investigation alter the metabolic enzyme levels; therefore, we have also investigated whether known genotoxicants alter (i.e. either increase or decrease) enzyme activities when they are applied to EpiDerm[TM] models under the same incubation conditions as those used in the RSMN assay. The design of these studies includes a 72 h total treatment period (i.e. 3 daily doses) for two reasons (1) some metabolic enzyme activities (e.g.

PXR or CAR mediated CYPs) require an induction period of up to 72 h [LeCluyse et al., 2000];

therefore, we wanted to maximize the chances of detecting an alteration in enzyme activities and (2) in

certain circumstances, the extension of the RSMN incubation time from 48 h to 72 h may be required,

especially for metabolically activated genotoxicants [Dahl et al., 2010].

Cyclophosphamide and B[a]P were chosen as model bioactivated genotoxicants for these studies.

B[a]P is metabolized mainly by CYP1B1, CYP1A1 and microsomal epoxide hydrolase [Hvastkovs et

al., 2007] and in part by CYP2C9, and CYP3A4 which produce the 3-hydroxy metabolite [Gautier et

al., 1996]. In the skin, pro mutagen and mutagen formations are dependent on the CYP1 family, which

is inducible by UV radiation and environmental poly aromatic hydrocarbons [Afaq et al., 2009,

Swanson, 2004], to the ultimate carcinogen, B[a]P-diolepoxide. Modulation of CYPs has been shown

to alter the amount of DNA adducts formed in HepG2 cells [Wei et al., 2009]; therefore, metabolism

plays an important role in the mechanism of B[a]P carcinogenesis. CYP1A1 is reported to be absent in

native human skin but is induced by B[a]P [Oesch et al., 2007], making this an appropriate test

chemical for our studies. Since CYP1A1 and CYP1B1 are responsible for the bioactivation of many

pro- genotoxicants [Pelkonen and Nebert, 1982], the O-deethylation of the CYP1 substrate

7-ethoxyresorufin (EROD) was measured in EpiDerm^{TM} models 24 h after each dose of test chemical.

Rather than add the substrate to the medium underneath the model, 7-ethoxyresorufin was added in

acetone to the surface – in the same way as the test chemicals. The presence of lipophilic solvents is

known to enhance compound penetration into the skin [Guy et al., 1990]; therefore, we dissolved both

test chemicals and substrates in acetone to maximize penetration into the models. Previous studies

have shown that treatment of the EpiDerm™ models with 10 µl acetone is not toxic and does not

cause an increased frequency of micronuclei compared to non-treated models [Dahl et al., 2010]. The

penetration into the deeper epidermal layers of the relatively lipophilic 7-ethoxyresorufin from the

model surface was considered to be greater than when it was added to the more hydrophilic medium.

The incubation time was set to 6 h to allow for both penetration of the substrate into the model and

metabolism (which is known to be much lower than in hepatic models [Oesch et al., 2007]). We found

3

that this was sufficient to allow some of the metabolites to be detected in the medium below the model.

The metabolism of cyclophosphamide is mainly via CYP2B6, and this enzyme is also induced by cyclophosphamide in human hepatocytes [Gervot et al., 1999]. Cyclophosphamide is also metabolized via CYP2A6, 2C8, 2C9, 2C19, 3A4 and 3A5 but these CYPs have a much lower contribution than CYP2B6 [Xie et al., 2003]. Notably, the expression of CYP2B6 is reported to be absent in the EpiDerm^{TM} donors (donor 1188 and 254) used in these studies [Hu et al., 2010b]. Of the other CYPs involved in cyclophosphamide metabolism, only CYP2C9 and CYP3A5 were expressed [Hu et al., 2010b]. We therefore used testosterone as a marker substrate for CYP2B6 (16β-hydroxide), CYP2C (producing 16α-hydroxide but also partly responsible for producing 16β-hydroxide) and CYP3A4 (6β-hydroxide and 2β-hydroxide) [Tachibana and Tanaka, 2001]. The major metabolite of testosterone in skin is androstenedione [Beckley Karty et al., 1997], which is catalyzed by 17β-hydroxysteroid oxidoreductase and CYP2C19 in the liver [Tachibana and Tanaka, 2001]. Therefore, this metabolite was also quantified in EpiDerm™ model incubates with testosterone. As with ethoxyresorufin, this lipophilic substrate was dissolved in acetone and added to the surface of the EpiDerm^{TM} models.

B[a]P is reported to also induce glutathione S-transferase (GST) activities in HepG2 cells, which confers protection against the formation of reactive metabolites [Wei et al., 2009]. The skin exhibits appreciable GST activity [Oesch et al., 2007], although still not in levels as high as those reported in human liver (300-500 nmol/min/mg protein in liver slices incubated with CDNB [Pushparajah et al. 2008b] and the EpiDerm^{TM} models used in our studies have been shown to express certain GSTs [Hu et al., 2010b]. Considering B[a]P induced GST activities in liver slices [Pushparajah et al. 2008b], it was of interest to determine whether B[a]P also alters the levels of this detoxification enzyme under the conditions of the 72 h RSMN assay. The reactive metabolites of cyclophosphamide are also detoxified by GSTs [Dirven et al., 1994]; therefore, the effect of both B[a]P and cyclophosphamide on the metabolism of the broad spectrum GST substrate, CDNB, was also measured. The conjugation of CDNB with glutathione is catalyzed by a number of GST isoenzymes, including the α, μ and π-classes

4

[Sherratt and Hayes, 2002] with π representing the predominant class in human skin [Raza et al. 1991]. It was not possible to measure GST activity by adding the substrate to the surface of the model; therefore, CDNB metabolism was measured in S9 prepared from the models 24 h after test chemical dosing.

The metabolites of B[a]P are also subject to conjugation by UDP-glucuronosyltransferases (UGTs, [Mackensie et al., 1993]), of which UGT1A6 is reported to be present in the EpiDerm™ donors used in our studies [Hu et al., 2010b]. Therefore, basal UGT activities in acetone and test chemical treated EpiDerm™ models were measured using 4-methylumbelliferone as a broad spectrum substrate. As with 7-ethoxyresorufin and testosterone, this substrate was dissolved in acetone and added to the surface of the EpiDerm™ models and the amount of glucuronide metabolite formed was determined by measuring the amount of 4-methylumbelliferone consumed over 6 h of incubation.

These studies were designed to determine basal metabolic enzyme activities over time under the same conditions as those used in the RSMN assay and whether the test chemicals themselves altered the activities. In addition to metabolic activities, the morphology of the EpiDerm™ models was monitored over 72 h. This allowed a comparison of activities with the visual differentiated state of the models with respect to time.

Methods

Materials

The EpiDerm™ Skin Model, EPI-200-MNA-kit (including the phenol red-free New Maintenance Medium (containing keratinocyte growth factor) and Ca^{2+}- and Mg^{2+}-free Dulbecco's phosphate-buffered saline (CMF-DPBS) was from MatTek, USA. The donors used were EPI-200-MNA-D2-254 (donor 254) and EPI-200-MNA-D2-2 1188 (donor 1188). All chemicals, unless otherwise specified, were purchased from Sigma-Aldrich (Germany) and were of the highest purity available.

Cryosectioning of EpiDerm™ models

EpiDerm™ models were retained for cryosectioning with hematoxylin-eosin staining at 24 h, 48 h and 72 h after arrival. Briefly, the models embedded in tissue freezing medium (Sakura TissueTek, USA) and frozen in a cryostat. The models were then cut into sections (8 µm) and mounted onto microscope slides (Thermo Superfrost, Germany). The sections were fixed in ice-cold acetone, dehydrated and stained with hematoxylin-eosin.

Treatment of EpiDerm™ models

An overview of the treatment of the EpiDerm™ models is shown in Figure 1. On the day of receipt (Day 0), 1 ml of warmed New Maintenance Medium was transferred into the appropriate wells of 6-well plates. The EpiDerm™ models were then transferred into 6-well plates. The EpiDerm™ models were incubated at 37 ± 1ºC in a humidified atmosphere of $5 \pm 1\%$ CO_2 in air (standard culture conditions) for 1 h before dosing with 10 µl of the test chemical, vehicle control, or reference compound on to the surface of the models. The term "reference compound" refers to compounds which are known to induce activities in human hepatocytes but not necessarily in skin models. The doses of test compounds were 2 µg/cm^2 and 50 µg/cm^2 B[a]P and 50 µg/cm^2 and 1000 µg/cm^2 cyclophosphamide. The top doses were based on those which are known to cause micronuclei in EpiDerm™ models [Aardema et al., 2010; Zhao et al., 1999]. The vehicle control, acetone, has been shown not to increase the rate of micronucleus formation in this model [Dahl et a., 2010] and can therefore be considered to be a "true negative" chemical. The models were incubated under standard

culture conditions. After 24 h (Day 1), 48 h (Day 2) and 72 h (Day 3), the medium from each model was collected and stored for lactate dehydrogenase measurement using the CytoTox 96® Non-Radioactive Cytotoxicity Assay from Promega Corp, USA. The lactate dehydrogenase activity in the medium without models was also determined. On Day 1 and 2, the medium was replaced with fresh warm New Maintenance Medium, and the model was dosed again and incubated under standard culture conditions. Twenty-four hours after each dose of test chemical (on Days 1, 2 and 3), the phase 1 and 2 enzyme activities were measured in 2-3 models per experiment (two experiments per enzyme activity measured). For each activity measured, the medium was refreshed 1 h prior to the addition of the substrate.

EROD activity was measured by applying the substrate, 7-ethoxyresorufin, directly to the epidermal model surface and measuring the metabolite, resorufin, in the tissue and medium. The phase 1 and 2 inhibitors, dicoumarol (which inhibits DT-diaphorase [Nims et al., 1984] and salicylamide (which inhibits sulfate- and glucuronide-conjugation [Bennet et al., 1975; Heath and Dingell, 1974]) did not significantly affect the production of resorufin under the conditions used in these studies (data not shown). Ethoxyresorufin (10 μl of 2.5 mM solution in acetone) was added to the surface of the models. The models were then incubated for 6 h in standard culture conditions. After this time the medium and models were separated. The models were homogenized in 200 μl homogenization buffer (0.25 M potassium phosphate, 0.15 M potassium chloride and 1 mM EDTA pH 7.25) using a Retsch TissueLyser and then centrifuged at 9000 ×g for 5 min at 4°C to remove debris. The fluorescence of a 100 μl aliquot of the medium, the model S9 fraction and appropriate control samples (to account for background fluorescence from the 7-ethoxyresorufin and medium components) was measured at an excitation wavelength of 544 nm and an emission wavelength of 590 nm. The amount of resorufin formed was calculated with respect to a standard curve.

Testosterone metabolism was measured by applying 10 μl of 50 mM testosterone (equivalent to a final concentration of 500 μM when considering the medium and skin volumes) to the surface of the models and incubating for 6 h under standard culture conditions. The concentration of testosterone

was in line with that used by others characterizing hepatic models [Brown et al., 2007] and was

purposely high to take into account maximum exposure of this substrate to all layers of the EpiDerm™

models. Preliminary results showed that testosterone hydroxides were not significantly conjugated

since inclusion of salicylamide in the incubation did not affect the amount of 6β-hydroxytestosterone

detected (data not shown). After 6 h, the medium and models were separated and immediately frozen

and stored at -80 °C until analysis. The internal standard, 11α-hydroxyprogesterone (50 µl of 5 µg/ml

solution in methanol:water 55:45 (v/v)) was added to 450 µl of medium. Dichloromethane (4 ml) was

added and the sample mixed. The organic phase was transferred to a new tube and evaporated using an

Eppendorf concentrator at 30°C for 30 min. The samples were reconstituted in 200 µl methanol:water

55:45 (v/v). The EpiDerm™ models were homogenized in 500 µl methanol:water (70:30 (v/v)) and

then spiked with 50 µl 11α-hydroxyprogesterone. The homogenized samples were centrifuged at 9000

×g for 10 min and the supernatant was extracted in the same way as for the medium samples. The

samples were analyzed by HPLC (Beckman Gold Nouveau System) using EC 250/4 Nucleosil 100-5

C18 column and a CC 8/4 Nucleosil 100-5 C18 guard column (Macherey-Nagel, Germany)

maintained at 37 °C. The mobile phases were (A) 100 % ultrapure HPLC water and (B) 100% MeOH

(Carl Roth, Germany). The gradient was as follows: 0-13 min 55 % B; 13-20 min 100 % B; 20-29 min

55 % B. Peak detection was carried out with a Shimadzu SPD UV detector set to 252 nm. The

chromatograms were analyzed with the Beckman Gold Nouveau software. Testosterone,

androstenedione and hydroxytestosterone metabolites were quantified using synthetic standards.

UGT activity was measured by adding the substrate, 4-methylumbelliferone, directly to the epidermal

model surface and measuring the decrease in fluorescence in the skin and medium compared to control

incubations (containing the same concentration of substrate in trans-wells without EpiDerm™

models). 4-Methylumbelliferone (10 µl of a 10 mM stock solution in acetone) was added to the

surface of the models which were then incubated for 6 h in standard culture conditions. After this time

the medium and models were separated. The models were homogenized in 100 µl methanol:water

70:30 (v/v), using a Retsch TissueLyser and then centrifuged at 9000 ×g for 5 min at 4°C to remove

debris. A 10 µl aliquot of the samples (medium and the model S9 fraction) was added to 190 µl 10

mM sodium hydroxide and the fluorescence was measured at 390 excitation and 460 nm emission

using a microplate spectrofluorimeter. The amount of substrate remaining was calculated with respect

to a standard curve of 4-methylumbelliferone. Background fluorescence from the medium was

measured and confirmed to have no influence on the measurement of the substrate.

Unlike the other three activities, GST activity was measured by addition of the substrate, CDNB, to

tissue S9 fractions. At each time point, the EpiDerm™ models were homogenized in 100 µl

homogenization buffer. The homogenized samples were centrifuged at 9000 ×g and 4 °C for 10 min to

remove debris. The resultant S9 fraction contained on average 3.6 ± 0.4 mg/ml protein). A 20 µl

aliquot was added to 180 µl of the reaction mixture. The reaction mixture contained 100 mM

potassium phosphate buffer (pH 6.5 (at which pH non-enzymic conjugation is minimal [Habig et al.,

1974]), 1 mM CDNB and 1 mM reduced glutathione. The reaction was started by the addition of

CDNB and the production of the conjugate was followed by measuring the rate of absorbance change

over 5 min in a plate reader set at 340 nm. Rates were calculated using the extinction coefficient 9.6

mM^{-1} cm^{-1} [Habig et al., 1974] adjusted to the path length of the solution per well (5.03 mM^{-1} cm^{-1}).

Statistical evaluation

Results were compared using the Student's unpaired t-test. $p < 0.05$ was considered significant. "n" is

the number of models in each experiment.

Results

Morphology of EpiDerm™ models over 72 h

Figure 2 shows the cross section of the EpiDerm™ models at 24 h, 48 h and 72 h in culture. After 24 h, the EpiDerm™ model contained basal, spinous, granular, and cornified layers, reflecting the structure of epidermis *in vivo*. There was notable stratum corneum thickening of the models over time. Apart from the thickness, there was little difference in the structure of the stratum corneum between 24 h and 48 h but by 72 h it was less compact than earlier time points. The basal, spinous, granular cells were still evident at 72 h.

Basal activities in EpiDerm™ models over 72 h

Table 1 summarizes the phase 1 and 2 activities measured in EpiDerm™ models treated with the vehicle control, acetone, over 72 h. These data are the average values from two experiments and up to six models and differences were based on the average value, as well as the reproducibility across the two experiments. EROD activities at all three time points were considered to be at the limits of detection of the assay design (0.025 pmol/min/model, considering the background fluorescence of the ethoxyresorufin present in either the EpiDerm™ models and medium, data not shown). The majority (97-90%) of the metabolite, resorufin, was detected in the medium at all incubation time points. The only hydroxy- metabolite, 6β-hydroxytestosterone, was present in all models at each time point measured. The majority (71-75%) of this metabolite was detected in the medium after the 6 h incubation at each time point. When testosterone 6β-hydroxylase activities from all models were averaged, this activity at 24 h was not significantly different from that at 48 h or 72 h. Although there was a statistically significant difference ($P<0.05$) in a single experiment (Figure 4A) between the 24 h and 72 h time points, the actual difference was 2 pmol/min/mg protein, which cannot be considered relevant when compared to the range of activities (thousands of pmol/min/mg) in human hepatocytes [LeCluyse et al., 2000]. Androstenedione was also formed by all EpiDerm™ models and, like 6β-hydroxytestosterone, most of this metabolite was detected in the medium (80 %). The production of androstenedione was similar in EpiDerm™ models incubated at 24 h, 48 h and 72 h. Unlike the metabolites of testosterone, the parent compound itself was mainly detected in the EpiDerm™ models

10

(66-73% of the total applied). The amount of testosterone remaining in the EpiDerm™ models was the same at all time points (73 ± 11%, 73 ± 15 and 66 ± 18% in the models at 24 h, 48 h and 72 h, respectively).

The average UGT conjugation of 4-methylumbelliferone in six EpiDerm™ models was maintained over 72 h and any statistically significant changes within a single experiment were not reproducible (Figure 6A and B). As with resorufin and the testosterone metabolites, the majority of the substrate, 4-methylumbelliferone, was detected in the medium (between 80 and 100%). GST activity was highest in models at 24 h and by 48 h the activity had decreased from 84.1 nmol/min/mg to approximately 50 nmol/min/mg. The GST activity did not decrease further between 48 h and 72 h.

Effect of B[a]P on phase 1 and 2 activities

The effect of B[a]P on the basal EROD activities is shown in Figure 3A. Both 2 μg/cm^2 and 50 μg/cm^2 B[a]P caused a significant increase in EROD activity in EpiDerm™ models. The effect was evident after 24 h and was still present after 72 h. The increase in EROD activity was not dose-dependent, for example, after 24 h treatment with 2 μg/cm^2 and 50 μg/cm^2 B[a]P, EROD activity increased from approximately 0.02 pmol/min/model to 0.12 ± 0.06 pmol/min/model and 0.16 ± 0.02 pmol/min/model, respectively. After 48 h, EROD activities in EpiDerm™ models treated with 2 μg/cm^2 and 50 μg/cm^2 B[a]P were marginally higher than at 24 h (0.18 ± 0.01 pmol/min/model and 0.19 ± 0.04 pmol/min/model, respectively, Figure 1A). After 72 h, the increase in EROD activity above acetone treated controls was diminished, whereby the activity in 2 μg/cm^2 treated models was only 0.10 ± 0.00 pmol/min/model. EROD activity in 50 μg/cm^2 B[a]P treated models was lower than those treated with the lower B[a]P dose, however, this was not due to cytotoxicity of B[a]P. The lactate dehydrogenase release into the medium in models treated with both doses of B[a]P was the same as vehicle control models at each time point (Table 2).

There were no significant effects of 2 μg/cm^2 and 50 μg/cm^2 B[a]P on testosterone 6β-hydroxylase activities in EpiDerm™ models at any of the three time points measured (Figure 4A). The activities

11

remained between 1.0 and 3.1 pmol/min/model. By contrast, the production of androstenedione was

statistically increased by 50 μg/cm^2 B[a]P after 24 h of treatment (Figure 5A). This effect was not

evident after 48 h of treatment and by 72 h, both 2 μg/cm^2 and 50 μg/cm^2 B[a]P caused the production

of androstenedione to significantly decrease compared to the acetone treated models (the production of

androstenedione was 23.7 ± 0.9 pmol/min/model in acetone treated models compared to 10.4 ± 1.4 and

14.6 ± 0.7 pmol/min/model in 2 μg/cm^2 and 50 μg/cm^2 B[a]P treated models, respectively).

UGT activity was not significantly affected by 2 μg/cm^2 and 50 μg/cm^2 B[a]P at any time point tested

(Figure 6). An additional reference compound was included to determine whether UGT activity could

be induced by a known hepatic UGT inducer under the conditions applied in these studies. Rifampin,

at a dose of 25 μg/cm^2 (equivalent to 20 μM if it was added to the medium) did not significantly alter

UGT activities after 72 h treatment (80.7 ± 3.4 pmol/min/model in rifampin treated EpiDerm™

models compared to 87.7 ± 6.6 pmol/min/model in acetone treated EpiDerm™ models).

GST activities in EpiDerm™ models treated with 2 μg/cm^2 B[a]P were equivalent to those in the

acetone control models (Figure 7A). GST activity was marginally higher in EpiDerm™ models treated

with 50 μg/cm^2 B[a]P after 48 h (63.1 nmol/min/mg compared to acetone treated models with 48.6

nmol/min/mg) but it was not possible to determine the statistical significance because only two models

were analyzed for this treatment. Additional EpiDerm™ models were treated with 5 μg/cm^2 beta-

naphthoflavone (equivalent to 50 μM if it was added to the medium) for 72 h, in which CDNB

metabolism in duplicate models was increased 1.6-fold above the duplicate acetone control treated

models (from 36.2 nmol/min/mg to 57.5 nmol/min/mg).

Effect of cyclophosphamide on phase 1 and 2 activities

EROD activities in EpiDerm™ models treated with 50 μg/cm^2 and 1000 μg/cm^2 cyclophosphamide

were equivalent to the corresponding acetone control models at each time point measured (Figure 3B),

which did not exceed the limits of detection of the method. Likewise, these doses of

12

cyclophosphamide had no effect on testosterone 6β-hydroxylase activities at any of the time points

measured and were between 1.8 and 3.0 pmol/h/model (Figure 4B). At 1000 μg/cm^2,

cyclophosphamide did significantly decrease androstenedione production compared to the acetone

treated models but this was evident at 72 h only (Figure 5B).

UGT activities were not significantly affected by 50 μg/cm^2 and 1000 μg/cm^2 cyclophosphamide, or

25 μg/cm^2 rifampin, at any time point tested (Figure 6B). UGT activities remained between 78.3 and

117.2 pmol/min/model. There was no dose-dependent effect of cyclophosphamide on GST activities

(Figure 7B). There was a decrease in activity at 72 h in models treated with 1000 μg/cm^2

cyclophosphamide compared to acetone control models at the same time point but it was not possible

to determine the statistical significance because only two models were analyzed for this treatment. The

decrease in GST activities measured in acetone treated EpiDerm™ models was also observed in

cyclophosphamide treated models (Figure 7B).

Discussion

These studies were designed to determine a number of basal metabolic enzyme activities under the same conditions as those used in the RSMN assay. The reason for this was that we wanted to investigate whether (a) selected activities were present in the EpiDerm™ models during the course of a 72 h RSMN assay, (b) they changed with time and (c) the test chemicals themselves altered the activities. At least for UGT and GST activities, it was also possible to measure any decreases since the basal levels were well above the limits of quantification.

Phase 2 detoxification pathways were clearly measureable in all models at each time point measured. Although there was some decrease in GST activities in acetone treated models between 24 h to 48 h, this drop did not continue between 48 h to 72 h. UGT activities remained constant throughout the 72 h experiment. In contrast to phase 2 activities, basal phase 1 bioactivating activities were at the limit of detection throughout the incubation. These findings are in agreement with others [Hu et al., 2010b] who found the overall expression of phase 2 enzymes to be more pronounced than that of Phase 1 enzymes in the EpiDerm™ model (as well as in human skin). The predominance of phase 2 pathways, which generally result in detoxication, over phase 1 activities supports the theory that skin acts as a barrier to toxins in terms of metabolic as well as a physical barrier. This is of significance for certain groups of cosmetic ingredients such as aromatic amines, which may be directly *N*-acetylated, rather than being hydroxylated to potentially genotoxic moieties [Skare et al., 2010; Goebel et al., 2009].

Although there was little change in the basal enzyme activities measured, there was some change in the morphology of the models. Over time, the stratum corneum increased in thickness. Despite this increase in the lipophilic nature of the upper layers of the models, the ratio of substrates and/or metabolites in the model and medium was unaltered. This is applicable to testosterone, which may have been expected to form a reservoir in the stratum corneum due to its highly lipophilic nature [van de Sandt et al., 2004]. However the amount of testosterone remaining in the EpiDerm™ models was the same at all time points. This may also have been true for B[a]P which is also highly lipophilic but the amount of this test compound was not determined in these studies.

We have shown that B[a]P, at doses which are known to induce micronuclei in the RSMN assay (data not shown), markedly induced EROD activity after 24 h. The induced levels were highest at 48 h, after which, they decreased during the last 24 h of the assay. The induction we observed can be expected because B[a]P is known to bind with high specificity to the aryl hydrocarbon receptor, which in turn modifies CYP1A1/2 and CYP1B1 expression [Li et al.,1998]. Others have also shown significant induction of aryl hydrocarbon hydroxylase, ethoxycoumarin O-deethylase, and/or EROD in rat skin after dermal application of a number of chemicals including polycyclic aromatic hydrocarbons and 3-methylcholanthrene [Khan et al., 1989; Raza and Mukhtar, 1993]. Topical application of BaP to rats has been shown to induce not only skin enzymes but also enzymes in other organs, although induction in the latter is lower than in the skin [Mukhtar and Bickers, 1981]. The induction of the expression of CYP1A1 and aryl hydrocarbon receptor in human *ex vivo* skin after application of B[a]P to the epidermis has also been demonstrated [Costa et al., 2010]. In their studies, the skin was placed epidermal side down in a 6-well plate containing 15 µl B[a]P but no medium for 18 h. The dose of B[a]P used was much lower (19 ng/cm^2) than used here and it was shown to cause significant loss of viability and lipid peroxidation. However, there were measureable amounts of basal CYP1A1 and aryl hydrocarbon receptor proteins (using western blotting) which were both increased by B[a]P (by approximately 10-fold) under these conditions. The doses of B[a]P used in our studies were not toxic to the models at any time point, according to the marker of viability, lactate dehydrogenase release, which was used in our studies. The EpiDerm™ models may be more robust than *ex vivo* skin discs since they are continually growing in the presence of specialized medium; whereas the *ex vivo* model lacked this form of functional maintenance. As a result of the continuing growth, the structure of the EpiDerm™ models changed over time, such that more stratum corneum was present by 72 h, possibly causing the B[a]P-induced EROD activities in the upper layers to be lower than at earlier times. Despite this decrease, it was still possible to measure induction of EROD activity over the entire RSMN assay duration. The induction of EROD activity after 24 h in EpiDerm™ models was also demonstrated by Curren et al. [2007] who treated them by adding 10 µM 3-methylcholanthrene to the medium. EROD activity was measured by incubating the models with 2.5 µM ethoxyresorufin and

15

33.3 μM dicoumarol for 30 min at 37ºC. The lack of effect of cyclophosphamide on EROD activities

over time was therefore not due to a general unresponsiveness of the models to aryl hydrocarbon

receptor mediated inducers - or due to cytotoxicity, since no increase of lactate dehydrogenase release

was observed at either cyclophosphamide dose. It is important to demonstrate that a model exhibits

induction responses similar to native skin since investigations in to the modulation of xenobiotic

metabolizing enzymes will enhance our knowledge of not just genotoxicity but also general skin

pathologies [Ahmad and Mukhtar, 2004].

Cyclophosphamide has been reported to induce a number of CYP activities in primary human

hepatocytes, including CYP3A4, CYP2C8, CYP2C9 and CYP2B6 levels [Chang et al., 1997; Gervot

et al., 1999; Lindley et al. 2002]. We therefore used testosterone as a substrate in our studies since it is

metabolized to a number of metabolites via CYP-selective pathways. In humans CYP2B6 catalyses

the formation of 16α-hydroxytestosterone, CYP3A3/4/5 catalyses the formation of formation of 2β-

and 6β-hydroxytestosterone and CYP2C9/19 catalyses the formation of androstenedione [Yamazaki

and Shimada, 1997; http://www.icgeb.org/~p450srv/]. In the skin, which generally lacks CYP2C

enzymes [Luu-The et al., 2009], androstenedione is most likely to be produced from the

interconversion of testosterone and androstenedione catalyzed by 17β-hydroxysteroid dehydrogenase

2, which is distributed around the basement layer of the epidermis [Hikima and Maibach, 2007]. The

kinetics of this enzyme have been investigated in cultured human keratinocytes [Milewich et al.,

1986]. The only metabolites detected in the EpiDerm™ models using non-radiolabelled testosterone

were 6β-hydroxytestosterone and androstenedione. Neither cyclophosphamide nor B[a]P altered the

production rate of 6β-hydroxytestosterone, suggesting that CYP3A4/5 is not affected by these test

compounds during the course of the RSMN assay. CYP3A4 is responsible for the metabolism of over

50% of marketed drugs [Zuber et al., 2002] and is therefore an important CYP to investigate;

therefore, future studies should include treatment of the EpiDerm™ models with known and FDA

recommended hepatic CYP3A4 inducers, such as rifampin [Huang and Stifano, 2006] to determine

whether this CYP is also inducible in skin models, especially if the 72 h dosing regimen is employed

in the RSMN assay. The production of androstenedione was significantly increased by the highest

16

dose of cyclophosphamide after 24 h but not at later times. This may reflect an induction of

CYP2C9/19 and/or 17β-hydroxysteroid dehydrogenase, the levels of which decrease over time due to

the increase in the number of corneocytes in the models. Further studies are needed to confirm the

reproducibility of this effect and CYP selective inhibitors could be included to identify which CYPs, if

any, are involved in the production of androstenedione.

GSTs play a role in metabolism of both B[a]P and cyclophosphamide; therefore, if GSTs are

modulated by these test chemicals, their genotoxic effects may also be modified. The π-class is

reported to be the predominant isoform in skin [Zhang et al., 2002] and is almost exclusively involved

in the detoxification of the ultimate B[a]P metabolite, (+)-anti-benzo[a]pyrene 7,8-dihydrodiol 9,10-

epoxide ((+)-anti-BPDE). Since EROD activity was significantly induced by B[a]P under the

conditions used here, we investigated whether GSTs could also be induced. The reference control

chemical, beta-naphthoflavone, increased GST activity by 1.6-fold, the magnitude of which may be

expected since the extent of induction of this enzyme is known to be low compared to the CYP1

family [Pushparajah et al., 2008b]. Likewise, B[a]P increased GST activities but only at 48 h and by

1.3-fold (the statistical significance of this result could not be made due to duplicates being taken for

most of the samples). Cyclophosphamide also caused a 1.3-fold increase in GST activity after 72 h at

the lower dose tested. Future studies will include the use of an isoform-selective substrate in order to

elucidate whether the lower induction of GST was due to the non-specificity of CDNB.

The aims of these studies were to determine whether selected phase 1 or 2 activities could be

measured and/or altered during the course of the RSMN assay. B[a]P and cyclophosphamide were

used as examples of chemicals which are bioactivated in the skin and caused significant micronuclei

formation in EpiDerm™ cells under the conditions used (data not shown) i.e. a local effect. This

shows that this model has the necessary metabolic capacity to bioactivate these chemicals and does not

require additional metabolic supplements (such as S9 and NADPH regenerating system). Other dermal

models may need additional S9-mix in the medium in order for this chemical to cause a genotoxic

effect [Flamand et al., 2006] However, it may be that the skin does not take part in the bioactivation of

17

a genotoxicant and that the site of bioactivation is systemic (e.g. via hepatic enzymes). In this case, the absorption of the chemical through the skin into the systemic circulation will affect the genotoxic potential of the chemical and the contribution of dermal metabolism will be negligible [Flamand et al., 2006]. Conversely, some dermally applied chemicals may be extensively detoxified by the skin before entering the circulation (e.g. hair dyes by N-acetyltransferase 1 [Goebel et al., 2009]); therefore, the presence of detoxification enzymes (GSTs, UGTs, N-acetyltransferase 1 etc) in the EpiDerm™ model is important to establish.

In conclusion, we have demonstrated the presence of basal phase 1 and 2 activities of EpiDerm™ models incubated according to the RSMN assay. With the exception of GST which decreased between 24 h and 48 h, all of the activities measured did not change over time. It was possible to measure enzyme induction using this assay design. Of the enzymes tested, EROD activity was significantly induced by B[a]P but not by cyclophosphamide. CPA and B[a]P had little or no reproducible effects on GST and UGT activities. Since a number of metabolic enzyme activities are present and at least the CYP1 family is inducible in the EpiDerm™ skin model, the RSMN assay may not require an exogenous metabolic activation system for compounds that are activated or detoxified via these pathways. Further studies investigating the effect of inclusion of cofactor regenerating systems will help to elucidate the contribution of dermal metabolic enzymes to the genotoxicity of selected positive control chemicals.

References

Aardema, MJ, Barnett, BC, Khambatta Z, Reisinger K, Ouedraogo-Arras G, Faquet B, Ginestet AC, Mun GC, Dahl EL, Hewitt NJ, Corvi R, Curren RD. (2010). International prevalidation studies of the EpiDerm 3D human reconstructed skin micronucleus (RSMN) assay: transferability and reproducibility. Mutat Res, 701(2), 123-31.

Ahmad N, Mukhtar H. (2004). Cytochrome p450: a target for drug development for skin diseases. J Invest Dermatol, 123(3), 417-25.

Afaq F, Zaid MA, Pelle E, Khan N, Syed DN, Matsui MS, Maes D, Mukhtar H. (2009). Aryl hydrocarbon receptor is an ozone sensor in human skin. J Invest Dermatol, 129(10), 2396-403.

Beckley-Kartey SAJ, Swales NJ, Hotchkiss SAM. (1997). The cutaneous metabolism of testosterone. Hum Exp Toxicol, 16, 51.

Bennet PN, Blackwell E, Davies DS. (1975). Competition for sulphate during detoxification in the gut wall. Nature (London), 258, 247-48.

Brown HS, Griffin M, Houston JB. (2007). Evaluation of cryopreserved human hepatocytes as an alternative in vitro system to microsomes for the prediction of metabolic clearance. Drug Metab Dispos, 35(2), 293-301.

Cao J, Leibold E, Beisker W, Schranner T, Nüsse M, Schwarz LR. (1993). Flow cytometric analysis of in vitro micronucleus induction in hepatocytes treated with carcinogens. Toxicol In Vitro, 7(4), 447-51.

Chang TK,Yu L, Maurel P,Waxman DJ. (1997). Enhanced cyclophosphamide and ifosfamide activation in primary human hepatocyte cultures: response to cytochrome P-450 inducers and autoinduction by oxazaphosphorines. Cancer Res, 57, 1946-54.

Costa C, Catania S, De Pasquale R, Stancanelli R, Scribano GM, Melchini A. (2010). Exposure of human skin to benzo[a]pyrene: role of CYP1A1 and aryl hydrocarbon receptor in oxidative stress generation. Toxicology, 271(3), 83-6.

Curren RD, Mun GC, Gibson DP, Aardema MJ. (2006). Development of a Method for Assessing Micronucleus Induction in a 3D Human Skin Model (EpiDermTM)". Mutat Res, 607, 192-204.

Curren, RD, Aardema M, Hayden PJ, Mun G, Hu T, Wilt N, Gibson D. (2007). Further development of a micronucleus assay using the human 3-D skin model EpiDerm™. Presented at the 46th Annual Society of Toxicology Meeting Charlotte, NC March 25-29, 2007. Poster number 427. http://www.mattek.com/pages/abstracts/abstractview/article/427-further-development-of-a-micronucleus-assay-using-the-human-3-d-skin-model-epidermTM/

Dahl EL, Curren R, Barnett BC, Khambatta Z, Reisinger K, Quedraogo G, Faquet B, Ginestet AC, Mun G, Hewitt NJ, Carr G, Pfuhler S, Aardema MJ. (2010). The reconstructed skin micronucleus assay (RSMN) in EpiDerm™: detailed protocol and harmonized scoring atlas. Mutat Res, 720(1-2), 42-52.

Dirven HA, van Ommen B, van Bladeren PJ. (1994). Involvement of human glutathione S-transferase isoenzymes in the conjugation of cyclophosphamide metabolites with glutathione. Cancer Res, 54(23), 6215-20.

Elhajouji A, Santos AP, Van Hummelen P, Kirsch-Volders M. (1994). Metabolic differences between

whole blood and isolated lymphocyte cultures for micronucleus (MN) induction by cyclophosphamide

and benzo[a]pyrene. Mutagenesis, 9(4), 307-13.

EU, 2003. EC - Directive 2003/15/EC of the European Parliament and of the Council of 27 February

2003 amending Council Directive 76/768/EEC on the approximation of the laws of the Member States

relating to cosmetic products. Official Journal L66, 11/03/2003 p.26.

Flamand N, Marrot L, Belaidi JP, Bourouf L, Dourille E, Feltes M, Meunier JR. (2006). Development

of genotoxicity test procedures with Episkin, a reconstructed human skin model: towards new tools for

in vitro risk assessment of dermally applied compounds? Mutat. Res, 606(1-2), 39-51.

Gautier JC, Lecoeur S, Cosme J, Perret A, Urban P, Beaune P, Pompon D. (1996). Contribution of

human cytochrome P450 to benzo[a]pyrene and benzo[a]pyrene-7,8-dihydrodiol metabolism, as

predicted from heterologous expression in yeast. Pharmacogenetics, 6(6), 489-99.

Gervot L, Rochat B, Gautier JC, Bohnenstengel F, Kroemer H, de Berardinis V, Martin H, Beaune P,

de Waziers I. (1999). Human CYP2B6: expression, inducibility and catalytic activities.

Pharmacogenetics, 9, 295-306.

Goebel C, Hewitt NJ, Kunze G, Wenker M, Hein DW, Beck H, Skare J. (2009). Skin metabolism of

aminophenols: human keratinocytes as a suitable in vitro model to qualitatively predict the dermal

transformation of 4-amino-2-hydroxytoluene in vivo. Toxicol Appl Pharmacol, 235(1), 114-23.

Guy RH, Mak VHW, Kai T, Bommannan D, Potts RO. (1990). Percutaneous penetration enhancers:

mode of Action. In: Scott, R.C., Guy, R.H., Hadgraft, J. eds. Prediction of Percutaneous Penetrationm

Methods, Measurements and Modelling. IBC, London, 213-23.

21

Habig WH, Pabst MJ, Jakoby WB. (1974). Glutathione S-transferases. The first enzymatic step in mercapturic acid formation. J Biol Chem, 249(22), 7130-9.

Heath EC, Dingell JV. (1974). The interaction of foreign chemical compounds with the glucuronidation of estrogens in vitro. Drug Metab Dispos, 2, 556-65.

Hikima T, Maibach HI. (2007). Gender differences of enzymatic activity and distribution of 17beta-hydroxysteroid dehydrogenase in human skin in vitro. Skin Pharmacol Physiol, 20(4), 168-74.

Hu T, Kaluzhny Y, Mun GC, Barnett B, Karetsky V, Wilt N, Klausner M, Curren R, Aardema MJ. (2009a). Intralaboratory and interlaboratory evaluation of the EpiDerm™ 3D human reconstructed skin micronucleus (RSMN) assay. Mutat. Res, 673, 100-8.

Hu T, Bailey RE, Morrall SW, Aardema MJ, Stanley LA, Skare JA. (2009b). Dermal penetration and metabolism of p-aminophenol and p-phenylenediamine: application of the EpiDerm human reconstructed epidermis model. Toxicol Lett, 188(2), 119-29.

Hu T, Khambatta, Z.S., Hayden, P.J., Bolmarcich, J., Binder, R.L., Robinson, M.K., Carr, G.J., Tiesman, J.P., Jarrold, B.B., Osborne, R., Reichling, T.D., Nemeth, S.T., Aardema, M.J., 2010. Xenobiotic metabolism gene expression in the EpiDermin vitro 3D human epidermis model compared to human skin. Toxicol In Vitro, 24(5), 1450-63.

Huang S-M, Stifano T. (2006). Guidance for industry: Drug interaction studies — study design, data analysis, and implications for dosing and labelling. Draft Guidance.
http://www.fda.gov/OHRMS/DOCKETS/98fr/06d-0344-gdl0001.pdf

Hvastkovs EG, So M, Krishnan S, Bajrami B, Tarun M, Jansson I, Schenkman JB, Rusling JF. (2007). Electrochemiluminescent arrays for cytochrome P450-activated genotoxicity screening. DNA damage from benzo[a]pyrene metabolites. Anal Chem, 79(5), 1897-906.

Khan WA, Park SS, Gelboin HV. (1989). Epidermal cytochrome P-450: Immunochemical characterization of isoform induced by topical application of 3-methylcholanthrene to neonatal rats. J. Pharmacol Exp Ther 249, 921–4.

LeCluyse E, Madan A, Hamilton G, Carroll K, DeHaan R, Parkinson A. (2000). Expression and regulation of cytochrome P450 enzymes in primary cultures of human hepatocytes. J Biochem Mol Toxicol 4(4), 177-88.

Li W, Harper PA, Tang BK, Okey AB. (1998). Regulation of cytochrome P450 enzymes by aryl hydrocarbon receptor in human cells: CYP1A2 expression in the LS180 colon carcinoma cell line after treatment with 2,3,7,8-tetrachlorodibenzo-p-dioxin or 3-methylcholanthrene. Biochem Pharmacol 56(5), 599–612.

Lindley C, Hamilton G, McCune JS, Faucette S, Shord SS, Hawke RL, Wang H, Gilbert D, Jolley S, Yan B, LeCluyse EL. (2002). The effect of cyclophosphamide with and without dexamethasone on cytochrome P450 3A4 and 2B6 in human hepatocytes. Drug Metab Dispos, 30, 814-22.

Luu-The V, Duche D, Ferraris C, Meunier JR, Leclaire J, Labrie F. (2009). Expression profiles of phases 1 and 2 metabolizing enzymes in human skin and the reconstructed skin models Episkin and full thickness model from Episkin. J Steroid Biochem, Mol. Biol. 116(3-5), 178-86.

Mackenzie PI, Rodbourn L, Iyanagi T. (1993). Glucuronidation of carcinogen metabolites by complementary DNA-expressed uridine 5'-diphosphate glucuronosyltransferases. Cancer Res, 53(7), 1529-33.

23

Milewich L, Kaimal V, Shaw CB, Sontheimer RD. (1986). Epidermal keratinocytes: a source of 5 alpha-dihydrotestosterone production in human skin. J Clin Endocrinol Metab, 62(4), 739-46.

Mukhtar H, Bickers DR. (1981). Comparative activity of the mixed function oxidases, epoxide hydratase, and glutathione-S-transferase in liver and skin of the neonatal rat. Drug Metab Dispos, 9, 311–4,

Mun GC, Aardema MJ, Hu T, Barnett B, Kaluzhny Y, Klausner M, Karetsky V, Dahl EL, Curren RD. (2009). Further development of the EpiDermTM 3D reconstructed human skin micronucleus (RSMN) assay. Mutat Res, 673, 92-9.

Nims RW, Prough RA, Lubet RA. (1984). Cytosol-mediated reduction of resorufin: a method for measuring quinone oxidoreductase. Arch Biochem Biophys, 229(2), 459-65.

Nohynek GJ, Duche D, Garrigues A, Meunier PA, Toutain H, Leclaire J. (2005). Under the skin: Biotransformation of para-aminophenol and para-phenylenediamine in reconstructed human epidermis and human hepatocytes. Toxicol Lett, 158(3), 196-212.

Oesch F, Fabian E, Oesch-Bartlomowicz B, Werner C, Landsiedel R. (2007). Drug-metabolizing enzymes in the skin of man, rat, and pig. Drug Metab Rev, 39(4), 659-98.

Pelkonen O, Nebert DW. (1982). Metabolism of polycyclic aromatic hydrocarbons: etiologic role in carcinogenesis. Pharmacol Rev, 34(2), 189-222.

Pushparajah DS, Umachandran M, Nazir T, Plant KE, Plant N, Lewis DFV, Ioannides C. (2008a). Up-regulation of CYP1 in rat lung and liver, and human liver precision-cut slices by a series of polycyclic

aromatic hydrocarbons; association with the Ah locus and importance of molecular size. Toxicol In Vitro, 22, 128–45.

Pushparajah DS, Umachandran M, Plant KE, Plant N, Ioannides C. (2008b). Up-regulation of the glutathione S-transferase system in human liver by polycyclic aromatic hydrocarbons; comparison with rat liver and lung. Mutagenesis, 23(4), 299-308.

Raza H, Mukhtar H. (1993). Differences in inducibility of cytochrome P-450 1A1, monooxygenases and glutathione-S-transferases in cutaneous and extra-cutaneous tissues after topical and parenteral administration of beta-naphthoflavone to rats. Int J Biochem, 10, 1511–6.

Raza H, Awasthi YC, Zaim MT, Eckert RL, Mukhtar H. (1991). Glutathione S-transferases in human and rodent skin: multiple forms and species-specific expression. J Invest Dermatol 96(4), 463-7.

Skare JA, Hewitt NJ, Doyle E, Powrie R, Elcombe C. (2009). Metabolite screening of aromatic amine hair dyes using in vitro hepatic models. Xenobiotica, 39(11), 811-25.

Sherratt PJ, Hayes JD. (2002). Glutathione S-transferases. In: Ioannides, C ed. Enzyme Systems that Metabolise Drugs and Other Xenobiotics. Wiley & Sons, Chichester, UK, 319–52.

Swanson HI. (2004). Cytochrome P450 expression in human keratinocytes: an aryl hydrocarbon receptor perspective. Chem Biol Interact 149(2-3), 69-79.

Tachibana S, Tanaka M. (2001). Simultaneous determination of testosterone metabolites in liver microsomes using column-switching semi-microcolumn high-performance liquid chromatography. Anal Biochem, 295(2), 248-56.

van de Sandt JJ, van Burgsteden JA, Cage S, Carmichael PL, Dick I, Kenyon S, Korinth G, Larese F, Limasset JC, Maas WJ, Montomoli L, Nielsen JB, Payan JP, Robinson E, Sartorelli P, Schaller KH, Wilkinson SC, Williams FM. (2004). In vitro predictions of skin absorption of caffeine, testosterone, and benzoic acid: a multi-centre comparison study. Regul Toxicol Pharmacol, 39(3), 271-81.

Wei W, Zhang C, Liu AL, Xie SH, Chen XM, Lu WQ. (2009). Effect of PCB153 on B[a]P-induced genotoxicity in HepG2 cells via modulation of metabolic enzymes. Mutat Res, 30, 675(1-2), 71-6.

Wu XJ, Lu WQ. (2003). Mersch-Sundermann V. Benzo(a)pyrene induced micronucleus formation was modulated by persistent organic pollutants (POPs) in metabolically competent human HepG2 cells. Toxicol Lett, 144(2), 143-50.

Xie HJ, Yasar U, Lundgren S, Griskevicius L, Terelius Y, Hassan M, Rane A. (2003). Role of polymorphic human CYP2B6 in cyclophosphamide bioactivation. Pharmacogenomics J, 3(1), 53-61.

Yamazaki H, Shimada T. (1997). Progesterone and testosterone hydroxylation by cytochromes P450 2C19, 2C9, and 3A4 in human liver microsomes. Arch Biochem Biophys 346(1), 161-9.

Zhang Y, Gonzalez V, Xu MJ. (2002). Expression and regulation of glutathione S-transferase P1-1 in cultured human epidermal cells. J Dermatol Sci 30(3), 205-14.

Zhao JF, Zhang YJ, Kubilus J, Jin XH, Santella RM, Athar M, Wang ZY, Bickers DR. (1999). Reconstituted 3-dimensional human skin as a novel in vitro model for studies of carcinogenesis. Biochem. Biophys. Res Commun, 254(1), 49-53.

Zuber R, Anzenbacherová E, Anzenbacher P. (2002). Cytochromes P450 and experimental models of drug metabolism. J Cell Mol Med, 6(2), 189-98.

26

Table 1. Phase 1 and 2 activities over 72 h in EpiDerm™ models treated with acetone. The number of

models (n) tested are shown. LOD = limits of detection (0.025pmol/min/model).

Activity	n	Time after first treatment		
		24 h	48 h	72 h
Phase 1				
EROD (pmol/min/model)	6	At LOD	At LOD	At LOD
Testosterone 6β-hydroxylation (pmol/min/model)	6	1.4 ± 0.6	3.0 ± 1.2	2.6 ± 0.5
ASD formation (pmol/min/model)	6	18.2 ± 5.3	19.4 ± 10.3	17.1 ± 7.3
Phase 2				
UGT (pmol/min/model)	6	110.4 ± 12.7	86.2 ± 19.4	97.3 ± 19.8
GST (nmol/min/mg protein)	3-4	84.1 ± 4.1	48.6 ± 4.5	50.4 ± 19.9

27

Table 2. Effect of (A) B[a]P and (B) CPA on LDH release from EpiDerm™ models over 72 h. The viability was expressed as the % LDH released from treated models compared to vehicle control. The amount of LDH in the medium from vehicle control samples compared to medium without Epiderm™ models was 164 ± 55%, 122 ± 26% and 116 ± 20% at 24 h, 48 h and 72 h, respectively.

Time (h)	B[a]P		CPA	
	$2\ \mu g/cm^2$	$50\ \mu g/cm^2$	$50\ \mu g/cm^2$	$1000\ \mu g/cm^2$
24	103 ± 5	98 ± 19	93 ± 1	105 ± 2
48	102 ± 3	102 ± 3	104 ± 2	109 ± 0
72	108 ± 2	114 ± 3	118 ± 8	110 ± 0

1
2
3
4
5
6
7
8
9
10
11
12
13
14
15
16
17
18
19
20
21
22
23
24
25
26
27
28
29
30
31
32
33
34
35
36
37
38
39
40
41
42
43
44
45
46
47
48
49
50
51
52
53
54
55
56
57
58
59
60

29

Xenobiotica

Figure 1

| DAY 0 | → | Day 1 | → | Day 2 | → | Day 3 |

First dose
1 h after arrival

Second dose
Measure activity
24 h after 1st dose*

Third dose
Measure activity
48 h after 1st dose*

Measure activity
72 h after 1st dose*
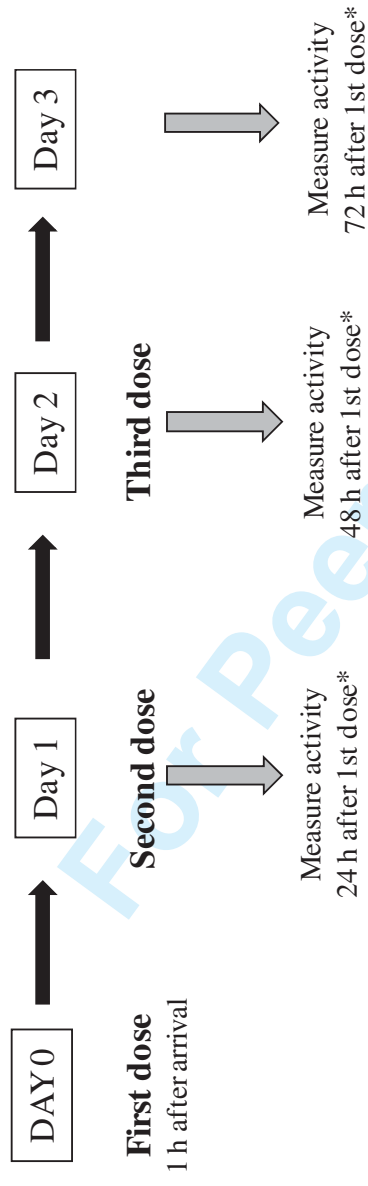
*Collect media from each time point to measure LDH activity
= cytotoxicity compared to control treated models

30

Figure 2

Figure 3.

(A)
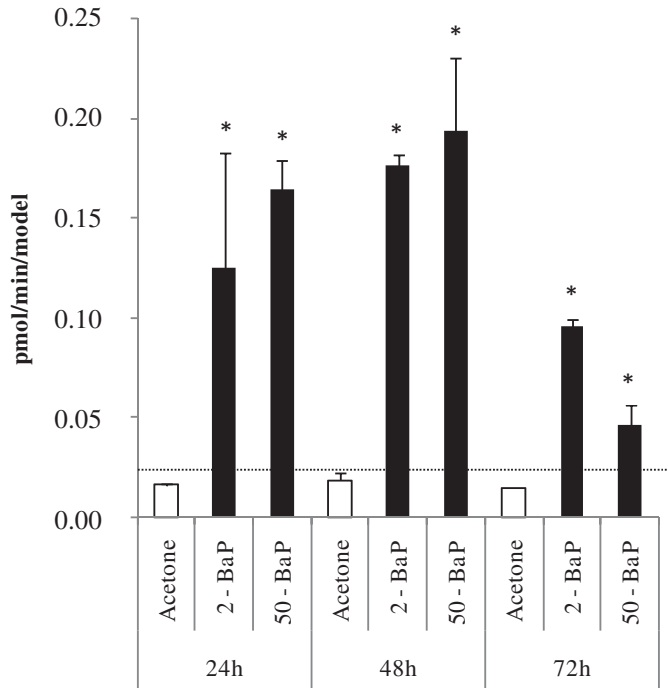
(B)

Figure 4.

(A)

(B)
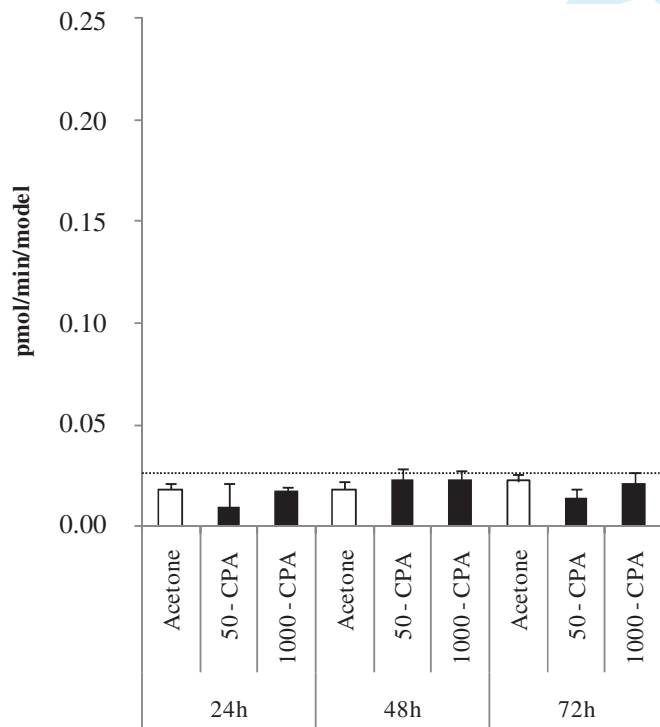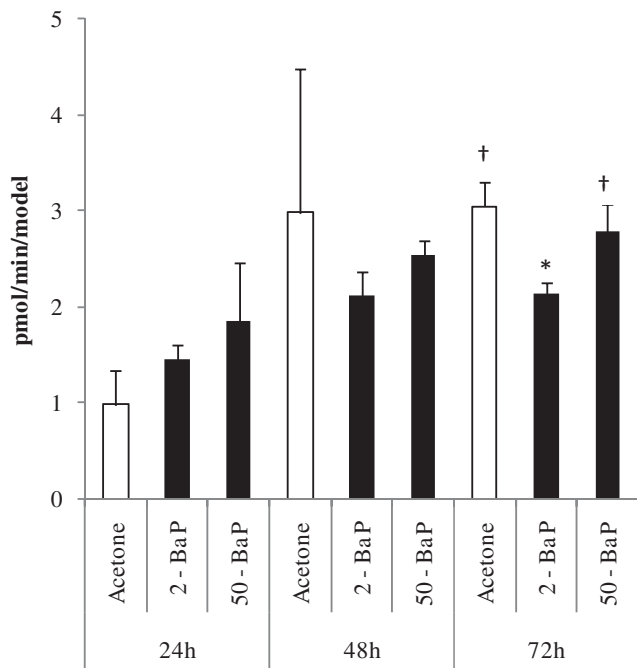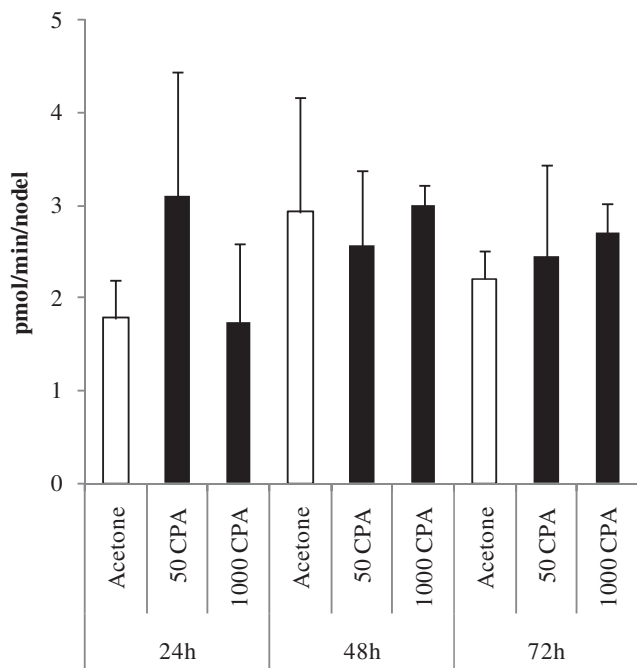
Figure 5
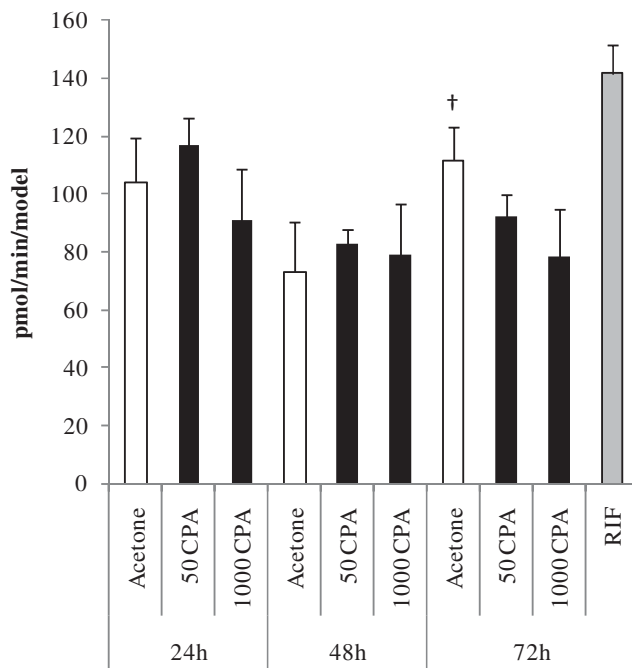
(A)

(B)

1
2
3
4
5
6
7
8
9
10
11
12
13
14
15
16
17
18
19
20
21
22
23
24
25
26
27
28
29
30
31
32
33
34
35
36
37
38
39
40
41
42
43
44
45
46
47
48
49
50
51
52
53
54
55
56
57
58
59
60

Figure 6.

(A)

(B)

Figure 7.

(A)
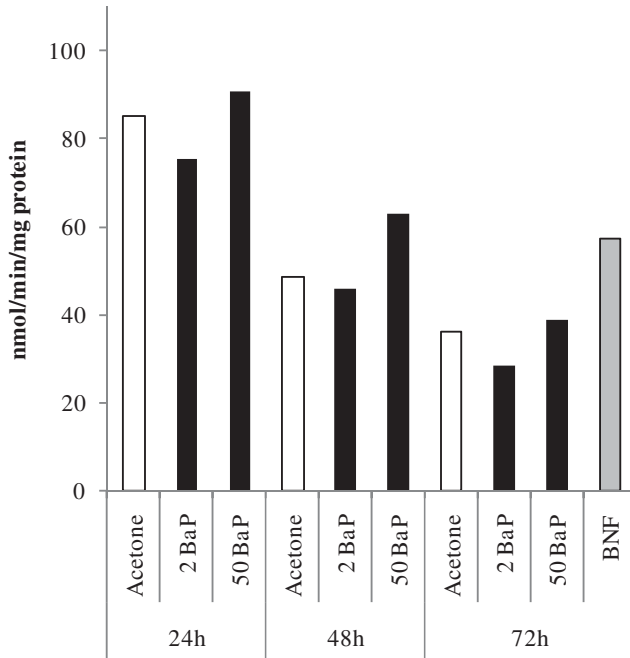
(B)
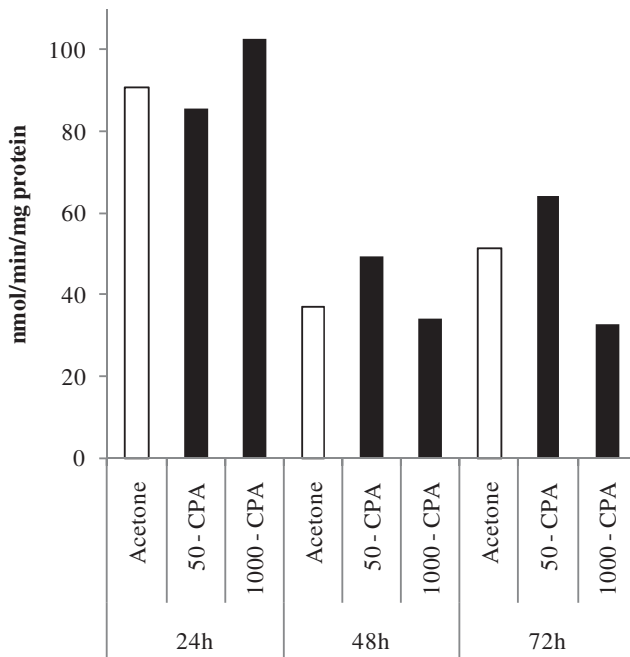
Figure legends

Figure 1. Overview of the dosing of test chemicals and enzyme activity determination.

Figure 2. Cross-sections of EpiDerm™ models incubated for 24 h, 48 h and 72 h. The pictures represent one (Donor 254) of the two donors analysed.

Figure 3. Effect of (A) B[a]P and (B) cyclophosphamide on ethoxyresorufin O-deethylase activities in EpiDerm™ models over 72 h. The doses were 2 μg/cm^2 and 50 μg/cm^2 B[a]P (denoted "2" and "50", respectively) and 50 μg/cm^2 and 1000 μg/cm^2 cyclophosphamide (denoted "50" and "1000", respectively). Mean ± SD. * denotes a statistical significance of <0.05. The dotted line represents the LOD.

Figure 4. Effect of (A) B[a]P and (B) cyclophosphamide on testosterone 6β-hydroxylase activities in EpiDerm™ models over 72 h. The doses were 2 μg/cm^2 and 50 μg/cm^2 B[a]P (denoted "2" and "50", respectively) and 50 μg/cm^2 and 1000 μg/cm^2 cyclophosphamide (denoted "50" and "1000", respectively). Mean ± SD, * = $p < 0.05$ difference from control at respective time point, † = $p < 0.05$ difference from 24 h acetone control, ‡= $p < 0.05$ difference between 2 μg/cm^2 and 50 μg/cm^2 B[a]P.

Figure 5. Effect of (A) B[a]P and (B) cyclophosphamide on androstenedione formation in EpiDerm™ models over 72 h. The doses were 2 μg/cm^2 and 50 μg/cm^2 B[a]P (denoted "2" and "50", respectively) and 50 μg/cm^2 and 1000 μg/cm^2 cyclophosphamide (denoted "50" and "1000", respectively). Mean ± SD. * = $p < 0.05$ difference from control at respective time point, † = $p < 0.05$ difference from 24 h acetone control, ‡= $p < 0.05$ difference between 2 μg/cm^2 and 50 μg/cm^2 B[a]P.

Figure 6. Effect of (A) B[a]P and (B) cyclophosphamide on UDP-glucuronosyltransferase activities in EpiDerm™ models over 72 h. The doses were 2 μg/cm^2 and 50 μg/cm^2 B[a]P (denoted "2" and "50", respectively) and 50 μg/cm^2 and 1000 μg/cm^2 cyclophosphamide (denoted "50" and "1000",

37

respectively). The reference compound was 25 μg/cm^2 rifampin (RIF) which was dosed in the same

way as B[a]P and cyclophosphamide but UDP-glucuronosyltransferase activities were only measured

after 72 h. Mean ± SD, * = $p < 0.05$ difference from control at respective time point, † = $p < 0.05$

difference from 24 h acetone control.

Figure 7. Effect of (A) B[a]P and (B) cyclophosphamide on glutathione S-transferase activities in

EpiDerm™ models over 72 h. The doses were 2 μg/cm^2 and 50 μg/cm^2 B[a]P (denoted "2" and "50",

respectively) and 50 μg/cm^2 and 1000 μg/cm^2 cyclophosphamide (denoted "50" and "1000",

respectively). The reference compound was 5 μg/cm^2 beta-naphthoflavone (BNF) which was dosed in

the same way as B[a]P and cyclophosphamide but GST activities were only measured after 72 h.

Mean of two models per treatment and time point.

Publikation Nr. 3

Effects of the genotoxic compounds, benzo[a]pyrene and cyclophosphamide on phase 1 and 2 activities in EpiDerm™ models

Christine Götz, Nicola J. Hewitt, Erich Jermann, **Julia Tigges**, Zippora Kohne, Ulrike Hübenthal, Jean Krutmann, Hans F Merk und Ellen Fritsche

– ▪ – ▪ – ▪ – ▪ – ▪ – ▪ – ▪ – ▪ – ▪ –

2.4   Publikation 4

AhRR function revisited: Investigations in adult primary human fibroblasts

Die Haut als Grenzflächenorgan des menschlichen Körpers hat als First-Pass-Organ für dermale Exposition die Fähigkeit, auf exogenen Noxen wie z.B. polyzyklischen aromatischen Kohlenwasserstoffe (PAK) oder ultraviolette (UV) Strahlung zu reagieren. In der Epidermis ist daher mit CYP und COX-Enzymaktivität Fremdstoffmetabolismus der Phase 1 vorhanden, durch den lipophile Substanzen funktionalisiert werden können. Die dafür notwendigen metabolischen Reaktionen führen jedoch auch zur Generierung von oxidativem Stress, was für die proliferativ aktiven Zellen der Epidermis nicht von großer Bedeutung ist, für die größtenteils nicht proliferierenden Fibroblasten der Dermis jedoch durch Akkumulation von zellulären Schäden wie Mutationen an der mitochondrialen DNS ein Problem darstellt. Aus diesem Grund ist es nicht verwunderlich, dass in der Vergangenheit in Fibroblasten ein nicht funktioneller AhR-Signalweg beschrieben wurde. Dieses soll mit einer hohen AhR-Repressor Expression in diesen Zellen zusammenhängen, von dem in Überexpressionsstudien gezeigt werden konnte, dass er mit ARNT dimerisiert, XRE im Promoterbereich von AhR-Zielgenen blockiert und somit in einer negativen Rückkopplungsschleife die Transkription AhR-regulierter Gene blockiert. In dieser Studie überprüfen wir dieses Konzept der „AhRR-Theorie" anhand von transkriptionellen und funktionellen Untersuchungen an 25 verschiedenen primären humanen Fibroblasten (NHDF). Dabei konnten wir bestätigen, dass der AhR-vermittelte Signalweg in humanen Fibroblasten in der Tat nicht funktionell ist. Dieses Phänomen korreliert jedoch nicht mit einer hohen AhRR-Expression, da der AhRR in primären humanen Fibroblasten, sowie in MEF Zellen, etwa 6-fach niedriger exprimiert wird, als in primären Keratinozyten. Des Weiteren konnten wir in exemplarisch durchgeführten funktionellen Untersuchungen zur EROD-Aktivität weder in NHDFs noch in MEF-Wildtyp-Zellen eine Induktion durch AhR-Liganden nachweisen. Interessanterweise war auch in AhRR-defizienten MEF-Zellen lediglich eine marginale EROD-Aktivität um das quantitative Detektionsminimum zu beobachten. Im Gegensatz dazu waren die als Positivkontrolle mitgeführten NCTC 2544 Keratinozyten durch beide AhR-Liganden gut induzierbar (um 100 pmol/min/mg). Des Weiteren konnten wir zwar auf transkriptioneller Ebene durch die Behandlung der

Zellen mit dem HDAC-Inhibitor TSA die in der Literatur beschriebenen „Superinduktion" von CYP1A1 verifizieren, in dieser Studie konnten wir aber erstmals zeigen, dass diese auf der Ebene der Enzymaktivität keine Auswirkung hat. Zusammenfassend zeigen wir in dieser Publikation, dass zwar der AhR-Signalweg in primären Fibroblasten nicht funktionell ist, dass dieses aber nicht mit einer hohen AhRR-Expression einhergeht.

AHRR FUNCTION REVISITED: INVESTIGATIONS IN PRIMARY ADULT DERMAL HUMAN FIBROBLASTS

Julia Tigges[1], Heike Weighart[1], Sandra Wolff[1], Christine Götz[1], Irmgard Förster[1], Zippora Kohne[1], Ulrike Huebenthal[1], Hans F. Merk[2], Thomas Haarmann-Stemmann[1], Josef Abel[1], Jean Krutmann[1], Ellen Fritsche[1,2]

[1] Leibniz Research Institute for Environmental Medicine at the Heinrich-Heine-University Düsseldorf, Germany

[2] Department of Dermatology and Allergology, University Clinic RWTH Aachen, Germany

Running title: AhRR function revisited

Keywords: skin; AhRR, CYP, fibroblast, MEF, EROD

Abbreviations: AhR = arylhydrocarbon receptor; AhRR = arylhydrocarbon receptor repressor; ARNT = AhR nuclear translocator; bHLH = basic helix-loop-helix; PAS = homologues of Period/ARNT/Single minded; XRE = xenobiotic response element; UV = ultraviolet; PAH = polycyclic aromatic hydrocarbons; CYP = Cytochrome P450; GST = Glutathion S-Transferase; NAT = N-Acetyltransferase; UGT = UDP-Glucuronosyltransferase; FICZ = 6-formylindolo-3,2b-carbazole; ROS = reactive oxygen species; MEF = mouse embryonic fibroblasts; NHEK = normal human epidermal keratinocyte; NHDF = normal human dermal fibroblast; MNF = 3'-methoxy-4'-nitroflavone; 3-MC = 3-methylcholanthrene; B(a)P= benzo(a)pyrene; TSA = Trichostatin A; HDAC = histone deacetylase; EROD = ethoxyresorufin O-deethylation; ER = Estrogen Receptor; LOQ = limit of quantification

ABSTRACT

The skin as the first pass organ for dermal exposure towards environmental and pharmaceutical agents exhibits the ability to react to exogenous noxae like polycyclic aromatic hydrocarbons or ultraviolet radiation by inducing cytochrome P450 (CYP)-catalyzed reactions. The drawback of CYP-mediated metabolism is generation of oxidative stress and its associated cellular damages. Such harm is especially dangerous for a tissue when the cellular turnover rate is low, like in postreplicative fibroblasts of the dermis, as then damage accumulates over time. Therefore, it has been thought that CYP1 activity is repressed by high aryl hydrocarbon receptor repressor (AhRR) expression in fibroblasts. Here we revisited this 'AhRR hypothesis' in primary human fibroblasts (NHDF) of 25 individuals and AhRR deficient ($^{-/-}$) mouse embryonic fibroblasts. According to the current literature, we found (i) AhRR expression in NHDFs, (ii) moderate CYP1A1 mRNA induction by AhR activators with large interindividual differences, and (iii) HDAC-dependent CYP1A1 mRNA induction. However, CYP1A1 mRNA induction at these low expression levels in NHDFs and in AhRR$^{-/-}$ does not translate into CYP1 enzyme activity. Therefore, our data confirm that CYP1 activity in NHDFs is repressed, but reveal that not the AhRR but a so far unidentified factor represses CYP1 activity in these cells.

INTRODUCTION

The arylhydrocarbon receptor (AhR) repressor (AhRR) – like the AhR itself - belongs to the group of basic helix-loop-helix (bHLH)-PAS (homologues of Period/ARNT(AhR nuclear translocator)/Single minded) proteins and is an integral part of the AhR signaling machinery (Mimura *et al.*, 1999a). The AhR is a ligand-dependent transcription factor which, in its unligated state, rests as a multi protein complex in the cytoplasm of most cells of the body including skin (Fujii-Kuriyama *et al.*, 1992;Bickers *et al.*, 1984). Upon ligand binding, the receptor sheds its co-factors, translocates into the nucleus where it dimerizes with its partner ARNT, binds to xenobiotic response elements (XREs) in the promoter region of AhR-dependent genes and initiates transcription (Rowlands and Gustafsson, 1997;Abel and Haarmann-Stemmann, 2010;Fujisawa-Sehara *et al.*, 1987). Besides genes which are involved in xenobiotic

metabolism, one gene of the AhR gene battery is the AhRR itself (Mimura *et al.*, 1999b). Overexpression studies suggest that the AhRR also forms heterodimers with ARNT also binding to XREs and blocking AhR target gene transcription (Mimura *et al.*, 1999b). This transcriptional hindrance is probably due to the lack of a transactivation domain in the AhRR protein that is present in the AhR (Sogawa *et al.*, 1995;Mimura *et al.*, 1999b). Thereby, the AhRR is thought to form a negative feedback loop on the AhR gene battery including its own transcription. Such AhR signaling was found in almost all cells of the body including skin (Ahmad *et al.*, 1996;Das *et al.*, 1986).

The skin is the largest organ of the human body and represents the body's protective surface as the first and outermost contact site for environmental noxae, which have the ability to overcome the physical barrier of the skin (Merk *et al.*, 2006;Oesch *et al.*, 2007;Swanson, 2004;Ahmad and Mukhtar, 2004). These include lipophilic chemicals like polycyclic aromatic hydrocarbons (PAH) or ultraviolet (UV) radiation. Not only liver - as the first-pass-organ for oral exposure – but also skin as the first-pass-organ for dermal exposure, possesses capacities for xenobiotic metabolism with the goal of eliminating lipophilic compounds (extensively reviewed in (Oesch *et al.*, 2007)). The ability of skin to metabolize PAH has long been described *in vivo* in animals and humans. Skin cells express the AhR and AhR-activation by PAH causes induction of Cytochrome P450 (CYP)1A1 and 1B1 which hydroxylate such xenobiotics (Levin *et al.*, 1972;Alvares *et al.*, 1973b;Alvares *et al.*, 1973a;Bickers *et al.*, 1984;Götz *et al.*, 2011). In contrast to inducible CYP enzymes, phase 2 drug metabolism enzymes like GST, NAT or UGT are constitutively present in skin and thus guarantee detoxification of hydroxylated metabolites (Oesch *et al.*, 2007;Götz C *et al.*, 2011). That the same drug metabolism is also essential for skin after UV exposure is a relatively new realization. We and others showed *in vitro* and *in vivo* that upon UV irradiation, natural AhR ligands are formed intracellularly from free tryptophan (Rannug *et al.*, 1987;Bergander *et al.*, 2004;Fritsche *et al.*, 2007;Wincent *et al.*, 2009;Wei *et al.*, 1999). Among those, 6-formylindolo-*3,2b*-carbazole (FICZ) is the most potent AhR ligand (Rannug *et al.*, 1987;Rannug *et al.*, 1995). FICZ is metabolized by CYP enzymes and thus induces their expression (Wei *et al.*, 2000;Bergander *et al.*, 2004;Wincent *et al.*, 2009;Wei *et al.*, 1998;Bergander *et al.*, 2003). Hence, AhR signaling is indispensable for skin xenobiotic metabolism of PAH and UV photoproducts.

The drawback of such CYP monooxygenase-catalyzed metabolic reactions is generation of oxidative stress (Puntarulo and Cederbaum, 1998;Morel *et al.*, 1999). A tissue with a high cellular turnover rate is up to a certain limit sparsely harmed by oxidative stress because structural cellular damages, like mitochondrial DNA mutations or other macromolecular modifications, do not accumulate over time. Such a tissue, where cells constantly proliferate, is the epidermis consisting of keratinocytes. A completely different situation is given in the dermis. Dermal fibroblasts are postreplicative and rest in the dermis for decades producing extracellular matrix (Fritsch, 2009). For them, accumulation of damage is pathogenic and causes tissue degeneration. Therefore, fibroblasts must try to keep their oxidative stress level low. As one source of reactive oxygen species (ROS) production is xenobiotic metabolism (reviewed in (Gonzales FJ, 2005)), repression of metabolism is a necessary consequence for the fibroblast, especially with regard to the fact that the epidermis as the outer barrier is metabolically competent (Du L *et al.*, 2006;Swanson, 2004;Afaq and Mukhtar, 2001;Pendlington *et al.*, 1994). Consequently, the function of the AhRR to repress AhR-mediated cyp1a1 mRNA expression and hence supposedly cyp metabolism in fibroblasts, an observation made in mouse embryonic fibroblasts (MEFs), seemed plausible (Oshima *et al.*, 2007).

In this study, we revisited this 'AhRR hypothesis' in primary human fibroblasts from 25 individual breast reduction donors. We confirmed that AhR-mediated signaling is impaired in human fibroblasts but that this is not due to high expression of the AhRR.

RESULTS

EXPRESSION OF AHR SIGNALING COMPONENTS IN HUMAN SKIN CELLS AND MEFs

It was previously reported that AhR signaling in fibroblasts is not functional due to the high levels of AhRR expression in those cells. The AhRR is thought to repress activation of the AhR via an internal feedback mechanism (Mimura *et al.*, 1999a). Real time RT-PCR analyses of NHDFs of 25 different donors from 5 age groups reveal for one that mRNA steady state levels of components of the AhR signaling pathway (AhRR, AhR and ARNT) are each expressed in similar copy numbers among the 25 individuals. The 5 different age groups also do not differ significantly from each other.

Thereby, the expressions of AhRR, AhR and ARNT do not exceed 0.01, 0.07 and 0.18 copies/10^4 transcripts β-Actin, respectively, in those cells (Fig. 1A-C). Comparison of these expression patterns to the distribution of AhR signaling components in NHEKs, AhRR$^{+/+}$ and AhRR$^{-/-}$ MEFs reveals that NHDFs express up to 6 times less AhRR than NHEKs, whereas the AhRR expression in AhRR$^{+/+}$ MEFs is at the same level as in NHDFs and AhRR$^{-/-}$ MEFs do not express the AhRR at all (Fig. 1D). A similar result was obtained for the expression of AhR (Fig. 1E) and ARNT (Fig. 1F): for both, gene expression was lowest in NHDFs (up to 0.07 and 0.18 copies/10^4 transcripts β-Actin, respectively), whereas AhR is highest expressed in NHEKs (~16/10^4 β-Actin) compared to AhRR$^{+/+}$ and AhRR$^{-/-}$ MEFs (up to 5.9 and 7.9 copies/10^4 transcripts β-Actin, respectively). In contrast, ARNT is highest expressed in AhRR$^{+/+}$ and AhRR$^{-/-}$ MEFs (152 and 109 copies/ 10^4 transcripts β-actin) followed by NHEKS (7.1 copies/ 10^4 transcripts β-actin). As shown as examples for the age groups 20-29 and > 60, the interindividual differences inside the different age groups are bigger than the differences between the different ages, but do not reach statistical significance (supplementary figure 1, Fig. 1A+B).

INDUCIBILITY OF AHR SIGNALING BY AHR AGONISTS IN HUMAN SKIN CELLS and MEFs

In order to verify that AhR signaling in fibroblasts is not functional as reported previously by others (reviewed in (Haarmann-Stemmann and Abel, 2006;Evans *et al.*, 2008)) we challenged the 25 different NHDF strains with 250 nM of the AhR agonist B(a)P (Fig. 2A-F). Indeed, B(a)P did not increase CYP1A1 copy numbers significantly. However, plotting the obtained data as x-fold of solvent control (supplementary figure 2) discloses a significant increase in CYP1A1 induction for the age groups 40-49, 50-59 and > 60. In the age group 50-59 preincubation of cells with the competitive AhR antagonist MNF (10 μM) inhibited this CYP1A1 induction significantly. However, figure 2B – F, which shows the detailed analysis of figure 2 A (each graph representing one age group) clearly demonstrates that the inducibility of CYP1A1 after treatment with B(a)P displays large interindividual differences. If these differences in inducibility of CYP1A1 in NHDF cells is due to respective AhRR content of the cells was determined by linear regression analyses. With a coefficient of determination (r^2) of 0.02 (Fig. 2I, basal) and 0.008 (Fig. 2J, induced) it is not likely that basal or inducible

CYP1A1 expression in NHDFs is determined by AhRR expression. In contrast to those findings, CYP1A1 of AhRR$^{-/-}$ MEFs is 3200-fold inducible by 10 μM of the AhR agonist 3-MC (Fig. 2G). However, this represents a change of copy numbers from 0.00003 to 0.1 copies/10^4 transcripts β-Actin. AhRR$^{+/+}$ MEFs do not show a significant change in CYP1A1 expression. In NHEKs CYP1A1 expression is significantly induced by 250 nM B(a)P approx. 3-fold (from ~100 to ~300 copies/10^4 β-actin).

CYP1A1 ENZYME ACTIVITY IN NHDFS COMPAIRED TO AHRR$^{+/+}$ AND AhRR$^{-/-}$ MEFS

Functional relevance of CYP1A1 induction reflects in CYP1 enzyme activity. Therefore, we measured for the first time EROD activity in NHDFs, AhRR$^{+/+}$ and AhRR$^{-/-}$ MEFs. For NHDFs, three individuals from the lowest (1) and highest (2) age group, respectively, which displayed the largest CYP1A1 mRNA induction upon AhR activation, were chosen for the functional analyses. NCTC 2544 cells, a keratinocyte cell line with known CYP1 induction upon AhR activation (Götz *et al.*, 2011), were used as a positive control. B(a)P and 3-MC (0.01, 0.1, 0.25, 1 and 10 μM) did not induce EROD activity above the limit of quantification (LOQ; indicated by dotted line) in any of the NHDFs under any condition tested, whereas NCTC cells presented a significantly inducible EROD substrate turnover (from basal 1 to induced 100 – 200 pmol min^{-1}mg^{-1}; Fig.3 A-C). EROD activity was also not detectable in AhRR$^{+/+}$ MEFs upon any treatment (Fig. 3D), whereas 1 μM B(a)P or 3-MC resulted in a marginal EROD activity at the level of the LOQ at 0.8 pmol min^{-1}mg^{-1} in AhRR$^{-/-}$ MEFs (Fig. 3E). Compared to keratinocytes, this turnover rate is negligible.

EFFECT OF HDAC INHIBITION ON EXPRESSION OF CYP1A1 AND AHRR MRNA AND EROD ACTIVITY IN NHDFS

Previous works from our own laboratory (Haarmann-Stemmann *et al.*, 2007) and others (Oshima *et al.*, 2007;Gradin *et al.*, 1999) showed that HDAC inhibition leads to a superinduction of CYP1A1 mRNA in fibroblasts. HDACs are recruited by the AhRR and they are necessary for its transcription inhibitory activity (Gradin *et al.*, 1999). In the same three NHDF cell strains already employed for the induction experiments in Fig.3, HDACs were inhibited by TSA (0.5 μM). As expected, TSA increased CYP1A1 mRNA expression, whereas in the same samples AhRR mRNA expression was

diminished (Fig. 4; A-F). However, EROD enzyme activity analyses in these cells for all three individuals demonstrated that the so far called 'superinduction' of CYP1A1 by HDAC inhibition does not lead to an increase in measurable EROD activity above the LOQ − despite the reduction in AhRR mRNA expression (Fig. 4G-I). None of these treatments decreased cell viability (Supplementary Fig. 3).

DISCUSSION

For a decade now it is thought that the AhRR represses AhR-dependent xenobiotic metabolism in HeLa cells or fibroblasts (reviewed in (Evans *et al.*, 2008;Haarmann-Stemmann and Abel, 2006)). This assumption is founded mainly on mRNA expression or overexpression experiments (Mimura *et al.*, 1999a). Therefore, we revisited this common knowledge 'AhRR hypothesis' by expanding the data base for (i) primary human fibroblasts from 25 different donors, (ii) physiological stoichiometry of AhR signaling compounds and involvement of HDACs in these not genetically manipulated cells and (iii) a functional readout, CYP1 activity. The data is confirmed by including AHRR$^{+/+}$ and AHRR$^{-/-}$ MEFs and set in relation to keratinocytes which are known to possess approximately 10% of liver CYP1 activity (Smith C.K. and Hotchkiss S.A.M., 2001). This thorough revisiting of the AhRR hypothesis revealed that - at least in primary human fibroblasts – the AhRR does not control AhR-dependent CYP activity. However, our data do not necessarily contradict the current literature, but extends the existing knowledge to primary cells from 25 individual adult human donors and the functional endpoint CYP activity, which had not been assessed with regard to the AhRR before.

Since the 1980s it has been known that inhibition of protein synthesis (e.g. by cycloheximide) causes superinduction of TCDD-induced CYP1A1 mRNA expression in liver cell lines (Israel *et al.*, 1985). Moreover, inhibitors of protein synthesis blocked the down-regulation of AhR function after short-time incubations with AhR-agonists (Lusska *et al.*, 1992). These interesting phenomena caused by protein synthesis inhibitors were ascribed to inhibited synthesis of a short-lived repressor of AhR function, the entity of which at that time remained elusive. Then, in 1993, Gradin et al. observed a lack of basal and inducible CYP1A1 by Northern Blot analyses in fibroblasts (Gradin *et al.*, 1993). XRE reporter gene experiments revealed a smaller luciferase

induction upon AhR-ligand exposure in fibroblasts than in keratinocytes and HepG2 cells. The clue for the AhRR was further established by an EMSA in the same study: nuclear protein of TCDF-treated fibroblasts showed 2 XRE-specific protein-DNA complexes. One of those did not react with the AhR antiserum and was also not visible in keratinocytes and HepG2 cells. This was thus the first identification of the AhRR, although the name had not been established yet. Final recognition of the AhR repressing molecular function was based on the observation that overexpression of a novel bHLH-PAS protein with N-terminal similarities to the AhR modulated AhR signaling (Mimura *et al.*, 1999a). Sequence identification of this now called AhRR facilitated expression analyses and certainly enriched research in the AhR field. One important observation was that AhRR expression level is tissue-specific (Tsuchiya *et al.*, 2003;Iwanari *et al.*, 2002). E.g. ACHN, A549, HT-1197, HeLa, and NEC14 cells express very different levels of AhRR. But not only in tumor cells of distinct origins but also in normal tissues of rodent and humans AhRR levels differ tremendously (Nishihashi *et al.*, 2006;Korkalainen *et al.*, 2004;Tsuchiya *et al.*, 2003;Yamamoto *et al.*, 2004;Bernshausen *et al.*, 2006;Hosoya *et al.*, 2008). This cell-specificity is indirectly supported by the above-mentioned XRE-reporter gene experiments from Gradin et al. (Gradin *et al.*, 1993). Their data suggest that two cell types, fibroblasts and keratinocytes, within the organ skin might contain high and low levels of AhRR expression, respectively. In the present study we found the AhRR, AhR and ARNT expressed in human fibroblasts and keratinocytes, not by northern blot analyses but by real time RT-PCR (Fig. 1). We identified gene expressions for AhRR in the same order of magnitude in both cell types and for AhR an up to 1500-times higher expression in keratinocytes compared to fibroblasts. Our findings are in contrast to previous work of Akintobi et al (Akintobi *et al.*, 2007) who found a 6-fold higher expression of AhRR vs. AhR in human fibroblasts than in human keratinocytes. These differences might be due to interindividual or gender variation (Supplementary Fig. 1), especially since the Akintobi study does not reveal how many individuals from which gender were tested.

Gene induction experiments with B(a)P from this study are in agreement with the work from Hosoya et al. (Hosoya *et al.*, 2008). While the CYP1A1 was induced up to 8-fold by B(a)P in NHDFs from this study, it was 25-fold induced by B(a)P in murine skin fibroblasts. Differences in magnitude of induction are possibly due to different B(a)P

concentrations (250 nM vs. 1 µM), incubation times (48 vs. 24 hrs), species or cellular age, as our donors were 20-60 year old females and the Hosoya study used skin fibroblasts from neonatal mice. In contrast, Gradin et al. (Gradin *et al.*, 1993) did not observe CYP1A1 induction by TCDF in fibroblasts derived from neonatal foreskin, which may be due to the method of detection, because real time RT-PCR is more sensitive than northern blot analysis, the age of the donors or even the skin location where fibroblasts were gained from. Fibroblasts of the same donor, prepared from skin from different parts of the body, display differences in their expression profile (Chang *et al.*, 2002). The role of the AhRR in magnitude of CYP1A1 induction in fibroblasts was tackled by the usage of AhRR proficient and deficient mouse fibroblasts. Hosoya et al. (Hosoya *et al.*, 2008) as well as this study (Fig. 2G) observed higher CYP1A1 induction after treatment with an AhR agonist in $AhRR^{-/-}$ MEFs (150- (Hosoya) and 3000-fold (this study), respectively). The differences in magnitude between the two studies might be explained by inducers (B(a)P vs. 3-MC), incubation times (24 vs. 48 hrs) or cell type (neonatal fibroblasts vs. MEFs).

To critically challenge the role of the AhRR in control of CYP1A1 expression in fibroblasts we took a step back from 'fold of gene induction' to the raw data, i.e. AhRR copy numbers, which were derived from a product-specific copy number standard. These analyses revealed that copy numbers of this gene are very low with 0.01 and 0.015 copies/10^4 transcripts β-Actin in fibroblasts and MEFs, respectively. As the actual gene copy numbers for the AhRR have not been reported previously, we cannot compare our data to any other study. But within our data we see that fibroblasts and MEFs express the AhRR in the same order of magnitude. Surprisingly, also primary keratinocytes express the AhRR at a similar very low level (0.06 copies / 10^4 transcripts β-Actin; Fig. 1D). Despite this low expression level we wanted to know if there is any functional relevance of the AhRR on AhR signaling. Therefore, we employed two strategies: first, we correlated gene copy numbers of basal and induced CYP1A1 expression with AhRR expression and second, we measured CYP1 enzyme activity with the EROD assay in primary fibroblasts as well as in the in $AhRR^{+/+}$ and $^{-/-}$ MEFs. Expression level of the AhRR does not correlate with neither basal nor induced CYP1A1 gene expression level (Fig. 2 I+G). However, CYP1A1 did not correlate with AhR or ARNT expression either (data not shown). AhRR expression and inducibility of

CYP1A1 also showed no association in nine different tumor cell lines in an earlier study (Tsuchiya *et al.*, 2003). Therefore, these data suggest that in the physiological stoichiometry of the cell, the AhRR does not necessarily determine AhR signalling. That this suggestion is true for human fibroblasts is strongly supported by our functional data. Measurements of enzyme activity in human fibroblasts (chosen were the individuals with highest CYP gene expression / induction) and in AhRR$^{+/+}$ and $^{-/-}$ MEFs clearly showed that in the copy number range of CYP1A1 gene expression (up to 10 copies hCYP1A1/10^4 transcripts β-Actin), there is no EROD activity measurable above the LOQ in primary human fibroblasts (Fig. 3 A-C). Wildtype MEFs also displayed no EROD activity, whereas AhRR$^{-/-}$ MEFs just reached the LOQ (at 1 pmol/min/mg Ethoxyresorufin) with inducer concentrations up to 1 μM (Fig. 3 D+E). As this enzyme activity is very low, especially in comparison to keratinocytes (100-200 pmol/min/mg Ethoxyresorufin; Fig. 3, (Götz *et al.*, 2011)), we doubt the physiological relevance of this pathway for CYP1A1 activity in fibroblasts.

Previous work identified the association of AhRR function with HDAC activity (Haarmann-Stemmann *et al.*, 2007;Oshima *et al.*, 2007). As this was supposed to be the molecular mechanism of CYP1A1 expression control, we treated our 3 best inducible individuals with the HDAC inhibitor TSA in presence or absence of B(a)P. Our study reproduces the previous results that CYP1A1 transcripts are strongly induced upon TSA exposure, which in our cells correlates with a down-regulation of AhRR expression. However, measuring EROD activities in those cells, the substrate turnover never reached the LOQ clearly showing that CYP1A1 mRNA expression is over all too low to be translated into physiologically relevant CYP1 activity in these cells.

Taken together, by revisiting the 'AhRR hypothesis' in primary human fibroblasts from 25 human individuals we reproduced the current literature by showing that (i) the AhRR is expressed in NHDFs, (ii) CYP1A1 mRNA is moderately induced in these cells by AhR activators and that (iii) HDAC inhibition by TSA elevates CYP1A1. However, CYP1A1 induction at these very low expression levels does not translate into CYP1 enzyme activity. Thus, although we agree that CYP activity in primary human fibroblasts is repressed, our data gives strong indications that not the AhRR but a so far unidentified other factor mediates the repression of CYP activity in these cells.

Practically, this is of relevance not only for environmentally-induced skin diseases, but also for therapeutical interventions as AhR modifying compounds are used as sunscreens as well as therapeutics. E.g. coal tar which contains a variety of AhR agonists has been used for psoriasis treatment (Goeckerman W, 1931) or the antifungal ketoconazole has recently been identified as an AhR agonist (Tsuji *et al.*, 2011). To understand the effects and side effects of such compounds on different skin cell types on a molecular basis, knowledge of regulation of AhR signalling is essential. This work contributes to the comprehension of AhR signalling in primary human fibroblasts.

MATERIALS AND METHODS

Chemicals and materials

All chemicals, if not otherwise specified, were purchased from Sigma-Aldrich (Germany) and were of highest purity available. Cell culture media were obtained from PAA (Austria) and PromoCell (Germany). The CBQCA protein quantification kit was purchased from Molecular Probes/Invitrogen (Germany). Cell Titer-Blue cell viability assay was purchased from Promega (USA). Multi-well plates and cell culture devices were obtained from Greiner (Germany) and Carl Roth GmbH (Germany).

Preparation of primary fibroblasts

NHDFs: Dermal fibroblasts from 25 healthy probands were prepared from skin samples from breast reduction surgery obtained from the hospital Kaiserswerther Diakonie in Düsseldorf, Germany. The samples originated from female patients of five different age groups (20-29, 30-39, 40-49, 50-59, >60; five each) and unknown pharmacological background. Patients were informed beforehand and agreed to donate removed tissue for scientific purpose. The preparation of primary human fibroblasts has been fully approved by the Ethics Committee, Heinrich-Heine-University of Düsseldorf (Project-Nr.: TOX_EF_D01/2008). Skin samples were collected immediately after surgery, kept cold during the transport (< 1h) and processed immediately. Briefly: subcutaneous fat and half of the dermis were removed before skin samples were cut into ~0.5 cm^2 pieces. Skin pieces were washed in 70 % Ethanol immediately followed by sterile PBS. Skin pieces were incubated with dispase (10 mg/ml in PBS, sterile filtered) at 37°C and 5 %

CO_2 for two hours, afterwards epidermal sheets were removed and dermal pieces were plated in cell culture dishes. Pieces were left to dry for 30 minutes, then medium was added. Fibroblasts started to migrate out of the dermal pieces approximately after 1-2 weeks. Cells were used for experiments in passages 1-7. Cell labeling: F = fibroblast; number = age; D + number = internal identification number; W = female (German: weiblich); B = breast.

MEFs: Murine embryonic fibroblasts (MEF) were generated from embryos of Wildtype and AhRR-deficient mice (H.W. and I.F. unpublished) at embryonic day 14. Cells were maintained in DMEM containing 10% FCS, 1% Glutamine, 0,1% 2-Mercaptoethanol and 1% Penicillin Streptomycin and were used as passage 3 cells for all experiments.

Cell culture

NHDFs were cultured in DMEM High Glucose with stable Glutamine containing 10 % (v/v) fetal calf serum (FCS) and 1 % (v/v) of antibiotic-antimycotic solution (PAA, Cat. No. P11-002). MEFs were cultured as mentioned above. NCTC 2544 were cultured in MEM containing 10 % (v/v) fetal calf serum (FCS) and 1 % (v/v) of antibiotic-antimycotic solution. Primary normal human epidermal keratinocytes (NHEK-c; PromoCell GmbH, Heidelberg, Germany) from a 29 year old female donor (breast) were cultured in full KGM2 Media (PromoCell, Germany) supplemented with supplement mix and 50 µg/ml gentamycin (PAA, Pasching, Austria) and 2.5 µg/ml amphotericyne (PAA). All cells were maintained under standard conditions at 37°C and 5 % CO_2. Treatment of cells was performed 24 h after seeding in 6-well plates (RNA analysis) or 48-well-plates (EROD/CTB) in the respective media. For subsequent EROD assay, the respective media were used without FCS supplementation.

RNA isolation, Reverse transcription-PCR and real time RT-PCR

Total RNA was isolated from cells using PeqLab Total RNA Kit (PeqLab, Erlangen, Germany) according to the manufacturer's instructions. RNA concentration was assessed by spectrophotometry at 260 nm. Reverse transcription was performed as follows: for cDNA synthesis 500 ng of total RNA, 1 µg of p(DT)15 primer (Roche, Switzerland) and 5 mM solutions of each dNTP were dissolved in 10 µl of H_2O and heated for 5 min at 65°C. The samples were chilled, and 4 µl of 4 x RT buffer (250 mM Tris HCl, 375 mM KCl, 15 mM $MgCl_2$) and 200 U of M-MLV reverse transcriptase

(Promega, Madison, USA) were added to a final volume of 20 µl. The samples were reverse transcribed at 37°C for 50 min, and the reaction was inactivated at 70°C for 15 min. Real time RT-PCR was performed by using the Rotor Gene Q device (Qiagen, Hilden, Germany). The PCR mix consisted of 1/10 volume of Quanti Tect SYBR Green FAST PCR Master Mix (Qiagen, Hilden, Germany), 0.5 µM solutions of each primer, 2.5 µl of cDNA (after RT-PCR diluted 1:2.5 with H_2O), in a final volume of 15 µl. The application started with an initial incubation step of 7 min at 95°C to activate the DNA polymerase. The conditions for PCR amplifications were 47 cycles of 10 sec at 95°C for denaturation, 35 sec at 60°C of primer annealing, elongation and fluorescence detection. PCR-primer sequences for human and murine CYP1A1, AhRR, AhR, ARNT and β-Actin are given in the supplementary materials Table 1. The quantification of PCR products was estimated from fragment-specific standard curves and was calculated with the Rotor Gene Q 1.7 (Qiagen, Hilden, Germany) software. Standard curves were prepared by using 1.5×10^2 to 1.5×10^7 cDNA copies per µl and amplified as described above. MEFs: For qPCR analyses 1×10^6 cells stimulated with 10µM 3MC or DMSO as control for 3h RNA was extracted using the Mini RNA Isolation kit^{TM} (Zymo Research, Heidelberg, Germany). First-strand cDNA was synthesized from 1 µg of total RNA using a mixture of oligo(dT)$_{12–18}$ primers and Revert Aid reverse transcriptase (Thermo Fisher Scientific, Bonn, Germany) according to the manufacturer's instructions.

EROD activity

For measuring CYP1A1 activities in living monolayer cultures, ethoxyresorufin (solved in DMSO) was employed according to a protocol described by (Rolsted et al., 2008). Resorufin as the reaction product in the respective media or assay solution was used to generate standard curves. Shortly, serum-free media containing 2.5 µM ethoxyresorufin and 10 µM dicumarol (to prevent metabolism of the reaction product resorufin by NQO1 (Asher et al., 2002) and Phase II enzymes) were applied to PBS-washed monolayer cells and resorufin formation kinetics were measured 21 min at 37°C at excitation and emission wavelength of 544 nm and 590 nm on a Thermo Ascent Fluoroscan fluorometric plate reader. Suitability of the EROD assay for both species, human and mouse, was shown by comparing EROD activities of liver microsomes for the two species (Götz et al., 2011). Cells were treated with the synthetic AhR agonist 3-

methylcholantrene (3-MC) and the environmentally relevant AhR agonist benzo(a)pyrene (B(a)P) dissolved in DMSO. These were added to the culture medium. Standard incubation times for induction were 24 h and final maximum solvent concentration was 0.2 % unless otherwise noted. All experiments were carried out three times in triplicate employing each three independent cell lots unless otherwise noted. For experiments with H-DAC inhibitor TSA (0.5 μM in EtOH) cells were coincubated with the respective inhibitor and B(a)P or respective solvent.

Cell viability and protein content assessment

Assay kit for measurement of cell viability (Cell Titer Blue, Promega Corp., Madison WI, USA) was applied as described by the manufacturer. Protein in monolayer cell culture was determined using the CBQCA protein quantification kit (Molecular Probes/Invitrogen, Germany) using bovine serum albumin as reference protein at ex 465 nm and em 550 nm on a Thermo Ascent Fluoroscan fluorometric plate reader.

Statistics

All experiments were conducted at least three times. Statistical analyses for significance were performed using the Student's unpaired t-test; $p < 0.05$ was considered significant. Data are presented as means ± SD. LOQ was defined as mean of blank measurements plus 9 times standard deviation of the blank. Correlations analyses were performed by using the GraphPad Prism 5 statistical Software.

CONFLICT OF INTEREST

The authors state no conflict of interest.

Reference List

1 Abel J, Haarmann-Stemmann T: An introduction to the molecular basics of aryl hydrocarbon receptor biology. Biol Chem 391:1235-1248 (2010).

2 Afaq F, Mukhtar H: Effects of solar radiation on cutaneous detoxification pathways. J Photochem Photobiol B 63:61-69 (2001).

3 Ahmad N, Agarwal R, Mukhtar H: Cytochrome P-450 and drug development for skin diseases. Skin Pharmacol 9:231-241 (1996).

4 Ahmad N, Mukhtar H: Cytochrome p450: a target for drug development for skin diseases. J Invest Dermatol 123:417-425 (2004).

5 Akintobi AM, Villano CM, White LA: 2,3,7,8-Tetrachlorodibenzo-p-dioxin (TCDD) exposure of normal human dermal fibroblasts results in AhR-dependent and -independent changes in gene expression. Toxicol Appl Pharmacol 220:9-17 (2007).

6 Alvares AP, Kappas A, Levin W, Conney AH: Inducibility of benzo( )pyrene hydroxylase in human skin by polycylic hydrocarbons. Clin Pharmacol Ther 14:30-40 (1973a).

7 Alvares AP, Leigh S, Kappas A, Levin W, Conney AH: Induction of aryl hydrocarbon hydroxylase in human skin. Drug Metab Dispos 1:386-390 (1973b).

8 Asher G, Lotem J, Kama R, Sachs L, Shaul Y: NQO1 stabilizes p53 through a distinct pathway. Proc Natl Acad Sci U S A 99:3099-3104 (2002).

9 Bergander L, Wahlstrom N, Alsberg T, Bergman J, Rannug A, Rannug U: Characterization of in vitro metabolites of the aryl hydrocarbon receptor ligand 6-formylindolo[3,2-b]carbazole by liquid chromatography-mass spectrometry and NMR. Drug Metab Dispos 31:233-241 (2003).

10 Bergander L, Wincent E, Rannug A, Foroozesh M, Alworth W, Rannug U: Metabolic fate of the Ah receptor ligand 6-formylindolo[3,2-b]carbazole. Chem Biol Interact 149:151-164 (2004).

11 Bernshausen T, Jux B, Esser C, Abel J, Fritsche E: Tissue distribution and function of the Aryl hydrocarbon receptor repressor (AhRR) in C57BL/6 and Aryl hydrocarbon receptor deficient mice. Arch Toxicol 80:206-211 (2006).

12 Bickers DR, Mukhtar H, Dutta-Choudhury T, Marcelo CL, Voorhees JJ: Aryl hydrocarbon hydroxylase, epoxide hydrolase, and benzo[a]-pyrene metabolism in human epidermis: comparative studies in normal subjects and patients with psoriasis. J Invest Dermatol 83:51-56 (1984).

13   Chang HY, Chi JT, Dudoit S, Bondre C, van de Rijn M, Botstein D, Brown PO: Diversity, topographic differentiation, and positional memory in human fibroblasts. Proc Natl Acad Sci U S A 99:12877-12882 (2002).

14   Das M, Asokan P, Don PS, Krueger GG, Bickers DR, Mukhtar H: Carcinogen metabolism in human skin grafted onto athymic nude mice: a model system for the study of human skin carcinogenesis. Biochem Biophys Res Commun 138:33-39 (1986).

15   Du L, Neis M, Ladd PA, Lanza DL, Yost GS, Keeney DS: Effects of the differentiated keratinocyte phenotype on expression levels of CYP1-4 family genes in human skin cells. Toxicol Appl Pharmacol 213:135-144 (2006).

16   Evans BR, Karchner SI, Allan LL, Pollenz RS, Tanguay RL, Jenny MJ, Sherr DH, Hahn ME: Repression of aryl hydrocarbon receptor (AHR) signaling by AHR repressor: role of DNA binding and competition for AHR nuclear translocator. Mol Pharmacol 73:387-398 (2008).

17   Fritsch: Dermatologie and Venerologie für das Studium. (Springer Medizin Verlag, Heidelberg 2009).

18   Fritsche E, Schafer C, Calles C, Bernsmann T, Bernshausen T, Wurm M, Hubenthal U, Cline JE, Hajimiragha H, Schroeder P, Klotz LO, Rannug A, Furst P, Hanenberg H, Abel J, Krutmann J: Lightening up the UV response by identification of the arylhydrocarbon receptor as a cytoplasmatic target for ultraviolet B radiation. Proc Natl Acad Sci U S A 104:8851-8856 (2007).

19   Fujii-Kuriyama Y, Imataka H, Sogawa K, Yasumoto K, Kikuchi Y: Regulation of CYP1A1 expression. FASEB J 6:706-710 (1992).

20   Fujisawa-Sehara A, Sogawa K, Yamane M, Fujii-Kuriyama Y: Characterization of xenobiotic responsive elements upstream from the drug-metabolizing cytochrome P-450c gene: a similarity to glucocorticoid regulatory elements. Nucleic Acids Res 15:4179-4191 (1987).

21   Goeckerman W: Treatment of psoriasis: continued observations on the use of crude coal tar and ultraviolett light. Arch Derm Syphilol 24:446-450 (1931).

22   Gonzales FJ: Role of cytochromes P450 in chemical toxicity and oxidative stress: studies with CYP2E1. Mutation Research 569:101-110 (2005).

23   Götz C, Pfeiffer R, Tigges J, Hübenthal U, Merk HF, Krutmann J, Edwards R, Abel J, Pease C, Goebel C, Hewitt N, Fritsche E: Xenobiotic metabolism capacities of human skin in comparison to 3D-epidermis models and keratinocyte-based cell culture as *in vitro* alternatives for chemical testing: Phase II . Exp Dermatol submitted (2011).

24 Götz C, Pfeiffer R, Blatz, Tigges J, Blatz V, Jäckh C, Hübenthal U, Ruwiedel K, Freytag E, Fabian W, Landsiedel R, Merk HF, Krutmann J, Edwards R, Abel J, Pease C, Goebel C, Hewitt N, Fritsche E: Xenobiotic metabolism capacities of human skin in coparison to a 3D-epidermal model and keratinocyte-based cell culture as an in vitro alternative for chemical testing: phase I. Exp Dermatol submitted (2011).

25 Gradin K, Toftgard R, Poellinger L, Berghard A: Repression of dioxin signal transduction in fibroblasts. Identification Of a putative repressor associated with Arnt. J Biol Chem 274:13511-13518 (1999).

26 Gradin K, Wilhelmsson A, Poellinger L, Berghard A: Nonresponsiveness of normal human fibroblasts to dioxin correlates with the presence of a constitutive xenobiotic response element-binding factor. J Biol Chem 268:4061-4068 (1993).

27 Haarmann-Stemmann T, Abel J: The arylhydrocarbon receptor repressor (AhRR): structure, expression, and function. Biol Chem 387:1195-1199 (2006).

28 Haarmann-Stemmann T, Bothe H, Kohli A, Sydlik U, Abel J, Fritsche E: Analysis of the transcriptional regulation and molecular function of the aryl hydrocarbon receptor repressor in human cell lines. Drug Metab Dispos 35:2262-2269 (2007).

29 Hosoya T, Harada N, Mimura J, Motohashi H, Takahashi S, Nakajima O, Morita M, Kawauchi S, Yamamoto M, Fujii-Kuriyama Y: Inducibility of cytochrome P450 1A1 and chemical carcinogenesis by benzo[a]pyrene in AhR repressor-deficient mice. Biochem Biophys Res Commun 365:562-567 (2008).

30 Israel DI, Estolano MG, Galeazzi DR, Whitlock JP, Jr.: Superinduction of cytochrome P1-450 gene transcription by inhibition of protein synthesis in wild type and variant mouse hepatoma cells. J Biol Chem 260:5648-5653 (1985).

31 Iwanari M, Nakajima M, Kizu R, Hayakawa K, Yokoi T: Induction of CYP1A1, CYP1A2, and CYP1B1 mRNAs by nitropolycyclic aromatic hydrocarbons in various human tissue-derived cells: chemical-, cytochrome P450 isoform-, and cell-specific differences. Arch Toxicol 76:287-298 (2002).

32 Korkalainen M, Tuomisto J, Pohjanvirta R: Primary structure and inducibility by 2,3,7,8-tetrachlorodibenzo-p-dioxin (TCDD) of aryl hydrocarbon receptor repressor in a TCDD-sensitive and a TCDD-resistant rat strain. Biochem Biophys Res Commun 315:123-131 (2004).

33 Levin W, Conney AH, Alvares AP, Merkatz I, Kappas A: Induction of benzo( )pyrene hydroxylase in human skin. Science 176:419-420 (1972).

34 Lusska A, Wu L, Whitlock JP, Jr.: Superinduction of CYP1A1 transcription by cycloheximide. Role of the DNA binding site for the liganded Ah receptor. J Biol Chem 267:15146-15151 (1992).

35 Merk HF, Baron JM, Heise R, Fritsche E, Schroeder P, Abel J, Krutmann J: Concepts in molecular dermatotoxicology. Exp Dermatol 15:692-704 (2006).

36 Mimura J, Ema M, Sogawa K, Fujii-Kuriyama Y: Identification of a novel mechanism of regulation of Ah (dioxin) receptor function. Genes Dev 13:20-25 (1999a).

37 Mimura J, Ema M, Sogawa K, Fujii-Kuriyama Y: Identification of a novel mechanism of regulation of Ah (dioxin) receptor function. Genes Dev 13:20-25 (1999b).

38 Morel Y, Mermod N, Barouki R: An autoregulatory loop controlling CYP1A1 gene expression: role of H(2)O(2) and NFI. Mol Cell Biol 19:6825-6832 (1999).

39 Nishihashi H, Kanno Y, Tomuro K, Nakahama T, Inouye Y: Primary structure and organ-specific expression of the rat aryl hydrocarbon receptor repressor gene. Biol Pharm Bull 29:640-647 (2006).

40 Oesch F, Fabian E, Oesch-Bartlomowicz B, Werner C, Landsiedel R: Drug-metabolizing enzymes in the skin of man, rat, and pig. Drug Metab Rev 39:659-698 (2007).

41 Oshima M, Mimura J, Yamamoto M, Fujii-Kuriyama Y: Molecular mechanism of transcriptional repression of AhR repressor involving ANKRA2, HDAC4, and HDAC5. Biochem Biophys Res Commun 364:276-282 (2007).

42 Pendlington RU, Williams DL, Naik JT, Sharma RK: Distribution of xenobiotic metabolizing enzymes in skin. Toxicol In Vitro 8:525-527 (1994).

43 Puntarulo S, Cederbaum AI: Production of reactive oxygen species by microsomes enriched in specific human cytochrome P450 enzymes. Free Radic Biol Med 24:1324-1330 (1998).

44 Rannug A, Rannug U, Rosenkranz HS, Winqvist L, Westerholm R, Agurell E, Grafstrom AK: Certain photooxidized derivatives of tryptophan bind with very high affinity to the Ah receptor and are likely to be endogenous signal substances. J Biol Chem 262:15422-15427 (1987).

45 Rannug U, Rannug A, Sjoberg U, Li H, Westerholm R, Bergman J: Structure elucidation of two tryptophan-derived, high affinity Ah receptor ligands. Chem Biol 2:841-845 (1995).

46 Rolsted K, Kissmeyer AM, Rist GM, Hansen SH: Evaluation of cytochrome P450 activity in vitro, using dermal and hepatic microsomes from four species and two keratinocyte cell lines in culture. Arch Dermatol Res 300:11-18 (2008).

47	Rowlands JC, Gustafsson JA: Aryl hydrocarbon receptor-mediated signal transduction. Crit Rev Toxicol 27:109-134 (1997).

48	Smith C.K., Hotchkiss S.A.M.: Allergic Contact Dermatitis: Chemical and Metabolic Mechanisms. (Taylor & Francis, London 2001).

49	Sogawa K, Iwabuchi K, Abe H, Fujii-Kuriyama Y: Transcriptional activation domains of the Ah receptor and Ah receptor nuclear translocator. J Cancer Res Clin Oncol 121:612-620 (1995).

50	Swanson HI: Cytochrome P450 expression in human keratinocytes: an aryl hydrocarbon receptor perspective. Chem Biol Interact 149:69-79 (2004).

51	Tsuchiya Y, Nakajima M, Itoh S, Iwanari M, Yokoi T: Expression of aryl hydrocarbon receptor repressor in normal human tissues and inducibility by polycyclic aromatic hydrocarbons in human tumor-derived cell lines. Toxicol Sci 72:253-259 (2003).

52	Tsuji G, Takahara M, Uchi H, Matsuda T, Chiba T, Takeuchi S, Yasukawa F, Moroi Y, Furue M: Identification of Ketoconazole as an AhR-Nrf2 Activator in Cultured Human Keratinocytes: The Basis of Its Anti-Inflammatory Effect. J Invest Dermatol (2011).

53	Wei YD, Bergander L, Rannug U, Rannug A: Regulation of CYP1A1 transcription via the metabolism of the tryptophan-derived 6-formylindolo[3,2-b]carbazole. Arch Biochem Biophys 383:99-107 (2000).

54	Wei YD, Helleberg H, Rannug U, Rannug A: Rapid and transient induction of CYP1A1 gene expression in human cells by the tryptophan photoproduct 6-formylindolo[3,2-b]carbazole. Chem Biol Interact 110:39-55 (1998).

55	Wei YD, Rannug U, Rannug A: UV-induced CYP1A1 gene expression in human cells is mediated by tryptophan. Chem Biol Interact 118:127-140 (1999).

56	Wincent E, Amini N, Luecke S, Glatt H, Bergman J, Crescenzi C, Rannug A, Rannug U: The suggested physiologic aryl hydrocarbon receptor activator and cytochrome P4501 substrate 6-formylindolo[3,2-b]carbazole is present in humans. J Biol Chem 284:2690-2696 (2009).

57	Yamamoto J, Ihara K, Nakayama H, Hikino S, Satoh K, Kubo N, Iida T, Fujii Y, Hara T: Characteristic expression of aryl hydrocarbon receptor repressor gene in human tissues: organ-specific distribution and variable induction patterns in mononuclear cells. Life Sci 74:1039-1049 (2004).

TABLES

Figure 1: Expression of AhR signaling components in human skin cells and MEFs
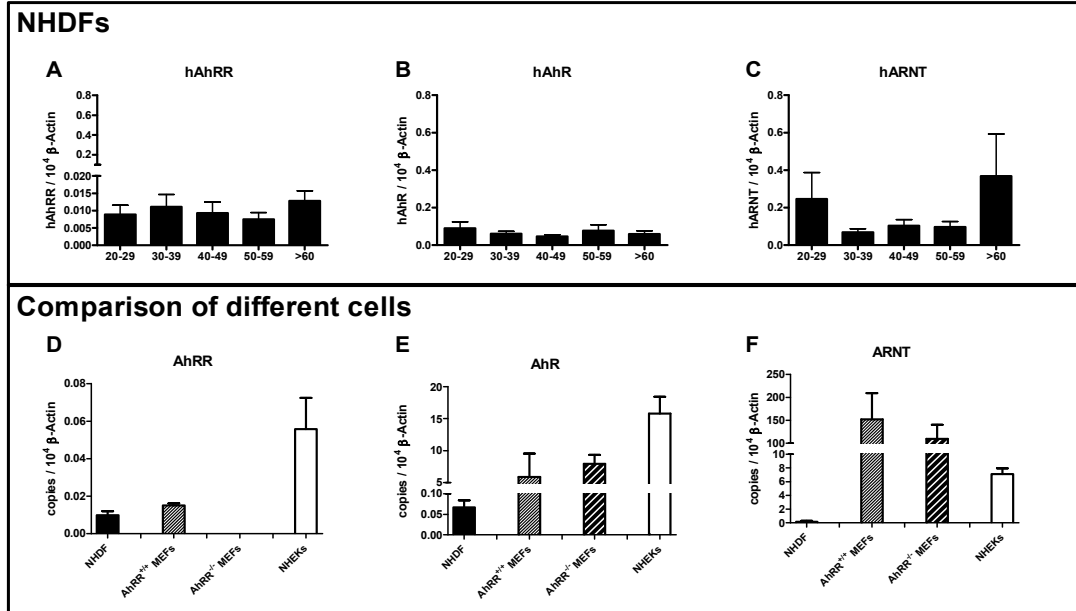
Figure 2: Inducibility of AhR signaling in human skin cells and MEFs
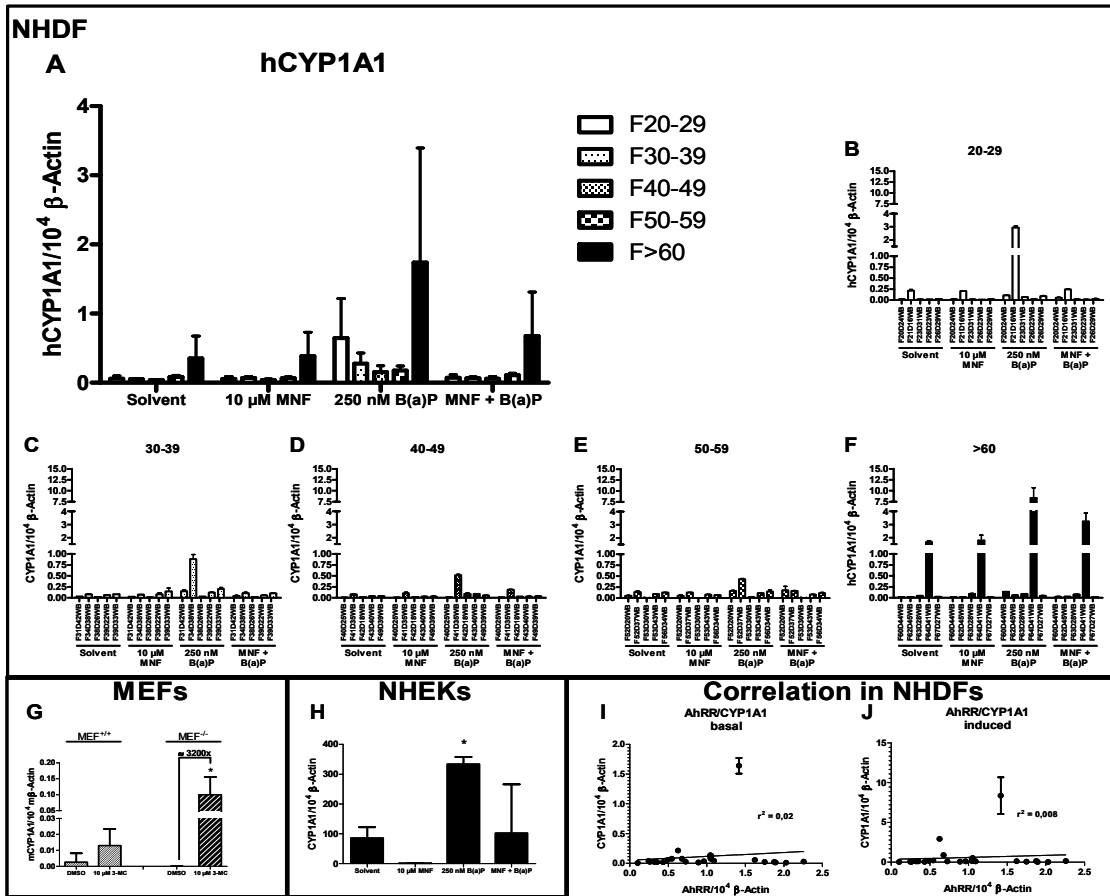
Figure 3: CYP1A1 enzyme activity in NHDFs compaired to AhRR$^{+/+}$ and AhRR$^{-/-}$ MEFs
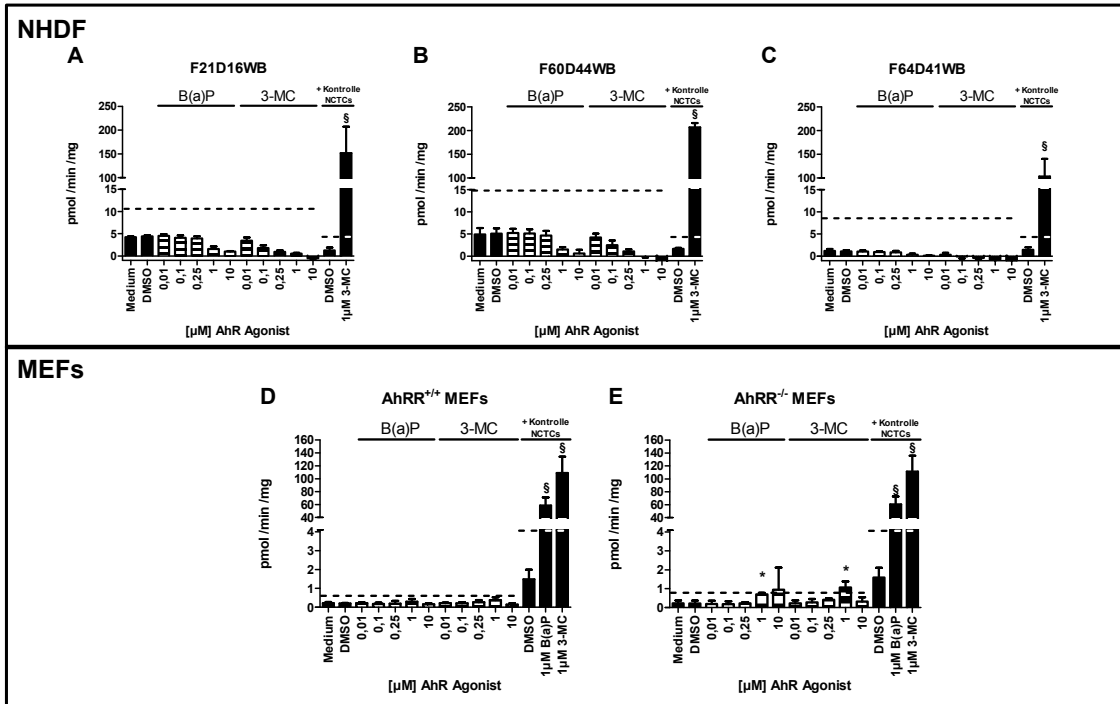
Figure 4: Effect of HDAC inhibition on expression of CYP1A1 and AhRR mRNA as well as EROD activity in NHDFs
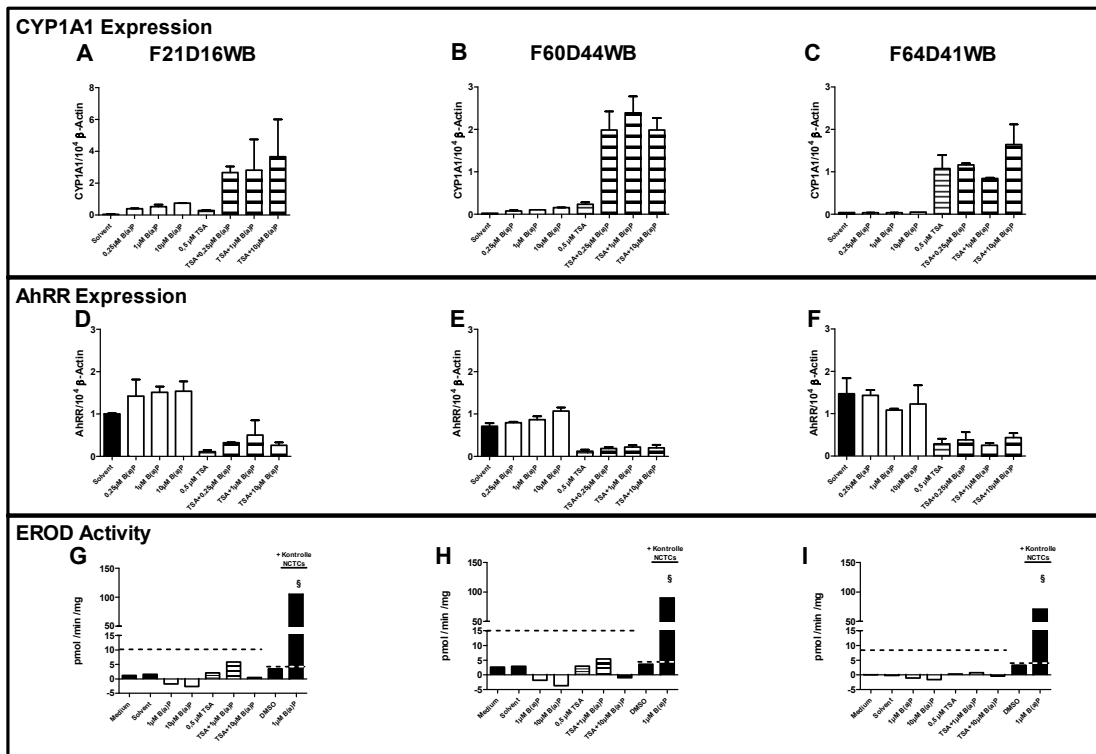
FIGURE LEGENDS

Figure 1: Expression of AhR signaling components in human skin cells and MEFs. Real-time RT-PCR detection of AhRR, AhR and ARNT in NHDFs of different aged donors (**A–C**), AhRR$^{+/+}$ and AhRR$^{-/-}$ MEFs, as well as NHEKs (**D–F**). Messenger RNAs of AhR signaling components were detected in different cells after 48 h in culture (if not otherwise noted), expression of each gene was normalized to 10^4 transcripts β-Actin.

A: Expression of AhRR in NHDFs cells of 5 different age groups, each bar representing 5 individuals (n = 25).

B: Expression of AhR in NHDFs cells of 5 different age groups, each bar representing 5 individuals (n = 25).

C: Expression of ARNT in NHDFs cells of 5 different age groups, each bar representing 5 individuals (n = 25).

D: Comparison of AhRR expression in NHDF (n = 25), AhR$^{+/+}$ MEFs (n = 2-5), AhR$^{-/-}$ MEFs (n = 2-5) and NHEKs (n = 3). AhRR expression in normalized to 10^4 copies β-Actin, analysis of MEF cells was performed after three hours.

E: Comparison of AhR expression in NHDF (n = 25), AhR$^{+/+}$ MEFs (n = 2-5), AhR$^{-/-}$ MEFs (n = 2-5) and NHEKs (n = 3). AhRR expression in normalized to 10^4 copies β-Actin, analysis of MEF cells was performed after three hours.

F: Comparison of ARNT expression in NHDF (n = 25), AhR$^{+/+}$ MEFs (n = 2-5), AhR$^{-/-}$ MEFs (n = 2-5) and NHEKs (n = 3). AhRR expression in normalized to 10^4 copies β-Actin, analysis of MEF cells was performed after three hours.

Figure 2: Inducibility of AhR signaling by AhR agonists in human skin cells and MEFs. Real-time RT-PCR detection of CYP1A1 in NHDFs of different aged donors (**A–F**), AhRR$^{+/+}$ and AhRR$^{-/-}$ MEFs (**G**), as well as NHEKs (**H**).

A: Summary of inducibility of CYP1A1 in NHDFs cells of five different age groups (20-29, 30-39, 40-49, 50-59 and > 60), each bar graph represents five different individuals (n = 25). Real-time RT-PCR detection of CYP1A1 was performed after pre-treatment with 10 μM MNF for 1 hour followed by 48 hours incubation with B(a)P (250 nM). Expression of CYP1A1 is normalized to 10^4 transcripts β-Actin.

B - F: Graphs show detailed analysis of A, each graph representing one age group (**B:** 20-29, **C:** 30-39, **D:** 40-49, **E:** 50-59 and **F:** > 60). Real-time RT-PCR analysis of CYP1A1 was performed after pre-treatment with 10 μM MNF for 1 hour followed by 48 hours incubation with B(a)P (250 nM). Expression of CYP1A1 is normalized to 10^4 transcripts β-Actin.

G: Inducibility of CYP1A1 in AhRR$^{+/+}$ and AhRR$^{-/-}$ MEFs. Real-time RT-PCR analysis of CYP1A1 was performed after treatment with 10 μM 3-MC for three hours. Expression of CYP1A1 is normalized to 10^4 transcripts β-Actin. * indicates significant increase compared to solvent control (DMSO), p < 0,05, n = 4-5.

H: Inducibility of CYP1A1 in NHEKs. Real-time RT-PCR analysis of CYP1A1 was performed after pre-treatment with 10 μM MNF for 1 hour followed by 48 hours incubation with B(a)P (250 nM). Expression of CYP1A1 is normalized to 10^4 transcripts β-Actin.

I-J: Correlation of AhRR and CYP1A1 (**I:** basal, **J:** induced by 250 nM B(a)P) expression in NHDFs. Basal AhRR expression is plotted on the x-axis, basal (**I**) or induced (**J**) CYP1A1 expression is plotted on the y-axis. Linear regression line and coefficient of determination (r^2) values are shown, n = 25.

Figure 3: Induction of EROD activity in NHDF-cells and MEFs by different concentrations of the AhR-agonists 3-MC and B(a)P (0,01 – 10 μM). The asterisks indicate significant differences (p < 0,05) to solvent (DMSO) control. NCTCs were used as a positive control, § indicates significant differences (p < 0,05) to solvent (DMSO) control of NCTCs. The red line indicates the LOQ for each cell strain. Each graph represents three independent experiments.

A: Induction of EROD activity in NHDF of a 21 year old female donor (F21D16WB) induced by different concentrations 3-MC and B(a)P. Activity is shown in pmol min^{-1} mg^{-1}.

B: Induction of EROD activity in NHDF of a 60 year old female donor (F60D44WB) induced by different concentrations 3-MC and B(a)P. Activity is shown in pmol min^{-1} mg^{-1}.

C: Induction of EROD activity in NHDF of a 64 year old female donor (F64D41WB) induced by different concentrations 3-MC and B(a)P. Activity is shown in pmol min^{-1} mg^{-1}.

D: Induction of EROD activity in wildtype MEFs (MEF$^{+/+}$) induced by different concentrations 3-MC and B(a)P. Activity is shown in pmol min^{-1} mg^{-1}.

E: Induction of EROD activity in AhRR knock out MEFs (MEF$^{-/-}$) induced by different concentrations 3-MC and B(a)P. Activity is shown in pmol min^{-1} mg^{-1}.

Figure 4: Effect of HDAC inhibitor Trichostatin A (TSA; 0,5 μM in EtOH) on expression of CYP1A1 (A-C) and AhRR (D-F) mRNA expression, as well as EROD activity (G-I) in three different NHDF cell strains (F21D16WB, F60D44WB, F64D41WB).

A – F: CYP1A1 and AhRR mRNA levels were quantified using real-time RT-PCR and normalized to 10^4 transcripts β-Actin. Cells were treated for 16 h with different concentrations of B(a)P (0,25, 1 and 10 μM) alone or cotreated with TSA. Each graph represents one experiments performed in duplicates, experiments were done in three different individuals (**A+D**: F21D16WB, **B+E:** F60D44WB, **C+F:** F64D41WB).

G – I: Change in EROD activity in NHDF-cells by different conentrations of B(a)P (1 and 10 μM) alone or cotreatment with TSA (0,5 μM in EtOH). NCTCs were used as a positive control, § indicated significant differences (p < 0,05) to solvent (DMSO) control of NCTCs. The red line indicates the LOQ for each cell strain. Each graph represents one experiment in triplicates (**G:** F21D16WB; **H:** F60D44WB; **I:** F64D41WB). Activity is shown in pmol min^{-1} mg^{-1}.

SUPPLEMENTARY MATERIAL

Supplementary Table 1: Primers used for real-time RT-PCR analysis.

Species	Gene	Accession number NCBI	Sequenz (5'-3')
homo sapiens	CYP1A1	NM_000499.3	F: cct tca tcc tgg aga cct tcc R: atg gtt gat ctg cca ctg gtt t
	AhRR	NM_020731.4	F: cag tta cct ccg ggt gaa ga R: cca gcg caa agc cat taa ga
	AhR	NM_001621.4	F: tgg tct ccc cca gac agt ag R: ttc att gcc aga aaa cca ga
	ARNT	NM_001668.3	F: ccc tag tct cac caa tcg tgg atc R: gta gct gtt gct ctg atc tcc cag
	β-Actin	NM_001101.3	F: ccc cag gca cca ggg cgt gat R: ggt cat ctt ctc gcg gtt ggc ctt ggg gt
	CYP1B1	NM_000104.3	F: aac gtc atg agt gcc gtg tgt R: ggc cgg tac gtt ctc caa atc
mus musculus	CYP1A1	NM_009992.4	F: ccc aca gca cca caa gag ata R: aag tag gag gca ggc aca atg tc
	AhRR	NM_009644.2	F: agg ctt acc atg gga gct ga R: cgc agg aca gaa agc ttg tc
	AhR	NM_013464.4	F: gac agt ttt ccg gct tct tg R: cgc ttc tgt aaa tgc tct cgt
	ARNT	NM_001037737.2	F: tgc ctc atc tgg tac tgc R: gaa cat gct gct cac tgg aa
	β-Actin	NM_007393.3	F: cta caa tga gct gcg tgt gg R: tag ctc ttc tcc agg gag ga
	CYP1B1	NM_009994.1	F: aca tcc cca aga ata cgg tc R: tag aca ggt tcc tca ccg atg

Supplementary Figure 1: Expression of AhR signaling components in different indivuals of primary human fibroblasts
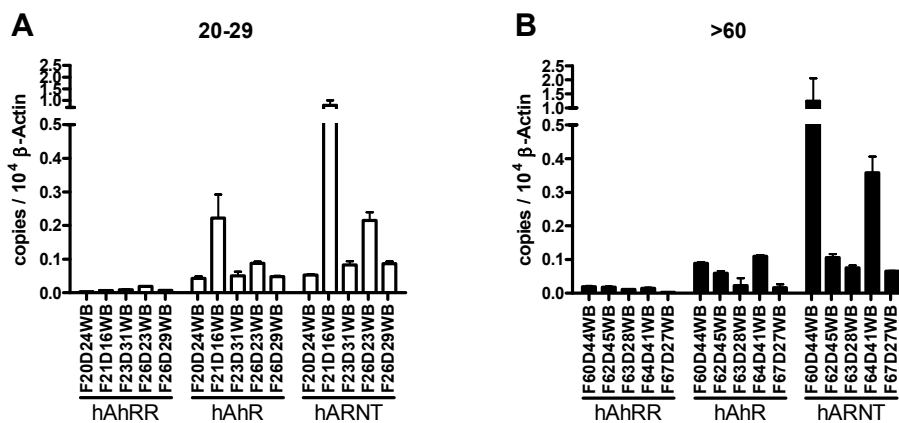
Supplementary Figure 1: Expression of AhR signaling components in different individuals of NHDFs. Graphs show detailed analysis of Figure 1 A-C, regarding the age-groups 20-29 (A) and > 60 (B). Real-time RT-PCR detection of AhRR, AhR and ARNT in NHDFs of different age groups. Messenger RNA of AhR signaling components were analyzed after 48 h in culture, expression of each gene was normalized to 10^4 transcripts β-Actin.

Supplementary Figure 2: Inducibility of AhR signaling by B(a)P in NHDF cells - fold of solven control
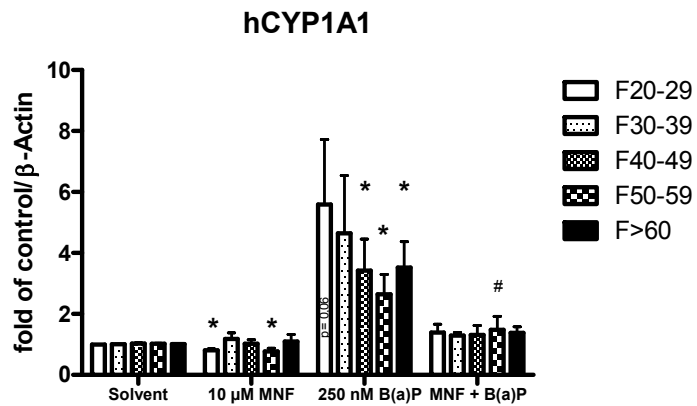
Supplementary Figure 2: Inducibility of AhR signaling by B(a)P in NHDF cells. Real-time RT-PCR detection of CYP1A1 in NHDFs of five different age groups (20-29, 30-39, 40-49, 50-59, > 60), each bar graph represents five different individuals (n = 25). Real-time RT-PCR detection of CYP1A1 was detected after pretreatment with 10 µM MNF for 1 hour followed by 48 hours incubation with B(a)P (250 nM). Expression of CYP1A1 is depicted as fold of solvent control, normalized to β-Actin. * indicates significant differences compared to solvent control, # indicates significant differences compared to B(a)P treated cells (p < 0,05).

Supplementary Figure 3: Effect of HDAC inhibition on cell viability in NHDFs
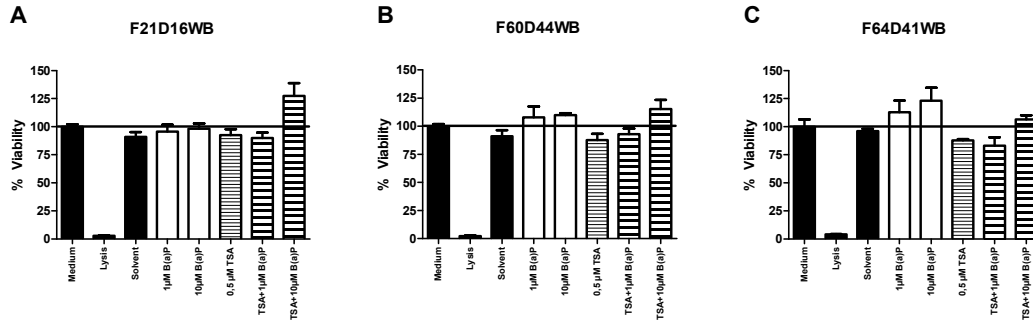
Supplementary Figure 3: Effect of HDAC inhibitor Trichostatin A (TSA; 0,5 µM in EtOH) on cell viability in three different NHDF cell strains (F21D16WB, F60D44WB, F64D41WB).

A - C: Change in cell viability in NHDF-cells by different conentrations of B(a)P (1 and 10 µM) alone or cotreatment with TSA (0,5 µM in EtOH). Lysis of the cells by adding 1:50 9 % Triton X was used as a positive control. The red line markes the approximately 100 % cell viability of untreaded (Medium) cells. Each graph represents one experiment in triplicates (**A:** F21D16WB; **B:** F60D44WB; **C:** F64D41WB).

Publikation Nr. 4

AhRR function revisited: Investigations in adult primary dermal human fibroblasts

Julia Tigges, Heike Weighart, Sandra Wolff, Christine Götz, Irmgard Förster, Zippora Kohne, Ulrike Huebenthal, Hans F. Merk, Thomas Haarmann-Stemmann, Josef Abel, Jean Krutmann und Ellen Fritsche

▬ ▪ ▬ ▪ ▬ ▪ ▬ ▪ ▬ ▪ ▬ ▪ ▬ ▪ ▬ ▪ ▬ ▪ ▬

2.5   Publikation 5

The Arylhydrocarbon Receptor (AhR) in keratinocytes is a universal sensor for environmental stress that mediates skin aging

Extrinsische Hautalterung ist durch den fortschreitenden Verlust von Kollagenfasern aus dem dermalen Kompartiment der Haut gekennzeichnet, was klinisch durch Faltenbildung gekennzeichnet ist und hauptsächlich auf die extrinsich-induzierte Genexpression der Kollagen-degradierenden MMP-1 zurückzuführen ist. Zu den Umweltfaktoren, die bekannterweise zu Hautalterung führen und die MMP-1 aktivieren, gehören sowohl Ultraviolet-B (UVB)-Strahlung, als auch Tabakrauch und durch Straßenverkehr verursachter Feinstaub, welche beide polyaromatische Kohlenwasserstoffe (PAK) wie Benzo(a)pyren (B(a)P) enthalten. In dieser Publikation zeigen wir, dass die Wirkung aller drei Umweltfaktoren durch den selben molekularen Signalweg, die Aktivierung des zytoplasmatischen Arylhydrocarbon-Rezeptors (AhR), vermittelt wird. So führt die Exposition von humanen erpidermalen Keratinozyten (NHEK) gegenüber UVB oder B(a)P zu einer Induktion der MMP-1 mRNS Expression und Enzymaktivität. Diese konnte durch Präinkubation der Zellen mit dem AhR-Inhibitor 3'-Methoxy-4'-nitroflavon (MNF) verhindert werden. Versuche mit pharmakologischen Inhibitoren deuten darauf hin, dass die AhR-mediierte MMP-1 Aktivierung über die src – *Epidermal Growth Factor Receptor* (EGFR) – MEK Signalkaskade vermittelt wird. Die *in vivo* Relevanz für den AhR-Signalweg in extrinsisch induzierter MMP-1-Expression konnte (i) im Nagermodel gezeigt werden, indem AhR-defiziente SKH-1 Mäuse untersucht wurden und (ii) durch eine Plazebo-kontrollierte humane *in vivo* Studie, in der der neuen AhR-Antagonisten 2-Benzyl-5,6-dimethoxy-3,3-dimethyl-indan-1-1 (BDDI) verwendet wurde. Diese Untersuchungen identifizieren die AhR-Aktivierung auf molekularer Ebene als den gemeinsamen Nenner der umweltinduzierten MMP-1 Aktivierung. Der AhR könnte folglich ein vielversprechendes Zielmolekül für die Prävention von extrinsischer Hautalterung abgeben.

THE ARYLHYDROCARBON RECEPTOR (AHR) IN KERATINOCYTES IS A UNIVERSAL SENSOR FOR ENVIRONMENTAL STRESS THAT MEDIATES SKIN AGING

Julia Tigges[1], Roland Pfeiffer[1], Christine Goetz[1], Sandra Wolff[1], Ulrike Huebenthal[1], Hans F. Merk[2], Jens W. Fischer[3], Katharina Röck[3], Charlotte Esser[1], Susanne Grether-Beck[1], Josef Abel[1], Thomas Haarmann-Stemmann[1], Jean Krutmann[1], Ellen Fritsche[1,2]

[1]IUF - Leibniz Research Institute for Environmental Medicine, Düsseldorf, Germany
[2]Dept. of Dermatology, University Hospital, RWTH Aachen, Germany
[3]Dept. of Pharmacology and clinical Pharmacology, Heinrich-Heine University Düsseldorf, Germany
Adress correspondence to: Ellen Fritsche, IUF – Leibniz Research Institute for Environmental Medicine, Dept. Molecular Toxicology, Auf'm Hennekamp 50, 40225 Düsseldorf, Germany. Tel.: 49-211-3389-217; Fax: 49-211-3190910; E-mail: ellen.fritsche@uni-duesseldorf.de.

   Extrinsic skin aging is characterized by progressive loss of collagen fibers from the dermal compartment of skin, which clinically presents as wrinkle formation and results to a major part from extrinsically-induced expression of collagen degrading MMP-1. Environmental stressors known to cause skin aging and to activate MMP-1 include Ultraviolet-B radiation (UV-B) as well as tobacco smoke and traffic related particulate matter, which both contain polyaromatic hydrocarbons such as benzo(a)pyrene (B(a)P). Here we provide evidence that all three environmental factors may act through the same molecular pathway, i.e. activation of the cytoplasmic arylhydrocarbon receptor (AhR). Accordingly, exposure of cultured human epidermal keratinocytes to either UV-B radiation or B(a)P induced MMP-1 mRNA expression and activity. This was prevented by pre-treatment of the cells with the AhR inhibitor 3'-methoxy-4'-nitroflavone (MNF). Pharmacological inhibition indicated that this AhR-mediated MMP-1 activation was mediated downstream via the src – epidermal growth factor receptor (EGFR) –MEK signalling cascade. *In vivo* relevance of AhR signalling in extrinsically induced MMP-1 expression was shown (i) in rodents by employing AhR-deficient SKH-1 mice and (ii) by a placebo-controlled human *in vivo* study employing the novel AhR antagonist 2-benzyl-5,6-dimethoxy-3,3-dimethly-indan-1-one (BDDI). These studies identify AhR activation as a common molecular denominator of environmentally-induced MMP-1 activation. The AhR may thus represent a promising target for the prevention of extrinsic skin aging.

   As an interface organ, skin is particularly affected by extrinsic aging. The most important environmental factors that initiate and propagate extrinsic skin aging are ultraviolet (UV) radiation from natural sunlight (1), tobacco smoke (2), and, as recently reported, traffic-related particulate matter (3). Chronic exposure to these exogenous noxae leads to a rarefaction of collagen fibers in the dermal compartment of skin, which clinically presents as coarse wrinkles. A series of very elegant studies has provided compelling evidence that this loss of collagen results to a major part from an extrinsically induced increased expression and activity of the collagen degrading MMP-1 and a lack of concomitant up regulation of its tissue-specific inhibitor TIMP-1 (4). The basic molecular mechanisms initiating extrinsically induced MMP-1 expression are an active field of investigation and are best understood for UV irradiation. It appears that at least part of the effect is initiated by UV-irradiation induced DNA damage in epidermal keratinocytes, since enhanced DNA repair prevents UV-induced MMP-1 expression (5). This inhibitory effect, however, was only partial, indicating the existence of additional mechanisms. Also, MMP-1 expression due to DNA photoproducts can not explain tobacco smoke and particulate matter-induced MMP-1 expression.

   In this regard we have recently shown that irradiation of keratinocytes with UV-B causes formation of tryptophan photoproducts, amongst them formylindolo(*3,2b*)carbazole (FICZ), inside the cells (6). This photoproduct is a high-affinity ligand of a nuclear receptor, the AhR and activates its signaling towards the nucleus and towards the cell membrane. As was previously described for polycyclic aromatic hydrocarbons (PAH) [e.g., B(a)P] and halogenated PAH [e.g.,

tetrachlorodibenzo-p-dioxin (TCDD)] (7;8), FICZ binding causes AhR translocation into the nucleus and activates genes including the xenobiotic metabolizing enzyme cytochrome P450 (CYP) 1A1 (6;9). AhR activation involves shedding of its chaperones Hsp90 and associated proteins such as c-src (pp60src; (10)), and nuclear dimerization with its partner ARNT. Dissociation of c-src from the ligand-activated receptor induces c-src translocation from the cytosol to the cell membrane (11), where it is thought to trigger the receptor for the epidermal growth factor (EGFR) and to induce downstream targets like cyclooxygenase (COX)-2 (12;13). Activation of the AhR by UV-B generated FICZ thus leads to signaling in two directions, towards the nucleus and towards the cell membrane, and it involves AhR translocation and src - ERK1/2 signaling, respectively (6;14).

Because the AhR is involved in UV-dependent, tryptophan-reliant signal transduction in keratinocytes, we hypothesized that AhR activation is implicated in extrinsic skin aging. This theory is supported by the observation that besides UV irradiation, cigarette smoke causes extrinsic skin aging (2) and that many of the tobacco smoke ingredients are PAH and thus ligands of the AhR (15). Furthermore, a recently published epidemiological study shows a close correlation between traffic-related air pollution with particulate matter and signs of extrinsic skin aging such as coarse skin wrinkles (3). Since traffic-born diesel exhaust particles are coated with combustion-derived PAHs (16-18), the AhR-pathway might be the common denominator in all three cases of extrinsic skin aging.

Experimental Procedures

Reagents: The AhR antagonists MNF and 2-benzyl-5,6-dimethoxy-3,3-dimethly-indan-1-one (BDDI) were generated by O. Koch (Symrise, Holzminden, Germany). All additional chemicals used (unless otherwise noted) were purchased from Sigma-Aldrich (Munich, Germany) and were of the highest purity available.

Cell Culture and UV-B Irradiation: The investigations were carried out with primary normal human epidermal keratinocytes (NHEK-c; PromoCell GmbH, Heidelberg, Germany). The cells were cultured in Keratinocyte Growth Medium 2 (PromoCell) supplemented with growth factors and 50 µg/ml gentamycine (PAA, Pasching, Austria) and 2.5 µg/ml aphotericyne (PAA, Pasching, Austria). The cells were kept at 37°C in a humidified atmosphere containing 5% CO_2. Cells were exposed to UV-B through PBS. For UV-B irradiation, a TL20W/12RS lamp, four tubes in parallel connection (Philips, Eindhoven, The Netherlands) was used, which emits most of its energy in the UV-B range (290-320 nm) with an emission peak at 310 nm. Sham-irradiated cells were subjected to the identical procedure without being UV-B-exposed. For inhibition of the AhR, cells were treated for 1 h with 10 µM MNF before irradiation. For inhibition of src kinases, MEK and EGFR, cells were treated for 1 h with 10 µM of the Inhibitors PP2, PD98059 and BPDIQII, respectively (Calbiochem, Darmstadt, Germany) before irradiation. B(a)P and FICZ treatment was carried out for indicated times and concentrations. Controls for MNF, PP2, PD98059, BPDIQII or FICZ were subjected to respective DMSO concentrations.

RNA isolation, Reverse transcription-PCR and real time RT-PCR: Total RNA was isolated from NHEK cells using PeqLab Total RNA Kit (PeqLab) according to the manufacturer's instructions. RNA concentration was assessed by spectrophotometry at 260 nm. Reverse transcription was performed as follows: for cDNA synthesis 500 ng of total RNA, 1 µg of p(DT)15 primer (Roche, Switzerland) and 5 mM solutions of each dNTP were dissolved in 10 µl of H_2O and heated for 5 min at 65°C. The samples were chilled, and 4 µl of 4 x RT-buffer (250 mM Tris HCL, 375 mM KCL, 15 mM $MgCl_2$) and 200 U of M-MLV reverse transcriptase (Promega, Madison USA) were added to a final volume of 20 µl. The samples were reverse transcribed at 37°C for 50 min, and the reaction was inactivated at 70°C for 15 min. real time RT-PCR was performed by using the Rotor Gene Q instrumentation (Qiagen, Hilden, Germany). The following forward and reverse primers were used: MMP-1 5'-CAA TTT CAT TTC TGT TTT CTG GC-3' and 5'-TGT AGA TGT CCT TGG GGT ATC C-3', TIMP-1 5'-GTG GGG ACA CCA GAA GTC AA-3' and 5'-GTG GGA CCT GTG GAA GTA, CYP1A1 5'-CCT TCA TCC TGG AGA CCT TCC-3' and 5'-ATG GTT GAT CTG CCA CTG GTT T-3', β-Actin 5'-CCC CAG GCA CCA GGG CGT GAT-3' and 5'-GGT CAT CTT CTC GCG GTT GGC CTT GGG GT-3'. The PCR mix consisted of 1/10 volume of

Qanti Tect SYBR Green FAST PCR Master Mix (Qiagen, Hilden, Germany), 0.5 µM solutions of each primer, 2.5 µl of cDNA (after RT-PCR diluted 1 : 2,5 with H_2O), in a final volume of 15 µl. The application started with an initial incubation step of 7 min at 95°C to activate the DNA polymerase. The conditions for PCR amplifications were 47 cycles of 10 sec at 95°C for denaturation, 35 sec at 60°C of primer annealing, elongation and fluorescence detection. PCR-primer sequences for human MMP-1, TIMP-1, CYP1A1 and β-Actin are given above. The quantification of PCR products was estimated from fragment-specific standard curves and was calculated with the Rotor Gene 6 software. Standard curves were prepared by using 1.5×10^2 to 1.5×10^6 cDNA copies per µl and amplified as described above.

MMP-1 activity assay: The MMP-1 activity was determined using the SensoLyte Plus 520 MMP-1 Assay Kit (AnaSpec, San Jose, CA). Briefly, 1 ml of conditioned media per well was collected from the companion plate after 48 hours. To measure MMP-1 activity, the conditioned media was ten-fold concentrated by an UFC501024 Amicon Ultra – 0,5 ml Centrifugal Filters device (Millipore). In the MMP-1 assay, 100 µl of concentrated conditioned media were added to each microplate well, which was precoated with an MMP-1 antibody. After MMP-1 was pulled down, the MMP-1 substrate 5-FAM/QXL520 FRET (fluorescence resonance energy transfer) peptide was added to the well. To measure total MMP-1 level, 1 mM p-aminophenylmercuric acetate (APMA) was added to the microplate wells to activate pro-MMP-1 for 1 h at 37°C. The fluorescence intensity representing the MMP-1 activity was measured at 490/520-nm wavelength over a period of 16 hours. Quantification of MMP-1 was calculated from the resulting gradient equation.

Generation of AhR-deficient SKH-1 mice: AhR-deficient SKH-1 hairless mice were generated by breeding AhR-/- mice (B6.129-Ahrtm1Bra/J, (19)) onto the SKH-1 (Charles River) background for 10 generations. Primers and protocol used for genotyping of the AhR deletion were previously described (20). All mice were kept under specific pathogen free conditios, at 12/12 hour light-darkness cycle, and had access to standard chow and water ad libitum. Mice were housed according to standard procedures. For experiments SKH-1:AhR-deficient mice and their SKH-1:AhR-proficient littermates were used.

Irradiation and preparation of mouse skin: Wildtype and AhR deficient SKH-1 mice were irradiated with 180 mJ/cm^2 UV-B. 24 and 48 hours after irradiation the mice were killed in a CO_2 chamber and dorsal and ventral skin (internal control) was dissected with a scalpel at the level of the subcutis just below the panniculus carnosus. After removal of the tissue debris skin samples were snap-frozen in liquid nitrogen. For RNA preparation pieces of approximately 1 cm^2 skin were disrupted in Total RNA Lysis Buffer (PeqLab) using the Tissue Disrupter device (Qiagen, Hilden, Germany). RNA isolation was performed using the PeqLab Total RNA Kit (PeqLab) according to manufacturer's instructions. RT-PCR and real time RT-PCR analysis were performed as stated above using the following forward and reverse primers: MMP-13 5'-ATC CTG GCC ACC TTC TTC TT-3' and 5'-TTT CTC GGA GCC TGT CAA CT-3', TIMP-1 5'-TCC CCA GAA ATC AAC GAG AC-3' and 5'-AAG AAG CTG CAG GCA CTG AT-3' and β-Actin 5'-CTA CAA TGA GCT GCG TGT GG-3' and 5'-TAG CTC TTC TCC AGG GAG GA-3'.

Human volunteers: Approval had been obtained from the Ethics Committee of the Heinrich-Heine University. The study has been conducted according to the ethical rules stated in the Declaration of Helsinki Principles and the ICH GCP guideline was observed insofar as applicable. Ten healthy human volunteers (5 female and 5 male) were enrolled after written informed consent. The age ranged from 24 to 55 years (mean 40.2 ± 10.5 SD, ± 3.3 SE) and all individuals had no history of any severe skin disease, especially no photosensitivity disorders. Skin types ranged from Fitzpatrick type II to III. Their buttock skin had not been exposed to natural or artificial UV radiation for a minimum of 1 year. None of the volunteers used dietary supplements during the study.

Topical treatment of human skin in vivo: For *in vivo* experiments two galenic formulations were prepared: the placebo containing the galenic preparation only and a galenic preparation containing 0.5 % BDDI. All volunteers were treated once daily on 4 consecutive days with the two test-products on a skin area of 16 cm^2 using 2 mg/cm^2 of the preparations. On the 4th day two hours post application of the substances volunteers were irradiated with UVB (1.5 MED).

3

Irradiation of human skin in vivo: MEDs (minimal erythema doses) for each volunteer were determined. The dose of 1.5 MED was chosen as it can be easily reached under physiological conditions and in previous studies was shown to consistently induce gene expression *in vivo* in human skin. In each volunteer, two of the treated and an untreated skin area (2,25 cm^2) of their buttock skin were exposed to a dose of 1.5 MED of broadband UVB from a Dermalight 80 with a maximum at 306 nm (Dr. K. Hönle Medizintechnik GmbH, Kaufering, Germany) irradiation device. 24 hours after irradiation, 4 mm punch biopsies were taken from (i) a sham-irradiated control area (no UVB), (ii) a UVB-irradiated skin area (UVB), (iii) a skin area, which was pretreated with BDDI and UVB-irradiated, and (iv) a skin area, which was pretreated with the placebo and UVB-irradiated. Biopsies were snap frozen in liquid nitrogen and stored at -20° C for further analysis. Total mRNA was isolated, reverse transcribed and analyzed by real-time RT-PCR as previously described (21).

Statistical Analysis: All data sets were analyzed by Student's *t* test as appropriate. Data are presented as means ± SEM. Statistical significance was assigned at the level of p < 0.05.

RESULTS

AhR dependent MMP-1 and CYP1A1 mRNA induction after UV-B and B(a)P treatment in normal human epidermal keratinocytes. If activation of the AhR by UV-B and PAH leads to increased MMP-1 expression and activity has not been examined previously. As is shown in figure 1, real time RT-PCR revealed that mRNA steady state levels of MMP-1 were not only significantly increased in NHEKs, if, as previously reported (22), cells were irradiated with UV-B (Fig. 1 A), but also after treatment with the PAH B(a)P (Fig. 1 B). Also, stimulation of unirradiated NHEKs with the UV-inducible endogenous AhR ligand FICZ resulted in increased MMP-1 mRNA expression levels similar to those observed in UV-B-irradiated or B(a)P stimulated cells (data not shown). Finally, pre-incubation of cells with the competitive AhR antagonist MNF inhibited the MMP-1 induction by both stimuli significantly (Fig. 1). Similar results were observed for the AhR signature gene CYP1A1 (Fig. 1). Importantly and in contrast to MMP-1, neither UV-B irradiation nor B(a)P

stimulation increased TIMP-1 mRNA expression (Fig. 1).

AhR-dependent MMP-1 activity after AhR activation in normal human epidermal keratinocytes. As mRNA expression does not necessarily correlate with expression of the respective protein, we next examined the MMP-1 enzyme activity using the SensoLyte Plus 520 MMP-1 Assay Kit (AnaSpec, San Jose, CA). As shown in Fig. 2 activation of the AhR by B(a)P or UV-B irradiation (data not shown) resulted in enhanced MMP-1 enzyme activity in the supernatants of NHEK cells which was inhibited by pretreatment of the cells with the AhR antagonist MNF (Fig. 2).

Pharmacological inhibitors of the EGFR pathway suppressed AhR-dependent MMP-1 induction. In previous work we showed that AhR-dependent gene activation by UV-B and its tryptophan product FICZ is transmitted towards the EGFR via c-src (6). FICZ treatment of NHEK cells leads to similar AhR-dependent MMP-1 induction than the UV-B and B(a)P stimuli investigated in this study (data not shown). Therefore, and based on the knowledge that MMP-1 expression is driven via the MAP kinase ERK1/2 (23), we hypothesized that the UV-B- and B(a)P-triggered MMP-1 induction is mediated through the src – EGFR – MEK signaling cascade. In order to investigate this hypothesis we pre-treated cells 1 hour with inhibitors (scr-kinase inhibitor: PP2; EGFR inhibitor: BPDIQII; MEK inhibitor PD98059) before they were stimulated with B(a)P or UV-B radiation (Fig. 3). All applied inhibitors antagonized AhR-dependent MMP-1 induction demonstrating the involvement of this pathway.

Expression of MMP-13 and TIMP-1 in irradiated dorsal skin of wildtype and AhR-deficient SKH-1 mice. In order to assess the *in vivo* relevance of our findings we generated AhR-deficient (AHR KO) SKH-1 hairless mice and AhR-proficient (WT) littermates. These mice were irradiated with 180 mJ/cm^2 UV-B and analyzed for MMP-13 (i.e. the functional mouse homologue to human MMP-1) and TIMP-1 expression 24 and 48 hours after irradiation. As expected, MMP-13 in skin of wildtype mice was induced significantly three- to four-fold 48 hours after irradiation (Fig. 4 A) while TIMP-1 expression was not altered (Fig. 4 B). In contrast, AhR-deficient mice lack this gene induction completely (Fig. 4 A)

demonstrating that the AhR mediates skin aging also *in vivo*.

AhR-dependent MMP-1 induction in human skin biopsies. To confirm the above human *in vitro* and mouse *in vivo* findings of AhR-mediated skin aging in human skin, we performed a human *in vivo* study. Skin of healthy volunteers was pretreated with an ointment containing a placebo or an AhR antagonist before irradiation with UV-B. Due to the high mutagenic potential of aromatic nitro compounds (24), we were not able to apply the AhR antagonist MNF and therefore developed a new AhR antagonist which is safe for cosmetic use, BDDI. BDDI is a benzylidene indanone derivative which was designed by assistance of force field minimization measurements based on the known structural properties of the AhR ligand binding site. Also, in independent studies[1], BDDI was shown to be effective in inhibiting UV-B radiation-induced AhR translocation and subsequent gene expression *in vitro* in cultured human epidermal keratinocytes and UV-B radiation-induced COX-2 expression *in vivo* in human skin. Analysis of MMP-1 mRNA levels in skin biopsies of ten healthy volunteers showed a significant increase of MMP-1 mRNA expression in untreated, irradiated or placebo pretreated, irradiated, but not in irradiated, BDDI pretreated skin (Fig. 5), as compared to placebo treated, unirradiated control skin.

DISCUSSION

Aging processes concern almost all organs of the human body and the environment's contribution to progression of deterioration has been long recognized (25). In skin, 'wear and tear' is most obvious and therefore skin is gladly used as a paradigmatic model organ for the study of mechanisms of extrinsic aging (4). Two environmental noxae which accelerate skin aging in humans have been well described: exposure towards the UV-B part of solar radiation (= photoaging) (4;26;27); and towards PAHs containing tobacco smoke (2;28;29); There is one common molecular pathway which is activated by both, UV-B irradiation (6) and PAHs (15), which is the AhR. If activation of the AhR by UV-B and PAH indeed leads to accelerated aging had not been studied yet. Here we provide evidence that

[1] E. Fritsche, manuscript in preparation

the AhR contributes to extrinsic skin aging via induction of MMP-1 in primary human epidermal keratinocytes *in vitro* and in mouse and human skin *in-vivo*. Given the well-documented and pivotal role of keratinocytes for collagen matrix destruction, which - based on zymographic as well as gene expression data - are the major cellular source of MMPs that are produced in response to exposure of human skin to solar UV irradiation in photoaged skin (30), we propose that the AhR serves as a sensor for environmental noxae relevant for extrinsic skin aging. Note that this sensor function may not be restricted to UV-B radiation and PAHs, as shown in this study, but include atmospheric ozone, although the relevance of ozone pollution for skin aging remains to be established (31).

The mechanisms of MMP-1 activation by UV irradiation were thought to be well known. For one, UV radiation causes direct DNA damage which contributes to cutaneous MMP-1 release (5). Secondly, common scientific knowledge identified reactive oxygen species (ROS), especially the superoxide anion, H_2O_2 and resulting hydroxyl radicals as the main detrimental molecules generated by UV irradiation. These ROS induce mitogen activated protein kinase (MAPK) signal transduction resulting in increased kinase activity of the MAPKs ERK1/2, JNK and p38 and a subsequent increase of transcription factor AP-1 which consists of c-Fos and c-Jun (27;32). AP-1 directly activates respective elements in the MMP-1 promoter causing gene induction (33).

We now add a novel element to this picture by showing that MMP-1 induction by UV-B irradiation in primary keratinocytes is dependent on the cytoplasmatic AhR. Two different strategies support this conclusion: (i) the induction of MMP-1 in NHEKs *in vitro* and in human skin *in vivo* is antagonized by the AhR antagonists MNF and BDDI (Fig.1 & 5, respectively), and (ii) MMP-13 is not induced by UV-B irradiation in the skin of AhR deficient mice *in vivo* (Fig.4). The responsible mechanism for AhR activation by UV-B is the intracellular formation of the UV-B-dependent tryptophan photoproduct FICZ (6) which is by far one of the most potent natural AhR ligands (34). This is supported by our observation that treatment of NHEKs with FICZ causes similar AhR-dependent MMP-1 induction than UV-B (data not shown). The involvement of the AhR in MMP-1 induction was additionally confirmed here

by application of the specific AhR ligand B(a)P (Fig.1 & 2). A potential role of the AhR in MMP-1 induction was previously suggested by Murphy et al. (35). However, in this study, the artificial, non-metabolized and thus persistent AhR ligand TCDD was used, although it is well known that TCDD-induced cellular actions beyond induction of CYP1A1 are distinct from those triggered by physiologically relevant, shorter-lived AhR ligands, an observation which might be explained by different kinetics and lack in metabolism (36-38). We also demonstrate for the first time that MMP-1 induction by UV-B or B(a)P is mediated through the src – EGFR – MEK signaling cascade (Fig. 2). Thus, MMP-1 induction does not happen through AhR nuclear translocation, ARNT dimerisation and XRE-binding as it is well known for the direct AhR target gene CYP1A1, but follows the trait which we already described for COX-2, involving MAPK signaling (14).

Our findings are also supported by indirect evidence in the literature. Accordingly, it is well known that small molecules with certain structural characteristics competitively inhibit AhR activation (39). Some of these molecules also prevent photoaging and/or inhibit UV-B-dependent MMP-1 induction. An example for a molecule which does both, AhR-inhibition and photoprotection, is the soy isoflavone genistein, which was shown to reduce UV-B-induced c-fos and c-jun gene expression in mouse skin (40), UV-induced AP-1 DNA-binding in a human keratinocyte cell line (41), to inhibit cutaneous aging induced by UV radiation in mice and to protect against photodamage in humans (42;43). Another example is luteolin, a flavone present e.g. in celery and green pepper, which was found to inhibit B(a)P-dependent AhR activation (44;45), to suppress the expression of MMP-1 in human skin fibroblasts (46), to reduce UV-B-induced collagenase activity and UV-dependent MMP induction in human dermal fibroblasts (47). Also, the flavonole quercetin, which is present in onions, apples, broccoli and green beans, antagonized B(a)P-dependent AhR activation (44) and prevented TPA-induced MMP-1 expression in human dermal fibroblasts by interfering with Erk1/2 signaling (48), i.e. a MAPK, which can be activated by UV radiation (49) via the AhR signaling pathway (6). Our finding that AhR activation is critically involved in UV-B-induced MMP-1 activation provides a scientific rational,

i.e. a common mechanistic explanation for the beneficial effects reported for these substances. It also indicates the possibility that other molecules that are already known to or may be synthesized to interfere with AhR signaling are suited for protection of skin against UV-induced aging. As an example for the 1st possibility we have recently found that the green tea catechins epigallocatechin (EGC) and epigallocatechin gallate (EGCG) can inhibit UV-B-dependent AhR activation[2]. Interestingly EGCG inhibits AhR function through a different mechanism than competitive antagonism by binding to Hsp90, an AhR chaperone, which then hinders its transcriptional activity (50). Green tea polyphenols improve photoaged skin 6 or 12 months after oral supplementation in humans (51) and EGCG hampers collagen destruction and collagenase up-regulation after UV-B irradiation in fibroblasts (52). Although the flavonoid's mechanisms of action have been mainly attributed to their antioxidative capacities, they might exert their beneficial effects through more than one mechanism, e.g. AhR inhibition.

As proof of principle for the second possibility, that is the development of novel AhR antagonist for the prevention of photoaging of human skin, we show in this study that topical application of BDDI is effective in preventing or reducing UV-B-induced MMP-1 expression. This molecule has been newly synthesized by us in a two step process from Benzaldehyde, Dimethyl acrylic acid ester and Veratrole (US 2009/0208433 A1) based on the known three dimensional structure of AhR ligands. By virtue of its optimized structure BDDI is capable of acting as a competitive antagonist to natural AhR ligands such as FICZ[3].

In summary, we here report that the AhR serves as a cytoplasmatic molecular sensor, which via the EGFR - MAPK signaling cascade mediates MMP-1 induction in the skin in response to such diverse environmental stimuli as UV-B radiation or PAHs. In the skin, AhR-mediated MMP-1 expression is not counteracted by concomitant TIMP-1 up regulation (Fig 1) and therefore likely to contribute to matrix degeneration and thus premature skin aging. We therefore consider the AhR as a promising target molecule for the prevention of extrinsic skin aging. In this regard, AhR

---

[2] E. Fritsche, unpublished observation

[3] E. Fritsche, manuscript in preparation

antagonism may not only protect against solar radiation and tobacco smoke induced skin aging, but also against the recently described skin aging promoting activity of traffic-related particles (3), which are generated in combustion processes and known to serve as Trojan horses for PAHs bound to the particles' surface (53;54). It was recently shown that particles reach most organs of the body when taken up by inhalation (55). In this context van Berlo and coworkers (56) showed that inhaled diesel exhaust particles activate AhR signaling not only in the rat lung, but also in an extrapulmonary organ. Therefore, such particles are also suspected to contribute to aging of other organs like the cardiovascular system (57). If this novel aging pathway is also of relevance for aging of other organs which are exposed to PAH has to be determined in future studies

Acknowledgements

REFERENCES

1. Bergfeld, W. F. (1997) *Int. J. Fertil. Womens Med.* **42,** 57-66

2. Morita, A. (2007) *J. Dermatol. Sci.* **48,** 169-175

3. Vierkotter, A., Schikowski, T., Ranft, U., Sugiri, D., Matsui, M., Kramer, U., and Krutmann, J. (2010) *J. Invest Dermatol.*

4. Gilchrest BA and Krutmann J (2006) Photoaging of skin. In Gilchrest BA and Krutmann J, editors. *Skin Aging*, Springer, New York

5. Dong, K. K., Damaghi, N., Picart, S. D., Markova, N. G., Obayashi, K., Okano, Y., Masaki, H., Grether-Beck, S., Krutmann, J., Smiles, K. A., and Yarosh, D. B. (2008) *Exp. Dermatol.* **17,** 1037-1044

6. Fritsche, E., Schafer, C., Calles, C., Bernsmann, T., Bernshausen, T., Wurm, M., Hubenthal, U., Cline, J. E., Hajimiragha, H., Schroeder, P., Klotz, L. O., Rannug, A., Furst, P., Hanenberg, H., Abel, J., and Krutmann, J. (2007) *Proc. Natl. Acad. Sci. U. S. A* **104,** 8851-8856

7. Kahl, G. F., Friederici, D. E., Bigelow, S. W., Okey, A. B., and Nebert, D. W. (1980) *Dev. Pharmacol. Ther.* **1,** 137-162

8. Knutson, J. C. and Poland, A. (1980) *Cell* **22,** 27-36

9. Wei, Y. D., Helleberg, H., Rannug, U., and Rannug, A. (1998) *Chem. Biol. Interact.* **110,** 39-55

10. Enan, E. and Matsumura, F. (1996) *Biochem. Pharmacol.* **52,** 1599-1612

11. Kohle, C., Gschaidmeier, H., Lauth, D., Topell, S., Zitzer, H., and Bock, K. W. (1999) *Arch. Toxicol.* **73,** 152-158

12. Buckman, S. Y., Gresham, A., Hale, P., Hruza, G., Anast, J., Masferrer, J., and Pentland, A. P. (1998) *Carcinogenesis* **19,** 723-729

13. Vogel, C., Boerboom, A. M., Baechle, C., El-Bahay, C., Kahl, R., Degen, G. H., and Abel, J. (2000) *Carcinogenesis* **21,** 2267-2274

14. Agostinis, P., Garmyn, M., and Van, L. A. (2007) *Sci. STKE.* **2007,** e49

15. Denison, M. S. and Nagy, S. R. (2003) *Annu. Rev. Pharmacol. Toxicol.* **43,** 309-334

16. Kotin, P., Falk, H. L., and THOMAS, M. (1954) *A M. A Arch. Ind. Hyg. Occup. Med.* **9,** 164-177

17. Kotin, P., Falk, H. L., MADER, P., and THOMAS, M. (1954) *A M. A Arch. Ind. Hyg. Occup. Med.* **9,** 153-163

18. Kotin, P., Falk, H. L., and THOMAS, M. (1955) *AMA. Arch. Ind. Health* **11,** 113-120

19. Schmidt, J. V., Su, G. H., Reddy, J. K., Simon, M. C., and Bradfield, C. A. (1996) *Proc. Natl. Acad. Sci. U. S. A* **93,** 6731-6736

20. Jux, B., Kadow, S., Luecke, S., Rannug, A., Krutmann, J., and Esser, C. (2011) *J. Invest Dermatol.* **131,** 203-210

21. Grether-Beck, S., Muhlberg, K., Brenden, H., Felsner, I., Brynjolfsdottir, A., Einarsson, S., and Krutmann, J. (2008) *Exp. Dermatol.* **17,** 771-779

22. Dazard, J. E., Gal, H., Amariglio, N., Rechavi, G., Domany, E., and Givol, D. (2003) *Oncogene* **22,** 2993-3006

23. Brauchle, M., Gluck, D., Di, P. F., Han, J., and Gram, H. (2000) *Exp. Cell Res.* **258,** 135-144

24. Sawatari, K., Nakanishi, Y., and Matsushima, T. (2001) *Ind. Health* **39,** 341-345

25. Martin, G. M., Austad, S. N., and Johnson, T. E. (1996) *Nat. Genet.* **13,** 25-34

26. Berneburg, M., Plettenberg, H., and Krutmann, J. (2000) *Photodermatol. Photoimmunol. Photomed.* **16,** 239-244

27. Fisher, G. J. and Voorhees, J. J. (1998) *J. Investig. Dermatol. Symp. Proc.* **3,** 61-68

28. Frances, C. (1998) *Clin. Dermatol.* **16,** 565-570

29. Schieke, S. M., Ruwiedel, K., Gers-Barlag, H., Grether-Beck, S., and Krutmann, J. (2005) *J. Invest Dermatol.* **124,** 857-859

30. Quan, T., Qin, Z., Xia, W., Shao, Y., Voorhees, J. J., and Fisher, G. J. (2009) *J. Investig. Dermatol. Symp. Proc.* **14,** 20-24

31. Afaq, F. and Mukhtar, H. (2001) *J. Photochem. Photobiol. B* **63,** 61-69

32. Rittie, L. and Fisher, G. J. (2002) *Ageing Res. Rev.* **1,** 705-720

33. Vincenti, M. P., White, L. A., Schroen, D. J., Benbow, U., and Brinckerhoff, C. E. (1996) *Crit Rev. Eukaryot. Gene Expr.* **6,** 391-411

34. Wincent, E., Amini, N., Luecke, S., Glatt, H., Bergman, J., Crescenzi, C., Rannug, A., and Rannug, U. (2009) *J. Biol. Chem.* **284,** 2690-2696

35. Murphy, K. A., Villano, C. M., Dorn, R., and White, L. A. (2004) *J. Biol. Chem.* **279,** 25284-25293

36. Matikainen, T., Perez, G. I., Jurisicova, A., Pru, J. K., Schlezinger, J. J., Ryu, H. Y., Laine, J., Sakai, T., Korsmeyer, S. J., Casper, R. F., Sherr, D. H., and Tilly, J. L. (2001) *Nat. Genet.* **28,** 355-360

37. Gassmann, K., Abel, J., Bothe, H., Haarmann-Stemmann, T., Merk, H. F., Quasthoff, K. N., Rockel, T. D., Schreiber, T., and Fritsche, E. (2010) *Environ. Health Perspect.*

38. Laub, L. B., Jones, B. D., and Powell, W. H. (2010) *Chem. Biol. Interact.* **183,** 202-211

39. Henry, E. C., Kende, A. S., Rucci, G., Totleben, M. J., Willey, J. J., Dertinger, S. D., Pollenz, R. S., Jones, J. P., and Gasiewicz, T. A. (1999) *Mol. Pharmacol.* **55,** 716-725

40. Wang, Y., Zhang, X., Lebwohl, M., DeLeo, V., and Wei, H. (1998) *Carcinogenesis* **19,** 649-654

41. Maziere, C., Dantin, F., Dubois, F., Santus, R., and Maziere, J. (2000) *Free Radic. Biol. Med.* **28,** 1430-1437

42. Wei, H., Saladi, R., Lu, Y., Wang, Y., Palep, S. R., Moore, J., Phelps, R., Shyong, E., and Lebwohl, M. G. (2003) *J. Nutr.* **133,** 3811S-3819S

43. Kang, S., Chung, J. H., Lee, J. H., Fisher, G. J., Wan, Y. S., Duell, E. A., and Voorhees, J. J. (2003) *J. Invest Dermatol.* **120,** 835-841

44. Zhang, S., Qin, C., and Safe, S. H. (2003) *Environ. Health Perspect.* **111,** 1877-1882

45. Bothe, H., Gotz, C., Stobbe-Maicherski, N., Fritsche, E., Abel, J., and Haarmann-Stemmann, T. (2010) *Arch. Biochem. Biophys.* **498,** 111-118

46. Kim, J. H., Cho, Y. H., Park, S. M., Lee, K. E., Lee, J. J., Lee, B. C., Pyo, H. B., Song, K. S., Park, H. D., and Yun, Y. P. (2004) *Arch. Pharm. Res.* **27,** 177-183

47. Sim, G. S., Lee, B. C., Cho, H. S., Lee, J. W., Kim, J. H., Lee, D. H., Kim, J. H., Pyo, H. B., Moon, D. C., Oh, K. W., Yun, Y. P., and Hong, J. T. (2007) *Arch. Pharm. Res.* **30,** 290-298

48. Lim, H. and Kim, H. P. (2007) *Planta Med.* **73,** 1267-1274

49. Bode, A. M. and Dong, Z. (2003) *Sci. STKE.* **2003,** RE2

50. Palermo, C. M., Westlake, C. A., and Gasiewicz, T. A. (2005) *Biochemistry* **44,** 5041-5052

51. Janjua, R., Munoz, C., Gorell, E., Rehmus, W., Egbert, B., Kern, D., and Chang, A. L. (2009) *Dermatol. Surg.* **35,** 1057-1065

52. Bae, J. Y., Choi, J. S., Choi, Y. J., Shin, S. Y., Kang, S. W., Han, S. J., and Kang, Y. H. (2008) *Food Chem. Toxicol.* **46,** 1298-1307

53. Park, S. S. and Kim, Y. J. (2005) *Chemosphere* **59,** 217-226

54. Vallius, M., Janssen, N. A., Heinrich, J., Hoek, G., Ruuskanen, J., Cyrys, J., Van, G. R., de Hartog, J. J., Kreyling, W. G., and Pekkanen, J. (2005) *Sci. Total Environ.* **337,** 147-162

55. Kreyling, W. G., Semmler-Behnke, M., Seitz, J., Scymczak, W., Wenk, A., Mayer, P., Takenaka, S., and Oberdorster, G. (2009) *Inhal. Toxicol.* **21 Suppl 1,** 55-60

56. van, B. D., Albrecht, C., Knaapen, A. M., Cassee, F. R., Gerlofs-Nijland, M. E., Kooter, I. M., Palomero-Gallagher, N., Bidmon, H. J., van Schooten, F. J., Krutmann, J., and Schins, R. P. (2010) *Arch. Toxicol.* **84,** 553-562

57. Schikowski, T., Sugiri, D., Ranft, U., Gehring, U., Heinrich, J., Wichmann, H. E., and Kramer, U. (2007) *Respir. Res.* **8,** 20

FOOTNOTES

[1]E. Fritsche, manuscript in preparation
[2]E. Fritsche, unpublished observation
[3]E. Firtsche, manuscript in preparation

FIGURE LEGENDS

Fig. 1. Real time RT-PCR detection of MMP-1, TIMP-1 and CYP1A1 in primary human keratinocytes. Messenger RNAs of MMP-1 (black), TIMP-1 (white) and CYP1A1 (grey) were detected in NHEK cells after pre-treatment with 10 µM MNF for 1 hour followed by 48 hours incubation after 100 J/m^2 UV-B (A) or with 250 nM B(a)P (B), respectively; n = 3, mean ± SEM, * $p < 0.05$ versus solvent control; # $p < 0.05$ versus UV-B (A) or B(a)P (B) treated cells.

Fig. 2. MMP-1 activity in primary human keratinocytes after AhR activation. MMP-1 concentration in concentrated conditioned media was determined by SensoLyte® Plus 520 MMP-1 Assay Kit (AnaSpec, San Jose, USA) after pre-treatment with 10 µM MNF for 1 hour followed by 48 hours incubation with 250 nM B(a)P. Each timepoint represents 6 individual datapoints. A shows a 16 hour kinetic; B reveals the quantitative accumulation of MMP-1 protein over time; mean ± SEM, * $p < 0.05$ versus solvent control; # $p < 0.05$ versus B(a)P treated cells.

Fig. 3. Real time RT-PCR detection of MMP-1 in primary human keratinocytes after pre-treatment with EGFR pathway related inhibitors (10 µM) for 1 hour followed by B(a)P (250 nM) treatment for 24 hours. *A*. B(a)P-treatment of pre-incubated cells; B. UV-B-irradiation of pre-incubated cells. (PP2: src-kinase inhibitor; BP: EGFR inhibitor; PD: MEK inhibitor; n = 3, mean ± SEM, * $p < 0.05$ versus solvent control; # $p < 0.05$ versus B(a)P (A) or UV-B (B) treated cells.

Fig. 4. Real time RT-PCR detection of MMP-13 in dorsal skin of SKH-1 WT and AhR KO littermates after UV-B irradiation. WT and AhR KO mice were irradiated with 180 mJ/cm^2 UV-B, samples of dorsal (UV-B) and ventral (internal control) skin were taken 24 and 48 hours after irradiation; n = 3-4, mean ± SEM, * $p < 0.05$ versus WT expression.

Fig. 5. MMP-1 expression in human skin biopsies after UV-B irradiation. Messenger RNAs of MMP-1 were detected in human skin biopsies after pre-treatment with 0.5 % BDDI or Placebo, respectively for 4 days every day followed by UV-B irradiation (1.5 MED) on day 4. 4 mm bunch biopsies were taken after another 24 hours. MMP-1 mRNA expression in unirradiated, untreated control skin were arbitrarily set as 1; n = 10, mean ± SEM, ** $p < 0.001$ versus placebo.

Figure 1
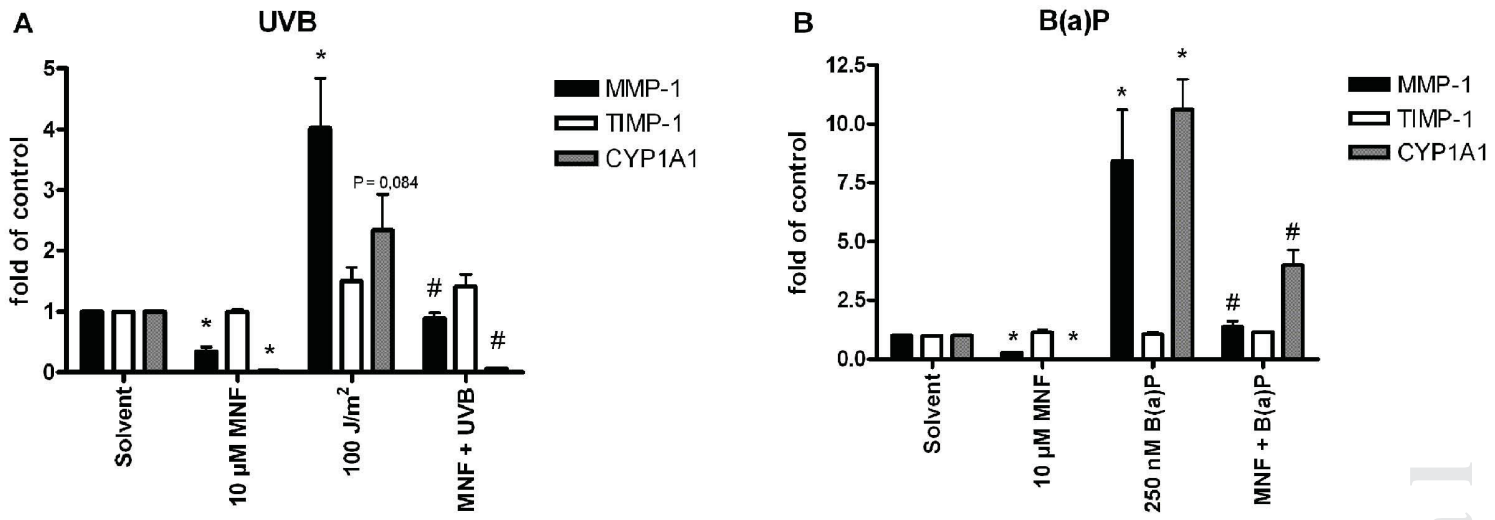
A UVB

fold of control

P = 0,084

Solvent | 10 µM MNF | 100 J/m^2 | MNF + UVB

- MMP-1
- TIMP-1
- CYP1A1

B B(a)P

fold of control

Solvent | 10 µM MNF | 250 nM B(a)P | MNF + B(a)P

- MMP-1
- TIMP-1
- CYP1A1

Figure 2

Figure 3

A **UVB**

B **B(a)P**

Figure 4

A   mMMP-13

B   mTIMP-1
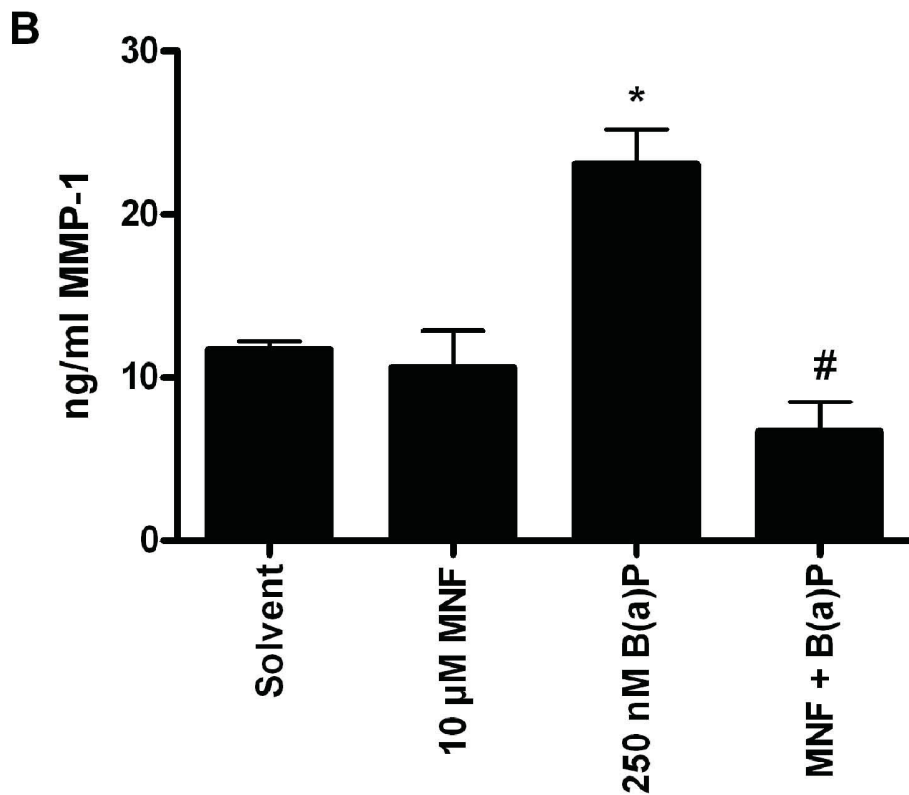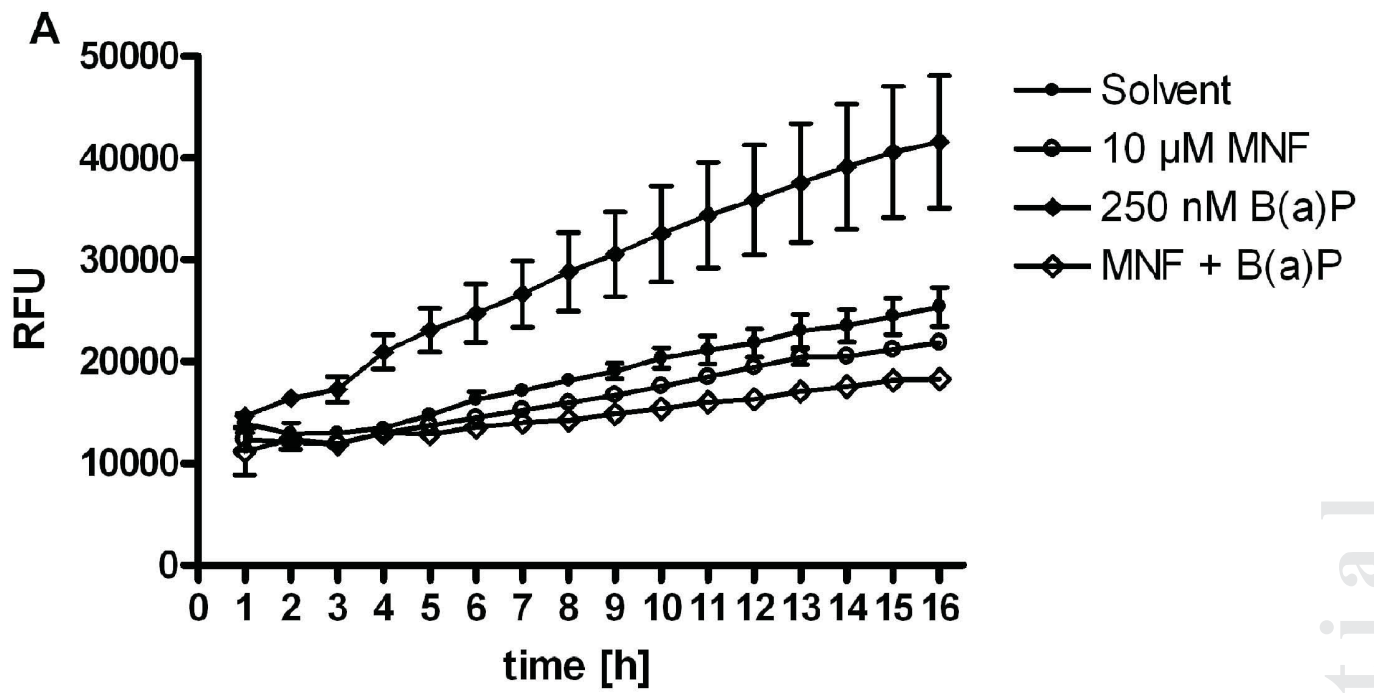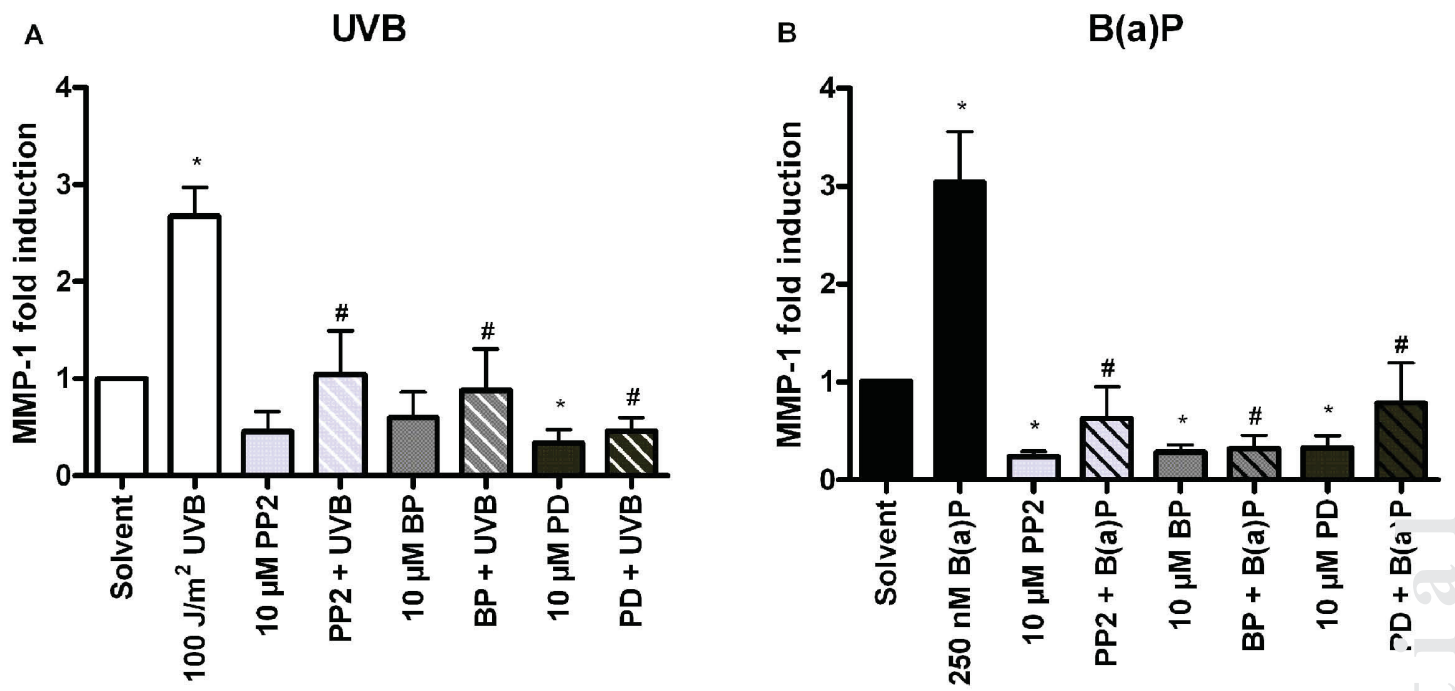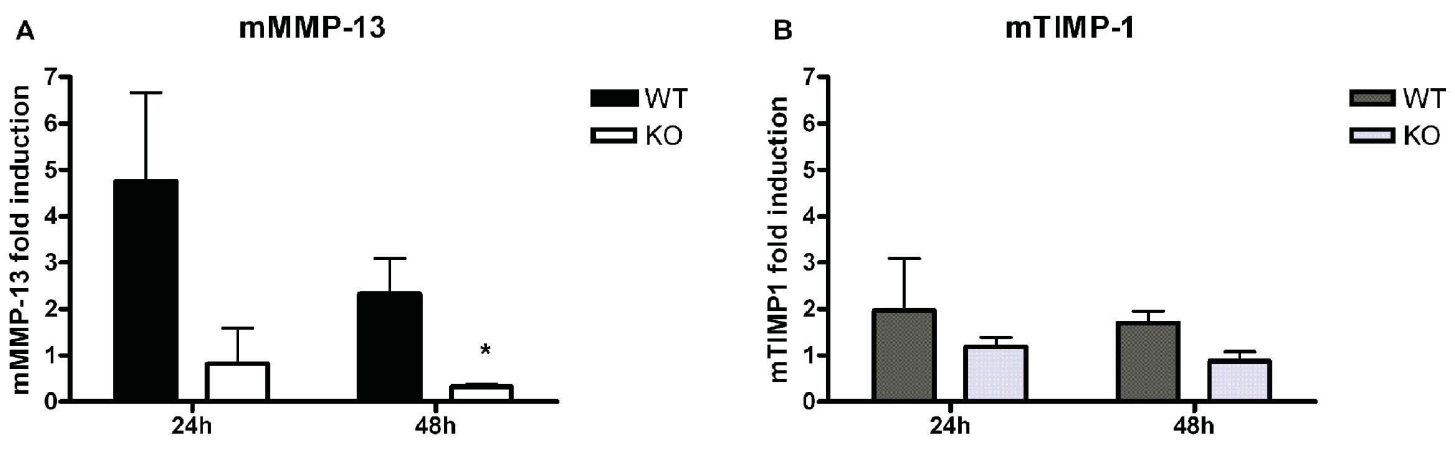
Figure 5
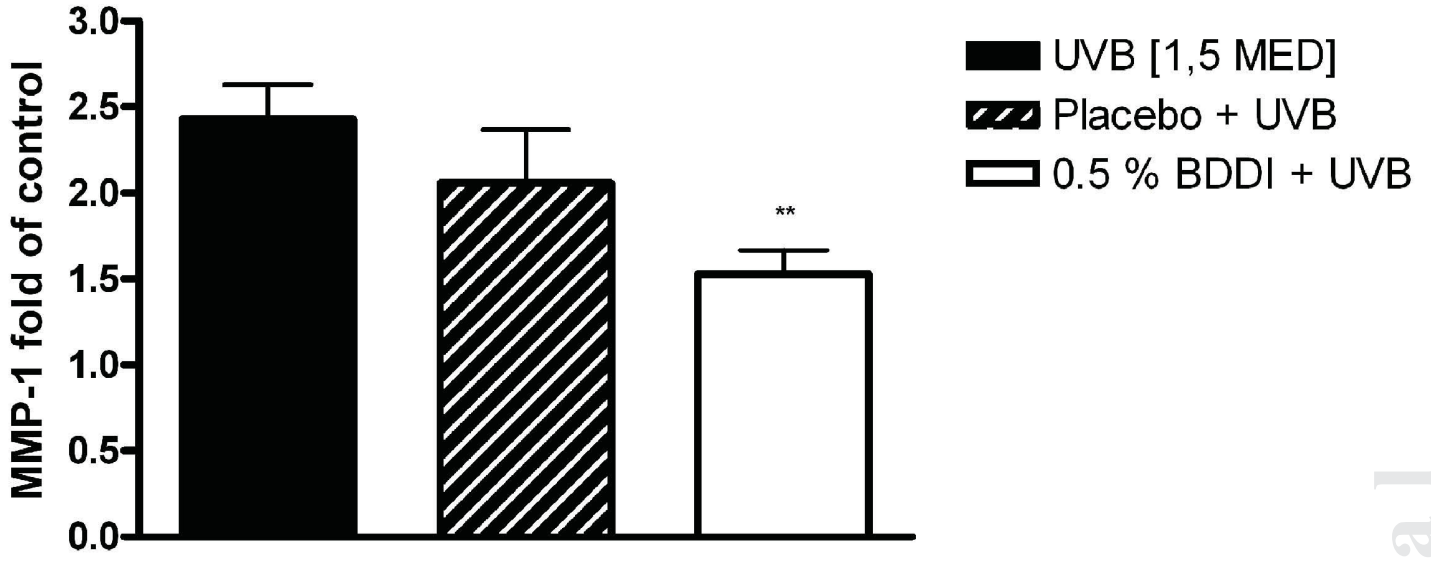
Publikation Nr. 5

The Arylhydrocarbon Receptor (AhR) in keratinocytes is a universal sensor for environmental stress that mediates skin aging

Julia Tigges, Roland Pfeiffer, Christine Goetz, Sandra Wolff, Ulrike Huebenthal, Hans F. Merk, Jens W. Fischer, Katharina Röck, Charlotte Esser, Susanne Grether-Beck, Josef Abel, Thomas Haarmann-Stemmann, Jean Krutmann und Ellen Fritsche

— ∙ — ∙ — ∙ — ∙ — ∙ — ∙ — ∙ — ∙ — ∙ — ∙ —

2.6   Publikation 6

Estradiol protects dermal hyaluronan/Versican matrix during photoaging by release of EGF from keratinocytes

Dermale Hyaluronsäuren (HA) und Versikane sind Schlüsselkomponenten der Dermis und responsiv gegenüber UVB-iduzierten Umstrukturierungen. Das Ziel dieser Studie war es, die molekularen Mechanismen der Östrogen (E_2)-vermittelten Effekte auf die HA-reiche extrazelluläre Matrix (ECM) während der Lichtalterung zu untersuchen. In haarlosen SKH-1 Mäusen, verursachten 10 Wochen UVB-Bestrahlung (3 x 1 MED (80 mJ/cm^2), wöchentlich) einen deutlichen Rückgang der dermalen HA, welcher durch Ovarektomie (OVX) noch verstärkt wurde. Subkutane Substitution mit Östrogen über *Controlled Release Pellets* hoben diese Effekte auf und bestätigten somit die protektive Rolle des E_2. Der Anstieg in dermaler HA korrelierte mit der Induktion der HA-Synthase HAS3 durch E_2. Zusätzlich wurde das HA-bindende Proteoglykan Versikan durch UVB induziert, der Effekt konnte durch E_2 sogar noch verstärkt werden. In kultivierten Hautfibroblasten reduzierte E_2 die Expression von HAS1 und Versikan und hatte keinen Effekt auf HAS3. Aus diesem Grund konnte die direkte Aufregulierung von HAS3 und Versikan über E_2 ausgeschlossen werden. E_2 induzierte jedoch die EGF-Expression in UVB bestrahlter Haut *in vivo* und in Keratinozyten *in vitro*. EGF seinerseits führte zu einer induzierten Expression von HAS3 und Versikan in dermalen Fibroblasten. Zusätzlich korrelierte die dermale HA- und Versikan-Induktion durch E_2 positiv mit der Proliferation (Ki67) und negativ mit der Akkumulation von inflammatorischen Makrophagen (Mac2) in der Dermis. Zusammengefasst weisen diese Daten darauf hin, dass E_2-Behandlung den Anteil an dermaler HA und Versikan über eine parakrine Freisetzung von EGF induziert, welches mit den pro-proliferativen und anti-inflammatorischen Effekten von E_2 in der Lichtalterung einhergehen könnte. Folglich ist E_2 in der Lichtalterung tatsächlich ein wichtiger Regulator des dermalen HA- und Versikan-Gehaltes. Vermittelt wird dieser Effekt zumindest zum Teil durch die parakrine Freisetzung von EGF aus Keratinozyten, welches dann die Expression von HAS3 und Versikan in Fibroblasten induziert. Als eine Konsequenz erhöht E_2 die Proliferation und hemmt die Inflammation. Dadurch identifiziert diese Publikation neue

molekulare Ziele des E_2, die die protektive Funktion dieses Hormons auf die dermale Matrix währen der extrinsischen Alterung mediieren.

Estradiol protects dermal hyaluronan/versican matrix during photoaging by release of EGF from keratinocytes.

Katharina Röck, Michael Meusch, Nikola Fuchs, [1]Julia Tigges, [2]Petra Zipper, [1]Ellen Fritsche, [1]Jean Krutmann, [2]Bernhard Homey, [2]Julia Reifenberger, Jens W. Fischer

Institut für Pharmakologie und Klinische Pharmakologie, Universitätsklinikum Düsseldorf, Heinrich-Heine-Universität Düsseldorf, Germany [1]IUF – Leibniz Institute for Environmental Medicine, Düsseldorf, Germany

[2]Department of Dermatology, Universitätsklinikum Düsseldorf, Heinrich-Heine-Universität Düsseldorf, Germany

Address correspondence to: Jens W. Fischer, Institut für Pharmakologie und Klinische Pharmakologie, Universitätsklinikum Düsseldorf, Heinrich-Heine-Universität Düsseldorf, Moorenstrasse 5, 40225 Düsseldorf, Germany. Tel.: 49-211-8112500; Fax: 49-211-8114781; E-mail: jens.fischer@uni-duesseldorf.de.

Dermal hyaluronan (HA) and versican are key components of the dermis and are responsive to UVB induced remodeling. Aim of the present study was to explore the molecular mechanisms of estrogen (E_2) mediated effects on HA-rich ECM during photoaging. In hairless Skh-1 mice 10 weeks of UVB irradiation (3 x 1 MED (80 mJ/cm^2), weekly) caused a marked decline of dermal HA, which was aggravated by ovariectomy (OVX). Subcutaneous substitution of estrogen (E_2) by means of controlled release pellets abolished these effects confirming the stimulatory role of E_2. The increase of dermal HA correlated with induction of HA synthase HAS3 by E_2. In addition the HA-binding proteoglycan versican was induced by UVB and further increased by E_2. In cultured skin fibroblasts E_2 reduced expression of HAS1 and versican and had no effect on HAS3. Therefore, direct upregulation of HAS3 and versican by E_2 was excluded. However, E_2 increased the expression of EGF in UVB irradiated skin *in vivo* and in keratinocytes *in vitro*. EGF in turn upregulated the expression of HAS3 and versican in dermal fibroblasts. Functionally, dermal HA and versican induction by E_2 correlated positively with proliferation and negatively with accumulation of inflammatory macrophages in the dermis. Collectively these data suggest that E_2 treatment increases the amount of dermal HA and versican via paracrine release of EGF which may be implicated in the pro- proliferative and anti-inflammatory effects of E_2 during photoaging.

INTRODUCTION

Photoaging of the skin inevitably occurs at the sun exposed areas such as face, neck and hands during life span. This process is characterized by overlap of intrinsic aging and extrinsic aging responses and also by an overlap with photo carcinogenesis (1). It is well established that the extracellular matrix (ECM) of the skin is involved in this aging process. In particular the cleavage of collagen by matrix metalloproteinases (MMP) has been demonstrated (2). The partially degraded collagen network heals imperfectly by *de novo* collagen synthesis leaving micro scars in the skin. Furthermore the collagen fragments that are released during MMP induced collagen cleavage are bioactive and participate in the regulation of fibroblast phenotype during photoaging. In this context it has been established that collagen fragments reduce collagen *de novo* synthesis (3). Matrix degradation and changes in matrix expression subsequently affect fibroblast phenotypes and

thereby possibly perpetuate UVB induced aging responses. In addition to collagen various reports have suggested that other ECM molecules are affected as well by UVB irradiation of the skin. Among these dermal hyaluronan (HA) and proteoglycans appear to be of great relevance (4-7). HA is abundant in the dermis and is supposed to contribute to the water content, the turgidity of the skin and the diffusion of soluble factors and nutrients (5). Furthermore, HA can support the proliferative phenotype of fibroblasts and possibly opposes apoptosis (8,9). HA is synthesized at the plasma membrane by HA synthase isoenzymes-1,-2 and -3 (HAS1-3) (10). These enzymes extrude HA into the extracellular space after assembly of UDP-glucuronic acid and UDP-N-acetyl-D-glucosamine into a growing chain of ß(1-3) linked D-glucuronic acid and N-acetyl-D-glucosamine disaccharides. The repeating disaccharides are linked by hexosaminidic ß(1-4) bonds that form high molecular weight HA of up to 10^7 Da and up to 20 µm in length (11). The HAS isozymes are expressed at a relatively low copy number per cell but can produce large amounts of HA in short time. In addition to transcriptional regulation of HAS enzymes it has recently been shown that regulation takes place on the posttranscriptional level by phosphorylation, glycosylation and mono-ubiquitination (12-14). As additional posttranscriptional mechanism the formation of homo- and hetereodimers has now been demonstrated (13).

With respect to skin aging it has been shown that HA is reduced by chronic UVB irradiation and likely contributes to the aged phenotype of skin (8,15-17). However opposing reports that detected no change of dermal HA have been published as well as studies that demonstrated increased HA in response to UVB

(15,18). The latter is likely an acute response associated with erythema and heliodermatitis.

Hyaluronan is bound by versican, a large chondroitin sulfate proteoglycan, through specific binding domains termed link modules that each consist of approximately 100 amino acids and are part of the link protein domain. The link protein domain is comprised of an immunoglobulin domain and two link modules and is present in the n-terminal globular G1 domain of versican (19). Because multiple versican molecules bind to one chain of HA, large networks of HA and versican are formed. These HA and versican-rich matrices are known to critically govern the proliferative and migratory phenotype of mesenchymal cells (20). Recently it has been demonstrated that versican accumulates in response to UVB irradiation (7). However little is known about how versican is affected during skin aging, what the specific functions of versican might be during skin aging and whether versican is responsive to estrogen.

Skin aging is accelerated after menopause and positive effects on the skin including increased thickness, increased moisture, decreased wrinkling and improved wound healing responses became obvious upon estrogen treatment of postmenopausal women (21). However hormone replacement therapy is confounded by thrombotic and malignant complications and is now restricted to short term use in selected cases (22). It is therefore of great interest to better understand the molecular mechanisms that underlie the protection of the skin matrix by E_2. The aim of the present study was to investigate the effect of E_2 on dermal hyaluronan and versican matrix during UVB-induced skin aging by use of ovariectomized and E_2 treated hairless skh-1 mice.

EXPERIMENTAL PROCEDURES
Materials

UVB Irradiation of Mice -Female hairless mice (Skh:Hr1) (Charles-River) were housed according to

standard procedures. Mice were randomly assigned to either sham procedure or bilateral ovariectomy (OVX) at the age of 8 weeks as described previously (23). OVX mice were subdivided into four treatment groups, which received either placebo or E_2 plus-minus UVB-irradiation. E_2 treatment was performed by implantation of subcutaneous slow-release hormone pellets (Innovative Research of America) prepared to dispense 1.1 µg/d E_2 for the entire experimental period of 10 weeks. Placebo (P) pellets served as control. After OVX and pellet implantation at 8 weeks half of the mice were irradiated with UVB light and the other half served as non–irradiated controls. Animals were exposed to UV radiation in an irradiation chamber as described previously (8) using UV lamps with fluorescent bulbs (280 to 320 nm with a peak at 313 nm TL 20W/12; Philips, Eindhoven, The Netherlands). UVB irradiation was performed three times per week at a dose of 80 mJ/cm² (irradiation time 1 minute 36 seconds) equaling 1 minimal erythema dose (MED) throughout a period of 10 weeks (figure 1A). The light intensity was determined by means of a UV meter (Waldmann, Villingen-Schwennigen, Germany). Skin biopsies from the dorsal skin of 1 by 2 cm^2 in size were obtained from control and UVB-irradiated animals after 10 weeks of UVB. Sham operated animals received placebo pellets plus-minus UVB irradiation. Thus six experimental groups were compared: 1) sham, placebo (S,P), 2) OVX, placebo (X,P), 3) OVX, E_2 (X, E_2), 4) sham, placebo, UVB (S,P,UVB), 5) OVX, placebo, UVB (X,P,UVB) and 6) OVX, E_2, UVB (X, E_2,UVB). All animal experiments have been approved by the local ethical committee for animal experiments.

Histology -Skin biopsies were frozen in tissue freezing medium (Leica Nussloch, Bensheim, Germany) in liquid isopentane at -40°C and 12 µm cryosections were prepared for immunohistochemical staining. Affinityhistochemistry of (HA) was performed with bovine HA binding protein (bHABP, Seikagaku, Tokyo, Japan), detected with biotin-labeled streptavidine (2 µg/ml, Calbiochem, Bad Soden, Germany). The following primary antibodies were used Versican (LF99, 1:400, rabbit anti-human, kindly provided by Dr. Larry Fisher, National Institute of Dental and Craniofacial Research, NIH, Bethesda, Md), HAS3 (H64, 1:500, Santa Cruz biotechnology, Santa Cruz, CA, USA), Mac2 (1:250, Cedarlane, Burlington, Canada), Ki-67 (1:50, Novus biological, Littleton, CO, USA). The respective biotinylated secondary antibodies (1:1000) were obtained from Calbiochem. Detection was performed using diaminobenzidine (Zytomed, Berlin, Germany) as a chromogen. Nuclei were stained with hemalaun solution (Merck, Darmstadt, Germany). The area fraction was determined by Image J software in the area of the papillary dermis excluding regions which contained hair follicles. This analysis was performed in a blinded fashion as described previously (8).

Cell culture -Human dermal fibroblasts from female donors were purchased from PromoCell (Heidelberg, Germany) and were maintained in monolayer cultures in Dulbecco`s modified Eagle's Medium (DMEM) without phenol red (Sigma Aldrich), supplemented with 10% heat inactivated, charcoal treated fetal bovine serum, 2 mmol/L L-glutamine, and antibiotics (100 units/ml penicillin, 50 mg/ml streptomycin-G). Normal human epidermal keratinocyte**s** (NHEK) were purchased from PromoCell and cultured in kerationocyte media 2 (PromoCell). The cells were maintained at 37°C, 5% CO_2 and 95% humidified air.

UVB irradiation of the cells was performed with a Bio-Sun irradiation system (Vilbert Lourmat, Munich)

containing two 30W UVB sources (312nm). During the UVB irradiation procedure (100 mJ/cm²; irradiation time approximately 10 seconds) cells were kept in phosphate buffered saline solution which was replaced by DMEM containing 10% charcoal treated FCS with or without 100 nM β-estradiol (Sigma Aldrich) shortly after the irradiation. Cells were harvested 24 hours after stimulation.

For the cell media transfer experiments NEHKs were UVB irradiated and E_2 stimulated as described above in keratinocyte media 2. The supernatant was collected 24 hours after stimulation and was transferred to fibroblasts in the presence or absence of erlotinb (3µM LC Laboratories, Woburn. MA, USA), EGF neutralizing antibody or isotype control (both 0.35 µg/mL, abcam, Cambridge, UK). Fibroblasts were harvested 24 hours after the media transfer.

RNA Isolation and Quantification of Gene Expression -Total RNA was isolated using RNeasy total RNA kits (Qiagen, Hilden, Germany). The RNA concentration was determined via photometric measurement at 260/280. Aliquots of total RNA (1 µg) were applied for cDNA synthesis using SuperscriptIII first-strand synthesis system for reverse transcriptase-polymerase chain reaction (RT-PCR) (Invitrogen, Karlsruhe, Germany). In order to analyze the mRNA expression primers were designed employing Primer Express 3.0 software (Applied Biosystems, Darmstadt, Germany) based on published mRNA sequences. The sequences are given in table 1. Each real time RT-PCR was performed in triplicates and the mean value calculated. PCR was carried out using SYBR Green PCR Master Mix (Applied Biosystems) as described [15]. The $2^{[-\Delta\Delta C(T)]}$ method was used for comparison of the relative expression between control and treated

cells. A melting curve analysis was performed after every run. Furthermore a negative control containing only master mix, the primer pair and control water was run on every plate.

Determination of HA and EGF in cell culture supernatants – HA concentration in the supernatants was determined by HA test Kit based on bHABP (Corgenix, Peterborough, UK) 24 hours after stimulation and was calculated as the ratio of HA and total cellular protein. EGF concentration in the supernatants was determined by EGF Human ELISA Kit (abcam, Cambridge, UK) 24 hours after stimulation according to the manufacturer's protocol.

HAS3 and versican immunoblotting. Versican from cell culture supernatants or skin extracts was first enriched by DEAE ionexchange chromatography, chondroitin ABC lyase-digested and subsequently core proteins were separated on SDS-PAGE and Western blotted as described previously. (24). LF99 (1:1000) was used as primary antibody.

HAS3 in skin homogenates or cell layer lysates was detected by immunoblotting using anti-mouse-HAS3 antibody (H64, 1:1000 Santa Cruz Biotechnology, Santa Cruz, CA, USA) and anti-human-HAS3 antibody (1:1000 Sigma Aldrich) respectively. β tubulin antibody was from Sigma-Aldrich (1:1000, Munich, Germany). Primary antibodies were detected by infrared-fluorescent coupled secondary antibodies (1:5000 LI-COR, Bad Homburg, Germany) allowing fluorescent detection (LI-COR Odyssey Infrared Imaging System).

Determination of HA and EGF in murine skin – For HA extraction murine skin biopsies were lyophilized, dry weight was determined and samples were digested by pronase (protease from *Streptomyces griseus*, 6 mg/ml in 100 mmol/L Tris-HCl, pH 8, 1 mmol/L CaCl2, and 1500 U/ml heparin, 60°C, 24 hours; Sigma-Aldrich). Subsequently HA was ethanol

precipitated (12 hours, -20°C) and recovered by centrifugation (10,000 x g, 4°C, 15 minutes). Samples were diluted 1:20,000, the HA concentration was determined by HA test Kit based on bHABP (Corgenix, Peterborough, UK) and normalized to dry weight (25).

EGF was detected in murine skin lysate, which was prepared by homogenization in modified RIPA buffer (50 mM Tris-HCl, pH 7.4, 1% Triton X-100, 0.2% sodium deoxycholate, 0.2% sodium dodecylsulfate (SDS), 1 mM sodium ethylenediaminetetraacetate, 1 mM phenylmethylsulfonyl flouride, 5 µg/ml of aprotinin, 5 µg/ml of leupeptin). Tissue and cell debris was removed by centrifugation. EGF concentration was determined by EGF Mouse ELISA Kit (abcam, Cambridge, UK) according the manufacturer's protocol. Protein concentration was analyzed with Bio-Rad protein assay (Bio-Rad Laboratories, Munich, Germany).

Statistical Analysis - All data sets were analyzed by ANOVA and the Bonferroni post hoc test. Only the data presented in figure 5 were analysed by Student's *t* test. Data are presented as means ± SEM. Statistical significance was assigned at the level of $p < 0.05$.

RESULTS

E_2 prevents loss of HA in response to UVB irradiation

Hairless skh-1 mice were ovariectomized (OVX) to deplete the animals from endogenous sex hormones. As a control E_2 was substituted in OVX mice by implantation of subcutaneous long release pellets (1.1 µg E_2/day/mouse). This non irradiated group allowed the characterization of the effect of E_2 on the intrinsically aged dermal HA matrix at 18 weeks of age. OVX caused a trend to reduced amounts of HA as shown by affinity histochemistry (Fig. 1B). Of note E_2 substitution reversed the effect of OVX and even elevated dermal HA accumulation strongly above the control level suggesting a stimulatory effect of E_2 on dermal HA.

To investigate the role of estrogen during photoaging skh1 mice were irradiated with UVB (3 x 1 MED (80 mJ/cm2), weekly) for 10 weeks. Subsequently, skin biopsies were collected from UVB exposed areas at the back. Clearly, loss of HA was induced by UVB (S,P UVB) and this loss was further aggravated by OVX (X,P UVB). Again substitution of E_2 compensated the decline of HA (X, E_2,UVB) even to the level of E_2-treated, non irradiated, non OVX controls (X, E_2 Fig. 1B). The results from the staining were confirmed by biochemical measurement of HA from skin extracts (Fig. 1C).

HAS3 is responsive to E_2 in the skin of UVB irradiated mice

To analyze the mechanisms that mediate the regulation of HA content in response to E_2 and UVB mRNA expression of HAS isozymes, hyaluronidases (Hyal) 1 and -2 were analyzed. Of note HAS3 expression followed the same pattern as the HA content in response to UVB and E_2 (Fig. 2A). In contrast HAS1 and HAS2 were regulated to a smaller degree and did not follow the pattern of HA in the skin (online figure 1 A, B). Therefore, HAS3 expression was further investigated in detail by ICC and immunoblotting which confirmed the regulation of mRNA expression (Fig. 2 B, C) and strongly suggests that HAS3 is induced by E_2 both in irradiated and non irradiated skin.

Furthermore, in non irradiated skin induction of Hyal2 in response to OVX was detected (supplemental Fig. 1D) which was rescued by E_2 substitution and could

therefore contribute to the decline of HA in response to OVX and the increase of HA in response to E_2 treatment. In contrast Hyal1 was not regulated in a fashion that could explain the observed changes in dermal HA. Finally HA-receptors, CD44 and receptor of HA mediated motility (RHAMM) were determined by qRT-PCR. CD44 expression was found to be unresponsive to both OVX/ E_2 and to UVB-irradiation. RHAMM however was clearly downregulated by OVX and rescued by E_2 substitution in both UVB-irradiated and non irradiated dermis which suggests that HA signaling via RHAMM is responsive to E_2 (online figure Fig. 1 E, F).

Furthermore, quantitation of E_2 receptors by qRT-PCR revealed that E2Rß was not detectable in the dermis of female hairless skh-1 mice in any of the experimental groups (data not shown). In contrast, the E2Rα receptor (supplemental Fig. 1G) was strongly expressed but the expression was not affected by any of the experimental interventions. These data suggest that the effects of estrogen were mediated by the E2Rα receptor.

E2 and UVB increase versican content in the dermal matrix

Subsequently, the response of the HA binding proteoglycan versican was characterized. Immunostaining of versican revealed that OVX did not affect versican but that substitution of E_2 caused marked dermal versican accumulation (Fig. 3A). Furthermore, in response to UVB versican was elevated in controls (S,P, UVB) and in OVX (X,P, UVB) mice. Still an additional increase of versican occurred after treatment of UVB irradiated X, E_2 mice (Fig. 3A). Four splicing variants of versican are known, V_0, V_1, V_2 and V_3. In order to obtain a readout of overall versican mRNA expression initially a primer was used that did not distinguish between the splicing variants. Although versican content increased in response to UVB the mRNA expression was not changed or even decreased (Fig. 3B). However, the increase of versican in response to E_2 in both non irradiated and irradiated skin was paralleled by induction of mRNA expression, which was particularly strong in UVB irradiated skin (Fig. 3B). Next immunoblotting of versican was performed in skin extracts and revealed a major versican band at approximately 200 kDa, which likely represented the versican splice variant V2 (Fig 3C) and closely resembled the regulation of versican as evidenced by immunostaining. Therefore, subsequently the mRNA expression versican V2 was analysed by realtime RT PCR (Fig. 3 D) and found to parallel the protein data shown in Fig. 3 A and C.

The changes of versican expression also occurred in the epidermis as evidenced by quantitation of immunostainings (data not shown) suggesting a similar response to E_2 in the epidermis. In contrast regulation of HAS3 was not detected in the epidermal compartment (data not shown). Therefore, future studies may address the effect of E_2 and versican in the epidermis.

In summary dermal HA was diminished by both E_2 depletion and UVB-irradiation in an additive manner whereas versican was markedly induced by UVB and exogenous E_2. Furthermore, the data suggest that HAS3 and versican V2 are the molecular targets of this regulation.

Effects of E_2 on HAS isozymes and versican in dermal fibroblasts *in vitro*

The above described *in vivo* results establish an important role of endogenous and exogenous E_2 on the composition of the dermal HA and versican matrix.

Specifically E_2 counteracts the decline of HA that is induced by UVB irradiation and elevates versican content of photoaged skin. In search of the underlying regulatory mechanisms two possibilities were considered. First, direct transcriptional effects of E_2 on HAS isozymes and versican may be responsible. Second, indirect effects of E_2 on the expression of growth factors that may in turn affect gene expression could be involved. Therefore, it was tested *in vitro* whether the HAS isozymes and versican are responsive to E_2 and UVB. In monolayer cultures of human skin fibroblasts HAS3 was not affected by UVB or E_2 and versican mRNA was downregulated in response to E_2 (Fig. 4 A,C). Furthermore immunoblotting of versican from supernatants revealed no effect on versican V2 (Fig. 4 D). In addition HAS1 and HAS2 were also downregulated 24 hours after stimulation with 100 μM E_2 (data not shown). To investigate whether the response of fibroblasts to E_2 and UVB would be different at lower E_2 concentrations or lower UVB doses experiments were performed with 0.1, 1 and 10 μM E_2 and in response to 10, 50 and 100 mJ UVB/cm^2. These experiments confirmed that HAS1, HAS2, HAS3 and versican were not directly induced by E_2 or UVB *in vitro* (data not shown). Since neither the estrogen response nor the acute UVB response *in vitro* mimicked the results obtained *in vivo*, a direct regulation of the involved genes in fibroblasts by E_2 and UVB appeared to be unlikely as a mechanism underlying the induction of HA and versican *in vivo*.

EGF is induced in response to E_2 in keratinocytes and mediates changes in HAS3 and versican expression.

Next a possible paracrine mechanism was addressed. For this purpose skin biopsies were examined with regard to differential regulation of growth factors known to be involved in the regulation of HA matrix. Specifically, it was searched for candidates that were diminished by OVX and increased by E_2 substitution both in non irradiated and irradiated skin. Interestingly, the expression level of EGF was indeed downregulated in OVX mice and was rescued by E_2 and therefore concurred with the regulation of HA, HAS3 and versican in non irradiated mice. Also in UVB irradiated mice EGF mRNA paralleled the changes of HA, HAS3 and versican expression (Fig. 5). Therefore, EGF expression was also investigated by immunostaining in the epidermis and measured in skin extracts using ELISA. The results confirmed that EGF is indeed induced in epidermis and in total skin extracts by E_2 (Fig.5 E,F). In contrast, TGFß1-3 did not correspond to the changes of HA, HAS3 and versican. Therefore, EGF was considered as a promising candidate for a paracrine mediator in response to E_2 and UVB and was studied in further detail.

The effect of E_2 and UVB on the expression of EGF in keratinocytes and dermal fibroblasts was examined *in vitro*. Fig. 6 shows that EGF induces HAS3 mRNA, HAS3 protein and HA synthesis in skin fibroblasts (Fig. 6 A-C). Furthermore, EGF induced total versican mRNA (Fig. 6D), versican V2 protein (Fig. 6 E) and versican V2 mRNA (Fig. 6 F). Next it was addressed whether UVB and E_2 affect the release of EGF from keratinocytes. Of note in keratinocytes E_2 induced expression and release of EGF from both non irradiated and irradiated keratinocytes (Fig. 7A,B). In dermal fibroblasts EGF expression was not detectable under the current experimental conditions (data not shown). Next, conditioned medium derived from keratinocytes exposed to E_2 and E_2 plus UVB was used to stimulate dermal fibroblasts and found to induce HAS3 and versican V2 mRNA expression. The induction of HAS3 and versican

V2 were blocked by both an EGF receptor kinase inhibitor, erlotinib, and by a neutralizing antibody against EGF (Fig. 7 C, D).

Therefore, it is proposed that *in vivo* E_2 induced expression and release of EGF from keratinocytes in a paracrine manner induced HAS3, HA and versican expression in fibroblasts of the papillary dermis.

Differential effects of E_2 on dermal cell proliferation and inflammation

Next it was attempted to link the specific changes of dermal HA and versican to functional effects in the dermis during photoaging. The proliferation of dermal fibroblasts as determined by Ki-67 immunostaining and mRNA expression was increased by E_2 both in non irradiated and in UVB irradiated skin (Fig. 8 A, B). This was further supported by the induction of TPX2 (microtubule-associated homolog) mRNA expression which is also indicative for proliferative activity (Fig. 8 C). It is conceivable that this proliferative response is in part due to the induction of HA and versican by E_2, because HA and versican are both thought to contribute to proliferation of dermal fibroblasts. It has also been suggested that HA plays a role in inflammation either after generation of HA-fragments or by supramolecular complexes of HA and HA-binding proteins that form HA cables and allow monocyte/macrophage adhesion. Interestingly, the UVB irradiated dermis of OVX mice, which contained the lowest HA and an elevated amount of versican, the Mac2 immunostaining and mRNA expression, indicative for macrophage content, were increased. Furthermore, Mac2 expression was strongly reduced by E_2 suggesting an anti-inflammatory effect of E_2 during skin aging (Fig. 8 D, E). To further support this hypothesis the expression profiles of chemokines and cytokines MCP-1, IL6 and TNFalpha were analysed and found be suppressed by E_2 (Fig. 8 F-H). Finally, the expression of inducible cyclooxygenase 2 (COX2) was analysed as an indicator of inflammatory activity. COX2 mRNA expression was also strongly responsive to E_2 (Fig. 8I). In summary, the *in vivo* data are consistent with a pro-proliferative and anti-inflammatory effect of estrogen that coincided with induction of both HAS3 and versican in UVB irradiated skin (Fig. 9).

DISCUSSION

Estrogen has been known for a long time to have beneficial effects on the skin which is particularly obvious after the onset of menopause or the initiation of estrogen treatment of post menopausal women (21). Estrogens partially protect from skin aging by increasing the thickness, reducing the wrinkling and augmenting the moisture of the skin (26-28). It has been demonstrated that estrogen treatment prevents loss of collagen type 1 and increases *de novo* collagen synthesis (29). Furthermore, estrogens increase dermal glycosaminoglycans which in turn may contribute to the thickness and moisture of the skin (30-32). Loss of HA from the skin appears to be part of the post menopausal aging response. In male mice the administration of estrogen increased the HA content of the skin (33). However systematic animal studies addressing the regulatory effect of estrogens on dermal HA, HAS isozymes, HA-receptors and hyaluronidases of females and importantly the underlying molecular mechanisms are lacking. Furthermore, up to date nothing is known about how E_2 may regulate the content and function of HA and versican in the skin. Therefore, the aim of the present study was to address changes of HA, HAS isozymes, hyaluronidases, HA receptors and the HA-binding proteoglycan versican in the context of photoaging and E_2 responses.

This study clearly shows that lack of endogenous E_2 results in marked loss of dermal HA in hairless skh-1 mice and that the lack of E_2 aggravates the additional loss of HA in response to UVB. Versican increased during photoaging and was further increased by E_2 treatment. The present data revealed that the molecular targets that mediate the response to E_2 differ between non irradiated and irradiated skin. The former was associated with changes in expression of HAS3 and Hyal2 whereas the latter corresponded mainly to changes in HAS3 expression. Therefore HAS3 was considered as a particularly important E_2-dependent regulator of dermal HA homeostasis during intrinsic and extrinsic skin aging.

E_2 mediates changes in gene expression by activation of intracellular E_2 receptors (E2R) α and $-\beta$, which translocate into the nucleus upon ligand binding and affect the expression of genes with estrogen response elements in the promoter region. In addition non genomic E_2 effects occur through the GPR30 pathway (34). It has been shown that both E2R α and $-\beta$ are expressed in the skin and that both are expressed in skin fibroblasts (21). However, considerable variability appears with respect to the ratio of both ER subtypes in various organs, ages and species (35,36). Therefore, the expression of E2R α and $-\beta$ was determined by realtime qPCR in hairless skh-1 mice in the present study. As a result the E2Rα receptor was strongly expressed in the skin biopsies whereas the E2Rβ receptor was not detectable by realtime qRT-PCR. Therefore the above mentioned effects of E_2 on dermal HA and versican during photoaging were attributed to E2R α. However contribution of non genomic effects can not be excluded on the basis of the present results.

Because the *in vivo* experiments showed that induction of HAS3 and versican mRNA likely played a key role in the estrogen response during photoaging, it was addressed whether E_2 directly induced the involved genes. However, it was found that HAS3 and versican were not directly induced in fibroblast monolayer cultures. Therefore, a direct transcriptional effect of E_2 on HAS3 and versican gene expression was ruled out as explanation for the *in vivo* results. As an alternative explanation induction of paracrine factors by E_2 that subsequently induce expression of HAS3 and versican appeared plausible. This hypothesis is in line with the report that E_2 indeed affects dermal ECM via paracrine mechanisms *in vivo*. It has been shown that postmenopausal loss of collagen might be due to lack of E_2 mediated transforming growth factor ß1 (TGFß1) expression (37).

Here it is demonstrated that EGF showed an expression pattern in response to ablation of endogenous sex steroids and E_2 substitution that paralleled the changes of the HA matrix both in photoaged skin and in non irradiated skin. Specifically, EGF mRNA and protein were reduced by OVX and induced by E_2. EGF is known to induce the expression of HAS2 and HAS3 in keratinocytes thereby promoting the pro-proliferative and migratory response to EGF (38,39). Because skin extracts were used to determine EGF mRNA and protein, which reflect epidermis plus dermis, both keratinocytes and fibroblasts might be the source of EGF in response to E_2. However, immunostaining of EGF already hinted to a pronounced EGF response in the epidermis. The *in vitro* experiments demonstrated that E_2 indeed induced EGF expression in keratinocytes but not in dermal fibroblasts. Subsequently, EGF released from keratinocytes in culture in response to E_2 and UVB was shown to stimulate HAS3 and versican expression in human skin fibroblasts. Therefore, it is proposed that E_2

stimulates keratinocytes to release EGF which in turn induces HAS3 and versican expression in dermal fibroblasts. The limitation of the *in vitro* experiments is that they reflect an acute response to single UVB irradiation whereas *in vivo* repetitive chronic dosing of UVB was applied. However, the results are agreeable with the observation in other biological systems that EGF is involved in various estrogen induced responses (40,41) or mimics E_2 responses (42) both *in vitro* and *in vivo*.

These findings might also be relevant with respect to the aged phenotype of fibroblasts. Interestingly, age associated resistance to phenotypic activation of fibroblasts is accompanied by reduced HA synthesis and the failure to upregulate HA in response to growth factors (43). EGF appears to be involved in this process, because EGF signaling is critically required for TGFß1 induced HA synthesis (44,45). Furthermore, fibroblast proliferation is stimulated by EGF and in aging fibroblasts this proliferative response declines partly due to downregulation of EGFR (46,47). Thus EGF is a growth factor that opposes the aging phenotype of dermal fibroblasts and this response involves in part HA-synthesis and HA-signaling. It is therefore likely that induction of EGF in keratinocytes by E_2 and paracrine stimulation of HA and versican in dermal fibroblasts is involved in the attenuation of the aged fibroblast and skin phenotype by E_2.

In vitro studies provided ample information about the function of individual, single matrix components including collagens, HA, HAS isozymes and versican. However it is obvious that during physiologic and pathophysiologic responses changes in matrix composition occur that involve simultaneously multiple matrix molecules. Thereby

the microenvironment of the cells changes dramatically and the cellular responses likely are the consequence of the combined effects of these complex changes. These include altered micromechanic forces, altered matrix receptor signaling including integrins, HA-receptors, CD44 and RHAMM and activation of alternative receptors by degraded matrix molecules such as toll like receptors that mediate "danger signals"(48). Therefore, a possibly important finding of the present study was that photoaging resulted in a dermal matrix characterized by low HA content and high versican content. At present it is unknown what the consequence of this shift in the relative abundance of HA and versican may be for the phenotype of cells and the aged phenotype of the skin. It is however very interesting that treatment with E_2 increases both HA and versican which resulted in a matrix with high HA and high versican content. Versican has 4 splicing variants that are characterized by loss of glycosaminoglycan bearing domains and therefore major differences in molecular weight and chondroitin sulfate content (49). The function of the different splice variants appears to be different, in part opposing, in various biological systems (50). The current data point towards versican V2 as the target of E2/EGF mediated regulation in the skin. Whereas the function in the skin has not been addressed, versican V2 has been suggested to regulate matrix assembly in the central nervous system (51). Therefore, versican V2 might be a interesting candidate for regulating matrix assembly and function in skin homeostasis and skin aging.

In the present study the proliferative capacity of fibroblasts in the dermis was closely correlated with HA and versican content in line with the pro-proliferative role of both pericellular HA and versican (20). Furthermore, estrogen clearly reduced the content of inflammatory macrophages, the expression of MCP-1, IL-6, TNFα and COX2 expression in UVB irradiated

skin. Vice versa inflammation was highest in the UVB-irradiated OVX mice that were characterized by dermal ECM with the lowest HA content and high versican content. It is believed that the supramolecular structure of the pericellular matrix determines whether the matrix acts homeostatic (5), pro-inflammatory (52) or pro-migratory (20). Therefore, it might be considered in the future that the ratio of HA and versican plays a role in the inflammatory response to UVB in the dermis. However, the present data do not prove the interrelationship between E2 induced matrix remodeling and effects on proliferation or inflammation.

In conclusion, during photoaging E_2 is indeed an important regulator of dermal HA and versican content in part by acting through paracrine release of EGF from keratinocytes which in turn induces the expression of HAS3 and versican in dermal fibroblasts. As a consequence proliferation is increased by E_2 and inflammation is inhibited. Thereby, the present study identifies novel molecular targets of E_2 that may contribute to the protective function of this hormone on dermal matrix during extrinsic aging responses.

Figure Legends

Figure 1 *Induction of HA by* E_2 *in vivo*. Hairless skh-1 mice were ovariectomized (X) at age 7-8 weeks or received a surgical sham procedure (S) and received either a subcutaneous placebo pellet (P) as control or a subcutaneous long-release E_2 pellet (1.1 µg E_2/day/mouse) (E2). Subsequently mice were subjected to UVB irradiation (3x 1 MED, weekly) for 10 weeks. At age of 18 weeks skin biopsies were obtained and the amount of HA was quantified. A, Experimental protocol and abbreviations. B, Affinity histochemistry of the skin using biotinylated bHABP and quantitative analysis (area fraction) of HA staining in the papillary dermis. C, Measurement of HA in skin extracts using a bHABP based kit. 100x magnification; n = 7-12, mean ± SEM, *, $p < 0.05$ versus S,P; #, $p < 0.05$ versus S,P UVB; ♦, $p < 0.05$ versus X,P; ▲ $p < 0.05$ versus X,P UVB.

Figure 2 *Induction of HAS3 by* E_2 *in vivo*. HAS3 expression was determined in skin biopsies from hairless skh-1 mice that were treated as detailed in figure 1. At age of 18 weeks skin biopsies were obtained and the amount of HAS3 was analysed. A, HAS3 mRNA expression in skin extracts. B, HAS3 immunostaining and quantitative image analysis of the dermal compartment. C, HAS3 immunoblotting (H64) of total skin extracts and quantitative analysis. 100x magnification; n = 7-12, mean ± SEM, *, $p < 0.05$ versus S,P; #, $p < 0.05$ versus S,P UVB; ♦, $p < 0.05$ versus X,P; ▲ $p < 0.05$ versus X,P UVB.

Figure 3 *Upregulation of versican in response to UVB and* E_2 *in vivo*. Versican expression was determined in skin biopsies from hairless skh-1 mice that were treated as detailed in figure 1. At age of 18 weeks skin biopsies were obtained and the amount of versican was analysed. A, pan-versican immunostaining and quantitative image analysis. B, mRNA expression of pan-versican in skin extracts. C, pan-versican immunoblotting (LF99) from skin extracts and quantitative analysis of the main band between 238 kDa and 171 kDa. D, versican V2 mRNA expression in skin

extracts. 100x magnification; n = 7-12, mean ± SEM, *, $p < 0.05$ versus S,P; #, $p < 0.05$ versus S,P UVB; ♦, $p < 0.05$ versus X,P; ▲ $p < 0.05$ versus X,P UVB.

Figure 4 *HAS3 and versican expression in human skin fibroblasts in response to UVB and E_2.* Fibroblasts were either untreated, received a single dose of UVB (100mJ/cm^2) or 100 nM E_2 or both and were analysed after 24 hours. A, HAS3 mRNA; B, HAS3 immunoblotting (H64) and quantitative analysis; C, pan-versican mRNA expression; D, pan-versican immunoblotting (LF99) and quantitative analysis; n= 3-6, mean ± SEM, *, $p < 0.05$ versus control.

Figure 5 *Gene expression profile in skin biopsies in response to UVB and E_2.* Mice were treated as detailed in the methods and in the legend of figure 1. Skin biopsies were obtained at 18 weeks of age and gene expression was determined by qRT-PCR. A, TGFß1; B, TGFß2; C, TGFß3; D, EGF; E, EGF in skin extracts determined by ELISA; F, EGF-immunostaining and quantitative image analysis of the epidermis; n = 5-12, mean ± SEM, *, $p < 0.05$ versus S,P; #, $p < 0.05$ versus S,P UVB; ♦, $p < 0.05$ versus X,P; ▲ $p < 0.05$ versus X,P UVB.

Figure 6 *HAS3 and versican expression in human fibroblasts in response to EGF.* Human skin fibroblasts were stimulated with EGF (10 ng/ml) for 24 hours. A, HAS3 mRNA expression; B, HAS3 immunoblotting (H64) and quantitative analysis; C, HA secreted into the medium during 24 hours after stimulation with EGF; D, pan-versican mRNA expression; E, pan-versican immunoblotting (LF 99) and quantitative analysis; F, versican V2 mRNA expression. n=3-6, mean ± SEM, *, $p < 0.05$ versus control.

Figure 7 *EGF release from keratinocytes in response to E2 and UVB.* A, Keratinocytes were treated with 100 nM E_2, UVB (100 mJ/cm2) or both. After 24 hours EGF expression was analyzed by qRT-PCR. B, EGF was determined by ELISA in cell culture supernatants of keratinocytes treated as in A. C, D, cell culture supernatants as in B were used to stimulate human skin fibroblasts. After 24 hours HAS3 mRNA expression and versican V2 expression were determined by qRT-PCR in the presence or absence of 3 µM erlotinib, EGF neutralizing antibody (EGF nAB, 0.35 µg/ml) or isotype control IgG (0.35 µg/ml). n=3-6, mean ± SEM, *, $p < 0.05$ versus control.

Figure 8 *Proliferation and macrophages in the dermis in response to E_2 and UVB in vivo.* Immunostaining of the papillary dermis of skin biopsies derived from 18 weeks old hairless skh-1 mice treated as described in the legend of figure 1. A-C, proliferation; A, immunohistochemistry of Ki67 and quantitative analysis of the papillary dermis. B, Ki67 mRNA expression. C, TPX-2 mRNA expression. D-I, inflammation; D, immunostaining of Mac2 as marker of inflammatory macrophages. E, Mac2 mRNA expression. F, MCP1 mRNA expression. G, IL6 mRNA expression. H, TNFα mRNA expression. I, COX2 mRNA expression as an inducible gene associated with inflammation and release of inflammatory chemokines and cytokines. n = 3-12, mean ± SEM, *, $p < 0.05$ versus S,P; #, $p < 0.05$ versus S,P UVB; ♦, $p < 0.05$ versus X,P; ▲ $p < 0.05$ versus X,P UVB.

Figure 9 UVB and E2 mediated remodeling of dermal matrix. Schematic drawing to summarize the working hypothesis that was deduced from the presented data. After chronic UVB exposure dermal matrix undergoes remodeling from HA-rich and versican poor matrix with low proliferative and low inflammatory activity (left) to HA-low and versican-rich ECM characterized by low proliferative but high inflammatory activity (middle). E2 upregulates

via paracrine release of EGF from the epidermis HAS3 and versican which cause transition into HA-rich and versican-rich dermal matrix with higher proliferative activity and reduced inflammation. This E2 mediated matrix remodeling partially overwrites the UVB induced degeneration of the dermal matrix possibly setting the stage for skin regeneration due to increased proliverative activity and by inhibition of inflammatory responses.

References

1. Fisher, G. J., Datta, S. C., Talwar, H. S., Wang, Z. Q., Varani, J., Kang, S., and Voorhees, J. J. (1996) *Nature* **379**, 335-339

2. Brennan, M., Bhatti, H., Nerusu, K. C., Bhagavathula, N., Kang, S., Fisher, G. J., Varani, J., and Voorhees, J. J. (2003) *Photochem Photobiol* **78**, 43-48

3. Varani, J., Spearman, D., Perone, P., Fligiel, S. E., Datta, S. C., Wang, Z. Q., Shao, Y., Kang, S., Fisher, G. J., and Voorhees, J. J. (2001) *Am J Pathol* **158**, 931-942

4. Koshiishi, I., Horikoshi, E., Mitani, H., and Imanari, T. (1999) *Biochim Biophys Acta* **1428**, 327-333

5. Stern, R., and Maibach, H. I. (2008) *Clin Dermatol* **26**, 106-122

6. Tammi, R., Agren, U. M., Tuhkanen, A. L., and Tammi, M. (1994) *Prog Histochem Cytochem* **29**, 1-81

7. Knott, A., Reuschlein, K., Lucius, R., Stab, F., Wenck, H., and Gallinat, S. (2009) *Biogerontology* **10**, 181-190

8. Dai, G., Freudenberger, T., Zipper, P., Melchior, A., Grether-Beck, S., Rabausch, B., de Groot, J., Twarock, S., Hanenberg, H., Homey, B., Krutmann, J., Reifenberger, J., and Fischer, J. W. (2007) *Am J Pathol* **171**, 1451-1461

9. Yoneda, M., Yamagata, M., Suzuki, S., and Kimata, K. (1988) *J Cell Sci* **90 (Pt 2)**, 265-273

10. Itano, N., and Kimata, K. (2002) *IUBMB Life* **54**, 195-199

11. Toole, B. P. (2004) *Nat Rev Cancer* **4**, 528-539

12. Bourguignon, L. Y., Gilad, E., and Peyrollier, K. (2007) *J Biol Chem* **282**, 19426-19441

13. Karousou, E., Kamiryo, M., Skandalis, S. S., Ruusala, A., Asteriou, T., Passi, A., Yamashita, H., Hellman, U., Heldin, C. H., and Heldin, P. (2010) *J Biol Chem* **285**, 23647-23654

14. Vigetti, D., Genasetti, A., Karousou, E., Viola, M., Clerici, M., Bartolini, B., Moretto, P., De Luca, G., Hascall, V. C., and Passi, A. (2009) *J Biol Chem* **284**, 30684-30694

15. Averbeck, M., Gebhardt, C. A., Voigt, S., Beilharz, S., Anderegg, U., Termeer, C. C., Sleeman, J. P., and Simon, J. C. (2006) *J Invest Dermatol*

16. Ghersetich, I., Lotti, T., Campanile, G., Grappone, C., and Dini, G. (1994) *Int J Dermatol* **33**, 119-122

17. Takahashi, Y., Ishikawa, O., Okada, K., Kojima, Y., Igarashi, Y., and Miyachi, Y. (1996) *J Dermatol Sci* **11**, 129-133

18. Schwartz, E. (1988) *J Invest Dermatol* **91**, 158-161

19. Day, A. J., and Prestwich, G. D. (2002) *J Biol Chem* **277**, 4585-4588

20. Evanko, S. P., Angello, J. C., and Wight, T. N. (1999) *Arterioscler Thromb Vasc Biol* **19**, 1004-1013

21. Verdier-Sevrain, S., Bonte, F., and Gilchrest, B. (2006) *Exp Dermatol* **15**, 83-94

22. Vickers, M. R., MacLennan, A. H., Lawton, B., Ford, D., Martin, J., Meredith, S. K., DeStavola, B. L., Rose, S., Dowell, A., Wilkes, H. C., Darbyshire, J. H., and Meade, T. W. (2007) *Bmj* **335**, 239

23. Freudenberger, T., Oppermann, M., Heim, H. K., Mayer, P., Kojda, G., Schror, K., and Fischer, J. W. (2010) *Basic Res Cardiol*

24. Chang, M. Y., Potter-Perigo, S., Tsoi, C., Chait, A., and Wight, T. N. (2000) *J Biol Chem* **275**, 4766-4773.

25. Papakonstantinou, E., Roth, M., Block, L. H., Mirtsou-Fidani, V., Argiriadis, P., and Karakiulakis, G. (1998) *Atherosclerosis* **138**, 79-89

26. Sator, P. G., Sator, M. O., Schmidt, J. B., Nahavandi, H., Radakovic, S., Huber, J. C., and Honigsmann, H. (2007) *Climacteric* **10**, 320-334

27. Sator, P. G., Schmidt, J. B., Sator, M. O., Huber, J. C., and Honigsmann, H. (2001) *Maturitas* **39**, 43-55

28. Kanda, N., and Watanabe, S. (2005) *J Dermatol Sci* **38**, 1-7

29. Castelo-Branco, C., Duran, M., and Gonzalez-Merlo, J. (1992) *Maturitas* **15**, 113-119

30. Grosman, N., Hvidberg, E., and Schou, J. (1971) *Acta Pharmacol Toxicol (Copenh)* **30**, 458-464

31. Uzuka, M., Nakajima, K., Ohta, S., and Mori, Y. (1981) *Biochim Biophys Acta* **673**, 387-393

32. Bentley, J. P., Brenner, R. M., Linstedt, A. D., West, N. B., Carlisle, K. S., Rokosova, B. C., and MacDonald, N. (1986) *J Invest Dermatol* **87**, 668-673

33. Sobel, H., and Cohen, R. A. (1970) *Steroids* **16**, 1-3

34. Hall, J. M., Couse, J. F., and Korach, K. S. (2001) *J Biol Chem* **276**, 36869-36872

35. Verdier-Sevrain, S., Yaar, M., Cantatore, J., Traish, A., and Gilchrest, B. A. (2004) *Faseb J* **18**, 1252-1254

36. Haczynski, J., Tarkowski, R., Jarzabek, K., Slomczynska, M., Wolczynski, S., Magoffin, D. A., Jakowicki, J. A., and Jakimiuk, A. J. (2002) *Int J Mol Med* **10**, 149-153

37. Ashcroft, G. S., Dodsworth, J., van Boxtel, E., Tarnuzzer, R. W., Horan, M. A., Schultz, G. S., and Ferguson, M. W. (1997) *Nat Med* **3**, 1209-1215

38. Pienimaki, J. P., Rilla, K., Fulop, C., Sironen, R. K., Karvinen, S., Pasonen, S., Lammi, M. J., Tammi, R., Hascall, V. C., and Tammi, M. I. (2001) *J Biol Chem* **276**, 20428-20435

39. Pasonen-Seppanen, S., Karvinen, S., Torronen, K., Hyttinen, J. M., Jokela, T., Lammi, M. J., Tammi, M. I., and Tammi, R. (2003) *J Invest Dermatol* **120**, 1038-1044

40. Ignar-Trowbridge, D. M., Nelson, K. G., Bidwell, M. C., Curtis, S. W., Washburn, T. F., McLachlan, J. A., and Korach, K. S. (1992) *Proc Natl Acad Sci U S A* **89**, 4658-4662

41. Nelson, K. G., Takahashi, T., Bossert, N. L., Walmer, D. K., and McLachlan, J. A. (1991) *Proc Natl Acad Sci U S A* **88**, 21-25

42. Gehm, B. D., McAndrews, J. M., Jordan, V. C., and Jameson, J. L. (2000) *Mol Cell Endocrinol* **159**, 53-62

43. Webber, J., Meran, S., Steadman, R., and Phillips, A. (2009) *J Biol Chem* **284**, 9083-9092

44. Simpson, R. M., Wells, A., Thomas, D., Stephens, P., Steadman, R., and Phillips, A. (2010) *Am J Pathol* **176**, 1215-1228

45. Simpson, R. M., Meran, S., Thomas, D., Stephens, P., Bowen, T., Steadman, R., and Phillips, A. (2009) *Am J Pathol* **175**, 1915-1928

46. Shiraha, H., Gupta, K., Drabik, K., and Wells, A. (2000) *J Biol Chem* **275**, 19343-19351

47. Reenstra, W. R., Yaar, M., and Gilchrest, B. A. (1993) *Exp Cell Res* **209**, 118-122

48. Stern, R. (2004) *Eur J Cell Biol* **83**, 317-325

49. Wight, T. N. (2002) *Curr Opin Cell Biol* **14**, 617-623

50. Sheng, W., Wang, G., Wang, Y., Liang, J., Wen, J., Zheng, P. S., Wu, Y., Lee, V., Slingerland, J., Dumont, D., and Yang, B. B. (2005) *Mol Biol Cell* **16**, 1330-1340

51. Dours-Zimmermann, M. T., Maurer, K., Rauch, U., Stoffel, W., Fassler, R., and Zimmermann, D. R. (2009) *J Neurosci* **29**, 7731-7742

52.   de La Motte, C. A., Hascall, V. C., Calabro, A., Yen-Lieberman, B., and Strong, S. A. (1999) *J Biol Chem* **274**, 30747-30755

Table 1: Primer sequences used for quantification of gene expression

Gene	Primer sequence
human CD44	f 5'-GCTATTGAAAGCCTTGCAGAG-3' r 5'-CGCAGATCGATTTGAATATAACC-3'
human COX2	f 5'-TGAGTGTGGGATTTGACCG-3' r 5'-TGTGTTTGGAGTGGGTTTCA-3'
human EGF	f 5'-AGTTTTTCTGAATGGGTCAAGG-3' r 5'-TCCAATTTATTGCCATTCCAG-3'
human GAPDH	f 5'-GTGAAGGTCGGAGTCAACG-3' r 5'-TGAGGTCAATGAAGGGGTC-3'
human HAS1	f 5´- TACAACCAGAAGTTCCTGGG -3´ r 5´- CTGGAGGTGTACTTGGTAGC-3´
human HAS2	f 5´-GTGGATTATGTACAGGTTTGTGA-3´ r 5´- TCCAACCATGGGATCTTCTT-3´
human HAS3v1	f 5´- GAGATGTCCAGATCCTCAACAA-3´ r 5´- CCCACTAATACACTGCACAC-3´
human Hyal1	f 5'-CCAAGGAATCATGTCAGGCCATCAA-3´ r 5'-CCCACTGGTCACGTTCAGG-3´
human Hyal2	f 5'-GGCTTAGTGAGATGGACCTC-3' r 5'-CCGTGTCAGGTAATCTTTGAG-3´
human RHAMM	f 5'-GAATATGAGAGCTCTAAGCCTG-3´ r 5'-CCATCATACTCCTCATCTTTGTC-3´
human Versican pan	f 5'-AGACTGTCAGATATCCCATCC-3´ r 5'-AATCCATAAGTCCTGACTCCT-3´
human Versican V1	f 5'-CGTCGAATGAGTGATTTGAG-3' r 5'-TTTCAGCCATTAGATCATGCAC-3´
human Versican V2	f 5'-AAGACAGGACCTGATCGCT-3´ r 5'-AGTGGCTCCATTACGACAGG-3´
human Versican V3	f 5'-ACGACCTGATCGCTGCAA-3´ r 5'-CAAGTGGCTCCATTACGACA-3´
human Versican Vo	f 5'-ACCAGGACCTGATCGCTGCAA-3´ r 5'-GTTCATTTTGCAGCGATCAG-3´
murine CD44	f 5'-CAAGTTTTGGTGGCACACAG-3´ r 5'-CTGTAGCGGCCATTTTTCTC-3´
murine COX2	f 5'-CCGGACTGGATTCTATGGTG-3´ r 5'-CCTTGAAGTGGGGTCAGGATG-3´
murine EGF	f 5'-GCCACGCTTACATTCATTCC-3´ r 5'-ATCGCCTTGCTTTTCAACAC-3´

murine E2R α	f 5'-AGCTGCTCCTCCACTTGGT-3´
	r 5'-GGCGTCGATTGTCAGAATTAG-3´
murine E2R β	f 5´-TACGGTGTCTGGTCCTGTGA-3´
	r 5'-TACACTGATTCGTGGCTGGA-3´
murine GAPDH	f 5'-TGGCAAAGTGGAGATTGTTGCC-3´
	r 5'-AAGATGGTGATGGGCTTCCCG-3´
murine HAS1	f 5'-TATGCTACCAAGTATACCTCG-3´
	r 5'-TCTCGGAAGTAAGATTTGGAC-3´
murine HAS2	f 5'-CGGTCGTCTCAAATTCATCTG-3´
	r 5'-ACAATGCATCTTGTTCAGCTC-3´
murine HAS3v1	f 5'-GATGTCCAAATCCTCAACAAG-3´
	r 5'-CCCACTAATACATTGCACAC-3´
murine Hyal1	f 5'-AAGTACCAAGGAATCATGCC-3´
	r 5'-CTCAGGATAACTTGGATGGC-3´
murine Hyal2	f 5'-GGTGGACCTTATCTCTACCAT-3´
	r 5'-TATTGGCAGGTCTCCATACTT-3´
murine IL6	f 5 '-GATGGATGCTACCAAACTGGA-3´
	r 5'-GGTACTCCAGAAGACCAGAGGA-3´
murine Ki-67	f 5'-CCAGCTGTCCTCAAGACAATC-3´
	r 5'-CACTGGAAGTCCTGCCTGAT-3´
murine Mac2	f 5'-TGAGAGTGGCAAACCATTCA-3´
	r 5'-GTCACCACTGATCCCCAGTT-3´
murine MCP1 (CcL2)	f 5'-CCCAATGAGTAGGCTGGAGA-3´
	r 5'-TCTGGACCCATTCCTTCTTG-3´
murine RHAMM	f 5'-GCCACTCAGAAGGACCTCAC-3´
	r 5'-TGCACAGCTAATTTCTTGGATG-3´
murine TGFβ1	f 5'-CTAATGGTGGACCGCAACA-3´
	r 5'-ACTGCTTCCCGAATGTCTGA-3´
murine TGFβ2	f 5'-CGAGGAGTACTACGCCAAGG-3´
	r 5'-GTAGAAAGTGGGCGGGATG-3´
murine TGFβ3	f 5'-TTCGACATGATCCAGGGACT-3´
	r 5'-TCTCCACTGAGGACACATTGA-3´
murine TNFα	f 5'-CGAGTGACAAGCCTGTAGCC-3´
	r 5'-AGCTGCTCCTCCACTTGGT-3´
murine TPX2	f 5'-TCCCTGGATGCTAAGAGAGC-3´
	r 5'-TTTCAACAGAGGCAACATGG-3´
murine Versican pan	f 5'-ACCATGTCACTGGCTGTGG-3´
	r 5'-AGCGGCAAAGTTCAGAGTGT-3´
murine Versican V1	f 5'-GCCTACTGCTTTAAACGTCGA-3´
	r 5'-GCAAACAGATCATGCAGTGG-3´
murine Versican V2	f 5'-ACAGGACCTGATCTCTGCAAAA-3´
	r 5'-CCATTCCGACAAGGGTTAGA-3´
murine Versican V3	f 5'-ACGACCTGATCTCTGCAA-3´

	r 5'-CCATTCCGACAAGGGTTAGA-3'
murine Versican Vo	f 5'-AAGACAGGTCGATTGAGTGATAT-3'
	r 5'-GCAAACAGATCATGCAGTGG-3'

Figure 1

A

10 weeks UVB irradtiation

8 weeks
OVX ± pellet

18 weeks
1st biopsy

age

Group	OVX	Placebo pellet	E2 pellet
S,P	-	+	-
X,P	+	+	-
X,E2	+	-	+

B Hyaluronan

S,P   X,P   X,E2

C

UVB
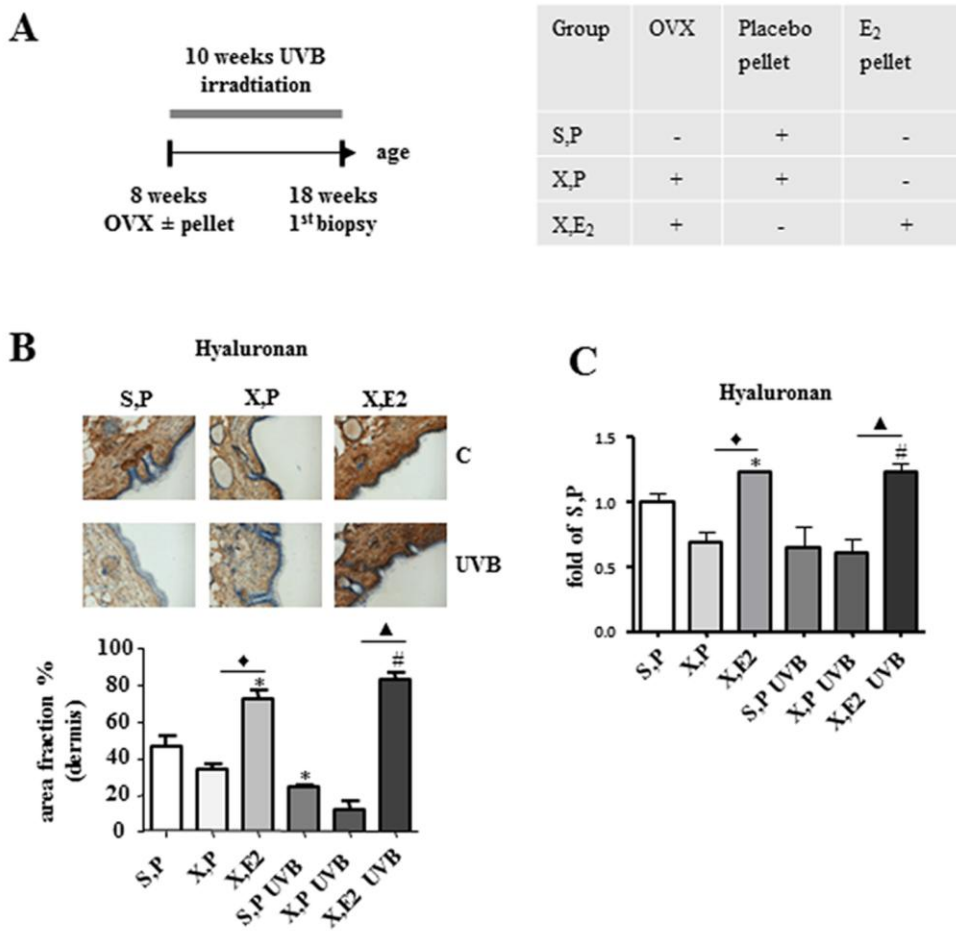
C Hyaluronan

Figure 2

A

B

C

Figure 3

Figure 4

A

HAS3

B

HAS3

◀ 63
◀ 55

C

Versican pan

D

Versican

◀ 268 kDa
◀ 238 kDa
◀ 171 kDa

Figure 5

A TGF ß 1

B TGF ß 2

C TGF ß 3

D EGF

E EGF

F

S,P   X,P   E2,P

C

UVB

EGF

Figure 6

A

HAS3

B

HAS3

◀ 63
◀ 55

C

Hyaluronan

D

Versican pan

E

Versican

◀268 kDa
◀238 kDa
◀171 kDa

F

Versican V2

Figure 7

A

EGF

B

EGF

C

HAS 3

D
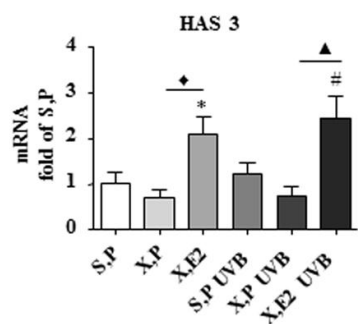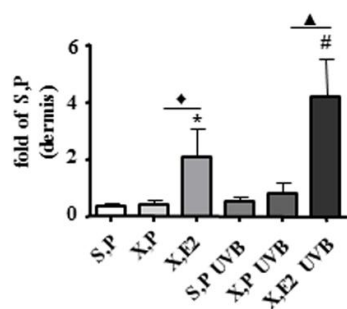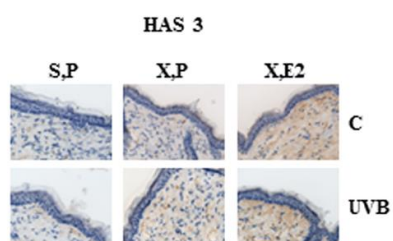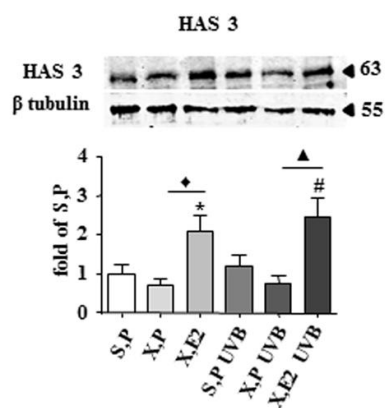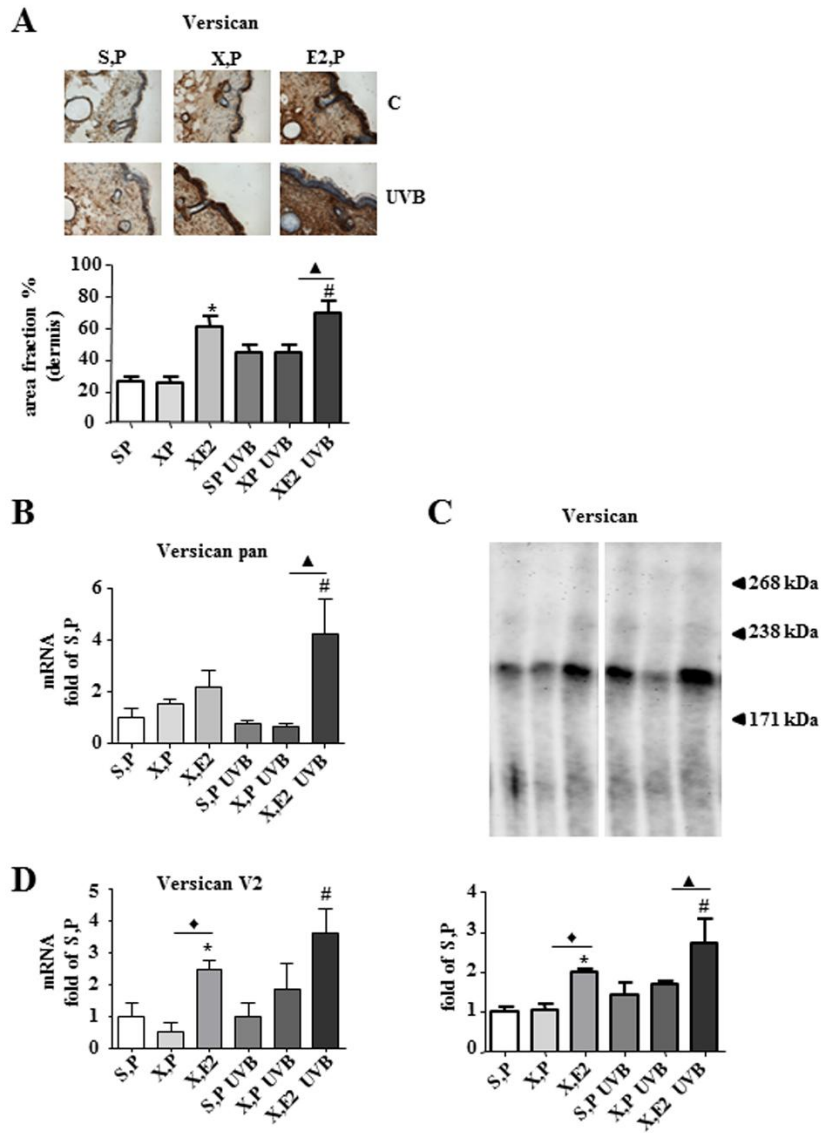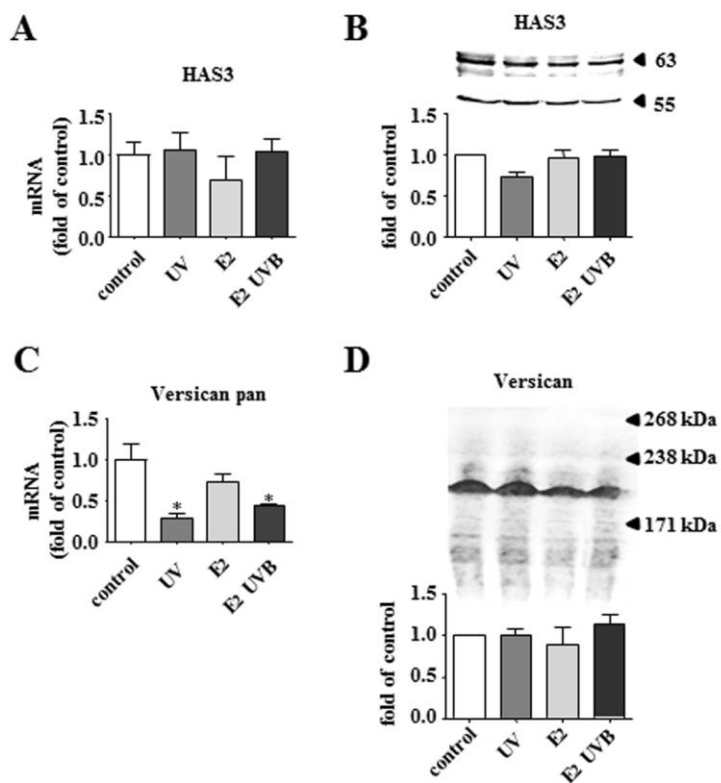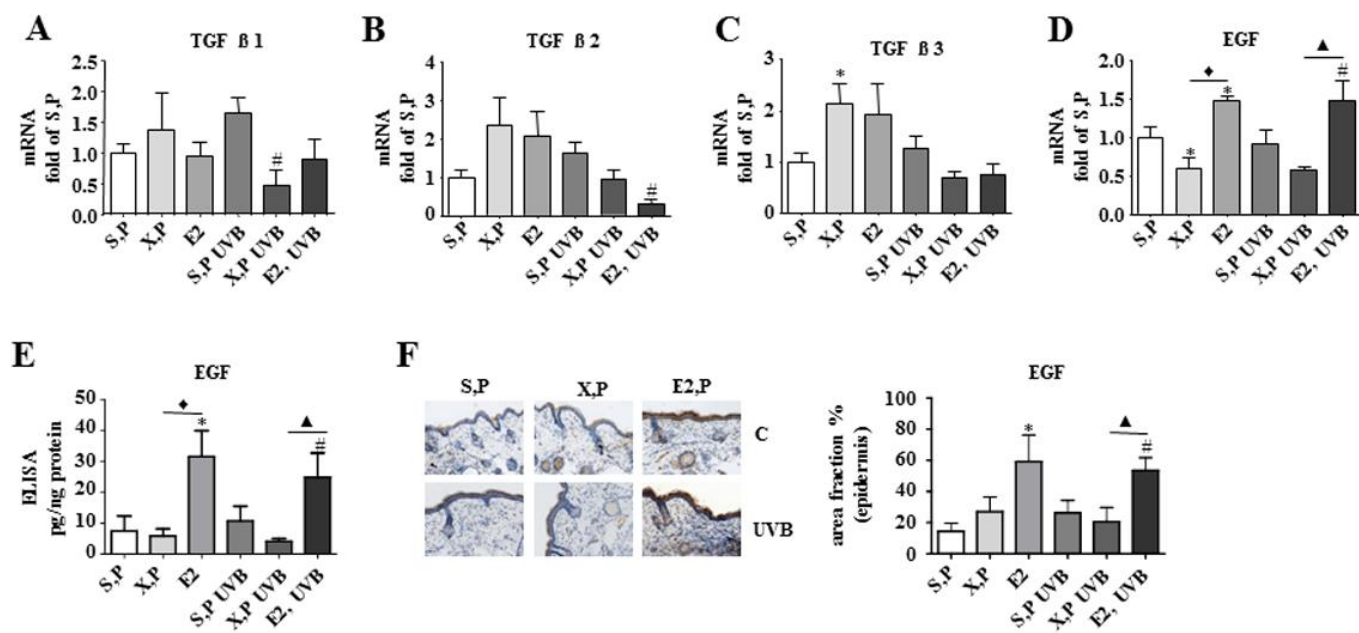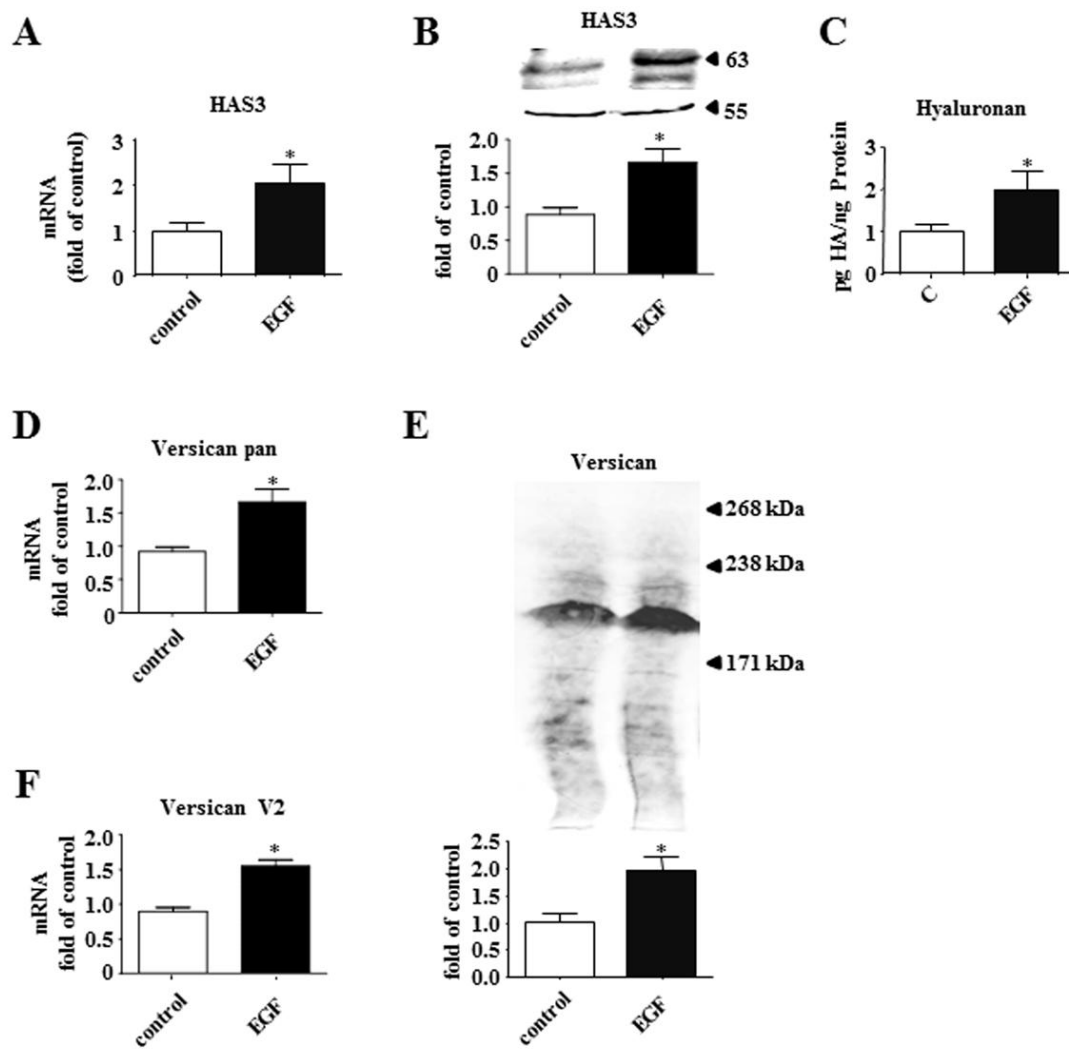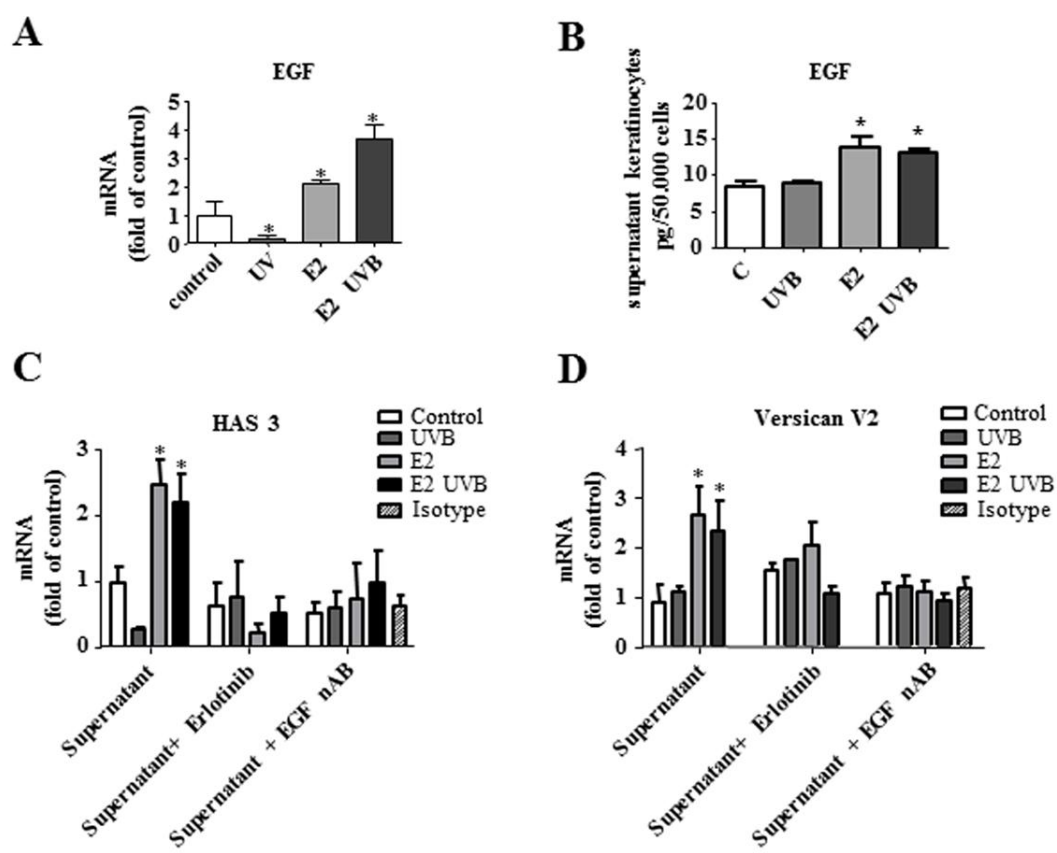
Versican V2
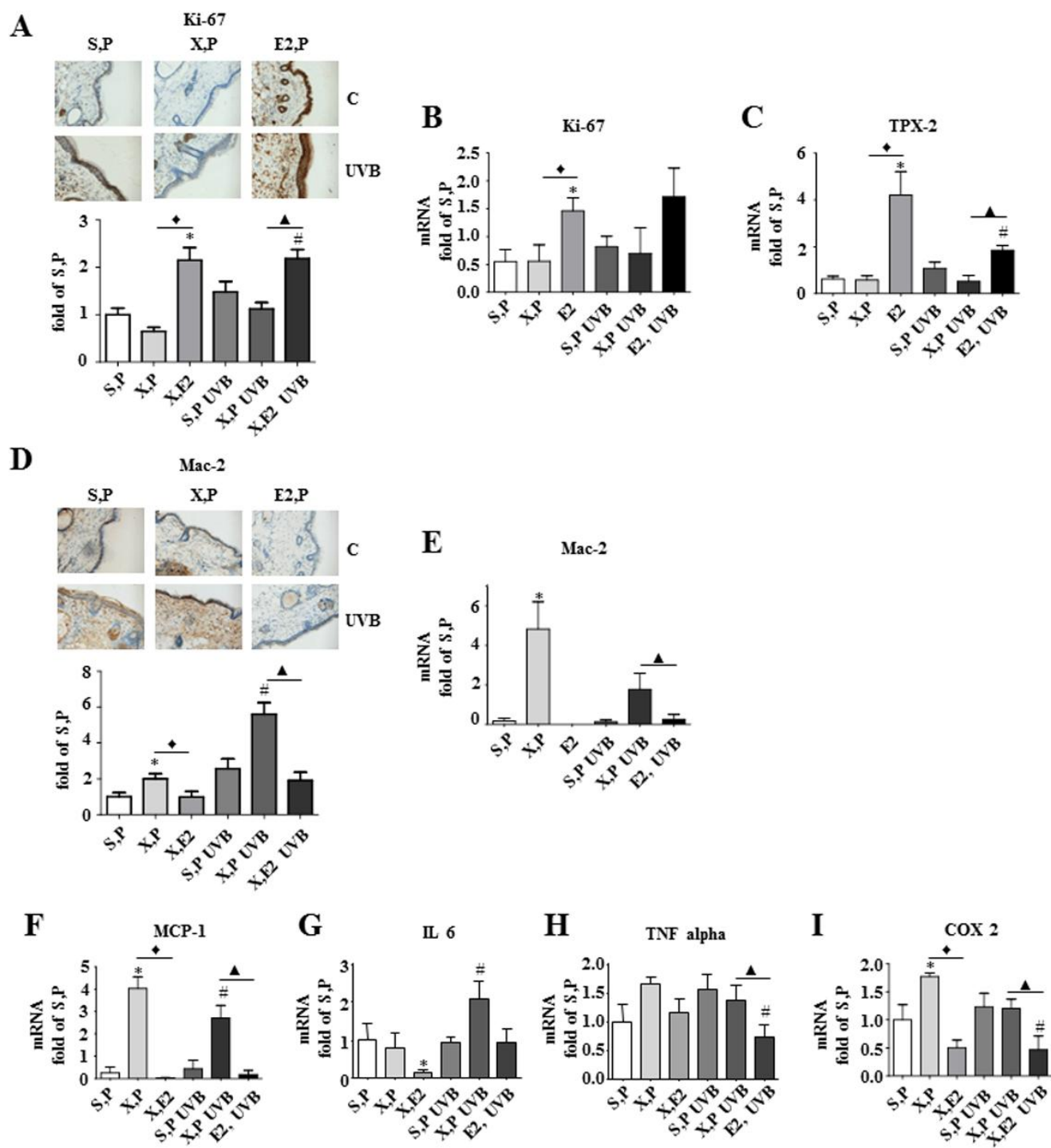
Figure 8

Figure 9
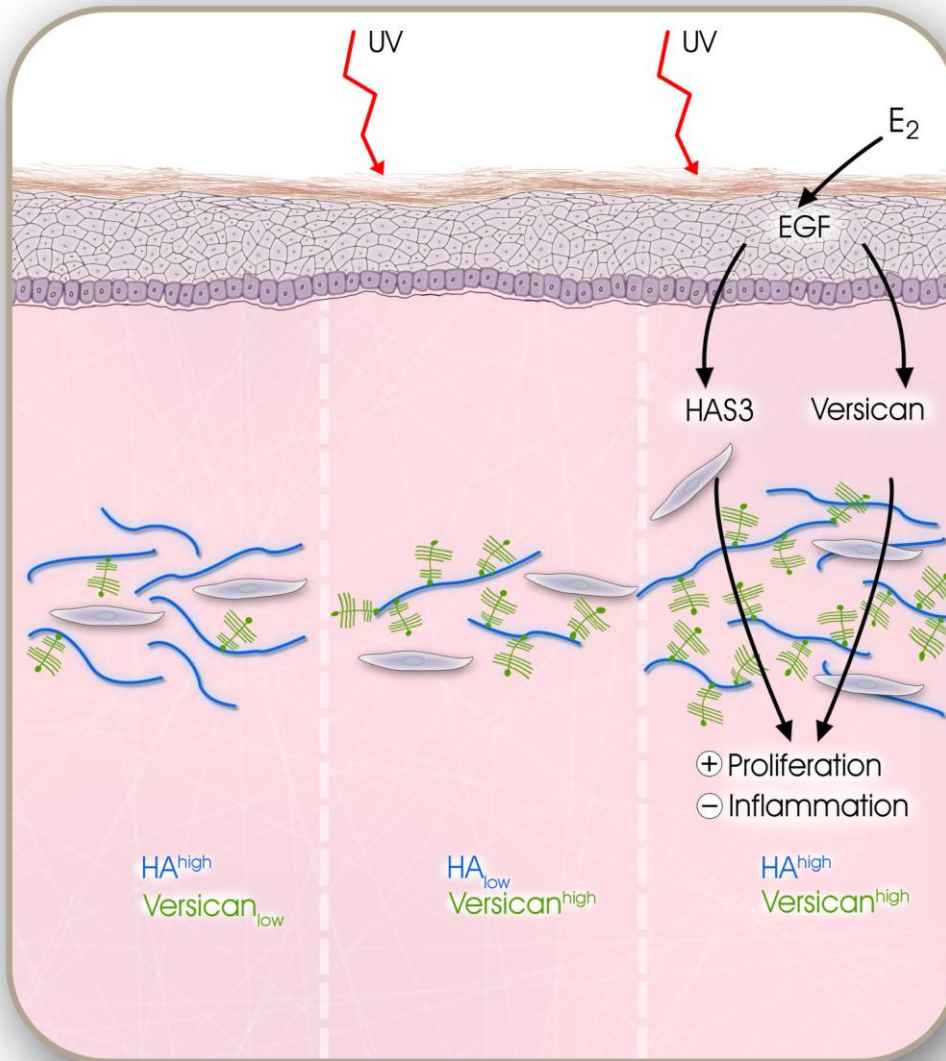
Publikation Nr. 6

Estradiol protects dermal hyaluronan/versican matrix during photoaging by release of EGF from keratinocytes

Katharina Röck, Michael Meusch, Nikola Fuchs, **Julia Tigges**, Petra Zipper, Ellen Fritsche, Jean Krutmann, Bernhard Homey, Julia Reifenberger, Jens W. Fischer

— · — · — · — · — · — · — · — · — · —

3   Abschlussdiskussion

Inhalt der vorliegenden Dissertation war es, die Reaktion der Haut auf exogene Noxen wie UV-Strahlung, Pharmazeutika, Kosmetika und Umweltschadstoffen, denen sie als Grenzflächenorgan des Körpers ständig ausgesetzt ist, näher zu charakterisieren. Dabei lag der Fokus auf Untersuchungen zur Rolle der AhR-Signalkaskade in der Haut vor allem in Bezug auf extrinsische Alterungsprozesse.

3.1   Die Haut als Grenzflächenorgan

Für die Homöostase des Organismus ist es essentiell, dass Hautzellen auf extrinsische Faktoren reagieren können (Merk *et al.*, 2006), denn die Haut, insbesondere die Epidermis, bildet als das größte der Grenzflächenorgane die äußerste Barriere des Körpers. Adverse Effekte von exogenen Noxen auf die Haut beinhalten Irritationen, Sensibilisierungen, Tumorentstehung sowie vorzeitige Alterungsprozesse. Während Irritationen der Haut physikalischer Natur sind, auf den physikochemischen Eigenschaften der Substanzen basieren und somit nicht durch Störungen zellulärer Prozesse verursacht werden, sind an der Sensibilisierung, der Tumorentstehung sowie vorzeitigen Alterungsprozessen intrazelluläre Signalprozesse beteiligt. Dass der Fremdstoffmetabolismus der Haut eine zentrale Rolle sowohl bei der Sensibilisierung (Ott *et al.*, 2009; Hagvall *et al.*, 2008) als auch bei der Hautkarzinogenese spielt, ist lange bekannt (Shimizu *et al.*, 2000; Ikuta *et al.*, 2009). Ob der Metabolismus auch in exogen induzierte Alterungsprozesse involviert ist, ist jedoch bisher nicht untersucht. Weiterhin spielt bei der Tumorentstehung sowie bei vorzeitigen Alterungsprozessen der Haut die zelluläre Signaltransduktion eine entscheidende Rolle. Ein für die Toxikologie zentrales Molekül, welches den Fremdstoffmetabolismus moduliert (zusammengefasst in Ramadoss *et al.*, 2005), an zellulären Signalprozessen beteiligt ist (zusammengefasst in Elferink, 2003; Marlowe und Puga, 2005; Dietrich und Kaina, 2010) und für welches eine Assoziation mit der Hauttumoriginese (Shimizu *et al.*, 2000) sowie vorzeitiger, extrinsischer Hautalterung beschrieben ist bzw. vermutet wird (Murphy *et al.*, 2004; Leung und Harvey, 2002; Lahmann *et al.*, 2001) ist der AhR. Daher werden

in den folgenden drei Unterabschnitten dieser Dissertation insbesondere die Rolle der AhR-Signalkaskade in der Haut diskutiert werden. Folgende Aspekte werden dabei fokussiert: (i) der Fremdstoffmetabolismus der menschlichen Haut, (ii) die Regulation des Fremdstoffmetabolismus in der menschlichen Haut durch den AhR und (iii) die Rolle des AhR bei vorzeitigen Alterungsprozessen der Haut.

3.1.1 AhR-abhängiger Fremdstoffmetabolismus in der Haut

Zu den AhR-abhängigen fremdstoffmetabolisierenden Enzymen der Phase 1, die in der Haut identifiziert werden konnten, gehören CYP1A1, 1B1, 2A6, 2B6, 2E1, 3A4 und 3A5 (Du L *et al.*, 2006; Swanson, 2004). Die meisten dieser Gene wurden bisher jedoch nur auf transkriptioneller Ebene untersucht. In Publikation 2.1 haben wir erstmals die Enzymaktivitäten in humaner Haut, epidermalen 3D-Äquivalenten, NHEKs, NCTCs und HaCaTs verglichen. Da der Hauptanteil des CYP-Metabolismus in der Haut im epidermalen Kompartiment stattfindet (Swanson, 2004; Baron *et al.*, 2001) wurden in Publikationen 2.1 – 2.3 ausschließlich epidermale *in vitro* Modelle auf ihre metabolische Kapazität hin untersucht. Eine Vielzahl an Studien hat die CYP-mRNS, Protein und / oder Aktivität von auf Keratinozyten basierenden *in vitro* Modellen unter-sucht (ausführlich zusammengefasst in Oesch *et al.*, 2007; Rolsted *et al.*, 2008; Gibbs *et al.*, 2007; Svensson, 2009; Rolsted *et al.*, 2008). Da die CYP-mRNS Expression oft nicht mit der tatsächlichen Enzymaktivität korreliert (Swanson, 2004; Svensson, 2009), wurde für die vorliegende Dissertation (Publikation 2.1 – 2.3) die CYP-mRNS Expression nicht berücksichtigt, sondern der wesentlich aussagekräftigere Endpunkt der Enzymaktivität untersucht.

Interessanterweise waren die basalen Aktivitäten der AhR-abhängigen Enzyme CYP1A1, 1B1 und 1A2 in allen untersuchten *in vitro* Modellen unterhalb des quantitativen Detektierminimums. Das Gleiche gilt für CYP2B6 und 3A, die beide über den *Pregnane X Receptor* (PXR) (Honkakoski *et al.*, 1998; Xie *et al.*, 2000) und den *Constitutive Androstane Receptor* (CAR) (Xu *et al.*, 2005) reguliert werden.

Im Bezug auf die Enzymaktivität finden sich in der Literatur widersprüchliche Ergebnisse. Während zum Beispiel eine Studie basale CYP1A1 und 1B1 Protein und

EROD Aktivität in humaner Epidermis nachweisen konnte (Katiyar *et al.*, 2000), war es anderen (Rolsted *et al.*, 2008) und uns nicht möglich, diese Ergebnisse zu verifizieren. Auch in 3D-Epidermis-Modellen konnte basale CYP1A1/1B1 Proteinexpression, sowie basale EROD Aktivität nicht nachgewiesen werden (Harris *et al.*, 2002; Neis *et al.*, 2010), was mit unseren Beobachtungen übereinstimmt. Diese Diskrepanzen sind möglicherweise durch Faktoren wie Lebensführung und Ernährung zu erklären, da einige Inhaltsstoffe von Lebensmitteln, wie z.B. Flavonoide, bekannte Induktoren für die AhR-abhängige CYP-Expression sind (Denison und Nagy, 2003). Eine andere Möglichkeit sind jahreszeitlich bedingte Variationen in der CYP-Expression, da diese von der saisonal bedingten UV-Exposition abhängig ist (zusammengefasst in Rannug und Fritsche, 2006). Diese Faktoren könnten in der CYP-Expression epidermaler 3D-Äquivalente eine Rolle spielen, da Keratinozyten zwar unter Standardbedingungen kultiviert werden, aber die Lagerung des Zellkulturmediums von der Produktion bis hin zum Endbenutzer nicht standdardisiert werden kann. Exposition von Medium gegenüber Sonnenlicht führt zur Entstehung von Tryptophanphotoprodukten, welche hochaffine AhR-Liganden sind und somit die basale CYP1-Expression in der Kultur unter ‚Standardbedingungen' modifizieren können (Oberg *et al.*, 2005).

Anders verhält es sich mit der induzierbaren CYP1-Aktivität in der Haut. (WATTENBERG *et al.*, 1962) konnten nach 3-MC Behandlung induzierte AHH-Aktivität in der Haut von Ratten nachweisen. Ähnliche Befunde wurden auch für die menschliche Haut berichtet (Levin *et al.*, 1972; Alvares *et al.*, 1973). Die in Publikation 2.1 identifizierte induzierbare EROD und MROD Aktivitäten durch das PAK 3-MC in 3D-Hautäquivalenten stimmt mit der Arbeit von Harris *et al.* überein, die ebenfalls funktionelles CYP Protein nachweisen konnte (Harris *et al.*, 2002).

Monolayer-Keratinozytenkulturen unterscheiden sich deutlich von den komplexeren 3D-Epidermis-Äquivalenten (EPI-200). Sowohl primäre humane Keratinozyten (NHEKs), als auch die immortalisierte Keratinozytenzelllinie NCTC 2544 zeigten basal sehr geringe CYP1A/1B-Aktivitäten, in HaCaT-Zellen konnte keine basale Aktivität detektiert werden. Des Weiteren wurde CYP1A/1B in allen *Monolayer*-Modellen durch den AhR-Liganden 3-MC induziert, in 3D-Modellen auch durch B(a)P, wobei NHEKs die niedrigsten Induktionsraten aufwiesen.

In allen *Monolayer*-Keratinozytenkulturen nahm die CYP1A/1B-Induktion ab, nachdem das Maximum der Induktion erreicht war. Da es sich dabei nicht um einen zytotoxischen Effekt von 3-MC handelte (gemessen durch LDH im Überstand), liegt der Grund wahrscheinlich in dem Phänomen der Substratinhibierung, was bereits in früheren Studien für Resorufin-basierte CYP-Substrate wie EROD aufgezeigt wurde (Lin *et al.*, 2001). Dieser Effekt war allerdings nicht in den 3D-Modellen zu beobachten. Dieses könnte auf einer unterschiedlichen Verteilung der Induktoren innerhalb der 3D-Modelle zurückzuführen sein, da in *Monolayer*-Kulturen alle Zellen durch das Medium exponiert werden. Des Weiteren ist das Verhältnis von Zellzahl zu Oberfläche in 3D-Modellen wesentlich höher. Diese Daten lassen vermuten, dass EPI-200-Modelle wegen ihrer 3D-Struktur eine brauchbare Alternative für die Untersuchung von CYP1A/1B-Induktion in der Haut sind.

Ein ganz anderes Bild ergibt sich bei der Untersuchung eines anderen AhR-abhängigen Phase 1 Enzyms: der Cyclooxygenase (COX). Von COX wird vermutet, dass es eine Hauptrolle in der Aktivierung von Chemikalien spielt, da während der COX katalysierten Peroxidase-Reaktion eine Vielzahl von elektrophilen Substanzen kooxidiert werden. Dieser Prozess ist besonders bedeutsam für Genotoxine und Allergene (Vogel *et al.*, 2000). COX-Enzymaktivitäten wurden in gut detektierbaren Mengen in allen getesteten Modellen reproduzierbar über verschiedene Donoren und Inkubationszeiten gemessen. Ein großer Unterschied zeigte sich jedoch zwischen immortalisierten und nicht-immortalisierten Zellsystemen: Die PGE_2 Produktion war in immortalisierten Zelllinien (HaCaT, NCTC) geringer als in primären Zellen (NHEK) oder *ex vivo* Haut. Dabei glichen die PGE_2-Produktionen von EPI-200 und HaCaTs denen, die von anderen Gruppen gefunden wurden (Natsch und Wasescha, 2007; Moeller *et al.*, 2008). Eine mögliche Erklärung für diese Unterschiede könnte im Verlust der zellulären PGE_2-Produktion während des zellulären Prozesses der Immortalisierung zu finden sein. Diese Hypothese wird von der Beobachtung bestätigt, dass die COX-2 Expression in Mammakarzinom-Zelllinien im Vergleich zu normalen epithelialen Brustzellen (hMEC) geringer ist und dass die Immortalisierung von hMEC zu einem dramatischen Rückgang in der COX-2 Expression führt, wobei der zugrunde liegende Mechanismus bisher nicht aufgeklärt ist (Zhao *et al.*, 2008). Kürzlich konnte die AG Fritsche zeigen, dass AhR-Aktivierung COX-2 Induktion in Maushaut und

HaCaT Zellen induziert (Fritsche *et al.*, 2007). In Publikation 2.1 wurde die PGE$_2$-Formation durch den AhR-Liganden 3-MC in HaCaTs, NHEKs und EPI-200-Modellen induziert. Dennoch war die Induktion lediglich in EPI-200-Modellen statistisch signifikant. Diese Daten zeigen, dass für die Studie der Oxidation von elektrophilen Substanzen *in vitro* Modelle auf der Basis von primären Zellen die Methode der Wahl sind und dass EPI-200-Modelle am geeignetsten für Experimente zur COX-Induktion sind. Zusammenfassend sind die basalen CYP-Aktivitäten im Vergleich zu den substantiellen COX-Aktivitäten in rekonstruierter Epidermis und humanen Hautmikrosomen in allen untersuchten Modellen sehr gering, lassen sich jedoch deutlich induzieren.

Zu den AhR-abhängigen fremdstoffmetabolisierenden Enzymen der Phase 2 gehören die UGT1A6 (Bock *et al.*, 1998) und die GSTA1 (Rushmore *et al.*, 1990), aber auch die N-Acetyltransferase (NAT) ist in der Haut sehr aktiv und wurde im Rahmen der Publikation 2.2 untersucht. Humane epidermale Keratinozyten exprimieren signifikante GST-Aktivität gegenüber dem universellen Substrat 1-Chor-2,4-dinitrobenzen (CDNB) (Zhang *et al.*, 2002) und auch im Zytosol menschlicher Haut konnte GST-Aktivität nachgewiesen werden (Raza *et al.*, 1991). Wir haben GST-Aktivitäten in zytosolischen Proteinen von menschlicher Haut (Epidermis und Dermis) und EPI-200-Modellen gemessen, wobei letztere etwa dreifach höhere GST-Aktivitäten aufwiesen (Publikation 2.2). Auch Harris *et al.* fanden höhere GST-Aktivitäten, allerdings in abgeschabten Epidermen (ohne Dermis) als in 3D-Epidermismodellen (Harris *et al.*, 2002). Daraus schlussfolgern wir, dass die basale zytosolische GST-Aktivität in EPI-200 Keratinozyten konstitutiv höher zu sein scheint als in humaner *ex vivo* Haut. Dabei kann nicht ausgeschlossen werden, dass interindividuelle Unterschiede der Donoren für die unterschiedlichen Aktivitäten verantwortlich sind. Um dieses zu ermitteln, müsste die n-Zahl der Keratinozytenspender für die Epidermismodelle erhöht werden. Auch Genexpressionsanalysen unterstützen diese Hypothese, da die Expressionen von GSTA4 und P1 in EPI-200-Modellen von zwei verschieden Donoren im Vergleich zu Vollhautbiopsien aus Gesäßhaut 2-3 mal höher waren (Hu *et al.*, 2010). GST-P wurde dabei als die dominante GST-Isoform in der Epidermis beschrieben (Raza *et al.*, 1991). Da die Firma MatTek nur EPI-200-Modelle von zwei verschiedenen Spendern zum

Verkauf anbietet, sind die Publikationen, die EPI-200 Modelle verwendet haben, alle von den gleichen Spendern.

Die basalen CDNB-Konjugierungsraten (Publikation 2.2) reproduzieren die bisherige Literatur (Zhang *et al.*, 2002; Hirel *et al.*, 1995). GST-Aktivitäten in Keratinozyten waren jedoch in allen intakten Monolayerzellen bis zu zweifach höher als in EPI-200-Modellen, der Unterschied zwischen EPI-200 und NHEK-Zellen war statistisch signifikant. Dabei bleibt jedoch zu beachten, dass die Aktivitäten aus intakten Zellen auf das zelluläre Gesamtprotein abgeglichen wurden, während die Aktivitäten in humaner Haut nur auf das zytosolische Protein bezogen wurden. Diese Tatsache erklärt wahrscheinlich die geringfügigen Unterschiede in den mittleren GST-Aktivitäten zwischen den verschiedenen Systemen. Entgegen der Erwartung ließ sich die GST-Aktivität weder in Monolayer-Keratinozytenkulturen, noch in epidermalen 3D-Äquivalenten durch den AhR-Liganden 3-MC induzieren. Dieser Befund deckt sich mit einer bereits 2001 veröffentlichten Studie, in der die basale GST-Aktivität in NCTC 2544-Zellen durch 3-MC ebenfalls nicht induzierbar war (Gelardi *et al.*, 2001). Dies könnte durch die bereits hohe basale GST-Aktivität erklärt werden.

Humane Haut und alternative *in vitro* Modelle (Publikation 2.2) besitzen GST-Aktivitäten im geringen nanomolaren Bereich (20 – 60 ng/min/mg), was im Vergleich zur Leber, dem wichtigsten Organ für Fremdstoffmetabolismus und Detoxifikation des Körpers, welches etwa 3 ng/min/mg GST-Aktivität aufweist (Pacifici *et al.*, 1988) relativ hoch ist. Dabei wurde die GST von allen untersuchten Enzymen als das Phase 2 Enzym in der Haut mit den höchsten Konjugationsraten identifiziert. Aus diesem Grund repräsentierten alle getesteten *in vitro* Modelle den GST-Metabolismus von *ex vivo* humaner Haut gut. Da GSTs auch eine wichtige Rolle im Metabolismus des genotoxischen AhR-Liganden B(a)P spielen, wurde in Publikation 2.3 weiterhin untersucht, ob EPI-200-Modelle in der Lage sind, B(a)P zu metabolisieren. Die dominante GST-Isoform in der Haut, GST-P (Zhang *et al.*, 2002) ist fast ausschließlich für die Detoxifikation des ultimativen B(a)P-Metaboliten 7,8-Dihydrodiol-9,10-Epoxids verantwortlich. In unserem Versuchsaufbau induzierte B(a)P die GST-Aktivität in EPI-200-Modellen, allerdings konnte die statistische Signifikanz nicht berechnet werden, da nur Werte aus Duplikaten vorlagen. Dennoch kann aus diesen Befunden der Schluss gezogen werden, dass EPI-200-Modelle genügend metabolische Kapazität besitzen, um

B(a)P zu metabolisieren und Substanzen auf ihr genotoxisches Potential zu testen, ohne dass eine weitere externe Zugabe von Enzymen, wie z.B. dem S9-Mix, erforderlich ist. Dabei sind die metabolischen Raten der EPI-200-Modelle mit denen der humanen Haut vergleichbar.

Ein weiteres in Publikation 2.2 untersuchtes AhR-abhängiges Phase 2 Enzym ist die UGT. Es gibt in der Literatur nur wenige Indizien für UGT-Aktivität in der Haut. Allerdings zeigen die Berichte über Indolylessigsäure-Glucuronide und die Bildung von Triclosan-Glucuroniden, dass UGT-Aktivität in der Haut vorhanden sein muss (Ademola *et al.*, 1993; Moss *et al.*, 2000). Unsere Daten aus Publikation 2.2 untermauern diese Befunde, indem wir UGT-Aktivität in der mikrosomalen Fraktion humaner *ex vivo* Haut identifizieren konnten. Die UGT-Aktivitäten von EPI-200-Mikrosomen waren vergleichbar mit denen aus Haut-Präparationen, was darauf hindeutet, dass sie die menschliche Haut in dieser Hinsicht gut widerspiegeln. Erstaunlicherweise betrug die Fähigkeit der menschlichen Haut, Fremdstoffe zu glucuronidieren, sogar ca. 50 % der UGT-Rate von humanen Lebermikrosomen. Basale UGT-Aktivitäten in HaCaT-, NCTC- und NHEK-*Monolayer*-Zellkulturen befanden sich im Bereich der EPI-200 Mikrosomen. Sowohl *in vitro* Keratinozyten als *Monolayer*-Kulturen, als auch epidermale 3D-Äquivalente repräsentieren also die UGT-Aktivität von humaner *ex vivo* Haut sehr gut.

In früheren Publikationen wurde die Induzierbarkeit von UGT mRNS durch den AhR-Liganden 3-MC in der Haut und in Hautzellen von verschiedenen Spezies gezeigt (ausführlich zusammengefasst in Oesch *et al.*, 2007). In denen zu Publikation 2.2 durchgeführten Experimenten konnten wir jedoch in keinem der untersuchten Modelle eine UGT-Induktion nach 3-MC feststellen. Diese Diskrepanz könnte daran liegen, dass bisher mRNS Analysen durchgeführt wurden, wir jedoch Enzymaktivität gemessen haben. Für CYP1A1 ist bekannt, dass diese beiden Endpunkte nicht immer gut korrelieren (Swanson, 2004; Svensson, 2009), das könnte auch hier eine Erklärung bieten.

Obwohl kein AhR-abhängiges Phase 2 Enzym, haben wir auch die NAT in Publikation 2.2 untersucht. Unsere Analysen bestätigen frühere Studien, die fanden, dass NAT in *ex vivo* Haut basal exprimiert wird (Kawakubo *et al.*, 1990; Kawakubo *et al.*, 2000). Des

Weiteren konnten wir auch in allen untersuchten *in vitro* Modellen NAT-Aktivitäten im unteren nanomolaren Bereich messen und belegen damit, dass im Bezug auf dieses Phase 2 Enzym auch *Monolayer*-Zellkulturen den Metabolismus der menschlichen Haut gut nachstellen.

3.1.2 Rolle des AhRR in der fehlenden Induzierbarkeit von primären Fibroblasten

Seit einem Jahrzehnt besteht bereits das Dogma, dass der AhRR den AhR-abhängigen Fremdstoffmetabolismus in einigen Zelltypen, darunter Fibroblasten, reprimiert (zusammengefasst in Haarmann-Stemmann and Abel, 2006; Hahn *et al.*, 2009). Da diese Annahme hauptsächlich auf Untersuchungen auf transkriptioneller Ebene basiert, haben wir in Publikation 2.4 dieses Dogma in primären adulten normalen humanen dermalen Fibroblasten (NHDF) von 25 verschiedenen weiblichen Donoren überprüft. Diese Neubetrachtung der AhRR-Hypothese offenbarte, dass zumindest in NHDF der AhRR nicht für die AhR-abhängige CYP-Aktivität verantwortlich ist. Dennoch sind unsere Daten in Einklang mit der aktuellen Literatur, sie erweitern die bisherige Daten-lage lediglich um die Erkenntnisse aus Untersuchungen an 25 adulten humanen Spendern, sowie die Analyse des funktionellen Endpunktes der CYP-Aktivität, die bisher im Bezug auf den AhRR noch nicht untersucht wurde. Unsere Ergebnisse zeigen zum einen, dass die Genexpression der drei wichtigsten Komponenten des AhR-Signalwegs, AhR, ARNT und AhRR, in NHDFs aller getesteter Individuen jeweils etwa in der gleichen Größenordnung liegt, wobei starke interindividuelle Unterschiede auf-traten. Im Gegensatz zu Befunden aus der Literatur, die in humanen Fibroblasten etwa zehnmal mehr AhRR identifizieren konnten als in Keratinozyten (Akintobi *et al.*, 2007), zeigen unsere Daten aber auch, dass der AhRR in NHDFs, AhRR-profizienten Maus-fibroblasten (MEF$^{+/+}$) und NHEKs in der gleichen niedrigen Größenordnung exprimiert wird. Diese Diskrepanz rührt wahrscheinlich von interindividuellen Unterschieden her, zumal aus der Literatur nicht hervorgeht, ob die Studie an einem oder mehreren Individuen durchgeführt wurde, oder welches Geschlecht die Zelldonoren hatten. Des Weiteren, in Übereinstimmung mit den Arbeiten von Hosoya (Hosoya *et al.*, 2008), die 25-fach induzierte CYP1A1 Induktion nach B(a)P- Behandlung in murinen

Hautfibroblasten gefunden haben, war die CYP1A1-Expression in NHDF durch B(a)P in unserer Studie bis zu achtfach induziert. Die marginalen Unterschiede in der Größenordnung der Induktion lassen sich auf verschiedene Weisen erklären: Zum einen wurden unterschiedliche B(a)P-Konzentrationen verwendet (Hosaya: 1 µM, Publikation 2.4: 250 nM), zum anderen unterschiedliche Inkubationszeiten (24 vs. 48 Std.). Des Weiteren können wir nicht ausschließen, dass die Spezies (Maus vs. Mensch) und das Alter der Fibroblasten eine Rolle spielen, denn in der Studie von Hosaya wurde Haut von neugeborenen Mäusen verwendet, während es sich bei unseren Zellen um adulte Donoren von 20-60 Jahren handelte. Zudem können Unterschiede schon alleine aus der Hautregion resultieren, aus der die Zellen isoliert wurden (Chang *et al.*, 2002). Im Gegensatz dazu gibt es eine weitere Studie (Gradin *et al.*, 1993), die in Fibroblasten keine CYP1A1-Induktion nach Belastung mit dem AhR-Liganden 2,3,7,8-Tetrachloro-dibenzofuran (TCDF) beobachten konnten. Dies ist jedoch wahrscheinlich auf die Methode der Detektion zurückzuführen. In der 1993er Studie wurde die Methode des Northern Blot verwendet, während wir in dieser Publikation die wesentlich sensitivere Methodik der quantitativen *real-time* RT-PCR angewandt haben. Um die Rolle des AhRR bei der CYP1A1-Induktion in Fibroblasten näher zu charakterisieren, wurden AhRR-profiziente (MEF$^{+/+}$) und AhRR-defiziente (MEF$^{-/-}$) Mausfibroblasten (MEFs) in die Studie miteinbezogen. Die beobachteten CYP1A1-Induktionen in MEFs$^{-/-}$ sind im Einklang mit der Literatur (Hosoya *et al.*, 2008), wobei auch hier Unterschiede in der Größenordnung durch verschiedene Induktoren (B(a)P vs. 3-MC), sowie Inkubations-zeit oder Zelltyp zustande gekommen sein könnten. Unsere Analysen offenbaren, dass, trotz signifikanter CYP1A1-Geninduktion in MEFs$^{-/-}$ um das etwa 3000-fache, die tatsächlichen Transkripte/10^4 Kopien β-Actin äußerst gering waren, nämlich NHDF: 0,01 / 10^4, MEF$^{-/-}$: 0,015 / 10^4 β-Actin. Da bisher in der Literatur die Kopienzahlen des AhRR nicht beschrieben wurden, können wir diese Ergebnisse nicht mit Daten aus anderen Studien vergleichen. Überraschenderweise exprimieren primäre Keratinozyten den AhRR in ähnlich niedrigen Quantitäten (0,06 Kopien / 10^4 β-Actin). Um die funktionelle Relevanz des niedrig exprimierten AhRR auf die Aktivierung des AhR-Signalwegs zu untersuchen, wurden in Publikation 2.4 sowohl die basalen, als auch die induzierten CYP1A1-Expressionen mit der entsprechenden AhRR-Expression korrelieren. Die Korrelationskoeffizienten von 0,02 und 0,008 lassen keinen Zusam-

menhang vermuten. Diese Erkenntnis wird durch Literaturdaten bestätigt, in denen – ebenfalls im Widerspruch zu landläufigen AhRR Hypothese - in neun verschiedenen Tumorzelllinien ebenfalls keine Korrelation der AhRR Expression mit der CYP1A1-Induzierbarkeit verzeichnet werden konnte (Tsuchiya *et al.*, 2003). Diese Daten deuten darauf hin, dass der AhRR im physiologischen Gleichgewicht der Zelle nicht an der Aktivierbarkeit des AhR-Signalwegs beteiligt zu sein scheint. Eine Annahme, die durch unsere funktionellen Daten bestätigt wird, denn des Weiteren haben wir die CYP1-Enzymaktivität mittels EROD-Assay in NHDFs, MEFs$^{+/+}$ und MEFs$^{-/-}$ ermittelt, wobei uns die gut induzierbare Keratinozytenzelllinie NCTC 2455 als Positivkontrolle diente. Diese Analysen machen deutlich, dass die Kopienzahlen von CYP1A1 (bis zu 10 Kopien hCYP1A1/10^4 β-Actin) in NHDFs keine messbare EROD-Aktivität über dem *limit of quantification* (LOQ) ergibt. Das Gleiche gilt für MEFs$^{+/+}$, während MEFs$^{-/-}$ mit 1 pmol / min / mg Ethoxyresorufin bei bis zu 1 µg AhR-Ligand Aktivitäten erreichen, die marginal über dem LOQ liegen. Besonders im Vergleich zu der als Positivkontrolle mitgeführten Keratinozytenzellinie NCTC 2455, die bei 100-200 pmol /min /mg Ethoxyresorufin liegen, ist diese Aktivität als sehr gering und unserer Meinung nach als nicht von physiologischer Relevanz einzuschätzen.

In vorhergehenden Arbeiten konnte ein Zusammenhang der AhRR-Funktion mit HDAC Aktivität identifiziert werden (Haarmann-Stemmann *et al.*, 2007; Oshima *et al.*, 2007). Aus diesem Grund behandelten wir verschiedene NHDF-Individuen mit dem HDAC-Inhibitor TSA sowie in Kobelastung mit B(a)P. Wir konnten die bisherige Datenlage reproduzieren und beobachteten eine starke Induktion von CYP1A1-mRNS nach TSA-Exposition, die in unserer Studie mit einem Rückgang der AhRR-mRNS-Expression einherging. Weitere funktionelle Analysen mittels EROD-Assay zeigten jedoch, dass der Substratumsatz auch hier nicht über den Level des LOQ hinausging und daher nicht in physiologisch relevante CYP1-Aktivität umgesetzt wurde.

Zusammengefasst konnten wir in unserer Studie zur Neuevaluierung der „AhRR-Hypothese" die bisherige Literatur reproduzieren, da wir zeigen konnten, dass der AhRR in NHDFs exprimiert wird, die CYP1A1-Expression auf mRNS-Ebene in diesen Zellen über AhR-Liganden induzierbar ist und dass HDAC-Inhibition in einer verringerten AhRR- und induzierter CYP1A1-Expression resultiert. Wir konnten jedoch auch zeigen, dass die interindividuellen Unterschiede in der CYP1A1-Induktion sehr

groß sind und dass die Geninduktion auf sehr geringem CYP1A1-Expressionsniveau nicht in physiologisch relevante CYP1-Enzymaktivität umgesetzt wird. Demnach stimmen wir zu, dass CYP-Aktivität in primären humanen Fibroblasten reprimiert ist, unsere Daten geben jedoch starke Anhaltspunkte, dass dieses Phänomen nicht auf die reprimierende Wirkung des AhRR, sondern auf einen bisher noch nicht identifizierten anderen Faktor zurückzuführen ist.

In der Praxis ist dieser Befund nicht nur von Relevanz für umweltinduzierte Hauterkrankungen, sondern auch für die therapeutische Intervention, da AhR-modifizierende Substanzen bereits sowohl als Sonnenschutz, als auch als Therapeutika im Einsatz sind. So enthält zum Beispiel der in der klassischen Psoriasis eingesetzte Teer eine Anzahl verschiedener AhR-Agonisten (Goeckerman W, 1931) und erst kürzlich konnte das Fungizid Kentoconazol als AhR-Induktor identifiziert werden (Tsuji *et al.*, 2011). Um die Effekte und Nebenwirkungen solcher Substanzen auf verschiedene Hautzellen auf molekularer Ebene zu verstehen, ist das Wissen über die Regulation des AhR-Signalwegs essenziell, wozu diese Arbeit beiträgt.

3.1.3   Rolle des AhR in der durch MMP-1 mediierten extrinsischen Hautalterung

Zwei Umweltnoxen, die zur beschleunigten Hautalterung beim Menschen führen, sind gut beschrieben: die Exposition gegenüber UV-Strahlung (Lichtalterung; Gilchrest BA und Krutmann J, 2006; Berneburg *et al.*, 2000; Fisher und Voorhees, 1998) und die Exposition gegenüber PAK-enthaltendem Zigarettenrauch (Morita, 2007; Frances, 1998). Es gibt einen molekularen Signalweg, der sowohl durch UV-Strahlung (zusammengefasst in Rannug und Fritsche, 2006), als auch durch PAKs (Denison und Nagy, 2003) aktiviert wird: die AhR-Signalkaskade. Ob die Aktivierung des AhR durch UVB und PAK tatsächlich zu beschleunigter Alterung führt, wurde vor den in Publikation 2.5 durchgeführten Studien noch nicht untersucht. Darin zeigen wir erstmals, dass der AhR über die Induktion von MMP-1 in primären humanen Keratinozyten *in vitro*, sowie in Maus- und humaner Haut *in vivo* zu extrinsischen Hautalterungsprozessen beiträgt. Mit dieser Publikation stellen wir die Hypothese auf, dass der AhR als Sensor für

Umweltnoxen dient, die in der extrinsischen Hautalterung eine Rolle spielen. Diese Funktion muss nicht auf die in dieser Studie untersuchten Parameter UVB-Bestrahlung oder Belastung mit PAKs beschränkt sein, sondern könnte auch atmosphärisches Ozon miteinbeziehen, obwohl die Relevanz von Ozonbelastung für die Alterung der Haut noch bestätigt werden muss (Afaq und Mukhtar, 2001).

Bislang schien der Mechanismus der MMP-1 Aktivierung durch UV-Strahlung bereits gut charakterisiert zu sein. Zum einen führt UV-Bestrahlung in der Haut zu DNS-Schäden, die zur Freisetzung von MMP-1 beitragen (Dong *et al.*, 2008). Zum anderen wurden Reaktive-Sauerstoff-Spezies (ROS) als Hauptursache für Schädigungen der Dermis nach UV-Bestrahlung identifiziert. Diese ROS induzieren die Signaltransduktion der Mitogen-aktivierten-Protein-Kinase (MAPK), welches letztendlich in der Induktion des Transkriptionsfaktors AP-1 resultiert (Fisher und Voorhees, 1998; Rittie und Fisher, 2002). AP-1 aktiviert dann direkt entsprechende Elemente in der MMP-1 Promoterregion uns führt somit zur Induktion des Gens (Vincenti *et al.*, 1996).

Mit Publikation 2.5 ergänzen wir diese bisherigen Erkenntnisse, indem wir zeigen, dass die MMP-1-Induktion durch UVB in primären Keratinozyten vom zytoplasmatischen AhR abhängig ist. Zwei Beobachtungen unterstützen diese Schlussfolgerung: Zum einen ist die Induktion von MMP-1 in NHEKs *in vitro* und in humaner Haut *in vivo* durch AhR-Antagonisten hemmbar und zum anderen ist MMP-13 in der Haut von AhR-defizienten Mäusen *in vivo* durch UVB-Bestrahlung nicht induzierbar. Der für diese Effekte verantwortliche Mechanismus ist die Bildung von Tryptophanphotoprodukten, wie z.B. FICZ, welches in NHEKs zu ähnlicher MMP-1-Aufregulierung führt wie UVB (unpublizierte Daten). Die Beteiligung des AhR an der MMP-1-Induktion konnte außerdem durch Applikation des spezifischen AhR-Liganden B(a)P bestätigt werden. Schon 2004 wurde eine mögliche Beteiligung des AhR an der MMP-1-Induktion be-schrieben (Murphy *et al.*, 2004). In dieser Studie wurde allerdings der nicht-matabolisierbare und daher persistente AhR-Ligand TCDD untersucht. Abgesehen von der CYP1A1-Induktion durch TCDD unterscheiden sich die Effekte dieses Liganden stark von physiologisch relevanteren, kurzlebigeren AhR-Liganden, was auf eine unter-schiedliche Kinetik und die fehlende Metabolisierung von TCDD zurückzuführen ist (Matikainen *et al.*, 2001; Gassmann *et al.*, 2010; Laub *et al.*, 2010). Wir zeigen in

Publikation 2.5 zudem erstmals, dass die AhR-abhängige MMP-1-Induktion durch UVB oder B(a)P durch die src-EGFR-MEK-Signalkaskade mediiert wird. Demnach erfolgt die MMP-1-Induktion nicht durch nukleäre Translokation des AhR, Dimerisierung mit ARNT und Bindung an ein XRE im MMP-1-Promoter, wie es für klassische AhR-Zielgene wie CYP1A1 beschrieben wurde, sondern folgt dem von uns bereits für COX-2 beschriebenen Weg, an dem die MAPK-Signalkaskade ebenfalls beteiligt ist. Direkte Anhaltspunkte aus der Literatur unterstützen diese Befunde. So ist gut beschrieben, dass kleine Moleküle mit bestimmten strukturellen Charakteristika die Aktivierung des AhR kompetitiv inhibieren (Henry *et al.*, 1999). Das Soja-Isoflavon Genistein ist eines dieser Moleküle. Es reduziert die UVB-induzierte c-fos- und c-jun-Genexpression in der Maushaut (Wang *et al.*, 1998), die UV-induzierte AP-1-DNS-Bindung in einer humanen Keratinozytenzelllinie (Maziere *et al.*, 2000) und kann vor durch UV-Bestrahlung verursachter Hautalterung in Mäusen und Menschen schützen (Wei *et al.*, 2003; Kang *et al.*, 2003). Ein weiteres Beispiel für eine solche Substanz ist Luteolin, ein Flavon aus Sellerie und grüner Paprika, das die B(a)P-abhängige AhR-Aktivierung inhibieren kann (Zhang *et al.*, 2003; Bothe *et al.*, 2010). Zusätzlich inhibiert es in humanen Hautfibroblasten die MMP-1-Expression (Kim *et al.*, 2004) und Aktivität (Sim *et al.*, 2007). Des Weiteren ist das Flavonol Quercitin zu nennen, welches in Zwiebeln, Äpfeln, Broccoli und grünen Bohnen vorkommt und die B(a)P-abhängige AhR-Aktivierung antagonisieren kann (Zhang *et al.*, 2003). Quercitin inhibiert außerdem die TPA-induzierte MMP-1-Expression in humanen dermalen Fibroblasten durch Interaktion mit der MAP-Kinase ERK1/2 (Lim and Kim, 2007), welche über UV-Bestrahlung (Bode and Dong, 2003) zumindest in Keratinozyten über den AhR-Signalweg aktiviert werden kann (Fritsche *et al.*, 2007). Unsere Befunde aus Publikation 2.5, dass AhR-Aktivierung an der UVB-induzierten MMP-1-Induktion beteiligt ist, liefern eine gemeinsame mechanistische Erklärung für die adversen Effekte, die durch diese Noxen vermittelt werden. Sie zeigen aber auch die Möglichkeit auf, dass bereits bekannte oder neu zu synthetisierende Moleküle, die mit der AhR-Signalkaskade interagieren, für den Schutz der Haut gegenüber UV-induzierter Alterung nützlich sein könnten und bieten damit einen wichtigen Ansatzpunkt für künftige präventivmedizinische Maßnahmen zum UV-Schutz. Ein Beispiel dafür sind die Grünteecatechine Epigallocatechin (EGC) und Epigallocatechin Gallat (EGCG). Diese beiden Moleküle sind in der Lage die UVB-

abhängige AhR-Funktion zu hemmen, indem sie an Hsp90, ein Chaperon des AhR, binden und somit die transkriptionelle Aktivität des AhR verhindern (Palermo *et al.*, 2005). Supplementierung mit Polyphenolen aus dem grünen Tee verbessern den Zustand der menschlichen Haut nach sechs bis zwölf Monaten (Janjua *et al.*, 2009) und EGCG inhibiert die Destruktion und Kollagenase-Induktion nach UVB-Bestrahlung in Fibroblasten (Bae *et al.*, 2008). Bislang wurden diese positiven Effekte auf die Hauthomöostase vor allem den antioxidativen Eigenschaften der Flavonoide zuge-schrieben, die Inhibierung der AhR-Signalkaskade könnte jedoch in diesem Zusammenhang ebenfalls eine Rolle spielen.

Zusammenfassend konnte in dieser Dissertation mit Publikation 2.5 erstmals gezeigt werden, dass der AhR als zytoplasmatischer molekularer Sensor dient, der über die EGFR-MAPK-Signalkaskade die Induktion von MMP-1 in der Haut als Antwort auf diverse Umwelteinflüsse wie UVB und PAKs mediiert.

In diesem Zusammenhang könnte die Antagonisierung des AhR nicht nur vor Licht- und Zigarettenrauch-induzierter Hautalterung schützen, sondern auch vor der erst kürzlich beschriebenen alternspromovierenden Aktivität von Feinstäuben, die in Abgasen von Autos enthalten sind (Vierkotter *et al.*, 2010) und auf ihrer Oberfläche oftmals mit PAKs überzogen sind (Park und Kim, 2005; Vallius *et al.*, 2005). Über Inhalation aufgenommene Partikel erreichen die meisten Organe des Körper (Kreyling *et al.*, 2009) und erst 2010 konnte nachgewiesen werden, dass inhalierte Partikel von Dieselabgasen den AhR-Signalweg nicht nur in der Rattenlunge, sondern auch in extra-pulmonalen Organen aktivieren können (van Berlo D. *et al.*, 2010). Aus diesen Beobachtungen lässt sich die Hypothese ableiten, dass diese PAK-überzogenen Partikel auch zur Alterung anderer Organe wie z.B. dem kardiovaskulären System beitragen könnten (Schikowski *et al.*, 2007). Ob der in dieser Dissertation (Publikation 2.5) neu identifizierte Alterns-Signalweg über den AhR auch eine funktionelle Relevanz für das Altern anderer Organe als der Haut hat, bleibt in künftigen Studien näher zu untersuchen.

3.2   Der protektive Effekt von Östrogen auf die Hauthomöostase

Der Zusammenhang zwischen Störungen des Hormonhaushaltes und Alterungsprozessen wird besonders bei Frauen in der Menopause offensichtlich. Ähnlich wie bei dermalen Veränderungen der extrinsischen Hautalterung durch UV-Strahlung gehen die postmenopausalen Hautveränderungen mit Faltenbildung und Reduzierung der Hautdicke einher und deuten auf eine Störung der ECM-Homöostase hin. Schon lange ist bekannt, dass Östrogen (E_2) sowohl die Hautdicke und den Feuchtigkeitsgehalt der Haut erhöht, als auch die Faltenbildung vermindert (Sator *et al.*, 2001; Sator *et al.*, 2007). Diese positiven Effekte des Östrogens werden vor allem durch den Schutz vor Verlust des Typ I Kollagens und der Neusynthese von Kollagen vermittelt (Castelo-Branco *et al.*, 1992). Dazu kommt, dass Östrogene den Gehalt an dermalen Glycosaminglykanen erhöhen, welche ihrerseits einen positiven Effekt auf Hautdicke und -Feuchtigkeit haben (Grosman *et al.*, 1971; Uzuka *et al.*, 1981; Bentley *et al.*, 1986). Ein weiteres Puzzelteil bei den postmenopausalen Alterungsprozessen der Haut scheint der Verlust von Hyaluronsäure (HA) zu sein. In männlichen Mäusen erhöhte der Einsatz von Östrogen den HA-Gehalt der Haut (Sobel and Cohen, 1970). Zusätzlich konnten Experimente an ovarioektomierten (OVX) Ratten zeigen, dass ein kausaler Zusammenhang zwischen Östrogen, dem Phänotyp der Hautalterung und UVB-Bestrahlung besteht (Tsukahara *et al.*, 2001). Diese Tiere entwickelten typische Symptome der Hautalterung, die durch UVB-Bestrahlung noch beschleunigt werden, was auf eine mögliche antagonistische Wirkung von Östrogen auf die Destruktion der Hauthomöostase hinweist. Dennoch fehlten bislang systematische Tierstudien, die den regulatorischen Effekt von Östrogen auf die dermale HA, HA-Synthase (HAS)-Isoformen, HA-Rezeptoren und Hyaluronidasen in weiblichen Mäusen untersuchen und wichtiger noch die zugrunde liegenden molekularen Mechanismen aufklären. So ist bis heute nichts darüber bekannt, auf welche Weise E_2 den Gehalt und die Funktion von HA und dem Proteoglykan Versikan in der Haut reguliert. Daher war das zugrunde liegende Ziel von Publikation 2.6 die Veränderungen von HA, HAS-Isoformen, Hyaluronidasen, HA-Rezeptoren und des HA-bindenden Proteoglykans Versikan im Kontext der Lichtalterung und der E_2-Antwort zu untersuchen.

Die Publikation zeigt deutlich, dass der Verlust von endogenem E_2 in haarlosen SKH-1 Mäusen zu einem Verlust der dermalen HA führt und dass das Fehlen von E_2 den Effekt

nach UVB-Bestrahlung noch verstärkt. Der Gehalt an Versikan hingegen wurde während der Lichtalterung erhöht, ein Effekt, der durch Östrogenbehandlung noch verstärkt wurde. Die Daten aus Publikation 2.6 zeigen, dass das molekulare Zielmolekül, welches die E_2-Antwort mediiert, in bestrahlter und unbestrahlter Haut ein anderes ist. In bestrahlter Haut kommt es zu einer Änderung der HAS3 und Hyl2 Expression, während in unbestrahlter Haut HAS1 und HAS3 moduliert sind. HAS3 scheint ein besonders wichtiger E_2-abhängiger Regulator der dermalen HA-Homöostase in intrinsischer und extrinsischer Hautalterung zu sein, da es in beiden Prozessen verändert ist. Östrogen mediiert Veränderungen in der Genexpression durch die Aktivierung intrazellulärer E_2-Rezeptoren (ER) −α und −β, welche nach Ligandenbindung in den Nukleus translozieren und dort die Expression von Genen mit *estrogenic regulatory elements* (ERE) in ihrer Promoterregion regulieren. Zusätzlich gibt es nicht genomische E_2-Effekte, die durch den GPR20-Signalweg vermittelt werden (Hall *et al.*, 2001). Es konnte gezeigt werden, dass sowohl ER α, als auch ER β in der Haut exprimiert werden und dass beide auch in den Fibroblasten der Haut zu finden sind (Verdier-Sevrain *et al.*, 2006). Im Verhältnis der beiden ER-Subtypen gibt es sowohl im Vergleich von verschiedenen Organen, als auch in Abhängigkeit vom Alter und der untersuchten Spezies eine hohe Variabilität (Verdier-Sevrain *et al.*, 2004; Haczynski *et al.*, 2002). In Publikation 2.6 wurde ER α in den Hautbiopsien von SKH-1 Mäusen hoch exprimiert, während ER β mittels quantitativer PCR nicht detektierbar war. Aus diesem Grund wurden die oben genannten Effekte von E_2 auf die dermale HA und Versikan während der Lichtalterung dem ER α zugeschrieben, obwohl nicht-genomische Effekte auf der Basis der vorliegenden Ergebnisse nicht ausgeschlossen werden können.

Da die *in vivo* Experimente in SKH-1 Mäusen ergeben haben, dass die Induktion von HAS3 und Versikan mRNS wahrscheinlich eine Schlüsselrolle in der E_2-Antwort während der Lichtalterung spielen, wurde weiterhin untersucht, ob E_2 direkt in die Regulation der involvierten Gene eingreifen kann. Da E_2 die HAS1- und Versikan-Expression in *in vitro* Fibroblasten-Kulturen inhibiert, während andere HA-assoziierte Gene keine Expressionsunterschiede zeigten, konnte ein direkter transkriptioneller Effekt von Östrogen auf die HAS3- und Versikan-Genexpression ausgeschlossen werden. Alternativ ist die Induktion von parakrinen Faktoren durch E_2, die nachfolgend die Expression von HAS3 und Versikan induzieren, denkbar. Tatsächlich kann

Östrogen *in vivo* über parakrine Mechanismen auf die ECM einwirken, denn der postmenopausale Verlust von Kollagen geht mit einem Verlust der E_2-mediierten Expression des *Transforming Growth Faktor* (TGF) β1 einher (Ashcroft *et al.*, 1997).

In Publikation 2.6. konnte gezeigt werden, dass das Expressionsprofil von EGF parallel mit den Veränderungen der HA-Matrix sowohl in lichtgealterter, als auch in nicht bestrahlter Haut verlief: so wurde EGF durch OVX reduziert und durch E_2 induziert. Des Weiteren ist von EGF bekannt, dass es die Expression von HAS2 und HAS3 in Keratinozyten induziert und dadurch sowohl proprolifertiv, als auch promigratorisch wirkt (Pienimaki *et al.*, 2001; Pasonen-Seppanen *et al.*, 2003). In *in vitro* Experimenten konnten wir zeigen, dass Östrogen in der Tat die EGF-Expression in Keratinozyten induziert, nicht aber in Fibroblasten. Nachfolgend stimulierte EGF, übereinstimmend mit früheren Berichten (Heldin *et al.*, 1989; Yamada *et al.*, 2004), die HAS3 und Versikan Expression in humanen Hautfibroblasten. Aus diesen Befunden schließen wir, dass E_2 in Keratinozyten die Freisetzung von EGF stimuliert, welches nachfolgend die HAS3- und Versikan-Expression in dermalen Fibroblasten induziert. Diese Befunde sind im Einklang mit Beobachtungen aus anderen biologischen Systemen, dass EGF in verschiedene E_2-induzierte Prozesse eingebunden ist (Ignar-Trowbridge *et al.*, 1992; Nelson *et al.*, 1991), bzw. in der Lage ist, die Östrogen-Antwort zu imitieren (Gehm *et al.*, 2000).

Interessanterweise konnte in der Vergangenheit gezeigt werden, dass phänotypisch gealterte Fibroblasten die HA-Synthese reduzieren und diese auch nach Stimulation mit Wachstumsfaktoren nicht hochregulieren (Webber *et al.*, 2009). Da EGF für die TGF β1 induzierte HA-Synthese benötigt wird (Simpson *et al.*, 2009; Simpson *et al.*, 2010), scheint dieses Signalmolekül daran beteiligt zu sein. Außerdem stimuliert EGF die Proliferation in Fibroblasten, welche in gealterten Fibroblasten durch die Herabregulierung des EGFR abnimmt (Shiraha *et al.*, 2000; Reenstra *et al.*, 1993). Dem zu Folge handelt es sich bei EGF um einen Wachstumsfaktor, der dem Alternsphänotyp von dermalen Fibroblasten entgegenwirkt. Daher ist es wahrscheinlich, dass die Induktion von EGF in Keratinozyten durch E_2 und parakrine Stimulation von HA und Versikan in dermalen Fibroblasten in der Dämpfung der Alternseffekte in Fibroblasten und der Haut durch E_2 beteiligt ist.

Ein weiterer Befund aus Publikation 2.6 ist, dass Östrogen in der Lage ist, den Gehalt an inflammatorischen Makrophagen und COX-2 in der Haut deutlich zu reduzieren. Dieser entzündungshemmende Effekt von E_2 könnte ebenfalls durch EGF-Freisetzung mediiert werden, denn die COX-2-Expression wurde in Fibroblasten durch EGF heruntergesetzt und die Entzündungsantwort war in UVB-bestrahlten OVX Mäusen am höchsten.

Da angenommen wird, dass die supramolekulare Struktur der die Zellen in der Dermis umgebenden Matrix bestimmt, ob diese Umgebung homöostatisch (Stern und Maibach, 2008), proinflammatorisch (de La Motte *et al.*, 1999) oder promigratorisch (Evanko *et al.*, 1999) wirkt, muss in künftigen Studien der Frage nachgegangen werden, ob das Verhältnis von HA zu Versikan eine Rolle in der Entzündungsantwort nach UVB-Bestrahlung spielt.

Zusammenfassend konnten wir in Publikation 2.6 zeigen, dass Östrogen in der Lichtalterung ein wichtiger Regulator des dermalen HA- und Versikan-Gehaltes ist, welches zumindest zum Teil durch die parakrine Freisetzung von EGF durch Keratino-zyten zustande kommt. Als Konsequenz daraus erhöht E_2 die Proliferation und hemmt die Entzündung. Dadurch werden in Publikation 2.6 neue molekulare Zielmoleküle von Östrogen identifiziert, welche die protektive Funktion dieses Hormons auf die dermale Matrix während extrinsischer Alterungsprozesse mediiert.

Ob der Arylhydrocarbon Rezeptor ebenfalls in diesem Prozess involviert ist, bleibt offen für weitere Untersuchungen. Aus Studien in humanen epidermalen Keratinozyten gibt es allerdings Befunde, dass in diesen Zellen EGF zu einer verminderten CYP1A1 Induktion sowohl auf mRNS, als auch auf Enzymebene nach Belastung mit TCDD führt (Sutter *et al.*, 2009). Diese Beobachtung stellt einen Bezug zwischen AhR- und EGFR-Signalweg her, der in die gleiche funktionelle Richtung deutet, denn Fremdstoffmetabolismus der Phase 1 durch CYP1A1 ist mit der Generierung von ROS assoziiert und kann somit zur vorzeitigen Hautalterung beitragen. Zudem konnte die Arbeitsgruppe um Fritsche zeigen, dass eine Aktivierung der AhR-Signalkaskade über c-src auch zu einer Aktivierung der EGFR-Signalkaskade und somit zur Transkription von COX-2 führt (Fritsche *et al.*, 2007), ein Phase 1 Enzym, welches vorwiegend

Entzündungsprozesse mediiert und ebenfalls mit Alterungsprozessen in Verbindung gebracht werden kann.

Inwiefern jedoch eine direkte Interaktion von AhR und ER in der extrinsischen Hautalterung von Bedeutung ist, ist bis heute noch nicht eingehend untersucht worden. Es wird jedoch schon lange ein inhibitorischer Crosstalk zwischen AhR- und ER-Signaltransduktion vermutet, da eine chronische Belastung von Ratten mit dem AhR-Liganden TCDD die Inzidenz von Mamma- und Uteruskarzinomen senkt (Kociba *et al.*, 1978). Mittlerweile zeigt eine große Anzahl von Studien die Inhibierung der Expression E_2-abhängiger Gene durch einen aktivierten AhR (Safe und Wormke, 2003). Der diesen Befunden zugrunde liegende molekulare Mechanismus ist bis zum heutigen Tag ungeklärt, es existieren aber verschiedene Hypothesen zur AhR/ER Interaktion (für ausführliche Übersichtsarbeiten siehe Matthews und Gustafsson, 2006; Pocar *et al.*, 2005). So wird eine direkte Inhibierung des ER durch ein aktiviertes AhR/ARNT Heterodimer über die Bindung an inhibitorische XRE in ER-Zielgenen diskutiert. Außerdem benötigen beide Rezeptoren (AhR und ER) zum Teil die gleichen Koaktivatoren, so dass ein aktivierter AhR durch Entzug dieser Kofaktoren zu einer geringeren E_2-Anwort führen kann. Des Weiteren sind die AhR-Zielgene CYP1A1 und 1B1 in der Lage, in die Östrogensynthese einzugreifen und der AhR selbst wirkt als Ubiquitinligase und kann somit zur Degradation des ER beitragen.

Diese Arbeiten deuten darauf hin, dass man in Bezug auf die extrinsische Hautalterung erwarten könnte, dass die Aktivierung des AhR die positiven Effekte des Östrogens auf die ECM antagonisiert. Erste Versuche, die im Rahmen dieser Dissertation dazu durchgeführt wurden, weisen jedoch darauf hin, dass das gewählte Zellsystem von primären Keratinozyten für diese Fragestellung allein nicht geeignet zu sein scheint. Diese Zellen exprimieren beide ER-Subtypen in äußerst geringem Maße und das gesamte E_2-System scheint nicht funktionell zu sein. Um die molekularen Mechanismen der AhR/ER-Interaktion im Bezug auf extrinsische Hautalterung aufzuklären, sind demnach *in vivo* Studien an AhR-defizienten Mäusen, oder aber zumindest Untersuchungen an Vollhautmodellen notwendig.

3.3 Humane *in vitro* Hautmodelle als Alternativmodell zur Untersuchung von exogenen Noxen auf die Haut

Es gibt einen dringenden Bedarf an hoch entwickelten und gut charakterisierten *in vitro* Modellen als Alternative für Tierversuche, um Risiken für die menschliche Gesundheit abschätzen zu können. Dieses gilt nicht nur im Rahmen der neuen EU-Chemikalienverordnung (1907/2007/EG) REACH (Registration, Evaluation and Authorisation of Chemicals), die seit dem 01. Juni 2007 in Kraft ist und sich im Bezug auf *in vivo* Versuche das Prinzip der 3Rs (*refine, reduce, replace*) von Russel und Burch auf die Fahne geschrieben hat (Russel WMS und Burch RL, 1959). Im Rahmen der 7. Änderung der EG-Kosmetik-Richtlinie (76/768/EWG) sind Tierversuche zur Testung von Kosmetika auf Endpunkte wie z.B. Genotoxizität bereits seit 2009 untersagt. Traditionell wurden Tests auf Haut-Verätzungen und –Irritationen mittels des in den 1940er Jahren entwickelten Draize Tests gemessen, bei dem die zu testenden Chemikalien/Kosmetika auf die Haut von Kaninchen aufgetragen wurden (DRAIZE *et al.*, 1948). Inzwischen müssen *in vitro* Hautmodelle, wie sie in dieser Dissertation in den Publikationen 2. 1 – 2. 3 untersucht wurden, den Platz dieses und anderer klassischer *in vivo* Modelle einnehmen. Allerdings ist die metabolische Kompetenz weder von humaner Haut, noch von alternativen *in vitro* Modellen bisher zufriedenstellend charakterisiert. Da die Haut das First-Pass-Organ für viele Chemikalien, darunter auch Kosmetika und Therapeutika ist, ist das aber von essentieller Bedeutung.

Die vorliegende Dissertation trägt in vielerlei Hinsicht dazu bei, funktionelle Reaktionen der Haut auf exogene Noxen besser zu verstehen. So haben wir in Publikation 2.4 zeigen können, dass humane dermale Fibroblasten keine funktionelle CYP1A1 Aktivität aufweisen und dass diese Tatsache nicht durch den AhRR vermittelt ist, wie bisher in der Literatur diskutiert wurde. Des Weiteren konnten wir in Publikation 2.5 den AhR als Sensor für extrinsische Noxen in der Haut identifizieren, der zur Destruktion der ECM beiträgt, indem er die MMP-1-Expression und Aktivität vermittelt. Zum anderen haben wir in den Publikationen 2.1 – 2.3 die fremdstoffmetabolisierenden Kapazitäten von *in vitro* Alternativmodellen im Vergleich zu humaner Haut ausgiebig untersucht und charakterisiert.

Zusammenfassend kommt diese Dissertation zu dem Schluss, dass 3D-Testmodelle wie das in Publikation 2. 1 – 2. 3 untersuchte EPI-200 besonders für die Testung von Chemikalien geeignet sind, da hier im Bezug auf die Phase 1 des Fremdstoffmetabolismus Enzymaktivitäten gefunden werden konnten, die denen in der menschlichen Haut sehr ähnlich sind, vor allem was die Aktivität der Cyclooxygenasen angeht. Des Weiteren konnte vor allem in Publikation 2.3 deutlich gemacht werden, dass die metabolische Kapazität des EPI-200 (hier im Bezug auf GST-Aktivität) ausreicht, auch genotoxische Substanzen zu identifizieren, ohne dass eine Zugabe von metabolischen Supplementen (z.B. S9-Mix) erforderlich ist. Für einige ausgesuchte Fragestellungen könnten auch Studien in *Monolayer*-Zellkulturen in Betracht kommen, insbesondere, wenn Enzyme des Phase 2 Fremdstoffmetabolismus im Fokus des Interesses stehen, denn dieser war in allen untersuchten *in vitro* Modellen (primäre Keratinozyten, NCTCs, HaCaTs, sowie den 3D-Epidermis-Äquivalenten EPI-200) sehr hoch und untereinander vergleichbar. Daher könnten in Abhängigkeit von der Fragestellung auch *Monolayer* Zellkulturen eine schnelle, kostengünstige und nützliche Alternative zu Versuchen in 3D-Epidermis-Äquivalenten bieten. Wie für B(a)P in Publikation 2. 3 gezeigt, wird es jedoch notwendig sein, eine größere Anzahl von Positiv- und Negativsubstanzen im Hinblick auf ihre Metabolisierbarkeit in 3D-Epidermis Äquivalenten und der korrekten Vorhersagbarkeit im Genotoxizitätstest in solchen Modellen zu untersuchen.

4   Zusammenfassung

Die Haut ist als größtes Grenzflächenorgan des menschlichen Körpers einer Vielzahl von exogenen Noxen wie UV-Strahlung, Pharmazeutika und Umweltschadstoffen direkt ausgesetzt. Daher ist es für die Homöostase des Organismus essentiell, dass Hautzellen als ‚First-pass-Organ' für dermale Exposition auf diese extrinsischen Faktoren reagieren können. Sind die Detoxifizierungskapazitäten der Haut erschöpft, resultieren Organpathologien wie Hauttumoren oder vorzeitige Hautalterung. Bei diesen Prozessen spielt der Arylhydrocarbon-Rezeptor (AhR) als intrazellulärer Stresssensor eine zentrale Rolle. Er reguliert den Fremdstoffmetabolismus (FSM), ist an zellulären Signalprozessen beteiligt und seine Überaktivierung wird mit extrinsischer Hauttumor-entstehung sowie Hautalterung assoziiert. Ziel dieser Arbeit war es daher, funktionelle Untersuchungen zur Reaktion der Haut auf exogene Noxen durchzuführen und die Rolle des AhR in diesem Kontext näher zu definieren.

Die vorliegende Dissertation erweiterte das Verständnis der metabolischen Kapazität (Enzymaktivitäten der Phase 1 und 2 des FSM) der menschlichen Haut, sowie verschiedener auf Keratinozyten basierender *in vitro* Modelle. Dabei erwies sich das 3D-Epidermisäquivalent (EPI-200) der FSM Phase 1 Kompetenz der humanen Haut *in vivo* am nächsten, wohingegen die Phase 2 von allen *in vitro* Modellen inklusive *Monolayer* Keratinozytenkulturen gut repräsentiert wird. Sollen solche *in vitro* Modelle als Alternativen zum Tierversuch zum Abschätzen des Gefährdungspotentials von Sub-stanzen genutzt werden, ist das Wissen um metabolische Potenzen im Vergleich zur menschlichen Haut von grundlegender Bedeutung.

Des Weiteren helfen die Ergebnisse dieser Arbeit, die funktionellen Reaktionen der Haut auf exogene Noxen besser zu verstehen. So wurde in dieser Arbeit die AhR-Repressor (AhRR)-Hypothese überprüft, die die Repression der AhR-abhängigen CYP1 Aktivität in dermalen Fibroblasten diesem Protein zuschreibt. Wir konnten nachdrücklich zeigen, dass nicht der AhRR, sondern ein bisher unbekanntes Protein diesen Effekt vermittelt. In den Keratinozyten der Epidermis hingegen wurde der AhR als gemeinsame Zielstruktur der umweltinduzierten Matrixmetalloproteinase (MMP)-1 Aktivierung durch polyzyklische aromatische Kohlenwasserstoffe (wie z.B. B(a)P) so-wie UVB-Strahlung identifiziert, die über den Abbau von Kollagenen zur Destruktion der extrazellulären Matrix beiträgt. Diesem wird durch Östrogen über eine parakrine Freisetzung von EGF aus Keratinozyten entgegengewirkt, da EGF in Fibroblasten einen positiven Effekt auf Makromoleküle der Extrazellulären Matrix hat.

Die Ergebnisse dieser Arbeit tragen dazu bei, die AhR-Signaltransduktion in der Physiologie und der Pathologie der Haut besser zu verstehen und somit den AhR als Zielstruktur für die Prävention von extrinsisch vermittelten Pathologien der Haut nutz-bar zu machen.

5   Abstract

The skin as the largest barrier organ of the human body is directly exposed to a variety of exogenous noxae like UV irradiation, therapeutic agents as well as environmental pollutants. Hence for the homeostasis of the organism it is essential that skin cells as "first-pass-organ" for dermal exposure are able to react to these extrinsic factors. Depletion of skin detoxification capacies leads to organ pathologies such as skin tumors or premature skin aging. In all of these processes the arylhydrocarbon receptor (AhR) plays a central role as a sensor for intracellular stress. This protein regulates the xenobiotic metabolism (XM), is involved in cellular signalling processes and its over-activation is associated with extrinsic tumor formation as well as skin aging. The aim of this study was therefore to investigate functional reactions of the skin after exposure to exogenous noxae and to define the role of the AhR in this context.

This dissertation extends the understanding of the metabolic capacity (enzyme activity of XM phase 1 and 2) of the human skin as well as of different keratinocyte-based *in vitro* models. Thereby the 3D-epidermis equivalent (EPI-200) was most similar to human skin *in vivo* in regard to XM phase 1, whereas phase 2 was represented well in all analysed *in vitro* models including monolayer keratinocyte cell cultures. For these *in vitro* models to be used as alternatives to animal models in order to evaluate the hazard potential of substances to human health, the knowledge of their metabolic potency in comparison with human skin is of essential.

Furthermore the results of this thesis help to better understand the functional reactions of the skin to exposure of exogenous noxae. Thus this work re-evaluated the AhR-Repressor (AhRR) hypothesis, which attributes the repression of AhR dependent CYP1 activity in dermal fibroblasts to this protein. We could show impressively that not the AhRR but a so far unknown protein mediates this effect. However in epidermal keratinocytes the AhR was identified as the common denominator of exogenously in-duced metrixmetalloproteinase (MMP)-1 activation by polycyclic aromatic hydrocarbons (e.g. B(a)P) as well as UVB irradiation, which, by degradation of collagens, accounts for destruction of the extracellular matrix. This effect is antagonized by estrogens via paracrine release of EGF from keratinocytes. EGF in turn has a posi-tive effect of macromolecules of the extracellular matrix.

The results of this thesis contribute to a better understanding of the role of the AhR signalling pathway in physiological and pathological stages of the skin and therefore utilizes the AhR as a target molecule for preventional strategies against extrinsically mediated pathologies of the skin.

6   Abkürzungsverzeichnis

2D	zweidimensional
3D	dreidimensional
3-MC	Methylcolanthren
AG	Arbeitsgruppe
AHH	Arylhydrocarbon Hydrolase (= CYP1A)
AhR	Arylhydrocarbon Rezeptor
AhRR	AhR-Repressor
AIP	AhR-interargierendes Protein
AP-1	Aktivator Protein-1
ARNT	*Arylhydrocarbon Receptor Nuclear Transkocator*
B(a)P	Benzo(a)pyren
BDDI	2-Benzyl-5,6-dimethoxy-3,3-dimethyl-indan-1-1
bHLH	*basic Helix-Loop-Helix*
bzw	beziehungsweise
CAR	*Constitutive Androstane Receptor*
CE	*Cornified Envelope*
CDNB	1-Chor-2,4-dinitrobenzen
COX	Cyclooxygenase
CPA	Cyclophosphamid
CYP	Cytochrom P450 Monooxygenase
DEJ	*Dermal/Epidermal Junction*
DNS	Desoxyribonukleinsäure
E_2	Östrogen
ECM	extrazelluläre Matrix
EGC	Epigallocatechin
EGCG	Epigallocatechingallat
EGF	epidermaler Wachstumsfaktor
EGFR	EGF-Rezeptor
EH	Epoxidhydrolase

ER	Östrogenrezeptor
ERE	*etrogenic regulatory element*
ERK	*extracellular signal-regulated kinase*
EROD	7-Ethoxyresorufin-O-Deethylierung
EPI-200	EpiDerm^{TM} (3D Epidermismodel)
FICZ	6-Formylindolo(3,2-*b*)carbazol
FMO	Flavin-abhängige Monooxygenase
FSM	Fremdstoffmetabolismus
GST	Glutathion S-Transferase
HA	Hyaluronsäure
HAK	halogenierte aromatische Kohlenwasserstoffe
HAS	Hyaluronsäure Synthase
HDAC	Histondeacetylase
hsp	Hitzeschockprotein
HWZ	Halbwertszeit
KO	*knock out*
LDH	Laktratdehydrogenase
LOD	*limit of detection*
LOQ	*limit of quantification*
LOX	Lysyloxidase
MAPK	mitogen-aktivierte Proteinkinase
MEC	normale epitheliale Brustzellen
MED	minimale Erythemdosis
MEF	Mausfibroblasten (*mouse embryonic fibroblasts*)
MMP	Matrixmetalloproeinase
MNF	3'-Methoxy-4'-nitroflavon
mt	mitochondrial
NAT	N-Acetyltransferase
NHDF	normale humane dermale Fibroblasten
NHEK	normale humane epidermale Keratinozyten
OVX	Ovarektomie

PAK	polyzyklische aromatische Kohlenwasserstoffe
PAS	Homologe von Per/ARNT/Sim
PCR	Polymerasekettenreaktion
Per	Period
PGE$_2$	Prostaglandin E2
PXR	*Pregnane X Receptor*
RNS	Ribonukleinsäure
ROS	reaktive Sauerstoffspezies
RSMN	Mikronukleus Assay in EPI-200 Modellen
RT	reverse Transkrition
Sim	*single minded*
SULT	Sulfotransferase
TCDD	2,3,7,8-Tetrachlorodibenzo-*p*-Dioxin
TCDF	2,3,7,8-Tetrachlorodibenzofuran
TGF	*transforming growth factor*
TIMP	*tissue inhibitor of matrixmetalloproteinases*
TPA	*tissue plasminogen activator*
TSA	Trichostatin A
UDP	Uridindiphosphat-Glucose
UGT	UDP-Glukuronosyltransferase
UV	ultraviolet
vs.	versus
XRE	Xenobiotika responsives Element
z.B.	zum Beispiel

7   Literaturverzeichnis

1.   Abbott BD, Schmid JE, Pitt JA, Buckalew AR, Wood CR, Held GA, Diliberto JJ: Adverse reproductive outcomes in the transgenic Ah receptor-deficient mouse. Toxicol Appl Pharmacol 155:62-70 (1999)

2.   Abel J, Haarmann-Stemmann T: An introduction to the molecular basics of aryl hydrocarbon receptor biology. Biol Chem 391:1235-1248 (2010)

3.   Ademola JI, Wester RC, Maibach HI: Metabolism of 3-indolylacetic acid during percutaneous absorption in human skin. J Pharm Sci 82:150-154 (1993)

4.   Afaq F, Mukhtar H: Effects of solar radiation on cutaneous detoxification pathways. J Photochem Photobiol B 63:61-69 (2001)

5.   Affinito P, Palomba S, Sorrentino C, Di CC, Bifulco G, Arienzo MP, Nappi C: Effects of postmenopausal hypoestrogenism on skin collagen. Maturitas 33:239-247 (1999)

6.   Agache PG, Monneur C, Leveque JL, de RJ: Mechanical properties and Young's modulus of human skin in vivo. Arch Dermatol Res 269:221-232 (1980)

7.   Agostinis P, Garmyn M, Van LA: The Aryl hydrocarbon receptor: an illuminating effector of the UVB response. Sci STKE 2007:e49 (2007)

8.   Ahmad N, Agarwal R, Mukhtar H: Cytochrome P-450-dependent drug metabolism in skin. Clin Dermatol 14:407-415 (1996)

9.   Ahmad N, Mukhtar H: Cytochrome p450: a target for drug development for skin diseases. J Invest Dermatol 123:417-425 (2004)

10. Akintobi AM, Villano CM, White LA: 2,3,7,8-Tetrachlorodibenzo-p-dioxin (TCDD) exposure of normal human dermal fibroblasts results in AhR-dependent and -independent changes in gene expression. Toxicol Appl Pharmacol 220:9-17 (2007)

11. Alvares AP, Kappas A, Levin W, Conney AH: Inducibility of benzo( )pyrene hydroxylase in human skin by polycylic hydrocarbons. Clin Pharmacol Ther 14:30-40 (1973a)

12. Alvares AP, Parli CJ, Mannering GJ: Induction of drug metabolism. VI. Effects of phenobarbital and 3-methylcholanthrene administration on N-demethylating enzyme systems of rough and smooth hepatic microsomes. Biochem Pharmacol 22:1037-1045 (1973b)

13. Amakura Y, Tsutsumi T, Nakamura M, Kitagawa H, Fujino J, Sasaki K, Toyoda M, Yoshida T, Maitani T: Activation of the aryl hydrocarbon receptor by some vegetable constituents determined using in vitro reporter gene assay. Biol Pharm Bull 26:532-539 (2003)

14. Ashcroft GS, Dodsworth J, van BE, Tarnuzzer RW, Horan MA, Schultz GS, Ferguson MW: Estrogen accelerates cutaneous wound healing associated with an increase in TGF-beta1 levels. Nat Med 3:1209-1215 (1997)

15. Bae JY, Choi JS, Choi YJ, Shin SY, Kang SW, Han SJ, Kang YH: (-)Epigallocatechin gallate hampers collagen destruction and collagenase activation in ultraviolet-B-irradiated human dermal fibroblasts: involvement of mitogen-activated protein kinase. Food Chem Toxicol 46:1298-1307 (2008)

16. Baron JM, Holler D, Schiffer R, Frankenberg S, Neis M, Merk HF, Jugert FK: Expression of multiple cytochrome p450 enzymes and multidrug resistance-associated transport proteins in human skin keratinocytes. J Invest Dermatol 116:541-548 (2001)

17. Bell DR, Poland A: Binding of aryl hydrocarbon receptor (AhR) to AhR-interacting protein. The role of hsp90. J Biol Chem 275:36407-36414 (2000)

18. Benn PA: Specific chromosome aberrations in senescent fibroblast cell lines derived from human embryos. Am J Hum Genet 28:465-473 (1976)

19. Bentley JP, Brenner RM, Linstedt AD, West NB, Carlisle KS, Rokosova BC, MacDonald N: Increased hyaluronate and collagen biosynthesis and fibroblast estrogen receptors in macaque sex skin. J Invest Dermatol 87:668-673 (1986)

20. Bergander L, Wincent E, Rannug A, Foroozesh M, Alworth W, Rannug U: Metabolic fate of the Ah receptor ligand 6-formylindolo[3,2-b]carbazole. Chem Biol Interact 149:151-164 (2004)

21. Berneburg M, Kamenisch Y, Krutmann J: Repair of mitochondrial DNA in aging and carcinogenesis. Photochem Photobiol Sci 5:190-198 (2006)

22. Berneburg M, Plettenberg H, Krutmann J: Photoaging of human skin. Photodermatol Photoimmunol Photomed 16:239-244 (2000)

23. Bernstein EF, Chen YQ, Kopp JB, Fisher L, Brown DB, Hahn PJ, Robey FA, Lakkakorpi J, Uitto J: Long-term sun exposure alters the collagen of the papillary dermis. Comparison of sun-protected and photoaged skin by northern analysis, immunohistochemical staining, and confocal laser scanning microscopy. J Am Acad Dermatol 34:209-218 (1996a)

24. Bernstein EF, Chen YQ, Tamai K, Shepley KJ, Resnik KS, Zhang H, Tuan R, Mauviel A, Uitto J: Enhanced elastin and fibrillin gene expression in chronically photodamaged skin. J Invest Dermatol 103:182-186 (1994)

25. Bernstein EF, Uitto J: The effect of photodamage on dermal extracellular matrix. Clin Dermatol 14:143-151 (1996)

26. Bernstein EF, Underhill CB, Hahn PJ, Brown DB, Uitto J: Chronic sun exposure alters both the content and distribution of dermal glycosaminoglycans. Br J Dermatol 135:255-262 (1996b)

27. Bickers DR, Mukhtar H, Dutta-Choudhury T, Marcelo CL, Voorhees JJ: Aryl hydrocarbon hydroxylase, epoxide hydrolase, and benzo[a]-pyrene metabolism in human epidermis: comparative studies in normal subjects and patients with psoriasis. J Invest Dermatol 83:51-56 (1984)

28. Birch-Machin MA, Tindall M, Turner R, Haldane F, Rees JL: Mitochondrial DNA deletions in human skin reflect photo- rather than chronologic aging. J Invest Dermatol 110:149-152 (1998)

29. Blackburn EH: Switching and signaling at the telomere. Cell 106:661-673 (2001)

30. Bock KW, Gschaidmeier H, Heel H, Lehmkoster T, Munzel PA, Raschko F, Bock-Hennig B: AH receptor-controlled transcriptional regulation and function of rat and human UDP-glucuronosyltransferase isoforms. Adv Enzyme Regul 38:207-222 (1998)

31. Bock KW, Kohle C: Ah receptor: dioxin-mediated toxic responses as hints to deregulated physiologic functions. Biochem Pharmacol 72:393-404 (2006)

32. Bode AM, Dong Z: Mitogen-activated protein kinase activation in UV-induced signal transduction. Sci STKE 2003:RE2 (2003)

33. Bodnar AG, Ouellette M, Frolkis M, Holt SE, Chiu CP, Morin GB, Harley CB, Shay JW, Lichtsteiner S, Wright WE: Extension of life-span by introduction of telomerase into normal human cells. Science 279:349-352 (1998)

34. Boehnke K: Etablierung und Charakterisierung eines Hautmodells zur Analyse epidermaler Regeneration, dermaler Histogenese und endothelialer Vaskulogenese in vitro 2009)

35. Bothe H, Gotz C, Stobbe-Maicherski N, Fritsche E, Abel J, Haarmann-Stemmann T: Luteolin enhances the bioavailability of benzo(a)pyrene in human colon carcinoma cells. Arch Biochem Biophys 498:111-118 (2010)

36. Brennan M, Bhatti H, Nerusu KC, Bhagavathula N, Kang S, Fisher GJ, Varani J, Voorhees JJ: Matrix metalloproteinase-1 is the major collagenolytic enzyme responsible for collagen damage in UV-irradiated human skin. Photochem Photobiol 78:43-48 (2003)

37. Brincat MP: Hormone replacement therapy and the skin. Maturitas 35:107-117 (2000a)

38. Brincat MP: Hormone replacement therapy and the skin: beneficial effects: the case in favor of it. Acta Obstet Gynecol Scand 79:244-249 (2000b)

39. Buckman SY, Gresham A, Hale P, Hruza G, Anast J, Masferrer J, Pentland AP: COX-2 expression is induced by UVB exposure in human skin: implications for the development of skin cancer. Carcinogenesis 19:723-729 (1998)

40. Castelo-Branco C, Duran M, Gonzalez-Merlo J: Skin collagen changes related to age and hormone replacement therapy. Maturitas 15:113-119 (1992)

41. Chang HY, Chi JT, Dudoit S, Bondre C, van de Rijn M, Botstein D, Brown PO: Diversity, topographic differentiation, and positional memory in human fibroblasts. Proc Natl Acad Sci U S A 99:12877-12882 (2002)

42. Chu DH, Haake AR, Holbrook K, Loomis CA: The Structure and Development of Skin: Fitzpatrick's dermatology in general medicine, pp 58-88 (McGraw-Hill Professional, New York 2003)

43. Ciolino HP, Daschner PJ, Yeh GC: Dietary flavonols quercetin and kaempferol are ligands of the aryl hydrocarbon receptor that affect CYP1A1 transcription differentially. Biochem J 340 (Pt 3):715-722 (1999)

44. Coumailleau P, Poellinger L, Gustafsson JA, Whitelaw ML: Definition of a minimal domain of the dioxin receptor that is associated with Hsp90 and maintains wild type ligand binding affinity and specificity. J Biol Chem 270:25291-25300 (1995)

45. Craven NM, Watson RE, Jones CJ, Shuttleworth CA, Kielty CM, Griffiths CE: Clinical features of photodamaged human skin are associated with a reduction in collagen VII. Br J Dermatol 137:344-350 (1997)

46. de La Motte CA, Hascall VC, Calabro A, Yen-Lieberman B, Strong SA: Mononuclear leukocytes preferentially bind via CD44 to hyaluronan on human intestinal mucosal smooth muscle cells after virus infection or treatment with poly(I.C). J Biol Chem 274:30747-30755 (1999)

47. Denis M, Cuthill S, Wikstrom AC, Poellinger L, Gustafsson JA: Association of the dioxin receptor with the Mr 90,000 heat shock protein: a structural kinship with the glucocorticoid receptor. Biochem Biophys Res Commun 155:801-807 (1988)

48. Denison MS, Nagy SR: Activation of the aryl hydrocarbon receptor by structurally diverse exogenous and endogenous chemicals. Annu Rev Pharmacol Toxicol 43:309-334 (2003)

49. Dietrich C, Kaina B: The aryl hydrocarbon receptor (AhR) in the regulation of cell-cell contact and tumor growth. Carcinogenesis 31:1319-1328 (2010)

50. Dohr O, Li W, Donat S, Vogel C, Abel J: Aryl hydrocarbon receptor mRNA levels in different tissues of 2,3,7,8-Tetrachlorodibenzo-p-dioxin-responsive and nonresponsive mice. Adv Exp Med Biol 387:447-459 (1996)

51. Dong KK, Damaghi N, Picart SD, Markova NG, Obayashi K, Okano Y, Masaki H, Grether-Beck S, Krutmann J, Smiles KA, Yarosh DB: UV-induced DNA damage initiates release of MMP-1 in human skin. Exp Dermatol 17:1037-1044 (2008)

52. DRAIZE JH, ALVAREZ E, .: Toxicological investigations of compounds proposed for use as insect repellents. J Pharmacol Exp Ther 93:26-39 (1948)

53. Du L, Neis M, Ladd PA, Lanza DL, Yost GS, Keeney DS: Effects of the differentiated keratinocyte phenotype on expression levels of CYP1-4 family genes in human skin cells. Toxicol Appl Pharmacol 213:135-144 (2006)

54. Eaton DL, Bammler TK: Concise review of the glutathione S-transferases and their significance to toxicology. Toxicol Sci 49:156-164 (1999)

55. El-Domyati M, Attia S, Saleh F, Brown D, Birk DE, Gasparro F, Ahmad H, Uitto J: Intrinsic aging vs. photoaging: a comparative histopathological, immunohistochemical, and ultrastructural study of skin. Exp Dermatol 11:398-405 (2002)

56. Elferink CJ: Aryl hydrocarbon receptor-mediated cell cycle control. Prog Cell Cycle Res 5:261-267 (2003)

57. Enan E, Matsumura F: Identification of c-Src as the integral component of the cytosolic Ah receptor complex, transducing the signal of 2,3,7,8-tetrachlorodibenzo-p-dioxin (TCDD) through the protein phosphorylation pathway. Biochem Pharmacol 52:1599-1612 (1996)

58. Escoffier C, de RJ, Rochefort A, Vasselet R, Leveque JL, Agache PG: Age-related mechanical properties of human skin: an in vivo study. J Invest Dermatol 93:353-357 (1989)

59. Evanko SP, Angello JC, Wight TN: Formation of hyaluronan- and versican-rich pericellular matrix is required for proliferation and migration of vascular smooth muscle cells. Arterioscler Thromb Vasc Biol 19:1004-1013 (1999)

60. Fernandez-Salguero P, Pineau T, Hilbert DM, McPhail T, Lee SS, Kimura S, Nebert DW, Rudikoff S, Ward JM, Gonzalez FJ: Immune system impairment and hepatic fibrosis in mice lacking the dioxin-binding Ah receptor. Science 268:722-726 (1995)

61. Fernandez-Salguero PM, Ward JM, Sundberg JP, Gonzalez FJ: Lesions of aryl-hydrocarbon receptor-deficient mice. Vet Pathol 34:605-614 (1997)

62. Fisher GJ, Quan T, Purohit T, Shao Y, Cho MK, He T, Varani J, Kang S, Voorhees JJ: Collagen fragmentation promotes oxidative stress and elevates matrix metalloproteinase-1 in fibroblasts in aged human skin. Am J Pathol 174:101-114 (2009)

63. Fisher GJ, Voorhees JJ: Molecular mechanisms of photoaging and its prevention by retinoic acid: ultraviolet irradiation induces MAP kinase signal transduction cascades that induce Ap-1-regulated matrix metalloproteinases that degrade human skin in vivo. J Investig Dermatol Symp Proc 3:61-68 (1998)

64. Frances C: Smoker's wrinkles: epidemiological and pathogenic considerations. Clin Dermatol 16:565-570 (1998)

65. Fritsch: Dermatologie and Venerologie für das Studium. (Springer Medizin Verlag, Heidelberg 2009)

66. Fritsche E, Schafer C, Calles C, Bernsmann T, Bernshausen T, Wurm M, Hubenthal U, Cline JE, Hajimiragha H, Schroeder P, Klotz LO, Rannug A, Furst P, Hanenberg H, Abel J, Krutmann J: Lightening up the UV response by identification of the arylhydrocarbon receptor as a cytoplasmatic target for ultraviolet B radiation. Proc Natl Acad Sci U S A 104:8851-8856 (2007)

67. Fuchs KO, Solis O, Tapawan R, Paranjpe J: The effects of an estrogen and glycolic acid cream on the facial skin of postmenopausal women: a randomized histologic study. Cutis 71:481-488 (2003)

68. Fujii-Kuriyama Y, Mimura J: Molecular mechanisms of AhR functions in the regulation of cytochrome P450 genes. Biochem Biophys Res Commun 338:311-317 (2005)

69. Gassmann K, Abel J, Bothe H, Haarmann-Stemmann T, Merk HF, Quasthoff KN, Rockel TD, Schreiber T, Fritsche E: Species-Specific Differential AhR-Expression Protects Human Neural Progenitor Cells Against Developmental Neurotoxicity Of PAHs. Environ Health Perspect (2010)

70. Gehm BD, McAndrews JM, Jordan VC, Jameson JL: EGF activates highly selective estrogen-responsive reporter plasmids by an ER-independent pathway. Mol Cell Endocrinol 159:53-62 (2000)

71. Gelardi A, Morini F, Dusatti F, Penco S, Ferro M: Induction by xenobiotics of phase I and phase II enzyme activities in the human keratinocyte cell line NCTC 2544. Toxicol In Vitro 15:701-711 (2001)

72. Ghersetich I, Lotti T, Campanile G, Grappone C, Dini G: Hyaluronic acid in cutaneous intrinsic aging. Int J Dermatol 33:119-122 (1994)

73. Gibbs S, van de Sandt JJ, Merk HF, Lockley DJ, Pendlington RU, Pease CK: Xenobiotic metabolism in human skin and 3D human skin reconstructs: a review. Curr Drug Metab 8:758-772 (2007)

74. Gilchrest BA, Krutmann J: Photoaging of skin, Gilchrest BA, Krutmann J (eds): Skin Aging, pp 33-44 (Springer, New York 2006)

75. Goebel C, Hewitt NJ, Kunze G, Wenker M, Hein DW, Beck H, Skare J: Skin metabolism of aminophenols: human keratinocytes as a suitable in vitro model to qualitatively predict the dermal transformation of 4-amino-2-hydroxytoluene in vivo. Toxicol Appl Pharmacol 235:114-123 (2009)

76. Goeckerman W: Treatment of psoriasis: continued observations on the use of crude coal tar and ultraviolett light. Arch Derm Syphilol 24:446-450 (1931)

77. Goerz G, Merk H, Bolsen K, Tsambaos D, Berger H: Influence of chronic UV-light exposure on hepatic and cutaneous monooxygenases. Experientia 39:385-386 (1983)

78. Gradin K, Toftgard R, Poellinger L, Berghard A: Repression of dioxin signal transduction in fibroblasts. Identification Of a putative repressor associated with Arnt. J Biol Chem 274:13511-13518 (1999)

79. Gradin K, Wilhelmsson A, Poellinger L, Berghard A: Nonresponsiveness of normal human fibroblasts to dioxin correlates with the presence of a constitutive xenobiotic response element-binding factor. J Biol Chem 268:4061-4068 (1993)

80. Grancharov K, Naydenova Z, Lozeva S, Golovinsky E: Natural and synthetic inhibitors of UDP-glucuronosyltransferase. Pharmacol Ther 89:171-186 (2001)

81. Greider CW: Telomere length regulation. Annu Rev Biochem 65:337-365 (1996)

82. Grosman N, Hvidberg E, Schou J: The effect of oestrogenic treatment on the acid mucopolysaccharide pattern in skin of mice. Acta Pharmacol Toxicol (Copenh) 30:458-464 (1971)

83. Haarmann-Stemmann T, Abel J: The arylhydrocarbon receptor repressor (AhRR): structure, expression, and function. Biol Chem 387:1195-1199 (2006)

84. Haarmann-Stemmann T, Bothe H, Kohli A, Sydlik U, Abel J, Fritsche E: Analysis of the transcriptional regulation and molecular function of the aryl hydrocarbon receptor repressor in human cell lines. Drug Metab Dispos 35:2262-2269 (2007)

85. Haczynski J, Tarkowski R, Jarzabek K, Slomczynska M, Wolczynski S, Magoffin DA, Jakowicki JA, Jakimiuk AJ: Human cultured skin fibroblasts express estrogen receptor alpha and beta. Int J Mol Med 10:149-153 (2002)

86. Hagvall L, Baron JM, Borje A, Weidolf L, Merk H, Karlberg AT: Cytochrome P450-mediated activation of the fragrance compound geraniol forms potent contact allergens. Toxicol Appl Pharmacol 233:308-313 (2008)

87. Hahn ME: Aryl hydrocarbon receptors: diversity and evolution. Chem Biol Interact 141:131-160 (2002)

88. Hahn ME, Allan LL, Sherr DH: Regulation of constitutive and inducible AHR signaling: complex interactions involving the AHR repressor. Biochem Pharmacol 77:485-497 (2009)

89. Hall JM, Couse JF, Korach KS: The multifaceted mechanisms of estradiol and estrogen receptor signaling. J Biol Chem 276:36869-36872 (2001)

90. Harley CB, Futcher AB, Greider CW: Telomeres shorten during ageing of human fibroblasts. Nature 345:458-460 (1990)

91. Harris IR, Siefken W, Beck-Oldach K, Brandt M, Wittern KP, Pollet D: Comparison of activities dependent on glutathione S-transferase and cytochrome P-450 IA1 in cultured keratinocytes and reconstructed epidermal models. Skin Pharmacol Appl Skin Physiol 15 Suppl 1:59-67 (2002)

92. Hart RW, Setlow RB: Correlation between deoxyribonucleic acid excision-repair and life-span in a number of mammalian species. Proc Natl Acad Sci U S A 71:2169-2173 (1974)

93. Hayes JD, Strange RC: Glutathione S-transferase polymorphisms and their biological consequences. Pharmacology 61:154-166 (2000)

94. Heckmann M: Taschenbuch Dermatologie. (Springer Verlag, Berlin 1999)

95. Heldin P, Laurent TC, Heldin CH: Effect of growth factors on hyaluronan synthesis in cultured human fibroblasts. Biochem J 258:919-922 (1989)

96. Henry EC, Kende AS, Rucci G, Totleben MJ, Willey JJ, Dertinger SD, Pollenz RS, Jones JP, Gasiewicz TA: Flavone antagonists bind competitively with 2,3,7, 8-tetrachlorodibenzo-p-dioxin (TCDD) to the aryl hydrocarbon receptor but inhibit nuclear uptake and transformation. Mol Pharmacol 55:716-725 (1999

97. Hirel B, Chesne C, Pailheret JP, Guillouzo A: In Vitro expression of drug metabolizing enzyme activities in human adult keratinocytes under various culture conditions and their response to inducers. Toxicol In Vitro 9:49-56 (1995)

98. Honkakoski P, Zelko I, Sueyoshi T, Negishi M: The nuclear orphan receptor CAR-retinoid X receptor heterodimer activates the phenobarbital-responsive enhancer module of the CYP2B gene. Mol Cell Biol 18:5652-5658 (1998)

99. Hosoya T, Harada N, Mimura J, Motohashi H, Takahashi S, Nakajima O, Morita M, Kawauchi S, Yamamoto M, Fujii-Kuriyama Y: Inducibility of cytochrome P450 1A1 and chemical carcinogenesis by benzo[a]pyrene in AhR repressor-deficient mice. Biochem Biophys Res Commun 365:562-567 (2008)

100.   Hu T, Khambatta ZS, Hayden PJ, Bolmarcich J, Binder RL, Robinson MK, Carr GJ, Tiesman JP, Jarrold BB, Osborne R, Reichling TD, Nemeth ST, Aardema MJ: Xenobiotic metabolism gene expression in the EpiDermin vitro 3D human epidermis model compared to human skin. Toxicol In Vitro 24:1450-1463 (2010)

101.   Hulmes DJS: Collagen Diversity, Synthesis and Assembly, Fratzl P (ed): Collagen: Structure and Mechanics, pp 15-47 (Springer Verlag, 2008)

102.   Hunzelmann N, Nischt R, Brenneisen P, Eickert A, Krieg T: Increased deposition of fibulin-2 in solar elastosis and its colocalization with elastic fibres. Br J Dermatol 145:217-222 (2001)

103.   Ignar-Trowbridge DM, Nelson KG, Bidwell MC, Curtis SW, Washburn TF, McLachlan JA, Korach KS: Coupling of dual signaling pathways: epidermal growth factor action involves the estrogen receptor. Proc Natl Acad Sci U S A 89:4658-4662 (1992)

104.   Ikuta T, Namiki T, Fujii-Kuriyama Y, Kawajiri K: AhR protein trafficking and function in the skin. Biochem Pharmacol 77:588-596 (2009)

105.   Itahana K, Campisi J, Dimri GP: Methods to detect biomarkers of cellular senescence: the senescence-associated beta-galactosidase assay. Methods Mol Biol 371:21-31 (2007)

106.   Janjua R, Munoz C, Gorell E, Rehmus W, Egbert B, Kern D, Chang AL: A two-year, double-blind, randomized placebo-controlled trial of oral green tea polyphenols on the long-term clinical and histologic appearance of photoaging skin. Dermatol Surg 35:1057-1065 (2009)

107.   Janmohamed A, Dolphin CT, Phillips IR, Shephard EA: Quantification and cellular localization of expression in human skin of genes encoding flavin-containing monooxygenases and cytochromes P450. Biochem Pharmacol 62:777-786 (2001)

108.   Jung EG: Dermatologie 4 ed. (Hippokrates Verlag, Stuttgart 1998)

109.   Kadler KE, Baldock C, Bella J, Boot-Handford RP: Collagens at a glance. J Cell Sci 120:1955-1958 (2007)

110.   Kadoya K, Sasaki T, Kostka G, Timpl R, Matsuzaki K, Kumagai N, Sakai LY, Nishiyama T, Amano S: Fibulin-5 deposition in human skin: decrease with ageing and ultraviolet B exposure and increase in solar elastosis. Br J Dermatol 153:607-612 (2005)

111.   Kang S, Chung JH, Lee JH, Fisher GJ, Wan YS, Duell EA, Voorhees JJ: Topical N-acetyl cysteine and genistein prevent ultraviolet-light-induced signaling that leads to photoaging in human skin in vivo. J Invest Dermatol 120:835-841 (2003)

112.   Karonen T, Jeskanen L, Keski-Oja J: Transforming growth factor beta 1 and its latent form binding protein-1 associate with elastic fibres in human dermis: accumulation in actinic damage and absence in anetoderma. Br J Dermatol 137:51-58 (1997)

113.   Katiyar SK, Matsui MS, Mukhtar H: Ultraviolet-B exposure of human skin induces cytochromes P450 1A1 and 1B1. J Invest Dermatol 114:328-333 (2000)

114.   Kawakubo Y, Merk HF, Masaoudi TA, Sieben S, Blomeke B: N-Acetylation of paraphenylenediamine in human skin and keratinocytes. J Pharmacol Exp Ther 292:150-155 (2000)

115.   Kawakubo Y, Ohkido M: Epidermal N-acetylation of p-aminobenzoyl glutamic acid: difference in response to ultraviolet B irradiation. J Dermatol Sci 16:99-103 (1998)

116.   Kawakubo Y, Yamazoe Y, Kato R, Nishikawa T: High capacity of human skin for N-acetylation of arylamines. Skin Pharmacol 3:180-185 (1990)

117.   Kazlauskas A, Poellinger L, Pongratz I: Evidence that the co-chaperone p23 regulates ligand responsiveness of the dioxin (Aryl hydrocarbon) receptor. J Biol Chem 274:13519-13524 (1999)

118.   Kazlauskas A, Poellinger L, Pongratz I: The immunophilin-like protein XAP2 regulates ubiquitination and subcellular localization of the dioxin receptor. J Biol Chem 275:41317-41324 (2000)

119.   Kim JH, Cho YH, Park SM, Lee KE, Lee JJ, Lee BC, Pyo HB, Song KS, Park HD, Yun YP: Antioxidants and inhibitor of matrix metalloproteinase-1 expression from leaves of Zostera marina L. Arch Pharm Res 27:177-183 (2004)

120.   Koch H, Wittern KP, Bergemann J: In human keratinocytes the Common Deletion reflects donor variabilities rather than chronologic aging and can be induced by ultraviolet A irradiation. J Invest Dermatol 117:892-897 (2001)

121.   Kohle C, Gschaidmeier H, Lauth D, Topell S, Zitzer H, Bock KW: 2,3,7,8-Tetrachlorodibenzo-p-dioxin (TCDD)-mediated membrane translocation of c-Src protein kinase in liver WB-F344 cells. Arch Toxicol 73:152-158 (1999)

122.   Kociba RJ, Keyes DG, Beyer JE, Carreon RM, Wade CE, Dittenber DA, Kalnins RP, Frauson LE, Park CN, Barnard SD, Hummel RA, Humiston CG: Results of a two-year chronic toxicity and oncogenicity study of 2,3,7,8-tetrachlorodibenzo-p-dioxin in rats. Toxicol Appl Pharmacol 46:279-303 (1978)

123. Kreyling WG, Semmler-Behnke M, Seitz J, Scymczak W, Wenk A, Mayer P, Takenaka S, Oberdorster G: Size dependence of the translocation of inhaled iridium and carbon nanoparticle aggregates from the lung of rats to the blood and secondary target organs. Inhal Toxicol 21 Suppl 1:55-60 (2009)

124. Lahmann C, Bergemann J, Harrison G, Young AR: Matrix metalloproteinase-1 and skin ageing in smokers. Lancet 357:935-936 (2001)

125. Laub LB, Jones BD, Powell WH: Responsiveness of a Xenopus laevis cell line to the aryl hydrocarbon receptor ligands 6-formylindolo[3,2-b]carbazole (FICZ) and 2,3,7,8-tetrachlorodibenzo-p-dioxin (TCDD). Chem Biol Interact 183:202-211 (2010)

126. Lee JL, Mukhtar H, Bickers DR, Kopelovich L, Athar M: Cyclooxygenases in the skin: pharmacological and toxicological implications. Toxicol Appl Pharmacol 192:294-306 (2003)

127. Leong J, Hughes-Fulford M, Rakhlin N, Habib A, Maclouf J, Goldyne ME: Cyclooxygenases in human and mouse skin and cultured human keratinocytes: association of COX-2 expression with human keratinocyte differentiation. Exp Cell Res 224:79-87 (1996)

128. Leung WC, Harvey I: Is skin ageing in the elderly caused by sun exposure or smoking? Br J Dermatol 147:1187-1191 (2002)

129. Levin W, Conney AH, Alvares AP, Merkatz I, Kappas A: Induction of benzo(a)pyrene hydroxylase in human skin. Science 176:419-420 (1972)

130. Li GZ, Eller MS, Firoozabadi R, Gilchrest BA: Evidence that exposure of the telomere 3' overhang sequence induces senescence. Proc Natl Acad Sci U S A 100:527-531 (2003)

131. Li W, Donat S, Dohr O, Unfried K, Abel J: Ah receptor in different tissues of C57BL/6J and DBA/2J mice: use of competitive polymerase chain reaction to measure Ah-receptor mRNA expression. Arch Biochem Biophys 315:279-284 (1994)

132. Lim H, Kim HP: Inhibition of mammalian collagenase, matrix metalloproteinase-1, by naturally-occurring flavonoids. Planta Med 73:1267-1274 (2007)

133. Lin Y, Lu P, Tang C, Mei Q, Sandig G, Rodrigues AD, Rushmore TH, Shou M: Substrate inhibition kinetics for cytochrome P450-catalyzed reactions. Drug Metab Dispos 29:368-374 (2001)

134. Lombard DB, Chua KF, Mostoslavsky R, Franco S, Gostissa M, Alt FW: DNA repair, genome stability, and aging. Cell 120:497-512 (2005)

135. Ma Q, Whitlock JP, Jr.: A novel cytoplasmic protein that interacts with the Ah receptor, contains tetratricopeptide repeat motifs, and augments the transcriptional response to 2,3,7,8-tetrachlorodibenzo-p-dioxin. J Biol Chem 272:8878-8884 (1997)

136. Marlowe JL, Puga A: Aryl hydrocarbon receptor, cell cycle regulation, toxicity, and tumorigenesis. J Cell Biochem 96:1174-1184 (2005)

137. Matikainen T, Perez GI, Jurisicova A, Pru JK, Schlezinger JJ, Ryu HY, Laine J, Sakai T, Korsmeyer SJ, Casper RF, Sherr DH, Tilly JL: Aromatic hydrocarbon receptor-driven Bax gene expression is required for premature ovarian failure caused by biohazardous environmental chemicals. Nat Genet 28:355-360 (2001)

138. Matthews J, Gustafsson JA: Estrogen receptor and aryl hydrocarbon receptor signaling pathways. Nucl Recept Signal 4:e016 (2006)

139. Maziere C, Dantin F, Dubois F, Santus R, Maziere J: Biphasic effect of UVA radiation on STAT1 activity and tyrosine phosphorylation in cultured human keratinocytes. Free Radic Biol Med 28:1430-1437 (2000)

140. Merk HF, Baron JM, Heise R, Fritsche E, Schroeder P, Abel J, Krutmann J: Concepts in molecular dermatotoxicology. Exp Dermatol 15:692-704 (2006)

141. Mimura J, Ema M, Sogawa K, Fujii-Kuriyama Y: Identification of a novel mechanism of regulation of Ah (dioxin) receptor function. Genes Dev 13:20-25 (1999)

142. Minchin RF, Hanna PE, Dupret JM, Wagner CR, Rodrigues-Lima F, Butcher NJ: Arylamine N-acetyltransferase I. Int J Biochem Cell Biol 39:1999-2005 (2007)

143. Mitchell RE: Chronic solar dermatosis: a light and electron microscopic study of the dermis. J Invest Dermatol 48:203-220 (1967)

144. Moeller R, Lichter J, Blomeke B: Impact of para-phenylenediamine on cyclooxygenases expression and prostaglandin formation in human immortalized keratinocytes (HaCaT). Toxicology 249:167-175 (2008)

145. Montagna W, Kirchner S, Carlisle K: Histology of sun-damaged human skin. J Am Acad Dermatol 21:907-918 (1989)

146. Morita A: Tobacco smoke causes premature skin aging. J Dermatol Sci 48:169-175 (2007)

147. Moss T, Howes D, Williams FM: Percutaneous penetration and dermal metabolism of triclosan (2,4, 4'-trichloro-2'-hydroxydiphenyl ether). Food Chem Toxicol 38:361-370 (2000)

148. Mukhtar H, DelTito BJ, Jr., Matgouranis PM, Das M, Asokan P, Bickers DR: Additive effects of ultraviolet B and crude coal tar on cutaneous carcinogen metabolism: possible relevance to the tumorigenicity of the Goeckerman regimen. J Invest Dermatol 87:348-353 (1986)

149. Murphy KA, Villano CM, Dorn R, White LA: Interaction between the aryl hydrocarbon receptor and retinoic acid pathways increases matrix metalloproteinase-1 expression in keratinocytes. J Biol Chem 279:25284-25293 (2004)

150. Narayanan DL, Saladi RN, Fox JL: Ultraviolet radiation and skin cancer. Int J Dermatol 49:978-986 (2010)

151. Natsch A, Wasescha M: Fragrance raw materials and essential oils can reduce prostaglandin E(2) formation in keratinocytes and reconstituted human epidermis. Int J Cosmet Sci 29:369-376 (2007)

152. Naylor EC, Watson RE, Sherratt MJ: Molecular aspects of skin ageing. Maturitas 69:249-256 (2011)

153. Nebert DW, Dalton TP, Okey AB, Gonzalez FJ: Role of aryl hydrocarbon receptor-mediated induction of the CYP1 enzymes in environmental toxicity and cancer. J Biol Chem 279:23847-23850 (2004)

154. Neis MM, Wendel A, Wiederholt T, Marquardt Y, Joussen S, Baron JM, Merk HF: Expression and induction of cytochrome p450 isoenzymes in human skin equivalents. Skin Pharmacol Physiol 23:29-39 (2010)

155. Nelson KG, Takahashi T, Bossert NL, Walmer DK, McLachlan JA: Epidermal growth factor replaces estrogen in the stimulation of female genital-tract growth and differentiation. Proc Natl Acad Sci U S A 88:21-25 (1991)

156. Nohynek GJ, Duche D, Garrigues A, Meunier PA, Toutain H, Leclaire J: Under the skin: Biotransformation of para-aminophenol and para-phenylenediamine in reconstructed human epidermis and human hepatocytes. Toxicol Lett 158:196-212 (2005)

157.   Oberg M, Bergander L, Hakansson H, Rannug U, Rannug A: Identification of the tryptophan photoproduct 6-formylindolo[3,2-b]carbazole, in cell culture medium, as a factor that controls the background aryl hydrocarbon receptor activity. Toxicol Sci 85:935-943 (2005)

158.   Oesch F, Arand M: Xenobiotic metabolism, Marquardt H, Schäfer S, McLellan D, Welsch C (eds): Toxicology, pp 84-110 (Academic Press, San Diego 1999)

159.   Oesch F, Fabian E, Oesch-Bartlomowicz B, Werner C, Landsiedel R: Drug-metabolizing enzymes in the skin of man, rat, and pig. Drug Metab Rev 39:659-698 (2007)

160.   Okey AB: An aryl hydrocarbon receptor odyssey to the shores of toxicology: the Deichmann Lecture, International Congress of Toxicology-XI. Toxicol Sci 98:5-38 (2007)

161.   Omdahl JL, Bobrovnikova EV, Annalora A, Chen P, Serda R: Expression, structure-function, and molecular modeling of vitamin D P450s. J Cell Biochem 88:356-362 (2003)

162.   Oshima M, Mimura J, Yamamoto M, Fujii-Kuriyama Y: Molecular mechanism of transcriptional repression of AhR repressor involving ANKRA2, HDAC4, and HDAC5. Biochem Biophys Res Commun 364:276-282 (2007)

163.   Ott H, Bergstrom MA, Heise R, Skazik C, Zwadlo-Klarwasser G, Merk HF, Baron JM, Karlberg AT: Cutaneous metabolic activation of carvoxime, a self-activating, skin-sensitizing prohapten. Chem Res Toxicol 22:399-405 (2009)

164.   Pacifici GM, Franchi M, Colizzi C, Giuliani L, Rane A: Glutathione S-transferase in humans: development and tissue distribution. Arch Toxicol 61:265-269 (1988)

165.   Paigen B, Ward E, Reilly A, Houten L, Gurtoo HL, Minowada J, Steenland K, Havens MB, Sartori P: Seasonal variation of aryl hydrocarbon hydroxylase activity in human lymphocytes. Cancer Res 41:2757-2761 (1981)

166.   Palermo CM, Westlake CA, Gasiewicz TA: Epigallocatechin gallate inhibits aryl hydrocarbon receptor gene transcription through an indirect mechanism involving binding to a 90 kDa heat shock protein. Biochemistry 44:5041-5052 (2005)

167.   Park SS, Kim YJ: Source contributions to fine particulate matter in an urban atmosphere. Chemosphere 59:217-226 (2005)

168. Pasonen-Seppanen S, Karvinen S, Torronen K, Hyttinen JM, Jokela T, Lammi MJ, Tammi MI, Tammi R: EGF upregulates, whereas TGF-beta downregulates, the hyaluronan synthases Has2 and Has3 in organotypic keratinocyte cultures: correlations with epidermal proliferation and differentiation. J Invest Dermatol 120:1038-1044 (2003)

169. Pavez LE, Li H, Vahlquist A, Torma H: The involvement of cytochrome p450 (CYP) 26 in the retinoic acid metabolism of human epidermal keratinocytes. Biochim Biophys Acta 1791:220-228 (2009)

170. Pienimaki JP, Rilla K, Fulop C, Sironen RK, Karvinen S, Pasonen S, Lammi MJ, Tammi R, Hascall VC, Tammi MI: Epidermal growth factor activates hyaluronan synthase 2 in epidermal keratinocytes and increases pericellular and intracellular hyaluronan. J Biol Chem 276:20428-20435 (2001)

171. Pocar P, Fischer B, Klonisch T, Hombach-Klonisch S: Molecular interactions of the aryl hydrocarbon receptor and its biological and toxicological relevance for reproduction. Reproduction 129:379-389 (2005)

172. Proksch E, Brandner JM, Jensen JM: The skin: an indispensable barrier. Exp Dermatol 17:1063-1072 (2008)

173. Radjendirane V, Joseph P, Jaiswal AK: Gene expression of DT-diaphorase (NQO1) in cancer cells, Henry JFEC (ed): Oxidative stress and signal transduction (Chapman & Hall, New York (NY) 1997)

174. Ramadoss P, Marcus C, Perdew GH: Role of the aryl hydrocarbon receptor in drug metabolism. Expert Opin Drug Metab Toxicol 1:9-21 (2005)

175. Rannug A, Fritsche E: The aryl hydrocarbon receptor and light. Biol Chem 387:1149-1157 (2006)

176. Rannug A, Rannug U, Rosenkranz HS, Winqvist L, Westerholm R, Agurell E, Grafstrom AK: Certain photooxidized derivatives of tryptophan bind with very high affinity to the Ah receptor and are likely to be endogenous signal substances. J Biol Chem 262:15422-15427 (1987)

177. Rannug U, Rannug A, Sjoberg U, Li H, Westerholm R, Bergman J: Structure elucidation of two tryptophan-derived, high affinity Ah receptor ligands. Chem Biol 2:841-845 (1995)

178. Raza H, Awasthi YC, Zaim MT, Eckert RL, Mukhtar H: Glutathione S-transferases in human and rodent skin: multiple forms and species-specific expression. J Invest Dermatol 96:463-467 (1991)

179. Reenstra WR, Yaar M, Gilchrest BA: Effect of donor age on epidermal growth factor processing in man. Exp Cell Res 209:118-122 (1993)

180. Rittie L, Fisher GJ: UV-light-induced signal cascades and skin aging. Ageing Res Rev 1:705-720 (2002)

181. Robert C, Lesty C, Robert AM: Ageing of the skin: study of elastic fiber network modifications by computerized image analysis. Gerontology 34:291-296 (1988)

182. Rolsted K, Kissmeyer AM, Rist GM, Hansen SH: Evaluation of cytochrome P450 activity in vitro, using dermal and hepatic microsomes from four species and two keratinocyte cell lines in culture. Arch Dermatol Res 300:11-18 (2008)

183. Rowlands JC, Gustafsson JA: Aryl hydrocarbon receptor-mediated signal transduction. Crit Rev Toxicol 27:109-134 (1997)

184. Rushmore TH, King RG, Paulson KE, Pickett CB: Regulation of glutathione S-transferase Ya subunit gene expression: identification of a unique xenobiotic-responsive element controlling inducible expression by planar aromatic compounds. Proc Natl Acad Sci U S A 87:3826-3830 (1990)

185. Russel WMS, Burch RL: The Principles of Human Experimental Technique. (Methuen, London 1959)

186. Saeki M, Saito Y, Nagano M, Teshima R, Ozawa S, Sawada J: mRNA expression of multiple cytochrome p450 isozymes in four types of cultured skin cells. Int Arch Allergy Immunol 127:333-336 (2002)

187. Safe S, Wormke M: Inhibitory aryl hydrocarbon receptor-estrogen receptor alpha cross-talk and mechanisms of action. Chem Res Toxicol 16:807-816 (2003)

188. Sarnstrand B, Eriksson G, Malmstrom A: Glucocorticoids change the nucleotide and sugar nucleotide pool sizes in cultured human skin fibroblasts. Arch Biochem Biophys 252:315-321 (1987)

189. Sator PG, Sator MO, Schmidt JB, Nahavandi H, Radakovic S, Huber JC, Honigsmann H: A prospective, randomized, double-blind, placebo-controlled study on the influence of a hormone replacement therapy on skin aging in postmenopausal women. Climacteric 10:320-334 (2007)

190. Sator PG, Schmidt JB, Sator MO, Huber JC, Honigsmann H: The influence of hormone replacement therapy on skin ageing: a pilot study. Maturitas 39:43-55 (2001)

191. Schieke S, Stege H, Kurten V, Grether-Beck S, Sies H, Krutmann J: Infrared-A radiation-induced matrix metalloproteinase 1 expression is mediated through extracellular signal-regulated kinase 1/2 activation in human dermal fibroblasts. J Invest Dermatol 119:1323-1329 (2002)

192. Schikowski T, Sugiri D, Ranft U, Gehring U, Heinrich J, Wichmann HE, Kramer U: Does respiratory health contribute to the effects of long-term air pollution exposure on cardiovascular mortality? Respir Res 8:20 (2007)

193. Schmidt JB, Binder M, Demschik G, Bieglmayer C, Reiner A: Treatment of skin aging with topical estrogens. Int J Dermatol 35:669-674 (1996a)

194. Schmidt JV, Su GH, Reddy JK, Simon MC, Bradfield CA: Characterization of a murine Ahr null allele: involvement of the Ah receptor in hepatic growth and development. Proc Natl Acad Sci U S A 93:6731-6736 (1996b)

195. Schwarz T: Photoimmunosuppression. Photodermatol Photoimmunol Photomed 18:141-145 (2002)

196. Shimada T, Sugie A, Shindo M, Nakajima T, Azuma E, Hashimoto M, Inoue K: Tissue-specific induction of cytochromes P450 1A1 and 1B1 by polycyclic aromatic hydrocarbons and polychlorinated biphenyls in engineered C57BL/6J mice of arylhydrocarbon receptor gene. Toxicol Appl Pharmacol 187:1-10 (2003)

197. Shimizu Y, Nakatsuru Y, Ichinose M, Takahashi Y, Kume H, Mimura J, Fujii- Kuriyama Y, Ishikawa T: Benzo[a]pyrene carcinogenicity is lost in mice lacking the aryl hydrocarbon receptor. Proc Natl Acad Sci U S A 97:779-782 (2000)

198. Shiraha H, Gupta K, Drabik K, Wells A: Aging fibroblasts present reduced epidermal growth factor (EGF) responsiveness due to preferential loss of EGF receptors. J Biol Chem 275:19343-19351 (2000)

199. Sim GS, Lee BC, Cho HS, Lee JW, Kim JH, Lee DH, Kim JH, Pyo HB, Moon DC, Oh KW, Yun YP, Hong JT: Structure activity relationship of antioxidative property of flavonoids and inhibitory effect on matrix metalloproteinase activity in UVA-irradiated human dermal fibroblast. Arch Pharm Res 30:290-298 (2007)

200. Simpson RM, Meran S, Thomas D, Stephens P, Bowen T, Steadman R, Phillips A: Age-related changes in pericellular hyaluronan organization leads to impaired dermal fibroblast to myofibroblast differentiation. Am J Pathol 175:1915-1928 (2009)

201. Simpson RM, Wells A, Thomas D, Stephens P, Steadman R, Phillips A: Aging fibroblasts resist phenotypic maturation because of impaired hyaluronan-dependent CD44/epidermal growth factor receptor signaling. Am J Pathol 176:1215-1228 (2010)

202. Situm M, Buljan M, Bulat V, Lugovic ML, Bolanca Z, Simic D: The role of UV radiation in the development of basal cell carcinoma. Coll Antropol 32 Suppl 2:167-170 (2008)

203. Smith C.K., Hotchkiss S.A.M.: Allergic Contact Dermatitis: Chemical and Metabolic Mechanisms. (Taylor & Francis, London 2001)

204. Sobel H, Cohen RA: Effect of estradion on hyaluronic acid in the skin of aging mice. Steroids 16:1-3 (1970)

205. Stern R, Maibach HI: Hyaluronan in skin: aspects of aging and its pharmacologic modulation. Clin Dermatol 26:106-122 (2008)

206. Sutter CH, Yin H, Li Y, Mammen JS, Bodreddigari S, Stevens G, Cole JA, Sutter TR: EGF receptor signaling blocks aryl hydrocarbon receptor-mediated transcription and cell differentiation in human epidermal keratinocytes. Proc Natl Acad Sci U S A 106:4266-4271 (2009)

207. Svensson CK: Biotransformation of drugs in human skin. Drug Metab Dispos 37:247-253 (2009)

208. Swanson HI: Cytochrome P450 expression in human keratinocytes: an aryl hydrocarbon receptor perspective. Chem Biol Interact 149:69-79 (2004)

209. Talwar HS, Griffiths CE, Fisher GJ, Hamilton TA, Voorhees JJ: Reduced type I and type III procollagens in photodamaged adult human skin. J Invest Dermatol 105:285-290 (1995)

210.   Taylor BL, Zhulin IB: PAS domains: internal sensors of oxygen, redox potential, and light. Microbiol Mol Biol Rev 63:479-506 (1999)

211.   Tsuchiya Y, Nakajima M, Itoh S, Iwanari M, Yokoi T: Expression of aryl hydrocarbon receptor repressor in normal human tissues and inducibility by polycyclic aromatic hydrocarbons in human tumor-derived cell lines. Toxicol Sci 72:253-259 (2003)

212.   Tsuji G, Takahara M, Uchi H, Matsuda T, Chiba T, Takeuchi S, Yasukawa F, Moroi Y, Furue M: Identification of Ketoconazole as an AhR-Nrf2 Activator in Cultured Human Keratinocytes: The Basis of Its Anti-Inflammatory Effect. J Invest Dermatol (2011)

213.   Tsukahara K, Moriwaki S, Ohuchi A, Fujimura T, Takema Y: Ovariectomy accelerates photoaging of rat skin. Photochem Photobiol 73:525-531 (2001)

214.   Tukey RH, Strassburg CP: Human UDP-glucuronosyltransferases: metabolism, expression, and disease. Annu Rev Pharmacol Toxicol 40:581-616 (2000)

215.   Uzuka M, Nakajima K, Ohta S, Mori Y: Induction of hyaluronic acid synthetase by estrogen in the mouse skin. Biochim Biophys Acta 673:387-393 (1981)

216.   Vallius M, Janssen NA, Heinrich J, Hoek G, Ruuskanen J, Cyrys J, Van GR, de Hartog JJ, Kreyling WG, Pekkanen J: Sources and elemental composition of ambient PM(2.5) in three European cities. Sci Total Environ 337:147-162 (2005)

217.   van Berlo D., Albrecht C, Knaapen AM, Cassee FR, Gerlofs-Nijland ME, Kooter IM, Palomero-Gallagher N, Bidmon HJ, van Schooten FJ, Krutmann J, Schins RP: Comparative evaluation of the effects of short-term inhalation exposure to diesel engine exhaust on rat lung and brain. Arch Toxicol 84:553-562 (2010)

218.   Verdier-Sevrain S, Bonte F, Gilchrest B: Biology of estrogens in skin: implications for skin aging. Exp Dermatol 15:83-94 (2006)

219.   Verdier-Sevrain S, Yaar M, Cantatore J, Traish A, Gilchrest BA: Estradiol induces proliferation of keratinocytes via a receptor mediated mechanism. FASEB J 18:1252-1254 (2004)

220.   Vierkotter A, Schikowski T, Ranft U, Sugiri D, Matsui M, Kramer U, Krutmann J: Airborne Particle Exposure and Extrinsic Skin Aging. J Invest Dermatol (2010)

221.   Vincenti MP, White LA, Schroen DJ, Benbow U, Brinckerhoff CE: Regulating expression of the gene for matrix metalloproteinase-1 (collagenase): mechanisms that control enzyme activity, transcription, and mRNA stability. Crit Rev Eukaryot Gene Expr 6:391-411 (1996)

222.   Visse R, Nagase H: Matrix metalloproteinases and tissue inhibitors of metalloproteinases: structure, function, and biochemistry. Circ Res 92:827-839 (2003)

223.   Vogel C, Boerboom AM, Baechle C, El-Bahay C, Kahl R, Degen GH, Abel J: Regulation of prostaglandin endoperoxide H synthase-2 induction by dioxin in rat hepatocytes: possible c-Src-mediated pathway. Carcinogenesis 21:2267-2274 (2000)

224.   Vondracek M, Xi Z, Larsson P, Baker V, Mace K, Pfeifer A, Tjalve H, Donato MT, Gomez-Lechon MJ, Grafstrom RC: Cytochrome P450 expression and related metabolism in human buccal mucosa. Carcinogenesis 22:481-488 (2001)

225.   Wallace DC: Mitochondrial genetics: a paradigm for aging and degenerative diseases? Science 256:628-632 (1992)

226.   Wang Y, Zhang X, Lebwohl M, DeLeo V, Wei H: Inhibition of ultraviolet B (UVB)-induced c-fos and c-jun expression in vivo by a tyrosine kinase inhibitor genistein. Carcinogenesis 19:649-654 (1998)

227.   Warren R, Gartstein V, Kligman AM, Montagna W, Allendorf RA, Ridder GM: Age, sunlight, and facial skin: a histologic and quantitative study. J Am Acad Dermatol 25:751-760 (1991)

228.   Wätjen W, Fritsche F: Fremdstoffmetabolismus, Vohr HW (ed): Toxikologie Band 1, pp 43-74 (WILEY-VCH Verlag GmbH & Co.KGaA, Weinheim 2010)

229.   Watson RE, Griffiths CE, Craven NM, Shuttleworth CA, Kielty CM: Fibrillin-rich microfibrils are reduced in photoaged skin. Distribution at the dermal-epidermal junction. J Invest Dermatol 112:782-787 (1999)

230.   WATTENBERG LW, LEONG JL, STRAND PJ: Benzpyrene hydroxylase activity in the gastrointestinal tract. Cancer Res 22:1120-1125 (1962)

231.   Webber J, Meran S, Steadman R, Phillips A: Hyaluronan orchestrates transforming growth factor-beta1-dependent maintenance of myofibroblast phenotype. J Biol Chem 284:9083-9092 (2009)
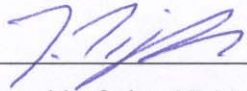
232. Wei H, Saladi R, Lu Y, Wang Y, Palep SR, Moore J, Phelps R, Shyong E, Lebwohl MG: Isoflavone genistein: photoprotection and clinical implications in dermatology. J Nutr 133:3811S-3819S (2003)

233. Wei YD, Rannug U, Rannug A: UV-induced CYP1A1 gene expression in human cells is mediated by tryptophan. Chem Biol Interact 118:127-140 (1999)

234. Williams SN, Shih H, Guenette DK, Brackney W, Denison MS, Pickwell GV, Quattrochi LC: Comparative studies on the effects of green tea extracts and individual tea catechins on human CYP1A gene expression. Chem Biol Interact 128:211-229 (2000)

235. Wincent E, Amini N, Luecke S, Glatt H, Bergman J, Crescenzi C, Rannug A, Rannug U: The suggested physiologic aryl hydrocarbon receptor activator and cytochrome P4501 substrate 6-formylindolo[3,2-b]carbazole is present in humans. J Biol Chem 284:2690-2696 (2009)

236. Xie W, Barwick JL, Simon CM, Pierce AM, Safe S, Blumberg B, Guzelian PS, Evans RM: Reciprocal activation of xenobiotic response genes by nuclear receptors SXR/PXR and CAR. Genes Dev 14:3014-3023 (2000)

237. Xu C, Li CY, Kong AN: Induction of phase I, II and III drug metabolism/transport by xenobiotics. Arch Pharm Res 28:249-268 (2005)

238. Yamada Y, Itano N, Hata K, Ueda M, Kimata K: Differential regulation by IL-1beta and EGF of expression of three different hyaluronan synthases in oral mucosal epithelial cells and fibroblasts and dermal fibroblasts: quantitative analysis using real-time RT-PCR. J Invest Dermatol 122:631-639 (2004)

239. Yamamoto J, Ihara K, Nakayama H, Hikino S, Satoh K, Kubo N, Iida T, Fujii Y, Hara T: Characteristic expression of aryl hydrocarbon receptor repressor gene in human tissues: organ-specific distribution and variable induction patterns in mononuclear cells. Life Sci 74:1039-1049 (2004)

240. Yang JH, Lee HC, Wei YH: Photoageing-associated mitochondrial DNA length mutations in human skin. Arch Dermatol Res 287:641-648 (1995)

241. Yengi LG, Xiang Q, Pan J, Scatina J, Kao J, Ball SE, Fruncillo R, Ferron G, Roland WC: Quantitation of cytochrome P450 mRNA levels in human skin. Anal Biochem 316:103-110 (2003)

242. Zhang S, Qin C, Safe SH: Flavonoids as aryl hydrocarbon receptor agonists/antagonists: effects of structure and cell context. Environ Health Perspect 111:1877-1882 (2003)

243. Zhang Y, Gonzalez V, Xu MJ: Expression and regulation of glutathione S-transferase P1-1 in cultured human epidermal cells. J Dermatol Sci 30:205-214 (2002)

244. Zhao X, Goswami M, Pokhriyal N, Ma H, Du H, Yao J, Victor TA, Polyak K, Sturgis CD, Band H, Band V: Cyclooxygenase-2 expression during immortalization and breast cancer progression. Cancer Res 68:467-475 (2008)

Eidesstaatliche Erklärung

Die hier vorgelegte Dissertation habe ich eigenhändig und ohne unerlaubte Hilfe angefertigt. Die Dissertation wurde in der vorgelegten oder einer ähnlichen Form noch bei keiner anderen Institution eingereicht. Ich habe bisher keine erfolglosen Promotionsversuche unternommen.

Düsseldorf, den 07.11.2011